2019

Volume : 8
Issue : 4
Page : 282- 377

e-ISSN : 2147-4249

Eurasian Journal of Soil Science

www.fesss.org

Published by Federation of Eurasian Soil Science Societies

EURASIAN JOURNAL OF SOIL SCIENCE

(Peer Reviewed Open Access Journal)

Published by Federation of Eurasian Soil Science Societies

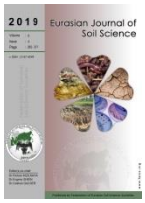

ABOUT THIS JOURNAL : Eurasian Journal of Soil Science is the official English language journal of the Federation of Eurasian Soil Science Societies. Eurasian Journal of Soil Science peer-reviewed open access journal that publishes research articles, critical reviews of basic and applied soil science in all related to soil and plant studies and general environmental soil science.

ABSTRACTING AND INDEXING: SCOPUS, CABI, FAO-Agris, EBSCOhost, ProQuest, DOAJ, OAJI, TR Dizin, TURKISH Journalpark, CrossRef, CiteFactor, CAS, etc.

Year: 2019, Volume: 8, Issue: 4, Page: 282 - 377 **e-ISSN 2147-4249**

Eurasian J Soil Sci 2019, 8 (4) 282 - 288

Eurasian Journal of Soil Science

Journal homepage : http://ejss.fesss.org

Effect of fertilizer, manure and irrigation on nutrient availability in soil of boro rice field

Md. Masfiqur Rahman [a], Md. Asaduzzaman Khan [a], Alok Kumar Paul [a] Md. Ashraful Hoque [b,*]

[a] Department of Soil Science, Sher-E-Bangla Agricultural University, Dhaka 1207, Bangladesh
[b] Department of Plant Pathology, Bangladesh Agricultural University, Mymensingh-2202, Bangladesh

Abstract

The experiment was conducted in the farm of Sher-e-Bangla Agricultural University, Dhaka, Bangladesh to study the effect of various organic manures and inorganic fertilizers with different water management on the nutrient availability of *boro* rice field. BRRI dhan29 was used as the test crop in this experiment. The experiment consists of 2 factors i.e. Irrigation and fertilizer plus manure. Two levels of irrigations (I_1= Continuous flooding and I_2= Saturated Condition) were used with 8 levels of fertilizer plus manure, as T_0: Control, T_1: 100% ($N_{120}P_{25}K_{60}S_{20}Zn_2$) Recommended dose of Fertilizer, T_2: 50% NPKSZn + 5 ton cow-dung ha^{-1}, T_3: 70% NPKSZn + 3 ton cow-dung ha^{-1}, T_4: 50% NPKSZn + 5 ton compost ha^{-1}, T_5: 70% NPKSZn+3 ton compost ha^{-1}, T_6: 50% NPKSZn + 3.5 ton poultry manure ha^{-1} and T_7: 70% NPKSZn+2.1 ton poultry manure ha^{-1}, with 16 treatment combinations and 3 replications. The pore-water samples were collected and analyzed during rice growing period. The higher concentrations of N, P and K were found in the pore water of T_6 (50% NPKSZn + 3.5 ton poultry manure ha^{-1}) and T_7 (70% NPKSZn + 2.1 ton poultry manure ha^{-1}) treatments where higher yield were obtained. The higher N, P, K & S concentrations and uptake were observed in the treatments where fertilizer plus manure were applied. The highest concentrations of grain N (1.31%), P (0.272%), K (0.195%) and S (0.091%) were recorded from T_5, T_3, T_7 and T_2 treatment respectively and lowest from T_0 (Control) treatment.

Keywords: Boro rice field, Effect of fertilizer, manure, irrigation, nutrient availability in soil.

Article Info

Received : 23.10.2018
Accepted : 17.06.2019

Introduction

Rice (*Oryza sativa*) is one of the major crops of the world. Rice is a semi aquatic annual grass plant and is the most important cereal crop in the developing world. Global rice production has tripled in the last five decades from 150 million tons in 1960 to 450 million tons in 2011, due to the rice Green Revolution in Asia (Rejesus et al., 2012). A study showed that most Asian countries won't be able to feed their projected population without irreversibly degrading their land resources, even with high levels of management inputs (Beinroth et al., 2001). The depleted soil fertility is a major constraint to higher crop production in Bangladesh. The increasing land use intensity has resulted in a great exhaustion of nutrients in soils. Rice-rice cropping system is the most important cropping system in Bangladesh.

Scientists are trying to improve the production systems with the help of combination of organic and inorganic sources of nutrients. The application of different levels of irrigation in *boro* rice affects the yield by affecting nutrient accumulation. More nutrients are leached out from soil when higher levels of irrigation water are added during *boro* rice growing period. Moisture levels affect the organic matter accumulation and

* Corresponding author.
Department of Plant Pathology, Bangladesh Agricultural University, Mymensingh-2202, Bangladesh
Tel.: +8801744515572 E-mail address: md.ashraful.hoque03@gmail.com
e-ISSN: 2147-4249 DOI: 10.18393/ejss.580833

mineralization. Yang et al. (2004) reported that application of chemical fertilizers with farmyard manure or wheat or rice straw in alternate wetting and drying condition increased N, P, & K uptake by rice plants.

This study was undertaken to: develop a suitable integrated dose of inorganic fertilizers combined with different manures for *boro* rice; evaluate the effects of inorganic and organic fertilizer with different water management on the nutrient concentration of *boro* rice; and investigate the improvement of soil fertility due to the use of organic manure in combination with chemical fertilizers.

This detailed study was under taken with the following objectives:

i. To maintain the soil health by adopting Integrated Nutrient Management system in rice cultivation.
ii. To investigate, the improvement of soil fertility due to the use of organic manure in combination with chemical fertilizers.
iii. To investigate the availability of N, P, K and S in pore water of cropped and un-cropped soil with different fertilizer application.

Material and Methods

The experiment was conducted in the Farm of Sher-e-Bangla Agricultural University, Dhaka, Bangladesh.

Experimental site and soil: The experiment was conducted in typical rice growing silt loam soil at the Sher-E-Bangla Agricultural University Farm, Dhaka during the *boro* season of 2012-13.

Climate: The climate of the experimental area is characterized by high temperature, high humidity and medium rainfall with occasional gusty winds during the *kharif* season (March-September) and a scanty rainfall associated with moderately low temperature in the *Rabi* season (October-March).

Planting material: BRRI dhan 29 was used as the test crop in this experiment.

Land preparation: Ploughing was done. Before transplanting each unit of plot was cleaned by removing the weeds, stubbles and crop residues. Finally each plot was prepared by puddling.

Experimental Design: The experiment was laid out in a split plot design (SPD) with three replications (Figure 1 and 2).

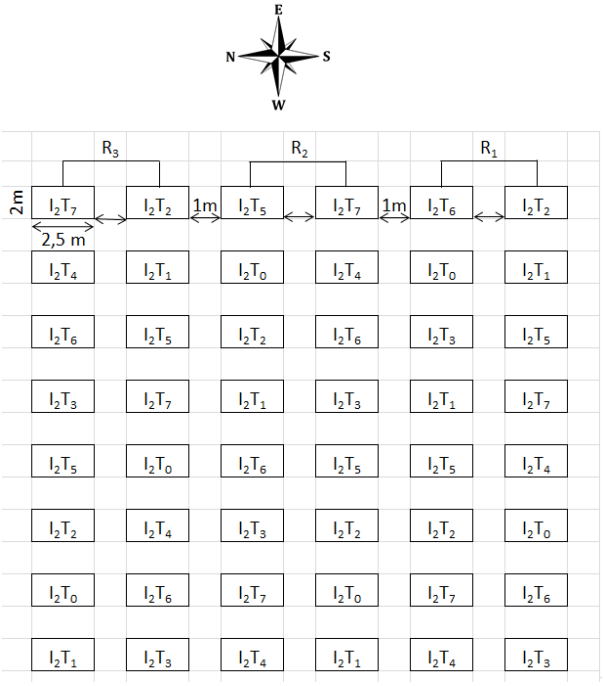

Figure 1. Layout of the experimental Plot of Boro Rice

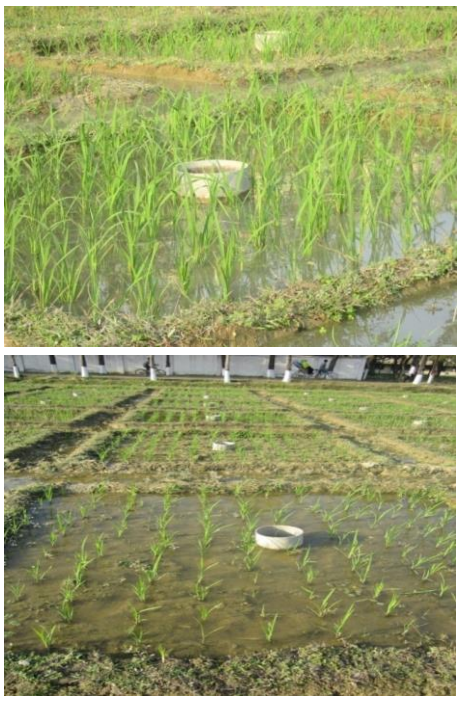

Figure 2. Main Field

Initial soil sampling: Before land preparation, initial soil samples at 0-15 cm depth were collected from different spots of the experimental field. The composite soil sample were air-dried, crushed and passed through a 2 mm (8 meshes) sieve. After sieving, the soil samples were kept in a plastic container for physical and chemical analysis of the soil.

Treatments: The experiment consists of 2 factors (i) irrigation and (ii) fertilizer plus manure. Details of factors and their combinations are presented below:

Factor A: 2 Level of ırrigation in the main plot

I_1= Continuous flooding

I_2= Saturated condition

Factor B: 8 Fertilizer, manure treatment in the sub plot

T_0: Control

T_1: 100% ($N_{120}P_{25}K_{60}S_{20}Zn_2$) recommended dose of fertilizer

T_2: 50% NPKSZn + 5 ton cow dung ha^{-1}

T_3: 70% NPKSZn + 3 ton cow dung ha^{-1}

T_4: 50% NPKSZn + 5 ton compost ha^{-1}

T_5: 70% NPKSZn + 3 ton compost ha^{-1}

T_6: 50% NPKSZn + 3.5 ton poultry manure ha^{-1}

T_7: 70% NPKSZn + 2.1 ton poultry manure ha^{-1}

Treatment combination

I_1T_0 = (Continuous flooding + Control)

I_1T_1 = Continuous flooding + 100% ($N_{120}P_{25}K_{60}S_{20}Zn_2$) (Recommended dose)

I_1T_2 = (Continuous flooding + 50% NPKSZn + 5 ton cow dung ha^{-1})

I_1T_3 = (Continuous flooding + 70% NPKSZn + 3 ton cow dung ha^{-1})

I_1T_4 = (Continuous flooding + 50% NPKSZn + 5 ton compost ha^{-1})

I_1T_5 = (Continuous flooding + 70% NPKSZn + 3 ton compost ha^{-1})

I_1T_6 = (Continuous flooding + 50% NPKSZn + 3.5 ton poultry manure ha^{-1})

I_1T_7 = (Continuous flooding + 70% NPKSZn + 2.1 ton poultry manure ha^{-1})

I_2T_0 = (Saturated condition + Control)

I_2T_1 = Saturated condition + 100% ($N_{120}P_{25}K_{60}S_{20}Zn_2$) (Recommended dose)

I_2T_2 = (Saturated condition + 50% NPKSZn + 5 ton cow dung ha^{-1})

I_2T_3 = (Saturated condition + 70% NPKSZn + 3 ton cow dung ha^{-1})

I_2T_4 = (Saturated condition + 50% NPKSZn + 5 ton compost ha^{-1})

I_2T_5 = (Saturated condition + 70% NPKSZn + 3 ton compost ha^{-1})

I_2T_6 = (Saturated condition + 50% NPKSZn + 3.5 ton poultry manure ha^{-1})

I_2T_7 = (Saturated condition + 70% NPKSZn + 2.1 ton poultry manure ha^{-1})

Fertilizer application: The amounts of N, P, K, S and Zn fertilizers required per plot were calculated as per the treatments. Full amounts of TSP, MP, Gypsum and Zinc sulphate were applied as basal dose before transplanting of rice seedlings. Urea were applied in 3 equal splits: one third was applied at basal before transplanting, one third at active tillering stage (30 DAT) and the remaining one third was applied at 5 days before panicle initiation stage (55 DAT).

Organic manure incorporation: Three different types of organic manure viz. cow-dung, poultry manure and compost were used. The rates of manure as 5&3, 3.5&2.1 and 5&3 tons per ha for cow-dung, poultry manure and compost per plot were calculated as per the treatments, respectively. Cow-dung, compost and poultry manure were applied before four days of final land preparation. Chemical compositions of the manures used have been presented in Table 1.

Table 1. Chemical compositions of the cow-dung, poultry manure and compost (Oven dry basis)

Sources of organic manure	Nutrient content			
	N (%)	P (%)	K (%)	S (%)
Cow-dung	1.46	0.29	0.74	0.24
Poultry manure	2.20	1.99	0.82	0.29
Compost	1.49	0.28	1.60	0.32

Transplanting: Forty days old seedlings of BRRI dhan29 were carefully uprooted from the seedling nursery and transplanted in 18 January, 2013 in well puddle plot.

Pore water collection: Pore-water samples were collected from inner and outside the cores during boro rice growing period by using rhizon sampler (Rhizon MOM 10 cm length, 2.5 mm OD, Rhizosphere Research Products, Wageningen, and The Netherlands) during the different dates of rice growing periods. The pore-water samples were filtered through Whatman no. 42 filter paper and analyzed for N, P, K and S contents by standard method (Plate 1 and 2).

Plate 1. Rhizon Samples

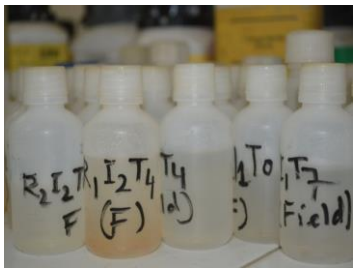

Plate 2. Pore Water Samples

Digestion of plant samples with sulphuric acid for N analysis: For the determination of nitrogen an amount of 0.5 g oven dry, ground sample were taken in a micro Kjeldahl flask. 1.1 g catalyst mixture (K_2SO_4: $CuSO_4.5H_2O$: Se in the ratio of 100: 10: 1), and 7 ml conc. H_2SO_4 were added. The flasks were heated at 160^{0}C and added 2 ml 30% H_2O_2 then heating was continued at 360 ^{0}C until the digests become clear and colorless. After cooling, the content was taken into a 50 ml volumetric flask and the volume was made up to the mark with de-ionized water. A reagent blank was prepared in a similar manner. Nitrogen in the digest was estimated by distilling the digest with 10 N NaOH followed by titration of the distillate trapped in H_3BO_3 indicator solution with 0.01N H_2SO_4 (Pequerul et. al. 1993).

Digestion of plant samples with nitric-perchloric acid for P, K and S analysis: A sub sample weighing 0.5 g was transferred into a dry, clean 100 ml digestion vessel. Ten ml of di-acid (HNO_3: $HClO_4$ in the ratio 2:1) mixture was added to the flask. After leaving for a while, the flasks were heated at a temperature slowly raised to 200^{0}C. Heating were stopped when the dense white fumes of $HClO_4$ occurred. The content of the flask were boiled until they were became clean and colorless. After cooling, the content was taken into a 100 ml volumetric flask and the volume was made up to the mark with de-ionized water. P, K and S were determined from this digest by using different standard methods.

Determination of P, K and S from plant samples

Phosphorus: Plant samples (grain and straw) were digested by di-acid (Nitric acid and Perchloric acid) mixture and P content in the digest was measured by blue color development. Phosphorus in the digest was determined by using 1 ml for grain sample and 2 ml for straw sample from 100 ml digest by developing blue color with reduction of phosphomolybdate complex and the color intensity were measured colorimetrical at 660 nm wavelength and readings were calibrated with the standard P curve (Jones, 2001).

Potassium: Ten milli-liters of digest sample for the grain and five ml for the straw were taken and diluted 50 ml volume to make desired concentration so that the flame photometer reading of samples were measured within the range of standard solutions. The concentrations were measured by using standard curves (Jones, 2001).

Sulphur: Sulphur content was determined from the digest of the plant samples (grain and straw) as described by Jones (2001). The digested S was determined by developing turbidity by adding acid seed solution (20 ppm S as K_2SO_4 in 6N HCl) and $BaCl_2$ crystals. The intensity of turbidity was measured by spectrophotometer at 420 nm wavelengths (Jones, 2001).

Statistical Analysis

The significance of the difference among the treatment means was estimated by the Duncan's Multiple Range Test (DMRT) at 5% level of probability.

Results

Effect of irrigation on the N and P concentration of pore-water during *boro* rice growing period

The higher levels of pore-water N concentrations were found inside the core where crop was not grown. There was no significant influence of irrigation on the pore-water P concentrations and higher levels of pore-water P were found in the saturated condition of rhizospheric zone of rice plant compared to continuous flooded condition (Table 2).

Table 2. Effect of Irrigation on the N and P concentrations of pore-water during *boro* rice growing period

		I_1	I_2
Nitrogen	Pore-water N conc. (ppm) in outside the core at 30 DAT	2.61	2.14
	Pore-water N conc. (ppm) in outside the core at 60 DAT	2.76	3.01
	Pore-water N conc. (ppm) into the core at 30 DAT	4.55	3.66
	Pore-water N conc. (ppm) into the core at 60 DAT	3.10	2.68
Phosphorus	Pore-water P conc. (ppm) in outside the core at 30 DAT	0.16	0.02
	Pore-water P conc. (ppm) in outside the core at 60 DAT	0.32	0.48
	Pore-water P conc. (ppm) into the core at 30 DAT	0.77	1.32
	Pore-water P conc. (ppm) into the core at 60 DAT	0.31	0.25
Potassium	Pore-water K conc. (ppm) In outside the core at 30 DAT	0.75	0.74
	Pore-water K conc. (ppm) in outside the core at 60 DAT	3.47	2.87
	Pore-water K conc. (ppm) inside the core at 30 DAT	2.85	1.48
	Pore-water K conc. (ppm) inside the core at 60 DAT	3.47	2.87
Sulphur	Pore-water S conc. (ppm) In outside the core at 30 DAT	2.60	2.19
	Pore-water S conc. (ppm) in outside the core at 60 DAT	2.86	1.91
	Pore-water S conc. (ppm) inside the core at 30 DAT	3.49	3.45
	Pore-water S conc. (ppm) inside the core at 60 DAT	2.45	2.81

Effects of fertilizer and manure on the pore-water N and P concentrations

The pore-water N, P, K and S concentrations were influenced by the application of different fertilizer treatments. The pore-water N, P, K and S concentrations in the cropped zone (outside the ring) were different from inside the core where root zone was absent. The higher pore-water P concentrations were found into the core and lower in the outside of the cores at 30 DAT and similar pore-water P concentrations were found in the pore-water of inside and outside the core at 60 DAT (Table 3).

Table 3. Effect of fertilizer and manure on the pore-water N concentration of 30 and 60 DAT

Treatments	Pore-water N conc. (ppm) outside the core		Pore-water N conc. (ppm) inside the core		Pore-water P conc. (ppm) outside the core		Pore-water P conc. (ppm) inside the core	
	at 30 DAT	at 60 DAT	at 30 DAT	at 60 DAT	at 30 DAT	at 60 DAT	at 30 DAT	at 60 DAT
T_0	1.50 c	1.56	2.68 b	2.03	0.11 c	0.30 c	0.33 d	0.08 c
T_1	2.65 ab	2.53	5.78 a	3.75	0.15 bc	0.38 abc	1.81 a	0.17 c
T_2	2.78 ab	4.29	3.28 b	3.22	0.15 bc	0.43 ab	0.66 cd	0.17 c
T_3	1.91 bc	2.80	3.85 b	2.35	0.20 a	0.38 abc	1.36 ab	0.40 b
T_4	2.35 abc	2.98	4.08 ab	2.95	0.14 bc	0.34 bc	1.34 ab	0.14 c
T_5	2.43 ab	2.65	4.09 ab	2.64	0.15 bc	0.41 abc	0.65 cd	0.16 c
T_6	2.53 ab	2.80	3.85 b	2.50	0.18 ab	0.50 a	1.14 bc	0.62 a
T_7	2.85 a	3.55	4.27 ab	3.65	0.22 a	0.45 ab	1.12 bc	0.49 b
SE (±)	0.26	0.38	0.49	0.26	0.013	0.04	0.19	0.04

in a column figures having similar letter(s) do not differ significantly whereas figures with dissimilar letter(s) differ significantly as per DMRT at 5% level of significance.

Combined effects of irrigation and fertilizer on the pore-water N and P concentration

The combined effects of different doses of fertilizer and irrigation on the pore-water N and P concentrations were significantly different (Table 4). The higher pore-water N concentrations were found into the core and outside the core at 30DAT than 60DAT. The higher levels of pore-water P concentrations were found in the pore-water samples of rice cropped area and non-cropped area where I_2T_6, I_2T_7 and I_1T_7 treatment combinations were applied (Table 4).

Table 4. Interaction effect of fertilizer and irrigation on the pore-water N d P concentration

Treatments	Pore-water N conc. (ppm) outside the core		Pore-water N conc. (ppm) inside the core		Pore-water P conc. (ppm) outside the core		Pore-water P conc. (ppm) inside the core	
	at 30 DAT	at 60 DAT	at 30 DAT	at 60 DAT	at 30 DAT	at 60 DAT	at 30 DAT	at 60 DAT
I_1T_0	2.25 bcde	1.42	3.55 abcd	2.10 def	0.11 d	0.22 f	0.20 e	0.07 d
I_1T_1	4.50 a	1.90	6.30 a	4.50 a	0.16 bcd	0.40 bcde	0.25 e	0.20 cd
I_1T_2	2.40 bcd	4.39	4.45 abcd	3.99 ab	0.16 bcd	0.44 bcd	0.59 cde	0.23 cd
I_1T_3	2.80 bcd	2.45	3.50 bcd	2.95 bcde	0.15 cd	0.31 def	0.96 bcde	0.44 b
I_1T_4	1.90 cdef	2.80	5.80 ab	2.45 cdef	0.14 cd	0.28 def	1.21 bcd	0.14 d
I_1T_5	1.55 def	3.20	3.28 cd	3.18 abcd	0.16 bcd	0.32 def	0.82 bcde	0.15 d
I_1T_6	3.10 bc	2.45	4.20 abcd	1.40 f	0.13 d	0.25 ef	0.83 bcde	0.78 a
I_1T_7	2.40 ef	3.45	4.34 abcd	4.20 ab	0.24 a	0.32 def	1.35 bcd	0.49 b
I_2T_0	0.75 f	1.70	2.80 cd	1.95 def	0.11 d	0.37 cdef	0.45 de	0.10 d
I_2T_1	0.80 f	3.15	5.25 abc	3.00 bcde	0.14 cd	0.36 cdef	3.37 a	0.14 d
I_2T_2	3.15 bc	4.20	2.10 d	2.45 cdef	0.13 d	0.42 bcde	0.73 cde	0.12 d
I_2T_3	1.03 ef	3.15	4.20 abcd	1.75 ef	0.25 a	0.45 bcd	1.76 b	0.35 bc
I_2T_4	2.80 bcd	3.15	2.35 d	3.45 abc	0.15 cd	0.40 bcde	1.48 bc	0.14 d
I_2T_5	3.30 ab	2.10	4.90 abc	2.10 def	0.15 cd	0.51 bc	0.47 de	0.18 cd
I_2T_6	1.95 cdef	3.15	3.50 bcd	3.60 abc	0.22 ab	0.75 a	1.44 bc	0.46 b
I_2T_7	3.30 ab	3.65	4.20 abcd	3.10 bcd	0.20 abc	0.57 b	0.88 bcde	0.49 b
SE (±)	0.37	NS	0.49	0.37	0.02	0.04	0.26	0.05

in a column figures having similar letter(s) do not differ significantly whereas figures with dissimilar letter(s) differ significantly as per DMRT at 5% level of significance.

Effect of irrigation on the K and S concentration of pore-water

The pore-water K and S concentrations were influenced by different irrigation management in the *boro* rice field. The higher levels of pore-water K concentrations were found inside the core where crop was not grown (Table 2).

Effects of fertilizer and manure on the pore-water K and S concentrations

The highest level of available K (4.64 ppm) in cropped area and (5.58 ppm) uncropped area were obtained from T_6 and T_7 (70% NPKSZn + 2.1 ton poultry manure/ha) treatments, respectively. The lowest pore-water K concentrations were found in the control treatment where fertilizer was not used. The similar concentrations of pore-water S were found in the root zone area (outside the core) and without cropped area (inside the core) (Table 5).

Table 5. Effect of fertilizer and manure on the pore-water K concentration of 30 and 60 DAT

Treatments	Pore-water K conc. (ppm) outside the core		Pore-water K conc. (ppm) inside the core		Pore-water S conc. (ppm) outside the core		Pore-water S conc. (ppm) inside the core	
	at 30 DAT	at 60 DAT	at 30 DAT	at 60 DAT	at 30 DAT	at 60 DAT	at 30 DAT	at 60 DAT
T_0	0.33 c	2.16 c	0.54 e	2.48 d	1.47	1.43 c	1.95 d	1.42 c
T_1	0.54 bc	2.45 c	1.69 d	4.89 ab	2.23	2.37 bc	4.19 ab	3.33 a
T_2	1.26 a	3.14 bc	1.75 d	3.78 bc	2.45	2.26 bc	2.51 d	2.40 ab
T_3	0.85 abc	3.72 ab	2.37 c	4.31 bc	2.88	2.77 ab	4.28 a	2.95 ab
T_4	0.68 bc	2.93 bc	2.17 cd	3.62 c	2.69	3.02 ab	3.53 c	2.57 ab
T_5	0.51 bc	3.25 bc	1.76 d	4.10 bc	2.46	2.07 bc	3.48 c	2.27 bc
T_6	0.79 abc	4.64 a	3.15 b	5.53 a	3.03	1.56 c	4.27 a	2.83 ab
T_7	0.98 ab	3.05 bc	3.91 a	5.58 a	1.97	3.58 a	3.57 bc	3.26 a
SE (±)	0.13	0.31	0.15	0.33	NS	0.27	0.19	0.27

in a column figures having similar letter(s) do not differ significantly whereas figures with dissimilar letter(s) differ significantly as per DMRT at 5% level of significance.

Combined effects of irrigation and fertilizer on the pore-water K and S concentrations

The pore-water K and S concentrations were significantly different due to combined application of different levels of fertilizer and irrigation. The higher pore-water K concentrations were found in the samples of inside the core compared to outside the core (Table 6). The highest pore-water K concentration of outside the core (4.71 ppm) was found in I_2T_6 (Saturated condition + 50% NPKSZn + 3.5 ton poultry manure ha^{-1}) treatment combination. The highest pore-water S concentration of outside the core (4.50 ppm) was found in I_1T_6 (Continuous flooding + 50% NPKSZn + 3.5 ton poultry manure ha^{-1}) treatment combination. The pore-water of 60 DAT of S (Table 6), outside the core (cropped area) was significantly affected by the interaction effects of irrigation and fertilizer and highest concentration of 4.58 ppm was obtained from I_1T_4 (Continuous flooding + 50% NPKSZn + 5 ton compost ha^{-1})treatment which was statistically similar with I_1T_3 and I_1T_7 and I_2T_7 treatments combinations at 30 DAT.

Table 6. Interaction effect of fertilizer and irrigation on the pore-water K and Sconcentration

Treatments	Pore-water K conc. (ppm) outside the core		Pore-water K conc. (ppm) inside the core		Pore-water S conc. (ppm) outside the core		Pore-water S conc. (ppm) inside the core	
	at 30 DAT	at 60 DAT	at 30 DAT	at 60 DAT	at 30 DAT	at 60 DAT	at 30 DAT	at 60 DAT
I_1T_0	0.36 c	1.98 e	0.68 hi	2.09	1.56	1.85 efgh	1.36 i	1.43
I_1T_1	0.64 bc	2.34 de	1.89 cdef	5.00	2.00	2.80 bcdef	2.79 fgh	2.90
I_1T_2	1.86 a	3.83 abcd	2.69 b	4.36	3.02	1.66 efgh	2.84 efgh	2.16
I_1T_3	1.04 bc	4.68 a	2.84 b	4.26	2.44	3.29 abcd	4.33 bc	2.89
I_1T_4	0.34 c	3.09 bcde	2.55 bcd	3.62	1.94	4.58 a	3.76 cde	2.91
I_1T_5	0.34 c	4.15 abc	2.31 bcde	4.36	2.56	2.68 bcdef	3.68 cdef	2.06
I_1T_6	0.64 bc	4.57 ab	4.60 a	6.38	4.50	2.37 bcdefg	4.86 ab	2.47
I_1T_7	0.78 bc	3.09 bcde	5.26 a	6.38	2.75	3.47 ab	4.30 bc	2.71
I_2T_0	0.28 c	2.34 de	0.41 i	2.87	1.38	1.02 gh	2.54 gh	1.41
I_2T_1	0.45 bc	2.55 de	1.49 fg	4.78	2.45	1.94 defgh	5.60 a	3.72
I_2T_2	0.68 bc	2.45 de	0.81 ghi	3.19	1.87	2.86 bcde	2.17 hi	2.64
I_2T_3	0.68 bc	2.77 cde	1.89 cdef	4.36	3.31	2.25 cdefg	4.23 bcd	3.02
I_2T_4	1.01 bc	2.76 cde	1.79 def	3.62	3.44	1.46 fgh	3.29 defg	2.25
I_2T_5	0.68 bc	2.34 de	1.22 fgh	3.83	2.35	1.47 fgh	3.29 defg	2.49
I_2T_6	0.95 bc	4.71 a	1.70 ef	4.68	1.56	0.76 h	3.68 cdef	3.18
I_2T_7	1.19 ab	3.02 bcde	2.57 bc	5.32	1.19	3.50 abc	2.83 efgh	3.81
SE (±)	0.18	0.44	0.21	NS	0.53	0.38	0.27	0.38

in a column figures having similar letter(s) do not differ significantly whereas figures with dissimilar letter(s) differ significantly as per DMRT at 5% level of significance.

Discussion

The experiment was conducted in the Farm of Sher-e-Bangla Agricultural University, Dhaka, Bangladesh. BRRI dhan 29 was used as the test crop in this experiment. The nutrient concentration in BRRI dhan29 rice plant was significantly affected by application of irrigation. The higher levels of grain N, K and S concentrations were recorded from I_1 (Continuous flooding) and P concentrations were recorded from I_2 (Saturated condition) treatment. The highest concentrations of grain N (1.31%), P (0.272%), K (0.195%), S (0.091%) were recorded from T_5 (70% NPKSZn + 3 ton compost ha^{-1}), T_3 (70% NPKSZn + 3 ton cow-dung ha^{-1}), T_1 (100% Recommended dose of Fertilizer), T_2 (50% NPKSZn + 5 ton cow-dung ha^{-1}), T_4 (50% NPKSZn + 5 ton compost ha^{-1}), T_7 (70% NPKSZn + 2.1 ton poultry manure ha-1) and T_2 (50% NPKSZn + 5 ton cow-dung ha^{-1}) treatment combination respectively which is supported the result of Golabi et. al. (2007). The highest concentrations of straw N (0.730%), P (0.057%), were recorded from T_2 (50% NPKSZn + 5 ton cow-dung ha^{-1}) treatment, K (1.63%) were recorded from T_3 (70% NPKSZn + 3 ton cow-dung ha^{-1}) and S (0.052%) were recorded from T_6 (50% NPKSZn + 3.5 ton poultry manure ha^{-1}) treatment as same as Palm et. al. (1997). The combined effect of fertilizer and manure significantly influenced the grain and straw N, P, K and S concentrations and higher levels grain nutrient concentrations were observed in the treatments where fertilizer plus manure more used.

Conclusion

The N, P, K and S concentrations were studied in the pore-water and the concentrations of N, P, K and S varied with the irrigation, fertilizer, cropped, without cropped areas and time in this experiment. The higher concentration of pore water N, P and K were found in the T_6 (50% NPKS + 3.5 ton poultry manure ha^{-1}) and T_7 (70% NPKSZn + 2.1 ton poultry manure per hectare) treatments where poultry manure and inorganic fertilizer were used. There was a good correlation between yield Vs Pore-water nutrient concentration and Pore-water nutrient Vs grain nutrient accumulation.

References

Beinroth, F.H., Eswaran, H., Reich, P.F., 2001. Land quality and food security in Asia. In: Response to land degradation. Bridges, E.M., Hannam, I.D. Penning de Vries, F.W.T., Scherr, S.J., Sombatpanit, S. (Eds.). Science Publishers, Enfield, USA, pp. 83-97.

Golabi, M.H., Denney, M.J., Iyekar, C., 2007. Value of composted organic wastes as an alternative to synthetic fertilizers for soil quality improvement and increased yield. *Compost Science and Utilization* 15(4): 267-271.

Jones, Jr.J.B., 2001. Laboratory guide for conducting soil tests and plant analysis. CRC Press, New York, USA. 363p.

Palm, C.A., Myers, R.J., Nandwa, S.M., 1997. Combined use of organic and inorganic nutrient sources for soil fertility maintenance and replenishment. In: Replenishing soil fertility in Africa. Buresh, R.J., Sanchez, P.A., Calhoun, F. (Eds.). Soil Science Society of America, Special Publication 51., Wisconsin, Madison, USA. pp.193-217.

Pequerul, A., Pérez, C., Madero, P., Val, J., Monge, E., 1993. A rapid wet digestion method for plant analysis. In: Optimization of Plant Nutrition. Fragoso, M.A.C., van Beusichem, M.L. Houwers , A. (Eds.). Developments in Plant and Soil Sciences, vol 53. Springer, pp. 3-6.

Rejesus, R.M., Mutuc, M.E.M., Yasar, M., Lapitan, A.V., Palis, F.G., Chi, T.T.N., 2012. Sending Vietnamese rice farmers back to school: further evidence on the impacts of farmer field schools. *Canadian Journal of Agricultural Economics* 60(3): 407-426.

Sahrawat, K.L., 1980. A rapid nondigestion method for determination of potassium in plant tissue. *Communications in Soil Science and Plant Analysis* 11(7): 753-757.

Yang, C., Yang, L., Yang, Y., Ouyang, Z., 2004. Rice root growth and nutrient uptake as influenced by organic manure in continuously and alternately flooded paddy soils. *Agricultural Water Management* 70(1): 67-81.

Eurasian J Soil Sci 2019, 8 (4) 289 - 297

Eurasian Journal of Soil Science

Journal homepage : http://ejss.fesss.org

Soil moisture adsorption capacity and specific surface area in relation to water vapor pressure in arid and tropical soils

Abdelmonem Mohamed Amer *

Department of Soil Science, Faculty of Agriculture, Menoufia University, 32511 Shebin El-Kom, Egypt

Abstract

This study is devoted to predict water vapour adsorption and hydro-physical properties of arid soils in middle Nile Delta (Farm of the Faculty of Agriculture, Shebin El-Kom, Egypt) and of tropical soils (Felix and INIAP Farms) in Quevedo zone, Los Rios, Ecuador. The vapour pressure and isothermal adsorption of water vapour is used to predict soil moisture adsorption capacity (*Wa*) and the specific surface area. To achieve these objectives, four soil profiles at different depths were investigated to indicate the status of hydro-physical properties of the studied area. The 1st & 2nd profiles are sandy loam (Felix Farm) and clay loam soils (Shebin El-Kom Farm), and 3rd & 4th are clay soils (INIAP Farm). Data of soil-water adsorption (W%) at different relative vapor pressures P/Po are obtained for the studied soil profiles, where the W% values increased with increasing P/Po from 1.87% to 10.01% in the 1st and 2nd sandy loam and clay loam soil profiles, and reached 27.44% in the 4th clay soil profile. The highest values of water adsorption capacity (*Wa*) were observed in the clay depths of 60 – 90 cm and 90 – 120 cm (INIAP-soil profiles) while the lowest values were in the subsurface depth (30 – 60 cm) of soil profiles 1st and 2nd. The other hygro-physical properties such as adsorbed layers and maximum hygroscopic water were obtained. The specific surface area (*S*) in sandy loam 1st&2nd soil profiles is ranged from 113m^2/g to 187m^2/g and raised to 385m^2/g and 553m^2/g in the 3rd & 4th clay soil profiles. The corresponded values of the external specific surface area (*Se*) ranged from 42m^2/g to 98m^2/g and 74 m^2/g to 252 m^2/g respectively. Two equations were assumed (1) to predict P/Po at water adsorption capacity (*Wa*), and (2) to apply *Wa* in prediction of soil moisture retention i.e., ψ(W) function at pF < 4.5.

Keywords: Water adsorption capacity, vapor pressure isotherm, soil hydro-physical properties, specific surface area, arid and tropical soils.

Article Info

Received : 11.12.2018
Accepted : 18.06.2019

Introduction

Agricultural and irrigation management practices, is largely depend on a timely and accurate characterization of temporal and spatial soil moisture dynamics in the root zone (Han, 2011). Consequently, measurements and detailed information about soil water sorption, water content and behavior are required. In that connection, water vapor adsorption is an important phenomenon in particular in drying periods in tropical soils as well as in arid and semi-arid regions (Amer, 2014) at which the high temperature and dry weather supports to more evapo-transpiration. Water vapor either reaches the soil from the atmosphere or is formed in the soil by the evaporation of water. The migration of water vapor in soil depends not only on the difference of vapor pressure in different sites but also on the capacity of soil particles surfaces to attract and absorb the molecules of vapor. A gain of water in the soil surface layer, not caused by rainfall or irrigation, can be caused by dew deposition or vapor adsorption. Dew deposition is a phenomenon recorded for most soil and climate types (Jacobs et al., 1999). It occurs during the night when dew point is reached, and it results in a discernible wetting of the surface.

* Corresponding author.
Department of Soil Science, Faculty of Agriculture, Menoufia University, 32511 Shebin El-Kom, Egypt
Tel.: +2050 2337480 E-mail address: amer_abdel@hotmail.com
e-ISSN: 2147-4249 DOI: 10.18393/ejss.580889

Under the right atmospheric and soil surface conditions, water is adsorbed from the atmosphere by a thin layer of top soil, generally during the afternoon and evening. The amounts of adsorbed water can be considerable up to 70% of daily evaporation (Kosmas et al. 1998, 2001; Agam and Berliner, 2004). Therefore, quantifying adsorption is important for agricultural water management, surface energy balance studies, ecological studies (Levy and Mamedov, 2002), and remote sensing investigations (changes in surface soil moisture content will affect land surface properties such as albedo, emissivity, and thermal inertia).

The objective of this work is devoted to study the isothermal adsorption of water vapour at different vapour pressures as applied to predict soil-water adsorption capacity, specific surface area, and hygro-physical properties in semiarid soils in the Nile Delta (Egypt) and in the tropical soils of Quevedo region-Los Rios Provence, Ecuador.

Material and Methods

Four soil profiles differ in their particles size distribution, salinity, and $CaCO_3$% were done in arid and tropical zones. Three tropical soil profiles (I, III, IV) were selected at different distances to Quevedo city, to represent the Quevedo region of the Los Rios Province, Ecuador. The investigated soils were cultivated mainly with Cacao, Banana and Corn crops. The arid soil profile No. II was taken from the Farm of Faculty of Agriculture, Menoufia University, Shebin El-Kom, (located at the Middle of the Nile Delta), Egypt. The profiles of Quevedo area is elevated 74m (243ft) above sea level and located at coordinates 1°20'30'' de latitude south and 79°28'30'' de longitude occidental, dentro de una zona subtropical (Figure 1). The first profile (I) was taken from the Felix Farm, which is located as far as 30 km from Quevedo city and cultivated with Cacao trees. The third and fourth profiles were taken from the INIAP Experimental Farms, Pichilingue, which located at 6 km to Quevedo. They were cultivated with Cacao and Corn crops respectively.

Disturbed and undisturbed soil samples were taken at depths, 0 – 30 cm, 30-60 cm, 60 - 90 cm for the first and second profiles, and 0 – 30 cm, 30 - 60 cm, 60 - 90 cm, 90 - 110 cm and 110 - 130 cm for the third profile and 0 – 30 cm, 30 - 60 cm, 60-90 cm, and 90 - 120 cm for the fourth one. The disturbed soil samples were air dried, gently crushed and sieved through a 2 mm sieve. Fractions below 2 mm were subjected to chemical and mechanical analysis in the laboratory. Soil texture (particle size distribution) was determined using the pipette method. The textural grade was assessed by texture triangle.

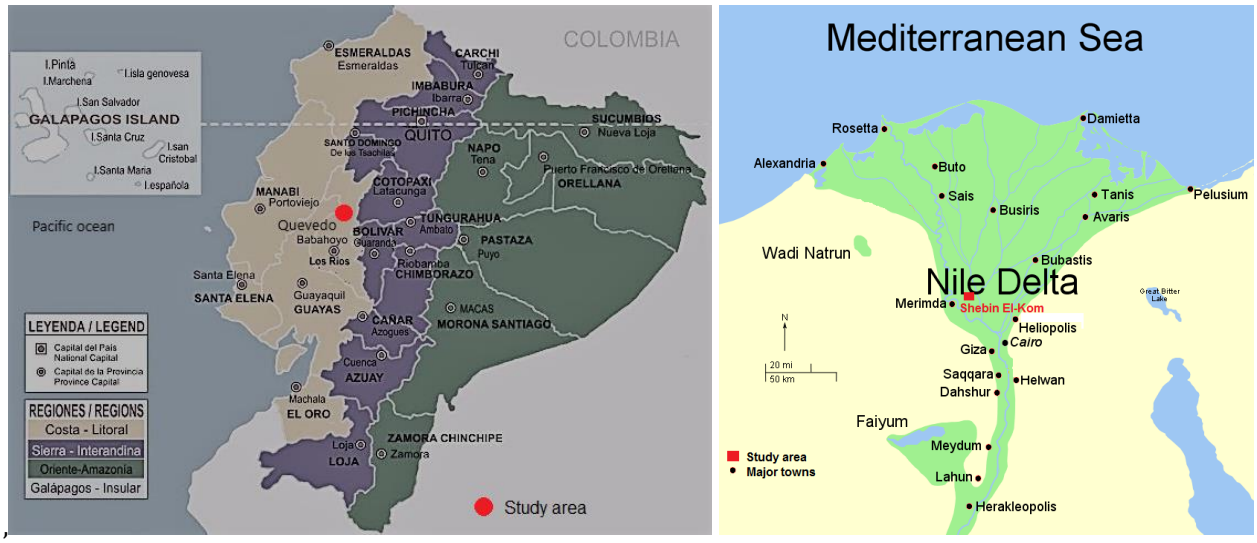

Figure1. Study areas (red color) in Los Rios province, Quevedo, Ecuador and in Nile Delta, Shebin El-Kom, Menoufia, Egypt

Physical and chemical analyses of the studied soils such as maximum hygroscopic water (*MH*), Particle size distribution %, EC, OM, $CaCO_3$% are determined according to Black et al. (1965) and Klute (1986). These analyses are shown in Tables 1 and 2.

Table 1. Particle size distribution of the studied soils

Profile Number & Soil location	Coarse Sand, %	Fine Sand, %	Silt, %	Clay, %	Texture Class
I- Felix Farm	38.50	20.50	24.10	16.90	Sandy Loam
II- Shebin El-Kom	15.76	18.35	27.32	38.57	Clay Loam
III-INIAP-Cacao Field	1.98	16.42	36.78	44.82	Clay
IV-INIAP-Corn Field	3.15	14.40	33.86	48.59	Clay

Table 2. Chemical analysis (mean values) of the studied soil profiles.

Chemical propertties	Felix Farm	Shebin El-Kom Farm	INIAP-Cacao Field	INIAP-Corn Field
pH	6.82	6.85	7.24	6.91
EC (dS/m)	0.73	1.24	1.10	1.96
Ca^{2+}	1.35	2.67	4.80	6.24
Mg^{2+}	1.40	2.23	1.92	2.88
Na^{+}	1.42	3.54	3.98	9.24
K^{+}	0.13	0.39	0.48	1.48
CO_3^{2-}	-	-	-	-
HCO_3^{-}	3.40	3.93	2.25	2.85
Cl^{-}	0.75	3.65	6.00	13.52
SO_4^{2-}	0.15	1.25	1.93	2.47
SAR	1.21	2.26	2.17	4.32
$CaCO_3$ (%)	1.12	3.42	0.43	0.34
OM (%)	1.38	2.21	2.72	2.99

Water vapour adsorption isotherms

The water vapour adsorption isotherm on dried soils is determined gravimetrically using saturated salt solutions such as $ZnCl_2$, $CaCl_2$, K_2CO_3, NH_4NO_3, KCl and K_2SO_4 whereas the corresponding P/Po values to these solutions at 20°C are 0.10, 0.35, 0.45, 0.65, 0.85 and 0.98 (Amer, 2009).

Matric suction at water vapour pressures

The soil matric suction values resulting from equilibrating the soil samples with salt solutions can be calculated using the pF formula:

$$pF = 6.502 + \log [2 - \log H] \quad (1)$$

where, pF = soil suction, expressed as the common logarithm of the suction (ψ) in cm of water, H is the relative humidity (H= P/Po x 100), and Relative water vapour pressure (P/Po) [P being the actual water vapour pressure on the sample particles and Po being the saturation vapour pressure of water at 20°C] were obtained by applying different appropriate salt solutions.

Moisture adsorption capacity

The property of moisture adsorption capacity (Wa) can be introduced as the critical limit between adsorbed and absorbed wetting films (pellicles) of soil moisture content (Amer, 2003), as well as corresponds to capillary condensation. So, the Wa values can be also derived from soil moisture retention curve at log (ψc) where ψc is the capillary condensation attitude.

Amer (1982, 1993) proved that the moisture adsorption capacity (Wa) is equal to three layers of adsorbed water as follows: $Wa = Wm + 2Wme$, where Wm is the moisture of the soil when water vapour adsorbed for monolayer, and Wme is the external mono-adsorbed layer of soil moisture content.

However, the moisture adsorption capacity (Wa), maximum hygroscopic water (MH) the specific surface area (S), and particle size composition are the most important indices characterizing the hydro-physical, physicochemical and heat properties of soil. Moreover, these parameters are inter-related, therefore the value of any of them can be obtained from the data of the other parameters.

Estimating Wm and Wme for predicting the moisture adsorption capacity and surface area

The relation between relative vapour pressure (P/Po) and moisture content ($W\%$) is experimental obtained by maintaining a soil sample in isothermal equilibrium with an atmosphere of water vapour as mentioned above.

The BET method (Brunauer et al., 1938) as modified and described by Orchiston (1954), Quirk (1955), Farrar (1963) and Globus (1996), was applied to predict the Wm and Wme, which they in turn were used to determine moisture adsorption capacity (Wa) and the total, external and internal specific surface areas (S, Se and Si).

Results and Discussion

BET theory as applied for adsorption isotherms

Brunauer et al. (1938), derived what has come to be known as the BET equation, based on multilayer adsorption theory. In BET theory, the explanation proposed for sigmoid type isotherm is that the adsorption in multi-molecular layers on the surface rather than a monomolecular one. Farrar (1963) and Amer (1982, 1993, 2009) used the water vapour adsorption isotherm method by applying BET theory based on the

assumption that the isotherm is made up of monolayer physical adsorption combined with capillary condensation as follows:

$$P/V(P_o\text{-}P) = (1/V_m\, C) + (C\text{-}1)\, P/V_m\, C\, P_o \quad (2)$$

Where, V is the volume of gas adsorbed at pressure P, V_m is the volume of a single layer of adsorbed molecules over the entire surface of the adsorbent (soil particles). P_o is the gas pressure required for monolayer saturation at the temperature of the experiment, and C is a constant for the particular gas, adsorbent, and temperature,

$$C = exp\, E_1\text{-}\, E_L / RT \quad (3)$$

whereas, E_1 is adsorption heat of the water adsorbed layer, E_L is condensation adsorption heat.

In this work we obtained experimentally and gravimetrically the relationship between relative vapour pressure (*P/Po*) and adsorbed moisture content, W% (wetting films) on soil particles which depending on the thermodynamic of adsorption of water vapor through the soil. Data for water vapor adsorption at *P/Po*; 0.10, 0.35, 0.45, 0.65, 0.85, and 0.98 for the studied soils are presented in Table 3. It is evident that the W% at different values of *P/Po* was higher in both clay soil profiles (III & IV) of INIAP Farms –in particular in the deeper depths (60-90 cm and 90-120 cm) of the 4th soil profile- than in the other two sandy loam and clay loam soils (1st & 2nd profiles).

Table 3. Water adsorption (*W%*) in the studied soils at different vapor pressures (*P/Po*).

Soil location & Profile number		Soil Depth, cm	*P/Po* Soil water content,%	0.10	0.35	0.45	0.65	0.85	0.98 (MH)
				Soil water adsorption					
		0 - 30	10.285	1.918	4.469	5.020	5.489	5.590	7.640
Felix Farm	I	30 - 60	8.359	1.874	4.241	4.790	5.031	5.372	6.955
		60 - 90	20.540	2.679	6.527	7.068	7.592	8.061	10.01
		0 - 30	19.120	2.689	6.423	6.980	7.322	7.873	9.878
Shebin El-Kom	II	30 -60	11.855	1.748	4.387	4.927	5.386	5.520	7.267
		60 - 90	15.135	1.887	4.844	5.388	5.656	6.165	8.012
		0 - 30	11.579	2.663	6.613	7.160	7.722	8.232	10.130
INIAP-Cacao		30 - 60	14.731	2.564	9.332	9.789	10.867	12.259	13.959
Field	III	60 - 90	30.252	2.974	10.470	10.920	11.458	13.604	15.521
		90 - 110	23.616	2.747	8.865	9.410	10.075	11.050	12.988
		110 - 130	17.063	3.864	10.044	10.587	11.532	12.611	14.720
		0 - 30	9.176	2.676	6.364	6.916	7.477	8.104	10.233
INIAP-Corn	IV	30 - 60	9.180	2.675	10.325	10.797	11.920	13.640	15.702
Field		60 - 90	17.198	3.879	15.504	16.050	18.131	20.005	22.647
		90 - 120	20.434	3.981	17.945	18.486	22.265	24.122	27.446

The W% values increased with increasing P/Po from 1.87% to 10.01% in the 1st soil profile of sandy loam soil, and from 1.75% to 9.88% in the 2nd clay loam profile. In clay soils, the increasing of W% values was from 2.56% to 15.52% in the 3rd soil profile, while it was more evident in the 4th profile where the increasing was from 2.67% to 27.44%. The clay content, mineralogical composition and salinity are the major factors that governed the absorbed water in the soils under investigation (Amer, 2009).

Solution of the BET equation for obtaining mono-adsorbed layers (*W*m & *W*me)

The BET equation can be applied in the following form using the gravimetric of a single layer of adsorbed molecules over the entire surface of the soil particles (Amer, 2009):

$$\frac{P}{W(Po-P)} = \frac{1}{WmC} + \frac{C-1}{WmC} \cdot \frac{P}{Po} \quad (4)$$

where *W*m is the moisture content when the soil surface is completely covered by a mono-molecular layer of water. *C* is a function of the state of the first adsorbed molecular layer of water and soil particles surface condition. *W* is adsorbed soil moisture content (%) equilibrated with *P/Po*, whereas P and *P*o are the actual and saturated water vapor pressures. By plotting P/W (*P*o–*P*) as ordinate versus *P/Po* at the segment 0 – 0.40 of the sorption isotherm as abscissa, a straight line would be obtained. The intercept on the y-axis is then $1/W_mC$ and the slope is $C - 1/W_mC$. Hence W_m and C can be determined.

Data for solution of BET equation are presented in Tables (4 and 5). From these data and linear equations, we can obtain W% at any P/Po values by using the next formula:

$$W = \frac{\frac{P}{Po}}{\left[1-\frac{P}{Po}\right]\left[\frac{1}{WmC}+\frac{C-1}{WmC}.\frac{P}{Po}\right]} \quad (5)$$

To determine W_{me} the BET equation (4) can be developed with some assumptions to the next form:

$$W = \frac{Wme}{\left[1 - Ke\frac{P}{Po}\right]}.\frac{Ce}{Ce + \frac{Po}{P} - Ke} + Wi \quad (6)$$

At high relative water vapor pressures, the amount Ce / (Ce + Po/P – Ke) is equal unit (Farrar, 1963), and then the equation (6) becomes (Amer, 2015):

$$W = \frac{Wme}{\left[1 - Ke\frac{P}{Po}\right]} + Wi \quad (7)$$

where the suffixes (e) and (i) refer to the external and internal surfaces respectively. The values of K_e in the indicated P/*P*o range were stated by Farrar (1963) as 0.9±0.01, but practically, it seems that K_e is an arbitrary coefficient ranged from 0.70 to 0.90 (Amer 1982, 2009). Equation (7) can be represented in linear equation; y = mx + c where y = W, m = W_{me} , x = 1 / 1 – K_e P/Po , and c = Wi, so W_{me} can be obtained graphically as the intercept on the y – axis.

Values of *Wm* and *Wme* are calculated for the studied soils as in Table 6. It is found that the highest values of *Wm* and *Wme* were in the deeper depths of the clay soils (INIAP farms) in particular the depths of 60 – 90 cm and 90 – 120 cm of INIAP crop field (profile IV).

Table 4. Using Equation (5) in solution of the BET equation for sandy loam and clay loam soil profiles (I and II)

Soil location	Soil Depth, cm	*P/Po*	0.10	0.20	0.30	0.35	*C*	Linear & adsorption equations
I Felix Farm	0 - 30	W%	1.920	3.200	4.050	4.470	7.472	P/W(Po-P)=0.036+0.233P/Po
		W(1-P/Po)	1.728	2.560	2.835	2.905		$W\% = \frac{\frac{P}{Po}}{\left[1-\frac{P}{Po}\right][0.036 + 0.233\frac{P}{Po}]}$
		P/W(Po-P)	0.058	0.078	0.106	0.120		
	30 -60	W%	1.874	3.000	3.800	4.241	10.238	P/W(Po-P)=0.03+0.277P/Po
		W(1-P/Po)	1.687	2.400	2.660	2.758		$W\% = \frac{\frac{P}{Po}}{\left[1-\frac{P}{Po}\right][0.03 + 0.277\frac{P}{Po}]}$
		P/W(Po-P)	0.059	0.083	0.113	0.127		
	60 - 90	W%	2.679	4.500	5.800	6.527	8.391	P/W(Po-P)=0.023+0.17P/Po
		W(1-P/Po)	2.411	3.600	4.060	4.243		$W\% = \frac{\frac{P}{Po}}{\left[1-\frac{P}{Po}\right][0.023 + 0.17\frac{P}{Po}]}$
		P/W(Po-P)	0.042	0.056	0.074	0.083		
II Shebin El-Kom	0 - 30	W%	2.689	4.480	5.750	6.423	10.548	P/W(Po-P)=0.019+0.1814P/Po
		W(1-P/Po)	2.420	3.584	4.025	4.175		$W\% = \frac{\frac{P}{Po}}{\left[1-\frac{P}{Po}\right][0.019 + 0.1814\frac{P}{Po}]}$
		P/W(Po-P)	0.037	0.055	0.074	0.083		
	30 - 60	W%	1.748	2.650	3.300	4.387	13.258	P/W(Po-P)=0.024+0.2942P/Po
		W(1-P/Po)	1.573	2.120	2.310	2.851		$W\% = \frac{\frac{P}{Po}}{\left[1-\frac{P}{Po}\right][0.024 + 0.2942\frac{P}{Po}]}$
		P/W(Po-P)	0.064	0.094	0.129	0.126		
	60 - 90	W%	1.887	3.400	4.560	4.844	11.324	P/W(Po-P)=0.03+0.2771P/Po
		W(1-P/Po)	1.698	2.720	3.192	3.149		$W\% = \frac{\frac{P}{Po}}{\left[1-\frac{P}{Po}\right][0.03 + 0.277\frac{P}{Po}]}$
		P/W(Po-P)	0.059	0.074	0.940	0.111		

Soil specific surface area

The specific surface of the adsorbent (soil) can be calculated by determining the number of molecules (volumetrically or gravimetrically) and multiplying this by the cross- sectional area of the molecules. Assuming that a single water molecule occupies some constant area on the sorbent surface (usually taken as 10.8 ˚A^2), the total specific surface area (S) of the soil then calculated as S = 36.16 W_m m^2/g.

Table 5. Using Equation (5) in solution of the BET equation for clay tropical soil profiles (III and IV).

Soil location	Soil Depth, cm	*P/Po*	0.10	0.20	0.30	0.35	*C*	Linear & adsorption equations
III INIAP-Cacao Field	0 - 30	W%	2.663	4.380	5.750	6.613	7.446	P/W(Po-P)=0.025+0.1611P/Po $W\% = \frac{\frac{P}{Po}}{\left[1-\frac{P}{Po}\right][0.025+0.1611\frac{P}{Po}]}$
		W(1-P/Po)	2.397	3.504	4.025	4.298		
		P/W(Po-P)	0.042	0.057	0.075	0.081		
	30 -60	W%	2.564	5.500	8.120	9.330	3.638	P/W(Po-P)=0.03+0.0791P/Po $W\% = \frac{\frac{P}{Po}}{\left[1-\frac{P}{Po}\right][0.03+0.0791\frac{P}{Po}]}$
		W(1-P/Po)	2.307	4.400	5.684	6.065		
		P/W(Po-P)	0.043	0.046	0.053	0.058		
	60 - 90	W%	2.974	6.740	9.200	10.470	5.486	P/W(Po-P)=0.02+0.0897P/Po $W\% = \frac{\frac{P}{Po}}{\left[1-\frac{P}{Po}\right][0.02+0.0897\frac{P}{Po}]}$
		W(1-P/Po)	2.677	5.392	6.440	6.806		
		P/W(Po-P)	0.037	0.037	0.047	0.051		
	90 - 110	W%	2.747	5.000	6.600	8.865	5.060	P/W(Po-P)=0.028+0.1157P/Po $W\% = \frac{\frac{P}{Po}}{\left[1-\frac{P}{Po}\right][0.028+0.1157\frac{P}{Po}]}$
		W(1-P/Po)	2.472	4.000	4.620	5.762		
		P/W(Po-P)	0.040	0.050	0.064	0.061		
	110 - 130	W%	3.864	6.200	8.510	10.044	2.929	P/W(Po-P)=0.032+0.0617P/Po $W\% = \frac{\frac{P}{Po}}{\left[1-\frac{P}{Po}\right][0.032+0.0617\frac{P}{Po}]}$
		W(1-P/Po)	3.478	4.960	5.957	6.529		
		P/W(Po-P)	0.029	0.403	0.050	0.054		
IV INIAP-Corn Field	0 - 30	W%	2.680	4.120	5.500	6.364	5.937	P/W(Po-P)=0.022+0.1864P/Po $W\% = \frac{\frac{P}{Po}}{\left[1-\frac{P}{Po}\right][0.022+0.1864\frac{P}{Po}]}$
		W(1-P/Po)	2.408	3.296	3.850	4.137		
		P/W(Po-P)	0.042	0.061	0.078	0.085		
	30 - 60	W%	2.675	5.880	8.750	10.325	3.245	P/W(Po-P)=0.029+0.0655P/Po $W\% = \frac{\frac{P}{Po}}{\left[1-\frac{P}{Po}\right][0.029+0.0655\frac{P}{Po}]}$
		W(1-P/Po)	2.408	4.704	6.125	6.711		
		P/W(Po-P)	0.042	0.043	0.049	0.052		
	60 - 90	W%	3.879	10.000	13.800	15.504	6.481	P/W(Po-P)=0.012+0.0652P/Po $W\% = \frac{\frac{P}{Po}}{\left[1-\frac{P}{Po}\right][0.012+0.0652\frac{P}{Po}]}$
		W(1-P/Po)	3.491	8.000	9.660	10.078		
		P/W(Po-P)	0.029	0.025	0.031	0.035		
	90 - 120	W%	3.981	11.500	16.320	17.945	5.937	P/W(Po-P)=0.011+0.0543P/Po $W\% = \frac{\frac{P}{Po}}{\left[1-\frac{P}{Po}\right][0.011+0.0543\frac{P}{Po}]}$
		W(1-P/Po)	3.583	9.200	11.424	11.664		
		P/W(Po-P)	0.028	0.022	0.026	0.030		

Data in Table 6, which based upon the water vapor adsorption isotherms show that the specific surface area (*S*) in the light textured soils ranged from 117 m^2/g to 187 m^2/g in the first profile and from 113 m^2/g to 180 m^2/g in the second profile. In clay tropical soils, the S values were from194 m^2/g to 385m^2/g in the third profile and from 173 m^2/g to 553 m^2/g in the fourth profile. Farrar (1963) deduced the soil external specific surface area (*Se*) by applying the relation (6) over the range of high relative vapor pressure (0.5 < P/*Po* > 0.8). However, the internal specific surface area (*Si*) may be calculated by the difference between *S* and *Se*.

The corresponding values of *Se* (Table 6) were 46 m^2/g to 98 m^2/g and 42 m^2/g to 93 m^2/g in the 1st and 2nd soil profiles and from 77m^2/g to 165m^2/g and 74 m^2/g to 252 m^2/g in clay soil profiles. Regarding the internal specific surface area (*Si*), it was found in loam soils that *Si* values are higher than *Se* in the surface (0 – 30 cm) and subsurface (30 – 60 cm) depths of the 1st profile (Felix farm), while the same observation was in the depths 30 – 60cm and 60 – 90cm of the 2nd profile (dry soil). In clay soils (INIAP farms) the *Si* values were higher than *Se* in all depths of the 3rd and 4th profiles. The results reflect different due to the difference of the investigated soils in their texture, clay content%, $CaCO_3$, salinity and mineralogical composition (El-Sharkawy, 1994; El-Fiky, 2002). However, the specific surface area is closely related to the physicochemical soil properties (Nerpin and Chudnovski, 1975), which is refer to the absence or presence of internal pores.

Whatever, the *Se*/*Si* ratio was less than unit in most depths of sandy loam soils and in all depths of the clay soils indicating that the *Si* values were higher than *Se* in most investigated tropical soils (Table 6). This result may refer to the mineralogical composition of these soils (Figure 2), whereas the montmorillonite, ferrous and hydrous mica are the prevailing minerals in the tropical soils as well as in the clay alluvial arid soils of the Nile Delta (El-Gabaly and Khadr, 1962).

Table 6. Water adsorption capacity (*Wa*), adsorbed layers (*Wm* & *Wme*) and specific surface area (*S, Se & Si*) of the studied soils.

Soil location	Soil Depth, cm	*Wm*	*Wme*	*Wc*	*Wa*	$[P/Po]_{wa}$	*S*,m^2/g	*Se*,m^2/g	*Si*, m^2/g	*Se/Si*	*Wa/S*
I	0 - 30	3.717	1.624	5.341	6.965	0.4662	134.430	58.72	75.710	0.775	0.0518
Felix	30 -60	3.256	1.274	4.530	5.804	0.4388	117.730	46.06	71.67 0	0.642	0.0493
Farm	60 - 90	5.181	2.735	7.916	10.651	0.5135	187.350	98.89	88.460	1.117	0.0568
II	0 - 30	4.989	2.581	7.570	10.151	0.5084	180.41	93.32	87.090	1.071	0.0562
Shebin	30 -60	3.143	1.188	4.331	5.519	0.4306	113.64	42.95	70.690	0.607	0.0485
El-Kom	60 - 90	3.222	1.248	4.470	5.718	0.4305	116.50	45.12	71.380	0.632	0.0491
III	0 - 30	5.372	2.148	7.520	9.668	0.4442	194.25	77.67	116.58	0.666	0.0497
INIAP-	30 -60	9.160	3.964	13.124	17.088	0.4636	331.30	143.34	187.960	0.762	0.0515
Cacao	60 - 90	9.115	4.240	13.355	17.595	0.4819	329.58	153.32	176.260	0.869	0.0533
Field	90 - 110	6.934	2.773	9.707	12.480	0.4424	250.74	100.27	150.470	0.666	0.0498
	110 - 130	10.670	4.568	15.238	19.806	0.4612	385.85	165.18	220.670	0.748	0.0513
IV	0 - 30	4.798	2.067	6.865	8.932	0.4628	173.51	74.74	98.770	0.756	0.0515
INIAP-	30 -60	10.550	4.542	15.092	19.634	0.4610	381.54	164.23	217.310	0.755	0.0514
Corn	60 - 90	12.965	5.837	18.802	24.639	0.4743	468.82	211.06	257.760	0.818	0.0525
Field	90 - 120	15.310	6.981	22.291	29.272	0.4768	553.63	252.43	301.190	0.838	0.0529


Figure 2. Clay soil samples were taken at depth >90 cm from INIAP research station- Pichilingue, Ecuador ~containing ferrous and ferric minerals with the highest values of surface area and water adsorption capacity (Amer, 2015).

Soil moisture adsorption capacity

Due to the soil – water adsorption capacity (*Wa*) is obeyed the mono-adsorbed layers (*Wm & Wme*) values (whereas, *Wa = Wm + 2Wme*), so it could be correlated with specific surface area. The *Wa/S* ratio was 0.0486 – 0.0568 for all the studied soils (Table 6). The values of *Wa* are the highest in the same deep depths, whereas *Wa* values in INIAP-profile IV reached 24.64% and 29.27% in the depths of 60 – 90 cm and 90 – 120 cm respectively, while reached 19.81% in the depth of 110 – 130 cm in the INIAP- profile III (Table 6). The high values of soil water adsorption capacity in the studied clay soils showed the importance of water adsorption phenomena in tropical soils.

The *Wa* values in the surface depth (0-30 cm) ranged from 6.97% to 10.15% in both sandy loam and clay loam soils under investigation. The lowest values for *Wa* were observed in the subsurface depth (30 – 60 cm) in soils profiles I and II, where, the *Wa* values were 5.80% and 5.52%, but increased to 17.09% and 19.63 in subsurface depth (30-60 cm) of the clay soil profiles III and IV respectively. This is indicated the significance of the soil texture and clay fraction content which play an important role in soil moisture content and its distribution along the soil profile depth. In general, high clay content in soil means increasing the soil moisture content & retention and water adsorption capacity. The same trend was ordinary observed with the other hygroscopic parameters such as boundary moisture films (*Wc*) and maximum hygroscopic water (*MH*). Hygroscopic water exists as a very thin film at the solid-liquid interfaces of the soil particles. At the maximum hygroscopic water (*MH*) the surface of soil particles is almost completely covered with individual molecules of water. However, It is known that the maximum hygroscopic water (*MH*) is determined practically at P/Po = 0.98. So, data in Table 3 indicate that the *MH* values (at *P/Po* = 0.98) are ranged from 6.95% –10.01% in soil profiles I & II, and from 10.13% – 27.44%, for the clay soils (profiles III &

IV). It is clear that the hygro-physical properties (*Wm, Wme, W*c, *W*a and *MH*) of the investigated soils are followed the same trend that observed in turn with the specific surface areas (*S* and *Se*).

Predict of P/Po at water adsorption capacity (Wa)

At higher water vapor pressure (*P*), the equation (4) can be developed to predict the vapor pressure *P/Po* at water adsorption capacity *Wa* as follows:

$$\frac{\frac{P}{Po}}{w(1-\frac{P}{Po})} = A + \mathrm{B}\frac{P}{Po} \quad (8)$$

Where, A = 1/WmC, and B = C-1/WmC

From equation (8) and at Po/P ≈ 1;

$$\mathrm{W}\ (1 - \mathrm{P/Po}) = 1/\ (\mathrm{A} + \mathrm{B}) \quad (9)$$

Then at Wa;

$$[\mathrm{P/Po}]_{wa} = 1 - [\mathrm{Wa}\ (\mathrm{A} + \mathrm{B})]^{-1} \quad (10)$$

Data in table (6) show that the relative vapor pressure $[P/Po]_{wa}$ at *Wa* is ranged between 0.43 to 0.51, indicating that at this range of P/Po the soil moisture reach water *adsorption* capacity. Above this range (P/Po > 0.51) the *absorption* process is prevailing, at which soil matric suction (ψ) values can be calculated using equation (1); pF = 6.502+log [2 – log P/P_o]. The ψ values expressed in pF at adsorption and absorption processes are ranged from 4.5 to 7.0. On the other hand, it may of interest to apply the water adsorption capacity (*Wa*) to predict soil moisture retention function ψ(W) at pF < 4.5 using the following suggested equation:

$$\Psi\mathrm{i} = \psi\mathrm{a}\ (W\mathrm{i} - W\mathrm{c}/W\mathrm{me})^{-n} \quad (11)$$

where *ψ*i and *ψ*a are capillary–sorption potentials at soil water content (*W*i) and moisture adsorption capacity (*W*a), respectively, and *n* is a constant. The decrease in soil water suction is associated with increasing thickness of the hydration envelopes covering the soil particles surfaces (Amer, 2009).

Conclusion

Soil-water adsorption W% values increased with increasing P/Po from 1.87% to 10.01% in the 1st and 2nd sandy loam and clay loam soil profiles, and reached 27.44% in the 4th clay tropical soil profile. The values of mono adsorbed layers (*Wm & Wme*), boundary moisture films (*Wc*), maximum hygroscopic water (*MH*), water adsorption capacity (*Wa*) and specific surface area (*S*), external (*Se*), internal (*Si*) of the tropical soils in the Quevedo region area (Ecuador) and in semiarid region of the Nile Delta (Egypt) are obtained experimentally.

Water adsorption capacity (*Wa*) is corresponding to P/Po = 0.43 – 0.51 for all soils under investigation. The absorption process is prevailing above this range.

The highest values of water adsorption capacity (*Wa*) were observed in the clay depths of 60 – 90 cm and 90 – 120 cm (INIAP-soil profiles) while the lowest values were in the subsurface depth (30 – 60 cm) of soil profiles 1st and 2nd. The specific surface area (*S*) in sandy loam & clay loam (1st & 2nd tropical and arid soil profiles) is ranged from 113m²/g to 187m²/g and raised to 385m²/g and 553m²/g in the 3rd & 4th clay tropical soil profiles. The corresponded values of the external specific surface area (*Se*) ranged from 42m²/g to 98m²/g and 74 m²/g to 252 m²/g respectively.

The internal specific surface area (Si) values were higher than the external specific surface area (Se) in all depths of the clay soil profiles, while they were higher than Se in sandy loam and clay loam soils only in the subsurface (30 – 60 cm) depth.

The results of specific surface area (*S, Se, Si*), mono adsorbed layers (*Wm & Wme*), water adsorption capacity (*Wa*) reflect different due to the texture and mineralogical composition of the investigated soils.

Clay soils at depth >90 cm in the farms of INIAP research station-Pichilingue, are containing ferrous and ferric minerals with the highest surface area and water adsorption capacity.

Results of soil water adsorption capacity show the significance of water adsorption capacity for moisture plant root zone – in particular- in clay soils.

Two new equations were assumed (1) to predict P/Po at water adsorption capacity (*Wa*), and (2) to predict the soil moisture retention function ψ(W) at pF < 4.5, depending on the water adsorption capacity *Wa*.

Acknowledgement

I am pleased to have the Prometheus Scholarship of the SENESCYT Prometeo Project of Ecuador during 2013/2014. The laboratorial support of SENESCYT for this work is acknowledged.

References

Agam, N., Berliner, P.R., 2004. Diurnal water content changes in the bare soil of a coastal desert. *Journal of Hydrometeorology* 5: 922–933.

Amer, A.M., 1982. Effect of the overburden pressure on the capillary sorption potential of water in swelling soils. PhD Thesis, Faculty of Soil Science, Lomosonov Moscow State University, Moscow, Russia. [in Russian].

Amer, A.M., 1993. Surface area measurements as related to water vapour adsorption in arid soils of Egypt. Proceedings of the IV International Conference on Desert Development. 25-30 July, Mexico City, Mexico. pp. 619–627.

Amer, A.M., 2003. Soil hydro-physics. First Part, Al-Dar Al-Arabia for Publishing Cairo, Egypt. 452p. [in Arabic].

Amer, A.M., 2009. Moisture adsorption capacity and surface area as deduced from vapour pressure isotherms in relation to hygroscopic water of soils. *Biologia* 64(3): 516-521.

Amer, A.M., 2014. Moisture dynamics and available water capacity in root zone as influenced by swelling pressure and water table in tropical soils. Final Report, submitted to SENESCYT, Prometeo Project, Ecuador.

Amer, A.M., 2015. Vapor adsorption capacity and soil wetting. In: Wetting and wettability. Aliofkhazraei, M. (Ed.). IntechOpen, pp.1-14.

Black, G.A., Evans, D.D., White, J.L., Ensminger, L.E., Clerk, F.E., 1965. Methods of soil analysis. Part 1&2. American Society of Agronomy - Soil Science Society of America, Madison, Wisconsin, USA.

Brunauer, S., Emmett, P.H., Teller, E., 1938. Adsorption of gases in multi-molecular layers. *Journal of the American Chemical Society* 60(2): 309-319.

El-Fiky, Y.S., 2002. Studies on hydro-physical and physicochemical properties of new reclaimed soils in Egypt. PhD Thesis, Soil Science Department, Faculty of Agriculture, Menoufia University, Egypt.

El-Gabaly, M.M., Khadr, M., 1962. Clay mineral studies of some Egyptian Desert and Nile alluvial soils. *European Journal of Soil Science* 13(2): 333–342.

El-Sharkawy, A.F., 1994. Study of water imbibition in some agricultural soils. MSc Thesis, Agricultural Engineering Department, Faculty of Agriculture, Menoufia University, Egypt.

Farrar, D.M. 1963. The use of vapour-pressure and moisture content measurements to deduce the internal and external surface area of soil particles. *Europen Journal Soil Science* 14(2): 303–321.

Globus, A.M., 1996. On specific soil surface area computing by one point on the water vapor sorption isotherm. *Eurasian Soil Science* 28(10): 154–155.

Han, E., 2011. Soil moisture data assimilation at multiple scales and estimation of representative field scale soil moisture characteristics. PhD. Thesis, Purdue University, West Lafayette, USA.

Jacobs, A.F.G., Heusinkveld, B.G., Berkowicz, S.M., 1999. Dew deposition and drying in a desert system: a simple simulation model. *Journal of Arid Environments* 42(3): 211–222.

Klute, A. 1986. Methods of soil analysis. Part I Physical and Mineralogical Methods. American Society of Agronomy - Soil Science Society of America, Madison, Wisconsin, USA.

Kosmas, C., Danalatos, N.G., Poesen, J., van Wesemael, B., 1998. The effect of water vapour adsorption on soil moisture content under Mediterranean climatic conditions. *Agricultural Water Management* 36(2): 157–168.

Kosmas, C., Marathianou, M., Gerontidis, St., Detsis, V., Tsara, M., Poesen, J., 2001. Parameters affecting water vapor adsorption by the soil under semi-arid climatic conditions. *Agricultural Water Management* 48(1): 61–78.

Levy, G.J., Mamedov, A.I., 2002. High-energy-moisture-characteristic aggregate stability as a predictor for seal formation. *Science Society of America Journal* 66(5): 1603-1609.

Nerpin, V., Chudnovski, A.F., 1975. Energy and mass-transfer in plant-soil-air system. Hydro-Meteo Izdat., Leningrad, Russia. [in Russian].

Orchiston, H., 1954. Adsorption of water vapour: II. Clays at 25^{0}C. *Soil Science* 78(6): 463–479.

Quirk, J.P., 1955. Significance of surface areas calculated from water vapour sorption isotherms by use of the BET equation. *Soil Science* 80(6): 423–430.

Eurasian J Soil Sci 2019, 8 (4) 298 - 303

Eurasian Journal of Soil Science

Journal homepage : http://ejss.fesss.org

Effects of iron sources and doses on plant growth criteria in soybean seedlings

Füsun Gülser [a,*], Halil İbrahim Yavuz [b], Tuğba Hasibe Gökkaya [a], Murat Sedef [b]

[1] Van Yüzüncü Yıl University, Faculty of Agriculture, Department of Soil Science and Plant Nutrition, Van, Turkey
[2] Van Yüzüncü Yıl University, Faculty of Engineering, Department of Mechanical Engineering, Van, Turkey

Abstract

In this study, effects of different iron sources and doses on plant growth criteria in soybean (*Glycine max* L.) seedlings were investigated. The experiment was conducted according to factorial experimental design with three replications under controlled conditions. Atakişi variety of soybean (*Glycine max* L.) cultivar was used as a plant material. Three soybean seeds were sown each plastic pot having 1.3 kg soil:sand mixed in 1:1 ratio. Three different Fe sources ($FeSO_4.7H_2O$, Fe-EDDHA and nanoFe) were applied to the pots with three different doses (0-15-30 mg Fe kg^{-1}). The experiment was ended after five weeks of seed sowing. Shoot length, shoot fresh and dry weights, root length, root fresh and dry weights and number of compound leaf in soybean seedlings were determined at the end of the experiment. The highest shoot fresh and dry weights, root fresh and dry weights, compound leaf number were determined in 15 mg kg^{-1} nano Fe applications as 3.56 g, 0.83 g, 2.30 g, 0.33 g and 5, respectively. Increasing the application dose of nano-Fe from 15 to 30 mg kg^{-1} caused to decrease in fresh and dry weights in soybean seedlings. Generally, shoot growth decreased and root length increased in soybean seedlings by increasing Fe application doses. Seedling growth in soybean generally increased depend on the Fe sources in the following order; $FeSO_4.7H_2O$ < Fe-EDDHA < nano-Fe.

Keywords: Soybean, seedling growth, nano Fe, Fe-EDDHA, $FeSO_4.7H_2O$.

Article Info

Received : 10.11.2018
Accepted : 25.06.2019

Introduction

Iron is an essential nutrient for all organisms (Zuo and Zhang, 2011). In plants, Fe is also one of the essential micro nutrient and participates in many physiological processes including RNA synthesis, chlorophyll biosynthesis, several enzyme activitions, respiration and redox reactions (Malakouti and Tehrani, 2005; Mimmo et al., 2014; Ye et al., 2015; Zargar et al., 2015). Although, micronutrient elements are needed in rather very small amounts for satisfactory plant growth and production, their deficiency may cause disorder in physiological and metabolic processes involved in the plant.

Iron deficiency is a wide spread agricultural problem in many crops especially in calcareous soils and semi-arid climates. Deficiencies are usually diagnosed by chlorosis in young leaves and are typically found among sensitive crops grown in calcareous soils covering over 30% of the world's surface soil. Excessive iron deficiency may lead to complete crop failure (Lindsay and Schwab, 1982; Chen and Barak, 1982).

Çakmak (2002) reported that even on the world scale, Fe deficiency is wide spread occurring in about 30-50% of cultivated soils. Iron content in soil is generally high, but a large proportion is fixed to soil particles (Mimmo et al., 2014; Bindraban et al., 2015) especially in aerobic soils and high pH levels. Fe is mainly in the insoluble form as ferric iron (Fe^{+3}). Mortvedt et al. (1991) reported that in calcareous soils less than 10 % of the Fe is available to plants. Therefore, these soils are usually deficient in the available form, ferrous iron (Fe^{+2}). (Ye et al., 2015). Because plants usually uptake Fe^{+2} from soil. When the soil-plant-animal-human food

* Corresponding author.
Van Yüzüncü Yıl University, Faculty of Agriculture, Department of Soil Science and Plant Nutrition 65080 Van, Turkey
Tel.: +90 432 2251024 E-mail address: fgulser@yyu.edu.tr
e-ISSN: 2147-4249 DOI: 10.18393/ejss.582231

chain considered, Fe deficiency does not only affect the plant growth and development but also lead to anemia in animals and humans (Li et al., 2014).

The application of Fe fertilizers is still the most effective way to improve Fe efficiency in plants. Inorganic Fe fertilizers chelated Fe fertilizer and organic Fe fertilizer are the common varieties of Fe fertilizers (Laurie et al., 1991). Iron ferrous sulphate ($FeSO_4.7H_2O$) and iron chelate products are generally used as inorganic fertilizer (Tisdale et al., 1993). Synthetic chelate iron (Fe-EDDHA) products are mostly applied to prevent or to remove Fe chlorosis in crops grown on calcareous soils. These products consist of a mixture of EDDHA components chelated to Fe.

Recently, the use of nanomaterials in agricultural production has increased (Gogos et al., 2012; Bindraban et al., 2015). Bindraban et al. (2015) and Montalvo et al. (2015) reported that nanomaterials have potential applications as crop fertilizers because of their physical and chemical attributes. The releasing of elements from fertilizers can be controlled and delayed with using of nanoparticles and nano powders. Nano materials consist of nano meter-scale particles with a very small diameter and large specific area (Hochella et al., 2008). Brunner et al. (2006) reported that nano-fertilizers are syhthesized or modified form of traditional fertilizers, fertilizers bulk materials or extracted from different vegetative or reproductive parts of the plant by different chemical, physical, mechanical or biological methods with the help of nanotechnology used to improve soil fertility. Nanoparticles can be made from fully bulk materials.

The plants sensitive to iron deficiency are apple, avocado, banana, bean, barley, cotton, citrus, grape, oats, peanut, potatoes, pecan, soybean, sorghum and various greenhouse flowers (Chen and Barak, 1982). These chelates increase Fe solubility and function as a transporter through solution to plant (Lucena et al., 1992). Fe-EDDHA (iron ethylenediamine hidroksi pheny acetic acid) is along the most effective synthetic Fe chelates under neutral and alkaline soil conditions (Lucena et al., 1992). Legumes and cereals are two most important foods to humans (Graham and Vance, 2003). Legumes have been used both for their medicinal, cultural as well as nutritional properties providing an important source of protein and oil which can also be converted into biodiesel (Libault et al., 2010). Soybean (*Glycine max* L.) is the highest produced legume crop. According to Food and Agriculture Organization statistic for 2009, about 230 million tons of soybean were produced over the world, ranking the on the world's top commodity production. The objective of this study was to investigate effects of different iron forms on growth criteria in soybean seedlings.

Material and Methods

The experiment was conducted according to factorial experimental design with three replications under controlled conditions in a growth chamber at 25±1ºC and irrigated with distilled water. Atakişi soybean variety was used as a plant material and three soybean seed was sown to each plastic pot having 1.3 kg soil:sand mixed in 1:1 ratio. Three different doses (0, 15, 30 mg kg^{-1}) of $FeSO_4.7H_2O$, FeEDDHA and nanoFe were used in the study. The experiment was ended after five weeks after sowing the seeds. Shoot length, shoot fresh and dry weights, root length, root fresh and dry weights and number of compound leaves were determined at the end of five weeks.

Some properties of the growth media were determined using the standard analysis methods (Kacar, 2010). According to the physical and chemical properties of the growth media (Table 1), it had loamy texture class, non-saline, slightly alkaline, low in organic matter, unsufficient in phosphorus and zinc contents, sufficient in calcium, magnesium, manganese and copper contents. Variance analysis of the experimental data was done by SPSS statistical program (SPSS, 2018).

Table 1. Some properties of the growth media used in this study.

Texture	pH	Salinity	Lime	OM	P	K	Ca	Mg	Fe	Mn	Zn	Cu
		dS m^{-1}	%		mg kg^{-1}							
Loamy	7.81	0.361	3.86	1.32	5.50	298	3034	405	5.58	29.84	0.58	0.81

Results and Discussion

The variance analysis of the results and the effects of different iron treatments on seedling growth criteria are given in Table 2 and Table 3, respectively.

Table 2.Variance analysis of the data for plant growth criteria in soybean seedling (F values).

Variation Sources	df	Shoot length	Shoot fresh weight	Shoot dry weight	Root length	Root fresh weight	Root dry weight	Comp. leaf number
Fe source (A)	2	5.43*	2.34	7.85**	0.10ns	5.02*	0.78	1.63ns
Fe dose (B)	2	22.14**	1.39	5.702*	11.55**	11.91**	8.94**	6.13**
AxB	4	2.68ns	3.90*	11.72**	1.49ns	16.21**	8.96**	2.38ns

*significant at 0.05, **significant at 0.01, ns not significant

According to the variance analysis, different iron sources significantly influenced shoot length, shoot dry weight and root fresh weight of soybean seedlings. Similarly Fe application doses had significant effect on all of the plant growth criteria of soybean seedlings, except shoot fresh weight. The effects of interaction between source and dose on shoot length, shoot fresh and dry weights, root fresh and dry weights were found to be significant statistically (Table 2).

According to the Fe application sources, the highest mean values for shoot length, shoot fresh and dry weights and root fresh and dry weights were obtained as 55.16 cm, 2.60 g, 0.54 g, 1.45 g and 0.22 g in nano-Fe application, respectively (Table 3). Increasing iron doses generally caused decreases in the mean values of plant growth criteria, except root length and compound of leaf number. Chakralhoseini et al. (2002) reported that iron at low concentration of 2.5 mg kg-1 in soil increased dry matter weight of soybean, but higher doses of iron decreased soybean growth. In a field experiment, Sheykhbaglou et al. (2010) determined that foliar application of nano-iron oxide at the concentration of 0.75 g L^{-1} was increased leaf + pod dry weight and pod dry weight over the control, but increasing the application dose from 0.75 to 1 g L^{-1} caused reduction in leaf + pod dry weight. They also reported that the highest yield was observed at 0.50 g L^{-1} application rate having 48% increase in grain yield compared with control. In this study, application of 15 mg kg^{-1} nano-Fe increased fresh and dry weights of shoot and root parts in the soybean seedlings over the control, but the highest dose (15 mg kg^{-1}) of nano-Fe application reduced the fresh and dry weights of the plants (Figures 1 and 2).

While the lowest mean values for shoot length (44.02 cm), shoot fresh (2.12 g) and dry (0.38 g) weights, root fresh (0.97 g) and dry (0.16 g) weights were found in 30 mg kg^{-1} Fe application dose, the highest mean values for root length (25.36 cm) was obtained in the highest Fe application dose (Table 3). According to the interactions between source and Fe dose, the highest values of shoot fresh (3.56 g) and dry (0.83 g) weights, root fresh (2.30 g) and dry (0.33 g) weights were determined in 15 mg kg^{-1} dose of nano-Fe application (Figure 1 and 2). Rui et al. (2016) found that application of iron oxide nanoparticles (Fe_2O_3NPs) as a fertilizer increased root length, plant height and biomass of peanut plants over the control and EDTA-Fe treatments. They reported that the root dry biomass did not display the statistical difference between Fe_2O_3NPs and EDTA-Fe treatments, and also no impact on biomass increases was found in the shoot dry weight. Alidoust and Isoda (2013) found that root length of soybean seedlings increased by 6, 8, 19, 27, 37, and 40% at 50, 100, 250, 500, 1000, and 2000 mg L^{-1} of nanoparticle Fe (IONPs) applications, respectively as compared to the controls. In another study, Liu (2016) determined that Fe nanoparticles (FeOxNPs) significantly increased root length of lettuce seedlings by 12–26 % as a Fe fertilizer at low application rates (5–20 ppm). Similarly in this study, at 15 and 30 mg kg^{-1} application doses of Fe, the mean values of shoot length decreased 25.54% and 27.28%, and the mean values of root length increased 24.64% and 31.53% over the control treatment, respectively.

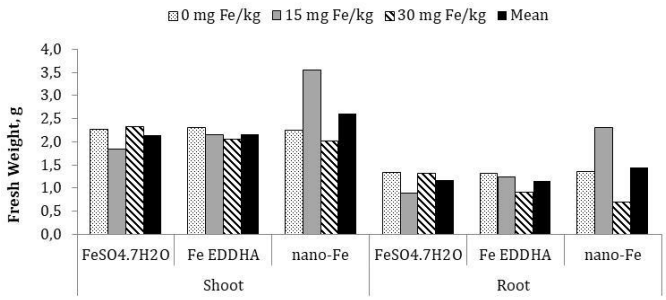

Figure 1. The effects of iron sources and doses on fresh weight in soybean seedlings

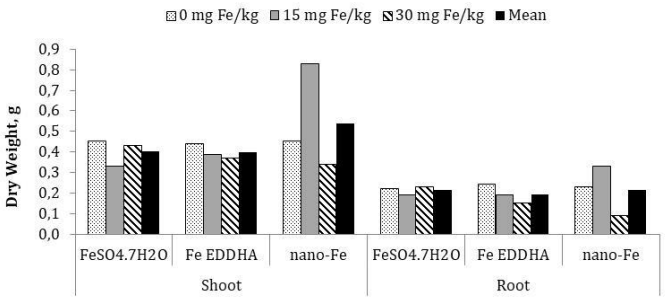

Figure 2. The effects of iron sources and doses on dry weight in soybean seedlings

In this study although the highest mean values of plant growth criteria were obtained in nano-Fe applications compare to the other Fe sources, 30 mg kg^{-1} Fe dose generally decreased plant growth. According to the results, it can be concluded that Fe application dose more than 15 mg kg^{-1} adversely affected seedling growth criteria in soybean.

According to the Fe sources, the highest mean values of plant growth criteria were generally found in 15 mg kg^{-1} iron doses of Fe-EDDHA and nano-Fe while the lowest means of these parameters were obtained in 15 mg kg^{-1} dose of $FeSO_4.7H_2O$. It was reported that soluble inorganic Fe fertilizer has little ameliorative effect to improve the available Fe content in alkaline calcareous soils (Cesco et al., 2000; Lucena et al., 2010). In this study, the mean values of plant growth criteria obtained in different iron sources showed the following decreasing trend: nano-Fe>Fe-EDDHA> $FeSO_4.7H_2O$.

Table 3. Effects of different iron sources and doses on growth criteria in soybean seedlings.

Plant Growth Criteria	Fe doses (mg kg^{-1})	Fe sources			Mean
		$FeSO_4.7H_2O$	Fe-EDDHA	Nano-Fe	
Shoot length (cm)	0	60.55 a*	60.58 a	60.46 a	60.53 A**
	15	42.27 cd	44.20 cd	48.75 bc	45.07 B
	30	39.10 cd	36.70 d	56.27 ab	44.02 B
Mean		47.31 B*	47.16 B	55.16 A	
Shoot fresh weight (g)	0	2.26 b*	2.29 b	2.24 b	2.27
	15	1.84 b	2.15 b	3.56 a	2.52
	30	2.32 b	2.04 b	2.00 b	2.12
Mean		2.14	2.16	2.60	
Shoot dry weight (g)	0	0.45 b**	0.44 b	0.45 b	0.45 AB*
	15	0.33 b	0.39 b	0.83 a	0.52 A
	30	0.43 b	0.37 b	0.34 b	0.38 B
Mean		0.40 B**	0.40 B	0.54 A	
Root length (cm)	0	19.25	19.32	19.28	19.28 B*
	15	22.63	23.77	25.70	24.03 A
	30	27.80	25.29	23.00	25.36 A
Mean		23.23	22.79	22.66	
Root fresh weight (g)	0	1.33 bc**	1.31 bc	1.34 b	1.33 A**
	15	0.89 de	1.24 bcd	2.30 a	1.48 A
	30	1.31 bcd	0.90 cde	0.69 e	0.97 B
Mean		1.18 B*	1.14 B	1.45 A	
Root dry weight (g)	0	0.22 bc**	0.24 b	0.23 bc	0.23 A**
	15	0.19 bc	0.19 bc	0.33 a	0.24 A
	30	0.23 b	0.15 cd	0.09 d	0.16 B
Mean		0.21	0.19	0.22	
Compound leaf number	0	4.00	4.00	4.00	4.00 B**
	15	4.67	5.00	5.00	4.89 A
	30	5.00	5.00	3.67	4.56 A
Mean		4.5 6	4.67	4.22	

*significant at 0.05 level, ** significant at 0.01 level.

Our results were corresponding with the results of similar researches. Mortvedt et al. (1972) reported that FeEDDHA application was more effective than ferrous sulphate at the same rate iron. Hassani et al. (2015) applied Fe fertilizer with chemical and nano form as their combination and separately. They determined that nano Fe had more effect on plant growth criteria than the chemical fertilizer in mint plant. Rui et al. (2016) determined that iron oxide nanoparticles increased root length, plant height, biomass values compare to chelated Fe application in the peanut plant. They also reported that iron oxide nanoparticles can replace traditional Fe-fertilizers. Similiarly, Sheykhbaglou et al. (2010), Nadi et al. (2013) and Singh et al. (2017) reported that nano Fe particles have beneficial effects on plant growth criteria and grain yield in soybean and fababean, respectively.

Previous researches showed that nano fertilizers lead an increase in the use efficiency of plant nutrients, reduce soil toxicity, decrease the potential adverse effects of excessive chemical fertilizer use and fertilizer application frequency (Brunner et al., 2006; Liu et al. 2016; Khadka et al., 2017). Nano fertilizers have large surface area and particle size less than the pore size of root and leaves of the plant which can increase penetration into the plant from applied surface and improve uptake and nutrient use efficiency of the nano fertilizer (Liscano et al., 2000). They can be applied frequently in small amounts and are environmentally friendly compare to traditional chemical fertilizers (Liu and Lal, 2016). On the other hand, Rameshaiah et al. (2015) reported that excessive doses of nano materials used in agricultural lands may be cause hazardous effects on living organisms and human health. The selection and cultivation of iron toxicity tolerant genotype may be another suitable option for its toxicity management (Khadka et al., 2017).

Conclusion

The different iron sources and application doses significantly influenced plant growth criteria in soybean seedlings. The highest shoot fresh and dry weights, root fresh and dry weights, compound leaf number were determined in 15 mg kg^{-1} nano Fe applications compared with the $FeSO_4.7H_2O$ and Fe-EDDHA treatments. The dose of 30 mg kg^{-1} nano-Fe application decreased fresh and dry weights in soybean seedlings, but increased the root length. Increasing the dose of Fe application from the different Fe sources generally

decreased shoot growth and increased root length. Effect of nano-Fe on the seedling growth was more effective than Fe-EDDHa and $FeSO_4.7H_2O$. As a result, it can be suggested that using of nano-Fe fertilizer will be beneficial on soybean seedling growth with an application dose lower than 30 mg kg^{-1}.

References

Alidoust, D., Isoda, A., 2013. Effect of γFe2O3 nanoparticles on photosynthetic characteristic of soybean (Glycine max (L.) Merr.): foliar spray versus soil amendment. *Acta Physiologiae Plantarum* 35(12): 3365–3375.

Bindraban, PS, Dimkpa, C., Nagarajan, L., Roy, A., Rabbinge, R., 2015. Revisiting fertilisers and fertilisation strategies for improved nutrient uptake by plants. *Biology and Fertility of Soils* 51(8): 897–911.

Brunner, T.J., Wick, P., Manser, P., Spohn, P., Grass, R.N., Limbach, L.K, Bruinink, A., Stark W.J., 2006. In vitro cytotoxicity of oxide nanoparticles: Comparison to asbestos, silica, and the effect of particle solubility. Environmental Science & Technology 40(14): 4374-4381.

Cakmak, I., 2002. Plant nutrition research: Priorities to meet human needs for food in sustainable ways. *Plant and Soil* 247(1): 3-24.

Cesco, S., Römheld, V., Varanini, Z., Pinton, R., 2000. Solubilization of iron by water-extractable humic substances. *Journal of Plant Nutrition and Soil Science* 163(3): 285–290.

Chakralhoseini, M.R., Ronaghi, A., Mafton, M., Karimian, N.A., 2002. Soybean response to application of iron and phosphorus in a calcareous soil. *Science and Technology Journal of Agriculture and Natural Resources* 6(4): 91-101.

Chen, Y., Barak, P., 1982. Iron nutrition of plants in calcareous soils. *Advances in Agronomy* 35(2): 17-40.

Gogos, A., Knauer, K., Bucheli, T.D., 2012. Nanomaterials in plant protection and fertilization: Current state, foreseen applications and research priorities. *Journal of Agricultural and Food Chemistry* 60(39): 9781–9792.

Graham, P.H., Vance, C.P., 2003. Legume importance and constraints to greater use. *Plant Physiology* 131(3): 872-877.

Hassani, A., Tajali, A.A., Mazinani, S.M.H., 2015. Studying the conventional chemical fertilizers and nano-fertilizer of iron, zinc and potassium on quantitative yield of the medicinal plant of peppermint (Mentha piperita L.) in Khuzestan. *International Journal of Agriculture Innovations and Research* 3(4): 1078-1082.

Hochella, M.F.Jr., Lower, S.K., Maurice, P.A., Penn, R.L., Sahai, N., Sparks, D.L, Twining, B.S., 2008. Nanominerals, mineral nanoparticles, and earth systems. *Science* 319(5870): 1631–1635.

Kacar, B., 2010. Toprak Analizleri. Genişletilmiş Baskı, XVIII, Nobel yayın Dağıtım, Ankara, Turkey. 468s. [in Turkish]

Khadka, D., Lamichhane, S., Shrestha, S.R., Pant, B.B., 2017. Evaluation of soil fertility status of Regional Agricultural Research Station, Tarahara, Sunsari, Nepal. *Eurasian Journal of Soil Science* 6(4): 295 -306.

Laurie, S.H., Tancock, N.P., Mcgrath, S.P., Sanders, J.R., 1991. Influence of complexation on the uptake by plants of iron, manganese, copper and zinc. *Journal of Experimental Botany* 42(237): 509–513.

Li, X., Gui, X., Rui, Y., Ji, W., Van Nhan, L., Yu, Z., Peng, S., 2014. Bt-transgenic cotton is more sensitive to CeO2 nanoparticles than its parental non-transgenic cotton. *Journal of Hazardous Materials* 274: 173–180.

Libault, M., Farmer, A., Joshi, T., Takahashi, K., Langley, R.J., Franklin, L.D., He, J., Xu, D., May, G., Stacey, G., 2010. An integrated transcriptome atlas of the crop model Glycine max, and its use in comparative analyses in plants. *The Plant Journal* 63(1): 86-99.

Lindsay, W.L., Schwab, A.P., 1982. The chemistry of iron in soils and its availability to plants. Journal of Plant Nutrition 5(4-7): 321-340.

Liscano, J.F., Wilson, C.E., Norman Jr, R.J., Slaton, N.A., 2000. Zinc availability to rice from seven granular fertilizers. Arkansas Agricultural Experiment Station Researh Bulletin 963, Fayetteville, Arkansas, USA. 31p. Available at [Access date: 10.11.2018]: http://digitalcollections.uark.edu/cdm/landingpage/collection/ArkBulletins

Liu, R., Lal, R., 2016. Nanofertilizers. In: Encyclopedia of Soil Science, Lal, R. (Ed.) 3rd Edition, CRC Press, pp:1511-1515.

Liu, R.Q., Zhang, H.Y., Lal, R., 2016. Effects of stabilized nanoparticles of copper, Zinc, manganese, and iron oxides in low concentrations on lettuce (Lactuca sativa) seed germination: nanotoxicants or nanonutrients? *Water, Air, & Soil Pollution* 227: 42.

Lucena, J.J., Gárate, A., Villén, M., 2010. Stability in solution and reactivity with soils and soil components of iron and zinc complexes. *Journal of Plant Nutrition and Soil Science* 173(6): 900–906.

Lucena, J.J., Manzanares, M., Gárate, A., 1992. Comparative study of the efficacy of commercial Fe-chelates using a new test. *Journal of Plant Nutrition* 15(10): 1995-2006.

Malakouti, M.J., Tehrani, M.M., 2005. The role of micronutrients in the increase in the yield and improvement of the quality of agricultural crops, micronutrients with macro effect. Tarbiyat Modares Publisher, Tehran, Iran. [In Persian].

Mimmo, T., Del Buono, D., Terzano, R., Tomasi, N., Vigani, G., Crecchio, C., Pinton, R., Zocchi, G., Cesco, S., 2014. Rhizospheric organic compounds in the soil–microorganism–plant system: their role in iron availability. *European Journal of Soil Science* 65(5): 629-642.

Montalvo, D., McLaughlin, M.J., Degryse, F., 2015. Efficacy of hydroxyapatite nanoparticles as phosphorus fertilizer in andisols and oxisols. *Soil Science Society of America Journal* 79(2): 551–558.

Mortvedt, J.J., 1991. Correcting iron deficiencies in annual and perennial plants: present technologies and future prospects. *Plant and Soil* 130(1-2): 273–279.

Mortvedt, J.J., Giordano, P., Lindsay, W., 1972. Micronutrients in agriculture. Soil Science Society of America, Madison. WI, USA. 666p.

Nadi, E., Aynehband, A., Mojaddam, M., 2013. Effect of nano-iron chelate fertilizer on grain yield, protein percent and chlorophyll content of Faba bean (*Vicia faba* L.). *International Journal of Biosciences* 3(9): 267-272.

Rameshaiah, G.N., Pallavi, J., Shabnam, S., 2015. Nano fertilizers and nano sensors-an attempt for developing smart agriculture. *International Journal of Engineering Research and General Science* 3(1): 314-320.

Rui, M., Ma, C., Hao, Y., Guo, J., Rui, Y., Tang, X., Zhao, Q., Fan, X., Zhang, Z., Hou, T., Zhu, S., 2016. Iron oxide nanoparticles as a potential iron fertilizer for peanut (Arachis hypogaea). *Frontiers in Plant Science* 7: 815.

Rui, Y., Zhang, P., Zhang, Y., Ma, Y., He, X., Gui, X., Li, Y., Zhang, J., Zheng L., Chu, S., Guo, Z., Chai Z., Zhao, Y., Zhang, Z., 2015. Transformation of ceria nanoparticles in cucumber plants is influenced by phosphate. *Environmental Pollution* 198: 8–14.

Sheykhbaglou, R., Sedghi, M., Shishevan, T.M., Sharifi, R.S., 2010. Effects of nano-iron oxide particles on agronomic traits of soybean. *Notulae Scientia Biologicae* 2(2): 112-113.

Singh, M.D., Chirag, G., Prakash, P.O., Mohan, M.H., Prakasha, G., Vishwajith, 2017. Nano fertilizers is a new way to increase nutrients use efficiency in crop production. *International Journal of Agriculture Sciences* 9(7): 3831-3833.

SPSS, 2018. IBM Corp. Released 2013. IBM SPSS Statistics for Windows, Version 21.0. Armonk, NY: IBM Corp.

Tisdale, S.L., Nelson, W.L., Beaton, J.D., 1993. Soil fertility and fertilizers. Macmillan Publishing Co. Inc. New York, USA. 634p.

Ye, L., Li, L., Wang, L., Wang, S., Li, S., Du, J., Zhang, S., Shou, H., 2015. MPK3/MPK6 are involved in iron deficiency induced ethylene production in Arabidopsis. *Frontiers in Plant Science* 6: 953.

Zargar, S.M., Agrawal, G.K., Rakwal, R., Fukao, Y., 2015. Quantitative proteomics reveals role of sugar in decreasing photosynthetic activity due to Fe deficiency. *Frontiers in Plant Science* 6: 592.

Zuo, Y., Zhang, F., 2011. Soil and crop management strategies to prevent iron deficiency in crops. *Plant and Soil* 339(1-2): 83–95.

Eurasian J Soil Sci 2019, 8 (4) 304 - 312

Eurasian Journal of Soil Science

Journal homepage : http://ejss.fesss.org

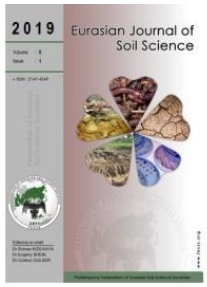

Role of soil physicochemical and microbiological properties in the occurrence and severity of chickpea's Fusarium wilt disease

Dahou Moutassem [a,c,*], Lakhdar Belabid [c], Yuva Bellik [a], Noureddine Rouag [b] Hanane Abed [a], Siham Ziouche [a], Faiza Baali [a]

[a] Characterization and Natural Resources Valorisation Laboratory (L.C.V.R) SNV-TU Faculty, Mohamed El Bachir El Ibrahimi Bordj Bou Arreridj University, Algeria

[b] Department of Agronomy, Faculty of Nature and Life Sciences, Ferhat Abbas Sétif 1 University, Sétif, Algeria

[c] Laboratory for Research on Biological Systems and Geomatics, Faculty of Nature and Life Sciences, Mustapha Stamboli Mascara University, Algeria

Abstract

The aim of the present study is to evaluate the relative disease severity of chickpea wilt in the most important chickpea growing areas in North Algeria and their relationship to soils properties. The physicochemical and biological parameters of 14 soils were analyzed and correlated to the disease index severity (*Dis*). Soil physicochemical factors were determined as a means of particle size distribution, pH, Electrical Conductivity (EC), $CaCO_3$ content, total Nitrogen (Total-N), Olsen-P and biological factors including Foc inoculum density (ID-Foc), *Trichoderma* spp propagule number (*TrPn*), *Pseudomonas* spp and *Bacillus* spp. The results revealed that the spread of the disease was evident in all prospected areas and recorded as low to medium with values ranging from 2.05 to3 9.8. The disease severity was positively correlated with EC (r=0.62), Total-N (r= 0.79), and ID-Foc (r=0.72), whereas negatively correlated with Olsen-P (r=-0.67), *TrPn* (r=-0.70) and *Pseudomonas* spp (r=-0.89). There was no correlation between *Dis* and soil physical (clay, loam and sand), chemical (pH, $CaCO_3$ content) and biological factors (*Bacillus* spp). As well, ID-Foc was positively correlated with Total-N and negatively correlated with Olsen-P. The results indicated that *TrPn* and *Pseudomonas* spp were positively correlated, whereas both were negatively associated with ID-Foc and D*is*. Our finding pointed out the critical role of some physicochemical and biological soil characteristics in the epidemic development of chickpea wilt under field conditions.

Keywords: Chickpea, *Fusarium oxysporum* f. sp *ciceris*, Nitrogen, Olsen-P, *Trichoderma spp*, *Pseudomonas spp*.

Article Info

Received : 10.09.2018
Accepted : 24.06.2019

Introduction

Fusarium wilt, caused by *Fusarium oxysporum* Schlechtend: Fr. f. sp. *ciceris* (Padwick Matuo and K. Sato) is the most important constraint to production of chickpea in the worldwide, particularly in the Mediterranean area and the Indian subcontinent (Haware, 1990). Pathogen can cause yield losses, with an annual average of 10–15%, although, the disease can destroy the crop completely under specific environmental conditions (Trapero-Casas and Jiménez-Díaz, 1985).

The disease is defined by a monocyclic epidemic nature induced by chlamydospores as primary inoculum wich survive on crop residues in soil for more than 6 years in the absence of susceptible host (Jiménez-Díaz

* Corresponding author.
Characterization and Natural Resources Valorisation Laboratory (L.C.V.R) SNV-TU Faculty, Mohamed El Bachir El Ibrahimi Bordj Bou Arreridj University 34030 Algeria
Tel.: +213555502797
E-mail address: moutassemdahou@gmail.com
e-ISSN: 2147-4249
DOI: 10.18393/ejss.585160

et al., 2015). Furthermore, the expression of epidemic *Fusarium* wilt can result from the complex interaction of population of chickpea, population of Foc, and soil properties (Mehmood et al., 2013).

Soil properties are considered as epidemiological factors that can influence the occurrence and severity of plant diseases (Ghorbani et al., 2008). Soil physicochemical properties such as pH, nitrogen and phosphorus play an important role in the growth and susceptibility of the host, multiplication and infectivity of the pathogen, or in the interaction of host plant and pathogen (Höper and Alabouvette, 1996; Elmer and Datnoff, 2014).

Research reports have demonstrated that soil intrinsic microbial communities or specific sub-populations have the potential to suppress pathogen infectivity of host plants (Shen et al., 2015). However, the degree of soil suppressiveness is associated to soil microorganism's biodiversity such as *Trichoderma* spp, *Bacillus* spp and *Pseudomonas spp*, which are commonly used as biological control agents (Lemanceau and Alabouvette, 1993), and which in turn are influenced by soil physicochemical properties (Lenc et al., 2011).

The associations between the soil properties on the behavior of microorganisms have been investigated intensively but are still imperfectly understood (Lucas, 2006). Furthermore, understanding the mechanism of the interaction between soil physicochemical properties and microorganisms is important for the successful disease control in a natural agro-system (Naseri and Hamadani, 2017).

In this context, the main objective of the present work is the study of the combined effects of soil physicochemical parameters (EC, N, P, pH) and antagonistic agents (*Pseudomonas* spp, *Bacillus* spp and *Trichoderma* spp) on the development of chickpea wilting as well as on the density of the inoculum and severity of *Fusarium* wilt in natural conditions.

Material and Methods

Farm assessment and soil sampling

This study was carried out during June 2015 indifferent cultivated fields' chickpea located in different agro-climatic zones in North Algeria, including Constantine (3 sites), Guelma (2 sites), Mascara (2 sites), Ain Témouchent (3 sites), Sidi Bel Abbes (2 sites) and Relizane (2 sites). Soil samples were collected from 14 fields' taken from the rhizosphere soil surrounding chickpea roots. Soil samples were initially sieved to remove all plant residues then air-dried and ground into 2-mm particles for physicochemical and biological analyses.

Soil physicochemical characterization

Soil samples were analyzed for particle size distribution (pipette method), soil acidity (pH) with a 1:2.5 w/v and electrical conductivity (EC) (1:5 w/v). Equivalent calcium carbonate ($CaCO_3$) was determined using the Bernard calcimeter (Hulseman, 1966). Total nitrogen was determined by the Kjeldahl method as described Jones (2001). Available phosphorus (Olsen-P) was determined by the method of Olsen et al. (1954).

Soil fungal and bacterial isolation

The dilution plate method described by Bulluck et al. (2002) by means of agar media was used for the determination of the different fungal species. 10 g of each soil sample were suspended and diluted into 90 ml of sterile distilled water then mixed for 30 minutes. Successive dilutions of 10 ml from this suspension were prepared with 90 ml sterile distilled water (10^{-2} and 10^{-3}). Each suspension was transferred onto 90 ml of agar media. Various suspensions were poured into Petri dishes (90 mm) and were incubated at 25°C for 3 to 15-days. Different colony types were transferred to potato dextrose agar (PDA) media and incubated for 7-days under the same conditions for taxonomic identification. The isolated *Fusarium oxysporum* strains were purified and identified by single-spore cultures and identified based on morphological and microscopic characteristics according to specific identification keys given by Messiaen and Cassini (1981).

The pathogenicity tests were performed according to pot screening procedure as described by Nene and Haware (1980). *Trichoderma* spp colonies which developed on PDA were identified based on visual macroscopic and microscopic observations according to Gams and Bissett (1998).

Regarding bacterial isolation, 1g from each soil was suspended in 9 ml of sterile distilled water according to Bulluck et al. (2002) technique. The suspensions were shaken and then heated at 50°C for 5 min. *Pseudomonas* Selective Agar (PSA) and Nutrient Agar were used for isolation of *Pseudomonas spp* and *Bacillus spp*, respectively. Here too, successive dilutions of 10 ml from this suspension were prepared with 90 ml sterile distilled water (10^{-2} and 10^{-3}). Aliquots (1 ml) of each dilution from each soil sample were transferred into 9 ml culture medium in Petri dishes. The plates were incubated at 28-37°C for 24-48h.Each colony of *Pseudomonas* spp and *Bacillus* spp was isolated and identified based on morphology and total density per sample (colony-forming units /g soil). All experiment was carried out in four replicates.

Fusarium wilt disease assessment, Foc isolation and pathogenicity test

Disease assessment in chickpea was carried out during the flooring stage to observe symptom development and disease evolution. Disease incidence (DI) was assessed according to Traperos-Casas and Jiménez-Díaz (1985) by counting the number of plants showing symptoms in three representative 10 m lengths of row, randomly chosen from each field. Severity of *Fusarium* wilt (ISM) was assessed on a scale of 0 to 4 according to the percentage of foliage with yellowing or necrosis (0 = 0%; 1 = 1 to 33%; 2 = 34 to 66%; 3 = 67 to 100% and 4 = dead plant). DI and ISM data (rated from 0 to 4) were used to calculate disease index intensity (*Dis*) using the equation *Dis* = (DI× ISM)/4.

A total of 10 wilted plants were collected from each field, for laboratory analysis. The infected plants were placed in paper envelopes, air-dried at room and stored at 4°C until used to isolate the pathogen. *F. oxysporum* cultures isolated from wilted plant were identified microscopically based on morphological characteristics. The pathogenicity tests were performed according to pot screening procedure (Nene and Haware, 1980).

Statistical analysis

One way analysis of variance (ANOVA) with post-hoc Newman-Keuls test was used to test differences between soil samples. The association between soil physicochemical, biological properties and D*is Fusarium* wilt were also calculated using the Pearson correlations. The association between physicochemical and biological soil properties as well as Dis was made by principal component analysis (PCA). The statistical analyses were done using the software package STATISTICA 8.

Results

Physicochemical properties of soils

The results in Table 1 show the variation in physicochemical proprieties of soils from the 14 sites. In terms of physical properties, sand, loam and proportion clay showed significant differences between the studied 14 sites. Particle size distribution varied significantly among the 14 sites ($P < 0.05$). The highest values of sand (46.3%), clay (61.4%) and loam (84.4%) were observed in S14, S9 and S3, respectively. In contrary, S3 was characterized by the lowest value of clay (11%). S9 presented the lowest value of silt (11%), whereas, S3 showed the lowest value of sand (4.4%).

Table 1. Physicochemical properties of different soil samples from 14 chickpea fields in North Algeria

Field sites	Silt (%) **	Clay (%) **	Sand (%) **	pH **	EC (µScm-1) **	Olsen-P (mg kg-1) **	N (g kg-1) **	$CaCO_3$ (%) **
S1	71.1±0.20c	19.4±0.14i	09.4±0.20h	8.0±0.05de	143.2±3.14k	4.9±0.53d	1.4±0.02h	27.3±0.02c
S2	70.5±0.20c	22.2±0.35h	07.2±0.45i	8.2±0.00ab	163.5±1.73j	6.4±0.24c	1.7±0.02g	31.2±0.45b
S3	84.4±0.24a	11.0±0.13k	04.4±0.11j	8.1±0.01bcd	173.9±1.57i	8.5±0.08b	0.7±0.02j	20.2±1.04d
S4	30.9±0.59h	40.8±0.56d	28.1±0.20b	8.1±0.02cd	167.3±1.25ij	5.4±0.08d	0.8±0.06ij	27.0±0.88c
S5	54.3±0.21f	24.5±0.15g	21.1±0.27d	7.0±0.03h	181.6±3.65h	10.5±0.19a	0.9±0.00ij	7.8±0.46f
S6	63.8±0.43d	21.5±0.32h	14.5±0.42f	7.5±0.00g	226.9±2.71e	2.6±0.11gh	0.9±0.03i	7.4±0.46fg
S7	60.3±0.32e	21.6±0.41h	17.9±0.41e	8.2±0.03bc	285.7±0.89b	4.2±0.30e	2.4±0.11cd	41.6±0.52a
S8	34.3±0.22g	35.6±0.66e	30.0±0.57e	7.5±0.07g	216.2±3.08f	3.2±0.11fg	2.6±0.05bc	21.0±1.21d
S9	23.9±0.36j	61.4±0.45a	14.6±0.16f	7.5±0.07g	242.1±0.97d	5.4±0.03d	2.1±0.04ef	5.7±0.23g
S10	77.8±0.91b	13.8±0.33j	8.3±0.58hi	8.3±0.01a	297.7±0.64a	4.1±0.03e	2.9±0.06a	42.6±0.75a
S11	30.5±0.31h	43.9±0.33c	25.4±0.40c	7.2±0.04h	144.8±1.32k	3.4±0.10f	2.3±0.11de	3.2±0.45h
S12	60.5±0.58e	27.2±0.57f	12.2±0.71g	7.9±0.02e	197.3±2.20g	3.6±0.13ef	2.7±0.09b	19.6±0.44d
S13	27.0±0.87i	44.2±0.74c	28.7±0.63b	7.7±0.10f	187.1±2.31h	5.4±0.30d	2.1±0.10f	01.8±0.50h
S14	34.9±0.38g	46.3±0.26b	18.6±0.49e	8.1±0.03cd	254.3±5.11c	2.5±0.05h	2.3±0.06de	11.3±0.58e
p-Value	<0.01	<0.01	<0.01	<0.01	<0.01	<0.01	<0.01	<0.01

Values represent the mean of four replicates ± SE (standard errors). Values of probability of one-way ANOVA. Within a column different letters denote significant difference ($P < 0.01$).

Statistical analysis showed that all chemical characteristic measures were significantly affected by site locality. Results showed that pH ranged from 7 to 8.3 in the top soils. As such, fifteen percent of the sites were rated as neutral to mildly alkaline with pH ranging from 7 to 7.9. The EC ranged from 143.2 to 297.7 µS cm^{-1} and was found higher, especially, in S10 and S14. In contrast, CE was very lower in S1 and S11. Soil $CaCO_3$ content across sites was low to medium, ranging from 1.8 to 42.6 % in top soils. Total-N in the different sites was evaluated as low to medium with values ranging from 0.7 to 2.9 g kg^{-1}. Olsen-P showed a large variation between sites which increased from 2.5 to 10.5 mg kg^{-1}. Av.P (Olsen-P) was lowest in S15, while the high Olsen-P content was observed in S6.

Biological properties of soils

Statistical analysis showed significant differences between all biological properties of soil samples. *TrPn*, *Pseudomonas* spp, *Bacillus* spp and ID-Foc varied significantly according to site locality (P<0.05). The ID-Foc varied between 3.25 × 10^3 and 29 × 10^3 Cfu g^{-1} soil. Seven fields showed a higher level of ID-Foc which varied from 12.25 × 10^3 to 29 ×10^3 Cfu g^{-1} soil. Based on the *Trichoderma* identification criteria, 439 *Trichoderma* isolates were found. *Trichoderma* isolates were mainly divided into eight species; *T. viride*, *T. harzianum*, *T. atroviride*, *T. virens*, *T. koningii*, *T. viridеisens*, *T. citrina*, *T. placentula* and T. *polysporum*. In the soil samples, *TrPn* varied between 3.75 ×10^3 to 13.75 × 10^3 Cfu g^{-1}soil (Figure 1a). Five fields showed a higher level of *TrPn*, varying from 13.25 to 13 × 10^3 Cfu g^{-1}soil. Based on biochemical, physiological and morphological properties, selected isolates were identified as *B. subtilis*, *B. circulans, B. lentus, B. aneurinilyticus, B. firmus and B. licheniformis.* Three species of *Pseudomonas* spp were identified including *P. aeruginosa, P. luteola* and *P. fluorescens*. Data analysis showed that *Pseudomonas* spp density varied between 1.4 to 14.88 ×10^7 Cfu g^{-1} soil (Figure 1b). Highest values were recorded in S1, S2 and S3. However, *Bacillus* spp density varied between 2.35×10^7 and 40.86 ×10^7 Cfu g^{-1} soil (Figure 1b).

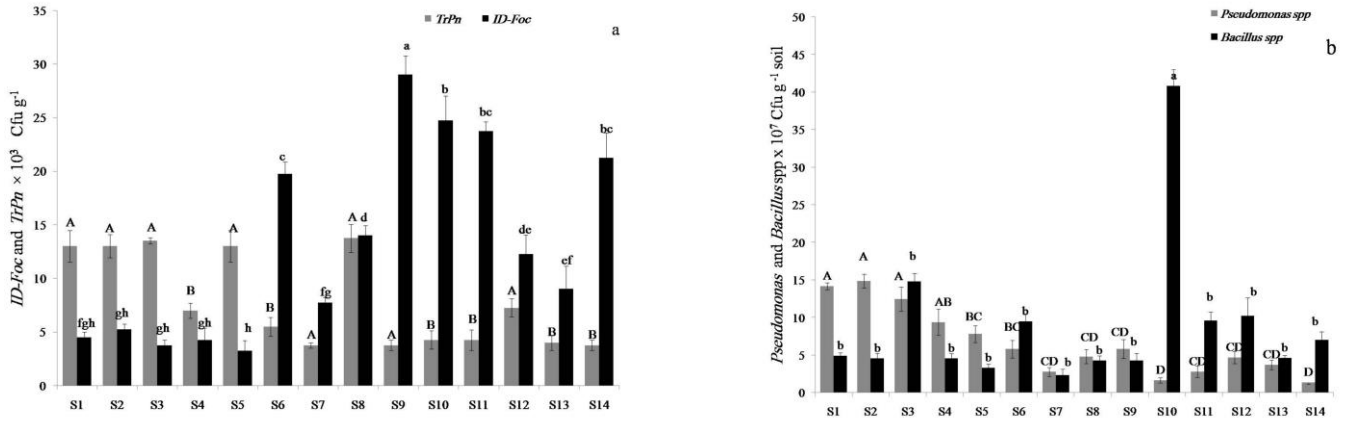

Figure 1. Biological properties of different soil from chickpea fields in Algeria a) ID- Foc and TrPn (expressed as Cfu g^{-1} soil); b) Total Pseudomonas spp and Bacillus spp communities. Data marked by different letters in a column indicate significant difference at P = 0.05 level according to Tukey test.

Disease assessment

Visual observation of symptoms in the field showed that contaminated plants exteriorize wilted or yellowed beaches (Figure 2a,b). The typical symptoms of wilting appeared mainly on the upper part of the leaves, then quickly gained the whole plant and finished with the death of the plants. In late attack, plants showed atypical symptoms of the disease where partial yellowing of the plants appeared at the lower part and then progressed to the upper part. It was found that the disease is widespread in all studied areas and his prevalence was 100%. The *Dis* values for each plot were presented in Figure 3. According to ANOVA, higher significant difference between D*is* values and soils locality was obtained (P<0.0001). The *Dis* revealed low to very high level with an average ranging between 2.05 in S1 to 39.83 in S10.

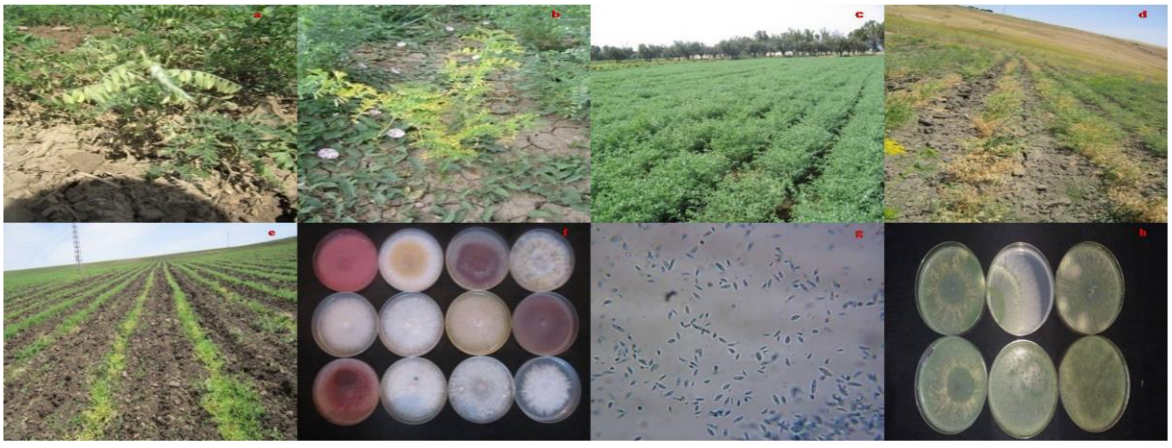

Figure 2. Symptoms of Fusarium wilt regarded in different fields (a- Typical symptoms b- atypical symptoms. Disease wilt regarded in different fields with different intensity (c, d and e). Morphotypical variation in Foc isolates obtained from wilted chickpea (f). Microscopic observation of Foc (g). Variation in Trichoderma isolates (h).

F. oxysporum and *F. solani* were most consistently isolated from stems showing symptoms of yellowing and wilting. Quantitative analysis of the fungi isolated from the stems effectively showed dominance of the *F. oxysporum* species with a rate of 95.14%. Nevertheless, a low occurrence was recorded for *F. solani* (4.86%). The selected Foc isolates (Figure 2f,g) obtained from the different wilted plants and soils completely expressed the symptoms of vascular wilt after inoculation of the latter on the susceptible variety ILC 482. Thus, isolates inoculated with this variety are certainly special forms *ciceri*, and constitute the isolates responsible for the vascular wilt of chickpea, noticed *in vivo*.

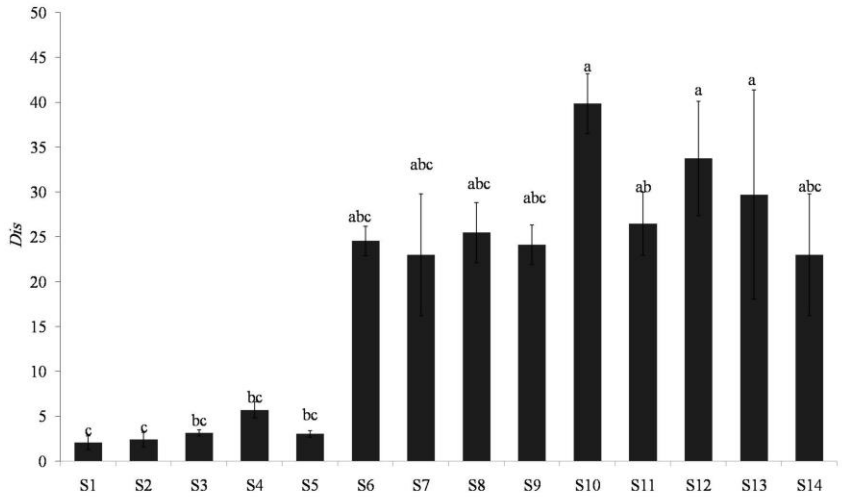

Figure 3. Evaluation of disease Index severity (Dis) of Fusarium wilts of chickpea in 14 investigated field during 2015 in North Algeria. Data were obtained in maturation point. Values represent the mean of four replicates ± SE (standard errors). Values of probability of one-way ANOVA (Site treatment).Data marked by different letters in a column indicate significant difference at $P < 0.0001$.

Relationship between wilt disease and soil properties

Relationship between soil physicochemical and biological properties and *Dis*

PCA plots represented the 14 experimental sites which were distributed normally according to 13 physicochemical and biological soil properties in relation to the disease index severity of wilt disease (Figure 4). The first and second ordination axis accounted for 41.19 and 28.96% of the total variance, respectively. Based on PCA analysis, Olsen-P, Total-N, ID-Foc, *Dis*, *TrPn* and *Pseudomonas* spp clustered together toward of the right side of the biplot, whereas loam, clay, sand, pH, EC, $CaCO_3$, and *Bacillus* spp were clustered at the opposite side. The D*is* was negatively correlated to Olsen-P, *TrPn, Pseudomonas* spp, and positively correlated to soil EC, ID-Foc and Total-N.

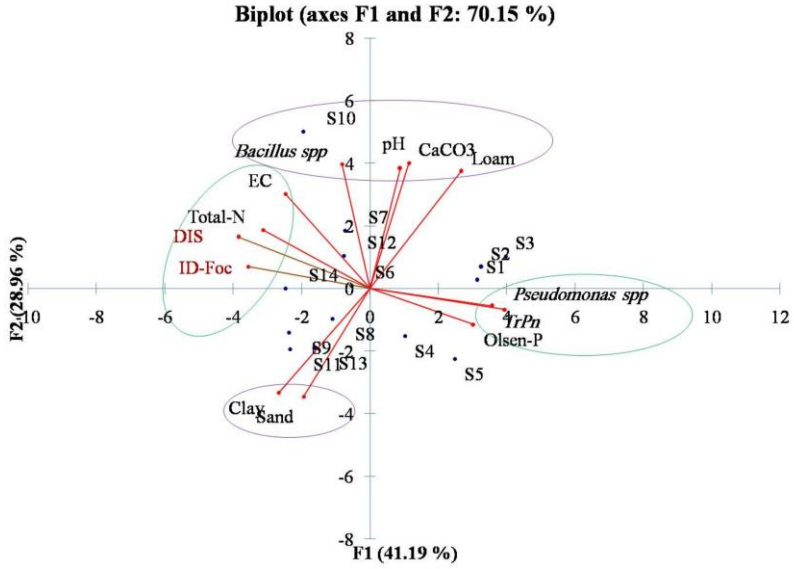

Figure 4. Principal component analysis of 14 chickpea fields: correlations among physicochemical (Laom, sand, Clay, olsen-P, Total-N, pH, CE) and biological characteristics (*Bacillus* spp, *Pseudomonas* spp, ID-Foc, *TrPn*) and D*is*. F1 accounted for 41.19% of the variance, and F2 accounted for 28.96%.

The Pearson correlation analysis (Table 2) of the total data from the 14 soil samples confirmed the results of PCA analysis and showed that D*is* was positively associated with EC, Total-N rate and ID-Foc, whereas negatively correlated with Olsen-P, *TrPn* and *Pseudomonas* spp. There was no correlation between D*is* and soil physical parameters (Loam, clay, and sand), chemical parameters (pH, $CaCO_3$ content) and biological factors (*Bacillus spp*). The analysis carried on EC showed a positive correlation with D*is* (r=0.62**). The increase in EC significantly increased D*is*, this was particularly evident in S7 and S8, where EC values were 285.72 and 216.28 µS cm^{-1}, respectively. While, low EC and D*is* values were recorded in S1 and S2. The studied soils showed a highly significant positive correlation between Total-N rate and D*is* (r= 0.79***). Accordingly, highest D*is* was observed in plots with a high concentration of Total-N particularly in S10 and S12. The results showed that Olsen-P deficiency increased significantly D*is* values, there was a negative relationship between Olsen-P and D*is*values (r = -0.67**). Analysis of S6 and S14 plots also showed lowest values of Olsen-P with values of 2.64 and 2.58 mg kg^{-1}, respectively. However, D*is* values were higher in the same sites. Pearson correlation indicated that D*is* was positively correlated with ID-Foc. Increased rate of ID-Foc increased significantly D*is*. The correlation analysis showed that *TrPn* were negatively correlated with D*is* (r=-0.70***). D*is* values decreased with the increase of *TrPn*. This was observed in S1and S2, while, D*is* values increased in S10 and S12 when the *TrPn* decreased. Analysis of bacterial outcomes, especially, *Pseudomonas* spp with Pearson correlation showed a negative correlation with D*is* (r=-0.89***). The results revealed highest concentrations of *Pseudomonas* spp in S2 and S3 while D*is* were lowest in same sites. In contrast, highest values of D*is* were observed both in S10 and S13 with lowest levels of *Pseudomonas* spp.

Relationship between soil physicochemical and biological parameters with ID-Foc

The correlation analysis showed that soil ID-Foc was significantly affected by Olsen-P, Total-N and *TrPn* (Table 2). Data showed that ID-Foc was positively correlated with the level of Total-N and negatively correlated with contents of Olsen-P. It was found that the rate of Total-N affected significantly ID-Foc in the soil, where a positive correlation was observed (r=0.56*). In fact, high levels of Total-N significantly increased ID-Foc. Inversely, the rate of Olsen-P was negatively correlated with ID-Foc (r=-0.58*). High level of Olsen-P significantly decreased ID-Foc. The latter significantly decreased in S6 and S14 when compared to S5 and S3. The results showed that *TrPn* were also negatively correlated with ID-Foc (r=- 0.65**). The concentration of ID-Foc decreased when *TrPn* increased. This was observed in S3 and S5 with high *TrPn* values. Otherwise, a negative correlation between ID-Foc and *Pseudomonas* spp (r =-0.65*) was recorded. These findings can be noticed in S1 and S2 with high rates of *Pseudomonas* spp.

Correlation of *TrPn* and *Pseudomonas* spp with soil characteristics

There was no correlation between *TrPn* and physical factors of soil (soil bulk), chemical factors (pH) and biological factors (*Bacillus spp*). Moreover, significant positive correlations were found between EC (r=-0.54*), Olsen-P (r=0.55*) and *TrPn*. The detailed summary of physical, chemical, and biological factors of the soils affecting *Pseudomonas* spp population was given in Table 2. The bacterial activity was negatively correlated with CE and Total-N. However, there was a positive correlation between *Pseudomonas* spp and *TrPn*.

Discussion

This study aimed to determine the impact of physicochemical and biological properties of soils on *Fusarium* wilt disease in chickpea growing in North-Algeria areas under commercial production conditions. A geographical variation in the occurrence of wilt chickpea was observed during the survey, with an important predominance of the disease in the investigated areas. The obtained result showed variation in disease levels within large geographical area which indicates that the soil physicochemical and biological proprieties affected significantly the ID-Foc and consequently the D*is*. The presence of Foc in the field can be irregular because of the nature of its dissemination and the variability of soil properties. Moreover, the variation of population size of Foc and D*is* in the studied fields might be attributed to variations in physicochemical and biological soils factors. The correlation analysis of 14 field's data showed that D*is* was positively correlated with EC, Total-N and ID-Foc, and negatively correlated with Olsen-P, *TrPn* and *Pseudomonas* sp. There was no correlation between D*is* and clay, loam, sand, pH, $CaCO_3$ and *Bacillus*.

The information regarding the effect of soil EC on Foc population and disease severity has been neglected. In our study, EC was positively correlated to D*is* and ID-Foc. This was probably due to the favorable environment for conidia germination and mycelium growth of Foc. Shim et al. (2002) reported a positive correlation between EC and germination rate of macroconidia and a consequent increase disease incidence of cucumber *Fusarium* wilt. In experimental conditions, results obtained by Naseri and Hamadani (2017) provided the importance of soil EC, as a population indicator for *F. oxysporum* in the soil under bean production conditions.

Table 2. Pearson correlations among Dis, soil physicochemical (Laom, Sand, Clay, Olsen-P, Total-N, pH, EC) and biological characteristics (*Bacillus* spp, *Pseudomonas* spp, ID-Foc, *TrPn*). The analysis is based on the total data set of 14 field plots analyzed during 2015.

	Loam	Clay	Sand	pH	EC	Olsen-P	N	$CaCO_3$	*Trichoderma spp*	*Bacillus spp*	*Psudomonas spp*	ID-Foc	*Dis*
Loam	1.00												
Clay	**-0.94*****	1.00											
Sand	**-0.83*****	**0.60*****	1.00										
pH	0.49^{ns}	-0.40^{ns}	-0.52^{ns}	1.00									
CE	0.05^{ns}	-0.01^{ns}	-0.10^{ns}	0.30^{ns}	1.00								
Olsen-P	0.26^{ns}	-0.26^{ns}	-0.19^{ns}	-0.14^{ns}	-0.37^{ns}	1.00							
Total-N	-0.22^{ns}	0.25^{ns}	0.11^{ns}	0.14^{ns}	0.52^{ns}	**-0.59***	1.00						
$CaCO_3$	**0.58***	**-0.59***	-0.40^{ns}	**0.78*****	0.35^{ns}	-0.05^{ns}	0.20^{ns}	1.00					
Trichoderma spp	0.43^{ns}	-0.48^{ns}	-0.23^{ns}	-0.03^{ns}	**-0.54***	**0.55***	-0.44^{ns}	0.15^{ns}	1.00				
Bacillus spp	0.47^{ns}	-0.42^{ns}	-0.43^{ns}	0.37^{ns}	0.43^{ns}	-0.13^{ns}	0.31^{ns}	**0.39***	-0.20^{ns}	1.00			
Pseudomonas spp	0.43^{ns}	-0.36^{ns}	-0.44^{ns}	0.19^{ns}	**-0.66****	**0.54***	**-0.65***	0.16^{ns}	**0.76*****	-0.30^{ns}	1.00		
ID-Foc	-0.35^{ns}	0.48^{ns}	0.03^{ns}	-0.20^{ns}	0.51^{ns}	**-0.59***	**0.56***	-0.27^{ns}	**-0.65***	0.40^{ns}	**-0.65***	1.00	
Dis	-0.25^{ns}	0.25^{ns}	0.20^{ns}	-0.04^{ns}	**0.62***	**-0.67****	**0.79*****	-0.07^{ns}	**-0.70****	0.46^{ns}	**-0.87*****	**0.72****	1.00

The table showed Pearson correlation coefficients and their level of significance. Pearson's correlation coefficients (r) are calculated by monowise comparison. Asterisks "*. ** and ***"denote significant difference at P< 0.05 and P < 0.01, respectively.

Nitrogen has been intensively studied in relation to host nutrition and disease severity because of its essential requirement for plant growth and its limited availability in soil (Ghorbani et al., 2008). The availability of N probably increased greatly the sporulation and mycelial growth of Foc isolates. Most studies on the effect of soil N on fungus sporulation have reported that high N content in the soil enhances sporulation of telluric pathogenic plant (Hoffland et al., 2000). Otherwise, abundant N enhanced succulent growth, prolonged vegetative period, and delayed maturity of the plant, which increased the period of susceptibility to pathogens (Ghorbani et al., 2008). In the present study, a positive correlation was obtained between Total-N, ID-Foc and *Dis*. A similar result was obtained by Sugha et al. (1994) who reported that the increase of N rate favored the frequency of wilt disease.

There are many researchers associating the level of soil P to the crop disease development. Ghorbani et al. (2008) reveled that subsequent careful monitoring and management of available P and its equilibrium with other nutrients could be considered as an important strategy for crop disease control. In the present study, a negative correlation was obtained between Olsen-P, ID-Foc and *Dis* of wilt disease in chickpea. These results could probably be explained by the indirectly role of Olsen-P in the inhibition of conidial germination and mycelial growth of Foc by enhancing biological control agents. Our results showed that Olsen-P was positively correlated with *Pseudomonas* spp. This is in agreement with the observations reached by Postma et al. (2013) who found that high P availability improved by *Pseudomonas chlororaphi* were able to control *P. aphanidermatum* and *F. oxysporum* f. sp. *radicis-lycopersici* in tomato plants. Prabhu et al. (2007) reported that improved root development by P nutrition may induce the plant to 'escape' attack by soil-borne fungal pathogens.

In our result a negative correlation between ID-Foc, D*is* and *TrPn* was observed, suggesting that *Trichoderma* species participate in the process of natural disease management. Indeed, Species of *Trichoderma* spp are probably limited sporulation and growth of Foc via various mechanisms such as hyperparasitism, antibiosis and induction of host resistance or through a combination of such mechanisms (Dubey et al., 2007). Otherwise, mineral nutrition is indispensable for growth and, within a narrower range, stimulatory of fungal secondary metabolism (Griffin, 1994). In this study, a positive relationship was recorded between Olsen-P and *TrPn*. The highest rate of Olsen-P in soil represents a positive factor for the growth and the antagonistic activity against Foc. This is in accordance with previous findings reporting that *Trichoderma* species increasing significantly the concentration of soluble phosphate (Saravanakumar et al., 2013).

Pseudomonas spp has habitually been showed to be responsible for the natural suppression of *Fusarium* wilt disease (Mazzola, 2002). In the present study, *Pseudomonas* spp strains were negatively correlated with D*is*, and contribute to the disease suppression of chickpea *Fusarium* wilt disease. The mechanism of action would be through direct antagonism such as production of bioactive metabolites, rapid exploitation of root exudates, colonization and multiplication in the environment and aggressive antagonism with other microbes (Thomashow and Weller, 1988). Abed et al. (2016) tested *Pseudomonas* spp for their antagonism ability against Foc *in vitro* conditions. The results showed a great variability in inhibiting mycelial growth of Foc isolates. The ability of bacterial *Pseudomonas* spp strains varied in terms of production of protease, gelatinase, amylase, cellulase, AIA, lipase, catalase and cyanid Hydrogen. The results obtained by Saikia et al. (2009) demonstrated that the strain of *Pseudomonas* controlled the severity of wilt disease of chickpea by systemically inducing resistance against *Fusarium* wilt of chickpea and decreased the disease severity up to 26–50% as compared to control.

The results obtained in this study showed a positive correlation between *TrPn* and *Pseudomonas* spp strains and both were negatively correlated with ID-Foc and D*is*. In a controlled experiment Liu et al. (2008) demonstrated that the incidence of Southern blight of tomato decreased while the *TrPn* and *Pseudomonas* spp increased.

Conclusion

In conclusion, the results from this study confirmed a great influence of soil physicochemical and biological characteristics in the occurrence and severity of the epidemic *Fusarium* wilt of chickpea. These results contribute in order to develop more efficient management strategies and exploitation of soil nutrients that might be indispensable in the context of an integrated pest management strategy and may even contribute significantly to reduce the abusive fungicides and synthetic fertilizers utilization.

References

Abed, H., Rouag, N., Mouatassem, D., Rouabhi, A., 2016. Screening for Pseudomonas and Bacillus antagonistic rhizobacteria strains for the biocontrol of Fusarium wilt of chickpea. *Eurasian Journal of Soil Science* 5(3): 182 – 191.

Bulluck, L.R., Brosius, M., Evanylo, G.K., Ristaino, J.B., 2002. Organic and synthetic fertility amendments influence soil microbial, physical and chemical properties on organic and conventional farms. *Applied Soil Ecology* 19(2): 147–160.

Dubey, S.C., Suresh, M., Singh, B., 2007. Evaluation of Trichoderma species against Fusarium oxysporum f. sp. ciceris for integrated management of chickpea wilt. *Biological Control* 40(1): 118–127.

Elmer, W.H., Datnoff, L.E., 2014. Mineral Nutrition and Suppression of Plant Disease. In: Neal VA. Encyclopedia of Agriculture and Food Systems, San Diego, Elsevier, pp 231–244.

Gams, W., Bissett, J., 1998. Morphology and Identification of Trichoderma. In: Kubicek C.P, Harman G.E. Trichoderma and Gliocladium. Basic Biology, Taxonomy and Genetics. London, Taylor and Francis Ltd, pp1–30.

Ghorbani, R., Wilcockson, S., Koocheki, A., Leifert, C., 2008. Soil management for sustainable crop disease control: a review. *Environmental Chemistry Letters* 6(3):149–162.

Griffin, D.H., 1994. Fungal Physiology, 2nd.New York, New York, USA, Wiley-Liss.

Haware, M.P., 1990. Fusarium wilt and other important diseases of chickpea in the Mediterranean area. Options Mediterr. Ser. Semin 9: 61–64.

Hoffland, E., Jeger, M.J., van Beusichem, M.L., 2000. Effect of nitrogen supply rate on disease resistance in tomato depends on the pathogen. *Plant and Soil* 218(1-2): 239–247.

Höper, H., Alabouvette, C., 1996. Importance of physical and chemical soil properties in the suppressiveness of soil to plant diseases. *European Journal of Soil Biology* 32(1): 41-58.

Hulseman, J., 1966. An inventory of marine carbonate materials. *Journal of Sedimentary Research* 36(2): 622– 625.

Jiménez-Díaz, R.M., Castillo, P., Jiménez-Gasco, M.M., Landa, B.B., Navas-Cortés, J.A., 2015. Fusarium wilt of chickpeas: Biology, ecology and management. *Crop Protection* 73: 16–27.

Jones, Jr.J.B., 2001. Laboratory guide for conducting soil tests and plant analysis. CRC Press, New York, USA. 363p.

Lemanceau, P., Alabouvette, C., 1996. Suppression of fusarium wilts by fluorescent pseudomonads: Mechanisms and applications. *Biocontrol Science and Technology* 3(3): 219–234.

Lenc, L., Kwaśna, H., Sadowski, C., 2011. Dynamics of the root/soil pathogens and antagonists in organic and integrated production of potato. *European Journal of Plant Pathology* 131: 603–620.

Liu, B., Deborah, G., Buckley, K., 2008. Trichoderma communities in soils from organic, sustainable, and conventional farms, and their relation with Southern blight of tomato. *Soil Biology and Biochemistry* 40(5): 1124–1136.

Lucas, P., 2006. Diseases caused by soil-borne pathogens. In: The Epidemiology of Plant Diseases. Cooke, B., Michael, Jones, D., Gareth, Kaye, Bernard (Eds.). Dordrecht, The Netherlands, Springer, pp 373–382.

Mazzola, M., 2002. Mechanisms of natural soil suppressiveness to soilborne diseases. *Antonie van Leeuwenhoek* 81(1-4): 557–564.

Mehmood,Y., Khan, M.A., Javed, N., Arif, M.J., 2013. Effect of soil and environmental factors on chickpea wilts disease caused by Fusarium oxysporum f. sp. ciceris. *Pakistan Journal of Phytopathology* 25 (1): 52–58.

Messiaen, CM., Cassini, R., 1981. Taxonomy of Fusarium. In: Fusarium. Diseases, biology and taxonomy. Nelson P.E., Toussoun T.A., Cook, R.J. (Eds). Pennsylvannia State University Press. University park, pp 427–445.

Naseri, B., Hamadani, S.A., 2017. Characteristic agro-ecological features of soil populations of bean root rot pathogens. *Rhizosphere* 3: 203–208.

Nene, Y.L., Haware, M.P., 1980. Screening chickpea for resistance to wilt. *Plant Disease* 64(4): 379–380.

Olsen, S.R., Cole, C.V., Watanabe, W.S., Dean, L.A., 1954. Estimation of available phosphorus in soil by extraction with sodium bicarbonate. Circular 939.USDA, Washington DC, USA.

Postma, J., Clematis, F., Nijhuis, E.H., Someus, E., 2013. Efficacy of four phosphate-mobilizing bacteria applied with an animal bone charcoal formulation in controlling Pythium aphanidermatum and Fusarium oxysporum f.sp. radicis lycopersici in tomato. *Biological Control* 67(2): 284–291.

Prabhu, A.S., Fageria, N.K., Berni, R.F., Rodrigues, F.A., 2007. Phosphorus and plant disease. In: Mineral Nutrition and Plant Disease. Datnoff, L.E., Elmer, W.H., Huber, D.M. (Eds.), APS Press, St. Paul, Minnesota, USA. pp. 45–55.

Saikia, R., Varghese, S., Singh, B.P., Arora, D.K., 2009. Influence of mineral amendment on disease suppressive activity of Pseudomonas fluorescens to Fusarium wilt of chickpea. *Microbiological Research* 164(4): 365–373.

Saravanakumar, K., Shanmuga, A.V., Kathiresan, K., 2013. Effect of Trichoderma on soil phosphate solubilization and growth improvement of Avicennia marina. *Aquatic Botany* 104: 101–105.

Shen, Z., Ruan, Y., Xue, C., Zhong, S., Li, R., Shen, Q., 2015. Soils naturally suppressive to banana Fusarium wilt disease harbor unique bacterial communitie. *Plant and Soil* 393(1-2): 21–33.

Shim, G.Y., Kim, H.K., Kang, S.W., 2002. Predisposing effect of soil salinity on the cucumber wilt caused by Fusarium oxysporum f. sp. cucumerinum. *Korean Journal of Plant Pathology* 8 (1): 14–21.

Sugha, S.k., kapoor, S.k., Singh M.B., 1994. Factors influencing Fusarium wilt of chickpea (Cicer arietinum). *Indian Journal of Mycology and Plant Pathology* 24 (2): 97–102.

Thomashow, L.S., Weller, D.M., 1988. Role of a phenazine antibiotic from Pseudomonas fluorescens in biological control of Gaeumannomyces graminis var. tritici. *Journal of Bacteriology* 170(8): 3499–3508.

Trapero-Casas, A., Jiménez-Díaz, RM., 1985. Fungal wilt and root rot diseases of chickpea in Southern Spain. *Phytopathology* 57: 1146–1151.

Eurasian J Soil Sci 2019, 8 (4) 313 - 320

Eurasian Journal of Soil Science

Journal homepage : http://ejss.fesss.org

Neem leaf and poultry manures soil amendment on growth and yield of Telfairia occidentalis

Norah Godwin Ekanem *, Leonard Itsede Akpheokhai

Department of Crop Science, Faculty of Agriculture, University of Uyo, Nigeria

Abstract

Telfairia occidentalis is a widely used leafy and seed vegetable in West Africa and adequate soil fertility management is essential for its higher productivity. Field experiments were conducted on neem leaf and poultry manures soil amendment to assess the growth and yields of *Telfairia occidentalis* between 2013 and 2014 cropping seasons. The experiment was laid out in a randomised complete block design with four replications to include 5 t ha^{-1} of neem leaf manure (NLM), 5 t ha^{-1} of poultry manure (PM), 2.5 t ha^{-1} of neem leaf manure plus 2.5 t ha^{-1} of poultry manure (NLM+PM) and control. Data collected on vegetative and yield related components were subjected to analysis of variance at $p \leq 0.05$ significance level. The results showed that number of leaves, vine length, leaf area and number of branches increased significantly ($p \leq 0.05$) in plants treated with NLM, PM and NLM+PM from 2-5 months after planting (MAP) compared to control. At five MAP, NLM+PM significantly ($p \leq 0.05$) produced more leaves (52.5; 56.4), longer vines (473.0; 488.4cm), more branches (14.6; 16.3) compared to sole treatment and control. In addition, foliar yield (4.29; 4.94 t ha^{-1}), number of pods/plant (3.09; 4.11), length of pods (72.80; 81.60cm), number of seeds/pod (87.62; 89.51), seeds yield (61.60; 62.54 t ha^{-1}) and pod yield (49.85; 50.15 t ha^{-1}) produced were higher in plants treated with combined manures in the two cropping seasons. The applied combined manures (neem leaf and poultry) could be exploited for soil improvement and sustainable yield increase of *Telfairia occidentalis* production.

Keywords: Fluted pumpkin, organic source, growth characters, yield components.

Article Info

Received : 31.10.2018
Accepted : 07.07.2019

Introduction

Fluted pumpkin (*Telfairia occidentalis* Hook F.) belongs to the family of cucurbitaceae. It is an herbaceous perennial cucurbit which climbs by means of coiled tendrils and bears large fruits (pods) of various sizes (Akoroda, 1986, 1990). It is widely cultivated across West Africa for its nutritional values and palatability (Longe et al., 1983; Axtell, 1992). The succulent young shoots and leaves are used in preparing various vegetable soups depending on the ethnic group. The seeds also are premium part of the crop in local diets of south-eastern region of Nigeria (Orluchukwu and Ossom, 1988). Akoroda (1990) reported that the production of vegetables have been found to be viable and profitable to farmers not only as a garden crop but also as commercial crop. In vegetables cultivation, organic fertilizer contributes to increase in yield by up to 80% depending on the rate of application (Olasantan, 1994; Ogbonna, 2008). The use of organic manures on agricultural lands is advantageous in nutrient recycling, improving soil structure and promoting biological activities of the soil thereby improving overall soil health, enhanced growth and productivity of crops (Arisah et al., 2003). Sometimes, application of organic manure serves as an alternative practice to mineral fertilization and improving soil structure (Idem et al., 2012). In most tropical soil, organic manure has become the determinant for improving soil fertility (Ikpe and Powel, 2002; Uwa, 2013).

According to Agyarko et al. (2006), soil nutritional status increased with addition of poultry manure and increasing levels of neem leaves in vegetable production across West Africa (Lombin et al., 1991). Neem

* Corresponding author.
Department of Crop Science, Faculty of Agriculture, University of Uyo, Nigeria
Tel.: +234 (0) 7030146317
E-mail address: norahgodwin75@yahoo.com
e-ISSN: 2147-4249
DOI: 10.18393/ejss.589439

leaves could be used for the preparation of vermin-compost having both fertilizer and pesticidal potential (Vethanayagam and Rajendran, 2010; Oyekunle and Abosede, 2012). Neem extract has been known to increase fruit weight and diameter of tomatoes (Moyin-Jesu et al., 2012). The phyto-chemicals such as liminoids in neem has demonstrated a dual purpose potential for bio-fertilizer source when ploughed into the soil; improves soil fertility and protects plant roots from nematodes and whiteflies in tomatoes production (Moyin-Jesu et al., 2012). Neem leaf manure (NLM) is gaining popularity due to being environmental friendly and could as well increase nitrogen and phosphorus content of the soil (Lokanadhan et al., 2012; Oyekunle and Abosede, 2012). Globally, growing awareness on health and environmental issues associated with the intensive use of inorganic inputs has led to interest in alternate forms of agriculture (FAO, 1999). Therefore, organic cropping system could be a way of ensuring a healthy agro-ecosystem, including concerns on biodiversity, biological cycles and soil biological activity. Awareness of crop quality and soil health has accelerated the attention of people towards organic farming (Sharma et al., 2008). Balanced use of nutrients through organic sources like farm yard manure, poultry manure (PM), vermicompost, green manuring, neem cake and biofertilizers, are prerequisites for sustaining soil fertility and producing maximal crop yields with optimal input levels (Dahiphale et al., 2003). Organic carbon build-up is increased when organic matter is applied to soil as organic manures leave behind residues in sufficient quantity for the next crop in the sequence (Singh et al., 1996; Baruah et al., 1999). In view of these, field experiments were conducted to evaluate the sole organic manure or combined organic manures soil amendment on growth and yield of fluted pumpkin.

Material and Methods

Description of pilot study area

The trial was carried out at the University of Uyo Teaching and Research Farm, Akwa Ibom State (Lat. $5^0$20´N and $5^0$30´ N, Long. $7^0$27´ E and 5´ 62 E at 68.0 m above sea level, average annual rainfall 2500 mm, relative humidity 79.8%, monthly mean temperature range: 26.88-32^0C (UCCDA, 1998), soil type: Ultisol, during the 2013 and 2014 cropping seasons (Agbede, 2015). The site had been under continuous cropping to various arable crops.

Soil sampling and analyses

Twenty-five core soil samples were collected randomly with a soil auger at the depth of 0-15 cm and 15-30 cm. The soil samples were thoroughly mixed, bulked, air dried, crushed with mortar and pestle and sieved using a 2 mm mesh sieve for physicochemical analyses in various methods described by Bouyoucos (1962), McLean (1965), Jackson (1967), Syers et al. (2012), AOAC (2016) and de Souza et al. (2016).

Collection and analysis of experimental materials

Neem leaves were obtained from Pharmacy Research Farm, University of Uyo. Poultry manure was obtained from Okpon Farm, Uyo. The pumpkin seeds were obtained from University of Uyo Teaching and Research Farm, Use Offot. Neem leaves and poultry manure samples were analysed for some physicochemical properties such as organic matter, nitrogen, potassium, calcium, magnesium, sodium in addition to percentages of sand, silt and clay.

Fresh neem leaves collected were chopped into bits using a knife, air-dried for five days and milled into powder with a mortar and pestle in the Pathology Laboratory, Department of Crop Science, University of Uyo. Similarly, poultry manure was air-dried for five days in the Screenhouse, Department of Crop Science, University of Uyo. Milled neem powder and poultry manure were thoroughly mixed in a 1:1 ratio to obtain 5tha^{-1} organic manure.

Field experiment and design

The land was manually cleared with a cutlass, ploughed, harrowed and beds were constructed according to Udoh et al. (2005). The beds were divided into four blocks and each block subdivided into four plots of 3 m x 2 m (6 m^2) each making a total of 16 plots separated by 1m furrow. Four treatments which include neem leaf powder applied at 5 t ha^{-1} (3 kg/plot), poultry manure applied at 5 t ha^{-1} (3 kg/plot), combined application (2.5 t ha^{-1} neem leaf manure plus 2.5 t ha^{-1} poultry manure) and control (no manure) were randomly incorporated into each plot before sowing. The experiment was laid out in a randomised complete block design (RCBD) and treatments replicated four times. One week later, two seeds of sun-dried fluted pumpkin were planted in a hole of 3 cm depth at 1 m x 1 m spacing giving a population of 12 plants per plot. Weeding was carried out regularly at 2, 5 and 12 weeks after planting. The experiment was repeated without any modification in order to validate the data. The plants were sprayed against insect pests using

Delthrin (content 100 g/ L cypermethrin E.C) at a rate of 50 ml to 20 ml of water using Knap-sack sprayer to control leaf defoliating insect. Four plants were randomly tagged per plot for data collection at 4, 8, 12, 16 and 20 weeks after planting (WAP).

Data collection

Data were collected on number of leaves/plant, vine length (cm) and leaf area (cm^2) by using the equation:

$$LA= 0.9467 + 0.2475\ LW + 0.9724\ LWN$$ (Akoroda, 1993);

where, LA = Leaf area, L = Length of the central leaflet, N= Number of leaflets in a leaf, W= Maximum width of the central leaflet and branches/plant.

At harvest, the length and diameter of pods (cm) were determined with a measuring tape, while the number of pods (fruits), number of ridges/pod, number of seeds/pod and seed yield (t ha^{-1}) were counted and recorded.

Statistical analysis

The trials were subjected to Analysis of Variance using Generalized Linear Models (GLM) of statistical analysis system 9.1 (SAS, 2002). Means were compared with Least Significant Difference (LSD) at 5% level of probability (Gomez and Gomez, 1984).

Results

The initial physicochemical properties that constituted soil fertility status were low before planting of *Telfairia occidentalis* during the two cropping seasons. The soil has low pH (5.50-5.80) values, which means that it is acidic. The organic matter (0.06 - 2.21%) and total nitrogen (0.05 – 0.06%) are low in soil fertility status compared with the recommended standard for organic matter and total nitrogen (Table 1) for crop production in Nigeria. Besides the low values obtained in exchangeable bases for magnesium (Mg) and sodium (Na), the soil texture was sandy loam (Table 1). The percentage composition of nutrients such as nitrogen (N), phosphorus (P), potassium (K), calcium (Ca) and magnesium (Mg) present in the various types of organic manures showed that nutrients in the mixture of milled neem leaves and poultry manure were significantly ($p \leq 0.05$) higher than those in the sole manure (neem leaves or poultry) used (Table 2). The lowest percentages of nutrients were present in milled neem leaves except sodium (Na) (1.56 and 1.61%) which was significantly ($p \leq 0.05$) higher than values in poultry manure and mixture of milled neem leaves and poultry manure applied (Table 2).

Table 1. Pre-planting physicochemical properties of experimental site

Parameters	2013		2014		Method of analysis
	Soil depths		Soil depths		
	0-15cm	15-30cm	0-15cm	15-30cm	
pH	5.50	5.70	5.66	5.80	pH meter
EC (dS/m)	0.08	0.05	0.06	0.06	Conductivity meter
Organic matter (%)	2.08	0.06	2.21	0.07	Dichromate oxidation
Total nitrogen (%)	0.05	0.05	0.06	0.05	Kjeldahl procedure
Available P (mg/kg)	20.16	6.05	22.09	7.14	Bray-P_1 method
Exchangeable K (cmol/kg)	0.08	0.08	0.12	0.06	Flame photometer
Exchangeable Ca (cmol/kg)	2.80	3.00	2.64	2.96	Flame photometer
Exchangeable Mg (cmol/kg)	1.10	1.14	1.30	1.41	AAS
Exchangeable Na (cmol/kg)	0.06	0.05	0.05	0.06	Flame photometer
CEC (cmol/kg)	6.62	6.85	6.55	6.68	Summation method
Base saturation (%)	65.65	67.59	53.60	58.47	Calculation
Sand (%)	90.60	86.60	88.50	80.70	Hydrometer method
Silt (%)	3.40	7.40	3.20	5.57	Hydrometer method
Clay (%)	6.00	6.00	6.21	6.54	Hydrometer method
Soil textural class	Sandy loam	Sandy loam	Sandy loam	Sandy loam	

At one month after planting (MAP), there was no significant difference ($p \geq 0.05$) in the number of leaves produced in plants treated with different manure and the control (Table 3). At three MAP, manure-treated *Telfairia occidentalis* significantly produced ($p \leq 0.05$) more leaves than the control. Plants treated with equal combination of milled neem leaf manure and poultry manure (NLM+PM) at 5 t ha^{-1} produced more leaves (37.2) followed by sole manure - poultry (33.1), neem leaf (30.8) (Table 3). At five MAP, similar trends in

leaf production were observed in manure treated plants (Table 3). The vine lengths of manure-treated plants were not significantly different ($p \geq 0.05$) at one MAP (Table 4). At five MAP, there were significant differences ($p \leq 0.05$) between the manure-treated plants and control. The longest vines were produced by the combination of NLM+PM at 5 t ha^{-1} (488.4 cm), followed by poultry manure at 5 t ha^{-1} (420.1 cm) and neem leaf manure (388.8 cm) at five MAP (Table 4).

From 1-2 MAP, there were no significant differences ($p \geq 0.05$) in the number of branches produced by manure-treated plants and the control (Table 5). However, equal combination of NLM+PM produced more branches (7.44 branches), followed by poultry manure (6.24 branches) and the least number of branches was produced by control (1.99) at three MAP (Table 5). At five MAP, number of branches produced in plants treated with NLM+PM increased significantly ($p \leq 0.05$) than poultry manure, neem leaf and the control (Table 5). The leaf area (cm^2) and foliar yield (t ha^{-1}) of manure-treated *Telfairia occidentalis* plants at five MAP were significantly ($p \leq 0.05$) better than the control (Tables 6 and 7). The leaf area of plants treated with poultry manure (64.48 cm^2) increased significantly ($p \leq 0.05$) than plants treated with combined sources (NLM+PM) (59.26 cm^2) and sole manure (neem leaf - 46.56 cm^2) (Table 6). Furthermore, manure-treated plants significantly ($p \leq 0.05$) produced more foliar yield than the control. The highest yield was obtained from equal proportion of NLM+PM (4.99 t ha^{-1}), followed by poultry manure (3.78 t ha^{-1}), neem leaf (3.33 t ha^{-1}) while the least foliar yield was obtained from control (1.92 t ha^{-1}) at three MAP (Table 7). In addition, manure-treated *Telfairia occidentalis* plants significantly ($p \leq 0.05$) produced more yield components (number of seeds/pod, length of pod (cm), pod diameter (cm), number of pods/plant, pod and seed yield (t ha^{-1}) at five MAP than the control (Table 8). The yield components of manure-treated and the control plants followed an increasing significant ($p \leq 0.05$) performance order: control < NLM < PM < NLM+PM (Table 8).

Discussion

Fluted pumpkin treated with organic manures at 5 t ha^{-1} revealed an increase in growth characters and yield-related components. This could be due to rapid availability and utilization of nitrogen for various internal processes in the plant in these treatments. Among the manure-treatments, equal combinations of neem leaf and poultry manures showed superiority in foliar yield and yield components and followed by sole application of poultry manure. Evidently, vegetative growth of manure-treated plants performed overwhelmingly better than control due to high availability of organic matter and nutrients in the soil for plant utilisation. Vimala et al. (2006) and Srinivasan et al. (2014) reported that the application of poultry manure and neem cake at 37.9 t ha^{-1} enhanced the rapid availability and utilisation of macro and micro nutrients in the soil significantly and consequently improve the uptake of nutrients such as nitrogen for various internal processes in cabbage. In addition, the lower significant values obtained in the control (no manure) could be attributed to low nutrients availability observed in the experimental plot. This observation agrees with the findings of Moyin-Jesu and Atoyosoye (2002) and Ogbonna (2008) that soil with low nutrients responded better to organic or inorganic fertilizer applications. Furthermore, poultry manure treated plants produced more leaves, increased vine length, more branches, increased foliar and seeds yield/ha better than the neem leaf manure treated fluted pumpkin. This is in contrast to the reports of Oyekunle and Abosede (2012) that neem manure could be preferred to poultry manure on its application to fluted pumpkin. The performance of poultry manure as shown on fluted pumpkin in this study could also be attributed to higher essential mineral components released for plant growth and development. Awodun (2007) demonstrated that poultry manure applied at 6 t ha^{-1} increased foliar growth and essential elements (N, P, K, Ca and Mg content) of fluted pumpkin in a field trial. The application of the combined poultry and neem leaf manures was superior in all growth and yield parameters evaluated compared with other treatments. In other words, their higher performance could also be attributed to high nutrients availability (N, P, K, Ca, Mg) compared to sole application of neem leaf and poultry manure. This corroborates the report of Moyin-Jesu et al. (2012) on superior performance of maize and watermelon treated with modified neem leaf extract in a field trial.

The organic-based soil amendment with neem leaf and poultry manures demonstrated higher effectiveness in the improvement of the experimental site. This finding agrees with Agbede (2015) which revealed that soil amendment could be utilized to enhance higher crop production. This also supports the reports of Schipper (2000) and Awodun (2007) that application of organic manures significantly influenced the growth and yield of fluted pumpkin.

Table 2. Mineral elements composition analysis of nutrient sources

Organic manure sources	2013						2014					
	N, %	P, %	K, %	Ca, %	Mg, %	Na, %	N, %	P, %	K, %	Ca, %	Mg, %	Na, %
Neem leaf	2.13	1.15	0.97	0.75	0.67	1.56	2.10	1.10	0.87	0.55	0.62	1.61
Poultry dropping	3.55	1.82	2.86	3.01	0.88	0.48	3.40	1.53	2.35	3.27	0.99	0.58
Neem leaf+ poultry	3.94	2.96	3.01	4.42	2.96	0.69	4.01	3.16	4.02	4.33	3.28	0.56
LSD ($p<0.05$)	0.41	0.96	0.33	1.15	0.45	0.55	0.40	0.84	0.31	1.11	0.40	0.63

Table 3. Influence of organic manure on the number of leaves per plant of *Telfairia occidentalis* in the field

Treatment	2013					2014				
	Months after planting (MAP)					Months after planting (MAP)				
	1	2	3	4	5	1	2	3	4	5
Neem leaf manure (5 t ha^{-1})	13.60	21.40	29.40	39.70	44.40	14.40	22.50	30.80	39.90	48.40
Poultry manure (5 t ha^{-1})	14.40	23.21	32.80	41.20	50.10	15.60	23.56	33.10	40.70	51.50
Neem leaf + poultry manure (2.5+2.5 t ha^{-1})	16.20	25.40	36.50	49.70	52.50	17.10	26.61	37.20	50.80	56.4
Control (0 t ha^{-1})	12.00	16.20	21.00	30.30	35.00	13.10	15.90	20.70	30.10	35.20
LSD ($p<0.05$)	ns	0.58	1.66	0.27	1.54	ns	0.59	1.66	0.38	1.46

NLM = Neem leaf manure; PM = poultry manure; ns = not significant

Table 4. Influence of organic manure on the vine length (cm) of *Telfairia occidentalis* in the field

Treatment	2013					2014				
	Months after planting (MAP)					Months after planting (MAP)				
	1	2	3	4	5	1	2	3	4	5
Neem leaf manure (5 t ha^{-1})	201.40	269.50	294.30	321.30	387.40	203.10	269.80	301.20	324.60	388.80
Poultry manure (5 t ha^{-1})	227.20	299.70	316.60	350.20	418.20	237.20	299.90	319.50	354.10	420.10
Neem leaf + poultry manure (2.5+2.5 t ha^{-1})	246.60	306.10	337.00	412.00	473.00	250.70	318.20	351.20	419.70	488.40
Control (0 t ha^{-1})	189.00	211.00	232.40	264.20	305.30	185.10	219.10	236.60	288.30	307.40
LSD ($p<0.05$)	ns	0.74	1.26	1.32	2.02	ns	0.78	1.32	1.57	2.12

NLM = Neem leaf manure; PM = poultry manure; ns = not significant

Table 5. Influence of organic manure on the number of branches in *Telfairia occidentalis* in the field

Treatment	2013					2014				
	Months after planting (MAP)					Months after planting (MAP)				
	1	2	3	4	5	1	2	3	4	5
Neem leaf manure (5 t ha^{-1})	0.18	1.74	5.30	6.65	10.40	0.17	1.81	6.30	6.71	11.60
Poultry manure (5 t ha^{-1})	0.22	2.25	5.74	9.42	11.20	0.24	2.27	6.24	9.48	10.90
Neem leaf + poultry manure (2.5+2.5 t ha^{-1})	0.27	2.98	6.45	13.20	14.60	0.37	2.62	7.44	14.60	16.30
Control (0 t ha^{-1})	0.11	1.20	1.97	3.24	5.10	0.14	1.41	1.99	4.14	6.11
LSD ($p<0.05$)	ns	ns	1.30	2.01	2.32	ns	ns	1.38	2.25	2.41

NLM = Neem leaf manure; PM = poultry manure; ns = not significant

Table 6. Influence of organic manure on leaf area (cm)^2 on *Telfairia occidentalis* in the field

Treatment	2013					2014				
	Months after planting (MAP)					Months after planting (MAP)				
	1	2	3	4	5	1	2	3	4	5
Neem leaf manure (5 t ha^{-1})	15.82	28.05	36.22	40.23	46.52	15.96	28.55	36.41	40.13	46.56
Poultry manure (5 t ha^{-1})	16.30	39.41	52.36	59.72	64.04	16.37	39.90	52.31	58.88	64.48
Neem leaf + poultry manure (2.5+2.5 t ha^{-1})	16.64	32.26	40.08	48.07	58.66	17.15	36.55	41.18	49.06	59.26
Control (0 t ha^{-1})	14.86	19.12	21.35	26.08	30.22	15.11	19.26	21.38	25.62	30.19
LSD($p<0.05$)	ns	ns	1.46	ns	2.05	ns	ns	1.55	ns	2.08

NLM = Neem leaf manure; PM = poultry manure; ns = not significant

Table 7. Influence of organic manure on foliar yield (t/ha) on *Telfairia occidentalis* in the field

Treatment	2013					2014				
	Months after planting (MAP)					Months after planting (MAP)				
	1	2	3	4	5	1	2	3	4	5
Neem leaf manure (5tha^{-1})	2.12	2.83	3.32	2.54	2.14	2.18	2.88	3.33	2.66	2.06
Poultry manure (5tha^{-1})	2.55	3.64	3.75	3.12	2.55	2.62	3.66	3.78	3.22	2.64
Neem leaf + poultry manure (2.5+2.5tha^{-1})	2.84	3.91	4.29	3.72	3.28	2.99	4.14	4.94	3.71	3.41
Control (0 tha^{-1})	0.90	1.00	1.60	1.20	0.81	0.88	1.07	1.62	1.40	0.62
LSD($p<0.05$)	0.54	1.02	0.83	0.06	1.03	0.53	1.04	0.92	0.08	1.05

NLM = Neem leaf manure; PM = poultry manure; ns = not significant

Table 8. Influence of organic manure on yield and yield component of *Telfairia occidentalis*

	2013						
	Yield components						
Treatment	No. of seed per pod	No. of ridges per pod	Length of pod (cm)	Pod dia-meter (cm)	No. of pods/ plant	Seed yield (tha^{-1})	Pod yield (tha^{-1})
Neem leaf manure (5 t ha^{-1})	58.24	10.00	54.51	43.21	2.40	39.26	30.00
Poultry manure (5 t ha^{-1})	66.50	10.00	67.63	54.02	2.50	46.73	38.37
NLM+PM (combined) (2.5 + 2.5 t ha^{-1})	87.62	10.00	72.80	65.20	3.09	61.60	49.85
Control (no manure)	35.81	9.30	40.12	33.64	1.10	13.84	16.22
LSD($p<0.05$)	0.84	Ns	0.46	0.24	0.02	0.04	0.98
	2014						
	Yield components						
Treatment	No. of seed per pod	No. of ridges per pod	Length of pod (cm)	Pod dia-meter (cm)	No. of pods/ plant	Seed yield (tha^{-1})	Pod yield (tha^{-1})
Neem leaf manure (5 t ha^{-1})	57.68	10.06	55.66	44.02	2.44	39.30	30.08
Poultry manure (5 t ha^{-1})	66.66	10.08	67.91	55.22	2.60	49.80	37.83
NLM+PM (combined) (2.5 + 2.5 t ha^{-1})	89.51	11.02	81.60	75.10	4.11	62.54	50.15
Control (no manure)	35.76	9.03	40.25	34.46	1.16	14.08	16.32
LSD($p<0.05$)	0.86	Ns	0.50	0.34	0.05	0.07	0.96

NLM = Neem leaf manure; PM = poultry manure; ns = not significant

Conclusion

The application of organic-based soil amendment promoted the growth characters, yield and yield-related components of fluted pumpkin production. Convincingly, the combined treatments applied was superior to sole treatments in yield and yield-related components evaluated. It further demonstrated that combined manure application improved soil fertility and enhanced the growth and yields of fluted pumpkin. These materials can easily be sourced locally by farmers for direct application to their farms for sustainable vegetable production.

Acknowledgements

The authors are grateful to Mr. O. Akpan, (Director, Okpon Farm), Mr. B. Etefia (Pharmacy Research Farm) and Mr. I. Ini (Soil Science Department) of University of Uyo for their technical support and cooperation.

References

Agbede, O.O., 2015. Assessment, development and conservation of soil fertility: Key to national food security, 1st Public Lecture organized by Landmark University, Omu-Aran, Kwara State, Nigeria. 50p. Available at [Access date: 31.10.2018]: https://eprints.lmu.edu.ng/id/eprint/497

Agyarko, K., Rwakye, P., Bonsu, M,, Osei, B., Frimpong, K., 2006. The effect of organic soil amendments on root-knot nematodes, soil nutrients and growth of carrot. *Journal of Agronomy* 5(4): 641-646.

Akoroda, M.O., 1986. Seed dessication and recalcitrance in *Telfairia occidentalis*. *Seed Science Technology* 14: 327-332.

Akoroda, M.O., 1990. Ethnobotany of *Telfairia occidentalis* (cucurbitaceae) among Igbos of Nigeria. *Economic Botany* 44(1): 29-39.

Akoroda, M.O., 1993. Non-destructive estimation of area and variation in shape of leaf lamina in the fluted pumpkin (Telfairia occidentalis). *Scientia Horticulturae* 53(3): 261-267.

AOAC, 2016. Association of Official Analytical Chemists (AOAC) International. Official methods of analysis. 20th Edition, Washington DC. USA.

Arisah, H.M., Gad, A.A., Younes, S.E., 2003. Responses of some pepper cultivar to organic and mineral nitrogen fertilizer under sandy soil condition. *Zag-Zag Journal of Agriculture Resources* 30:1675-1699.

Awodun, M.A., 2007. Effect of poultry manure on growth, yield and nutrient content of fluted pumpkin (Telfairai occidentalis Hook F.) *Asian Journal of Agricultural Research* 1(2): 67-73.

Axtell, B., 1992. Minor oil crops. Food and Agriculture Organisation (FAO)Agriculture Service Bulletin No. 94, Rome, Italy. Available at [Access date: 31.10.2018]: http://www.fao.org/3/X5043E/x5043E00.htm#Contents

Baruah, R., Haridev, T., Talukdar, N.C., 1999. Soil chemical properties as influenced by the application of fertilizers and farm yard manure (FYM). *International Journal of Tropical Agriculture* 17:153-158

Bouyoucos, G.J., 1962. Hydrometer method improved for making particle size analyses of soils. *Agronomy Journal* 54(5): 464-465.

Dahiphale, A.V., Giri, D.G., Thakre, G.V., Gin, M.D., 2003. Effect of integrated nutrient management on yield and yield contributing parameters of the scented rice. *Annal Plant Physiology* 17:24-26.

de Souza, D.M., de Oliveira Morais, P.A., Matsushige, I., Rosa, L.A., 2016. Development of alternative methods for determining soil organic matter. *Revista Brasileira de Ciência do Solo* Vol.40.

FAO, 1999., 1999. Guidelines for the production, processing, labelling and marketing of organically produced foods. Food and Agriculture Organisation (FAO), Rome, Italy. Available at [Access date: 31.10.2018]: http://www.fao.org/organicag/doc/glorganicfinal.pdf

Gomez, K.A., Gomez, A.A., 1984. Statistical Procedures for Agricultural Research. 2nd edition. John Wiley and Sons, New York. USA. 704p.

Idem, N.U.A., Ikeh, A.O., Asikpo, N.S., Udoh, E.I., 2012. Effect of organic and inorganic fertilizer on growth and yield of fluted pumpkin (Telfairia occidentalis, Hook F.) in Uyo, Akwa Ibom State, Nigeria. *Journal of Agriculture and Social Research* 12(2):74-84.

Ikpe, F.N., Powel, J.M., 2002. Nutrient cycling practices and changes in soil properties in the crop-livestock farming systems of western Niger Republic of West Africa. *Nutrient Cycling in Agroecosystems* 62(1): 37-45.

Jackson, M.L., 1967. Soil chemical analysis. Englewood Cliffs, Prentice Hall Inc. New York.

Lokanadhan, S., Muthukrishnam, P., Jeyaraman, S., 2012. Neem products and their agricultural applications. *Journal of Biopesticides* 5: 72-76.

Lombin, L.G., Adepetu, J.A., Ayolade, A.K., 1991. Organic fertilizer in the Nigerian agriculture, present and future, F.P.D.D Abuja, pp. 146-162.

Longe, O.G., Faniru, G.O., Fetuga, B.L., 1983. Nutritional value of the fluted pumpkin (*Telfaria occidentalis*). *Journal of Agricultural and Food Chemistry* 31(5): 989-992.

McLean, E.O., 1965. Aluminium In: Method of soil analysis Part 2 Chemical and microbiological properties. Black, C.A., Evans, D.E., White, J.L., Ensminger, L.E. and Clark, F.E. (Eds.). Agronomy No. 9, American Society of Agronomy, Madison Wisconsin, USA. p. 927-932.

Moyin-Jesu, E.I., Atoyosoye, B., 2002. Utilisation of agricultural wastes for the growth, leaf and soil chemistry composition of cocoa seedlings in the nursery. *Pertanika Journal of Tropical Agricultural Science* 25(1): 53-62.

Moyin-Jesu, E.I., Micah, O., Akinola, M.O., 2012. Comparative evaluation of modified neem leaf and wood ash extracts on soil fertility status growth and fruit yields of tomato (*Lycopersicon esulentum* L). *Global Journal of Bio-science and Biotechnology* 1(2):271-276.

Ogbonna, P.E., 2008. Effects of combined application of organic and inorganic fertilizer on fruits yield of eggplant (Solanum melongena). 42nd Annual Conference in Agricultural Society of Nigeria (ASN). 19-23 October 2008, Abakaliki, Nigeria. Book of Proceedings, pp.236-250.

Olasantan, F.O., 1994. Fertilizer use in vegetable production in Nigeria. *Outlook Agriculture* 23(3): 213-222.

Orluchukwu, J.A., Ossom, E.M., 1988. Effect of management practice on weed infestation, yield and nutrient concentration of the fluted pumpkin, Telfairia occidentalis Hook. *Tropical Agriculture* 65(4):317-320.

Oyekunle, O.J., Abosede, O.T., 2012. Growth, yield and nutritional compositions of fluted pumpkin (Telfairia occidentalis) as affected by fertilizer types on Ogbomoso, South West Nigeria. *Bulletin of Environment, Pharmacology and Life Sciences* 1(9):81-88.

SAS, 2002. SAS Institute, SAS User's Guide: Statistics, version 9.1e SAS Institute, Cary. NC. USA.

Schipper, R.R., 2000. African indigenous vegetables: an overview of the cultivated species. National Resources International Limited, Aylesford, United Kingdom. 214p

Sharma, M., Pandey, C.S., Mahapatra, B.S., 2008. Effect of biofertilizers on yield on nutrient uptake by rice and wheat in rice-wheat cropping system under organic mode of cultivation. *Journal of Eco-Friendly Agriculture* 3(1):19-23.

Singh, A., Singh, R.D., Awasthi, R.P., 1996. Organic and inorganic sources of fertilizers for sustained productivity in rice (Oryza sativa)-wheat (Triticum aestivum) sequences on humid hilly soils of Sikkim. *Indian Journal of Agronomy* 41: 191-194.

Srinivasan, R., Rao, K.J., Sailaja, V., Kalaivanan, D., 2014. Influence of organic manures and fertilizers on nutrient uptake, yield and quality in cabbage-baby corn cropping sequence. *Journal of Horticultural Sciences* (1):48-54.

Syers, J.K., Williams, J.D.H., Walker, T.W., 2012. The determination of total phosphorus in soils and parent materials. *New Zealand Journal of Agricultural Research* 11(4): 757-762.

Udoh, D.J., Ndon, B.A., Asuquo, P.E., Ndaeyo, N.U., 2005. Crop production techniques for the tropics. Concept Publication Ltd., Lagos, Nigeria. 464p.

Uwa, O., 2013. The Impact of organic and inorganic manure on the cultivation of pumpkin (Cucurbita maxima). *IOSR Journal of Pharmacy and Biological Sciences* 8(1):18-20.

UCCDA, 1998. Uyo Capital City Development Authority (UCCDA), Yearly Report of Uyo Capital City: Akwa Ibom State, Nigeria. pp.24-26.

Vethanayagam, S.M., Rajendran, S.M., 2010. Bioefficacy of neem insecticidal soap (NIS) on the disease incidence of bhendi, Abelmoschus esculentus (L.) Moench under field conditions. *Journal of Biopesticides* 3(1): 246-249.

Vimala, P., Illias, M.K., Sabbiah, H., 2006. Effect of rates of organic fertilizer on growth, yield and nutrient content of cabbage (Brassica oleracea var. capitata) grown under shelter. *International Symposium on Greenhouses, Environmental Controls and In-house Mechanization for Crop Production in the Tropics and Sub-Tropics - ISHS Acta Horticulturae* 710: 391-397.

Eurasian J Soil Sci 2019, 8 (4) 321 - 328

Eurasian Journal of Soil Science

Journal homepage : http://ejss.fesss.org

Estimation of soil loss by USLE Model using Remote Sensing and GIS Techniques - A Case study of Coastal Odisha, India

Ramasamy Srinivasan [a,*], Surendra Kumar Singh [b], Dulal Chandra Nayak [c], Rajendra Hegde [a], Muniasami Ramesh [a]

[a] ICAR-National Bureau of Soil Survey and Land Use Planning, Regional Centre, Hebbal, Bangalore, India
[b] ICAR- National Bureau of Soil Survey and Land Use Planning, Amravati Road, Nagpur, Maharashtra, India
[c] ICAR- National Bureau of Soil Survey and Land Use Planning, Regional Centre, Salt Lake, Kolkata, West Bengal, India

Abstract

Globally, Soil erosion is the major land degradation problem, which impacts seriously on economic and environmental status. Geospatial techniques support and provided quantitative approach to estimate soil erosion in different conditions. In the present study, Revised Universal Soil Loss Equation (RUSLE) integrated with GIS has been used to estimate soil loss in the part of coastal Odisha system. The study area, Ganjam block have undulating topography covering 0-35% slopes. The quantitative soil loss was estimated and classified into different classes and soil erosion map was generated. The soil erosion map is classified into seven classes from very slight (<5 t ha^{-1} yr^{-1}) to extremely severe (>80 t ha^{-1} yr^{-1}). The results indicate that 90.9% (22330 ha) of the study area falls in very low erosion category, which may be due to level topography and regular vegetation cover. The other erosion classes such as moderate, high and very high erosion occurred in the range of 2.12%, 2.23% and 1.49 %, respectively. The high soil erosion risk is spatially situated in the foothills and upper steep slope of the area. The results can certainly aid in implementation of soil management and conservation practices to reduce the soil erosion in the coastal Odisha regions of Eastern India.

Keywords: Soil erosion risk, land use, Remote sensing, GIS, coastal Odisha.

Article Info

Received : 18.01.2019
Accepted : 25.07.2019

Introduction

Soil erosion is one of the important land degradation problems in agricultural land and consider as critical environmental hazard in modern time, worldwide (Lu et al., 2003; Kim et al., 2005). It is one of the most serious problems as it removes plant essential nutrients from the top soil and increases natural level of sedimentation in rivers and reservoirs which in turn reduce their storage capacity and water availability to plants (Devatha et al., 2015).The coastal systems have different kind of ecological problems due to various anthropogenic and natural interventions and regular prone to different kinds of erosion, sedimentation, floods and cyclones (Vinayaraj et al., 2011; Monalisha and Panda, 2018).

Coastal ecosystems provide livelihood to around 60% of world's population. Overall about 50-70% of population lives in coastline covering only about 4% of earth's land (Poyya Moli and Balachandran, 2008). The coastal agro-ecosystem occupies 19.6 m ha (6.2%) area of land in India (Sehgal et al., 1992). About 14.2% of the total population of India lives in coastal areas. In coastal agro-ecosystem, with the increasing human and animal population, the competition between various land uses has become intensive. Besides, unsuitable land is brought under cultivation and thereby causing physical and chemical degradation on land (Renschler et al., 1999; Srinivasan et al., 2015). Odisha coast line has extended from east to southern, about 445 km (Bandyopadhyay et al., 1984). Besides, there is narrow strip of land of few km in width along the sea

* Corresponding author.
ICAR-National Bureau of Soil Survey and Land Use Planning, Regional Centre, Hebbal, Bangalore 560024, India
Tel.: +91 80-23412242 E-mail address: srinivasan.surya@gmail.com
e-ISSN: 2147-4249 DOI: 10.18393/ejss.598120

coast prone for salt problems (Chaudhary et al., 2008). The soil loss in the deltaic areas of Odisha is estimated to be 10-20 MT/ha/yr. (Singh et al., 1992).

Soil loss is accelerated by anthropogenic or human induced soil degradation (Bai et al., 2008). There are different steps of soil erosion viz. sheet, rill and gully involving detachment, transport, and accumulation of soil particles in catchment area, which deteriorating the soil quality as well as reducing the productivity of potential lands (Tideman, 1996; Fernandez et al., 2003). Among the erosion, sheet erosion is the most serious soil erosion problems in India (Narayana and Babu, 1983). A proper assessment of the erosion problem is greatly dependent on its spatial, economic, environmental and agricultural context (Ganasri and Ramesh, 2016). A better soil loss management will be reducing the land degradation and water quality in contest of siltation and sedimentation to the water body (Karthick et al., 2017). More dependable soil erosion rates are required for land use planning and extension of soil water conservation works in coastal India.

Soil erosion assessment and mapping of soil loss susceptible area will be helpful to select or adoptthe suitable or appropriate soil conservation and ecosystem management techniques in the different scale of the maps (Shi et al., 2004). The mean annual soil loss information per unit land area could be ascertained by employing Universal Soil Loss Equation (USLE) and the Revised Universal Soil Loss Equation (RUSLE) (Wischmeier and Smith, 1978; van Remortel et al., 2001; Lee and Lee, 2006).

Remote sensing and GIS techniques are better tools for assessing erosion at larger scales. For this reason use of these techniques have been widely adopted and used in several studies that show the potential of remote sensing techniques integrated with GIS in soil erosion mapping (Parveen and Kumar, 2012).

Soil erosion is a complex phenomenon governed by a large number of factors such as rainfall erosivity, soil erodibility, slope, land use, and conservation measures. Estimating the soil loss and its spatial distribution are one of the key factors for successful erosion assessment (Bera, 2017). Spatial and quantitative information on soil erosion on a regional scale contributes to conservation planning, erosion control and management of the environment. Identification of erosion prone areas and quantitative estimation of soil loss rates with sufficient accuracy are of extreme importance for designing and implementation (Sharda et al., 2013). Keeping in view of the above aspects, case study was attempted in Ganjam block, part of coastal system to estimate the soil erosion.

Material and Methods

Description of study area

The study area Ganjam block belongs to Ganjam district of Odisha is a part of Indian peninsular subtropics, having tropical climate and sub-humid temperate region, which is located close to the Bay of Bengal coast and lies between 19º 22' 07'' to 19º 32' 24'' N and 84º 58'04" to 85º 10'30" E (Figure 1).

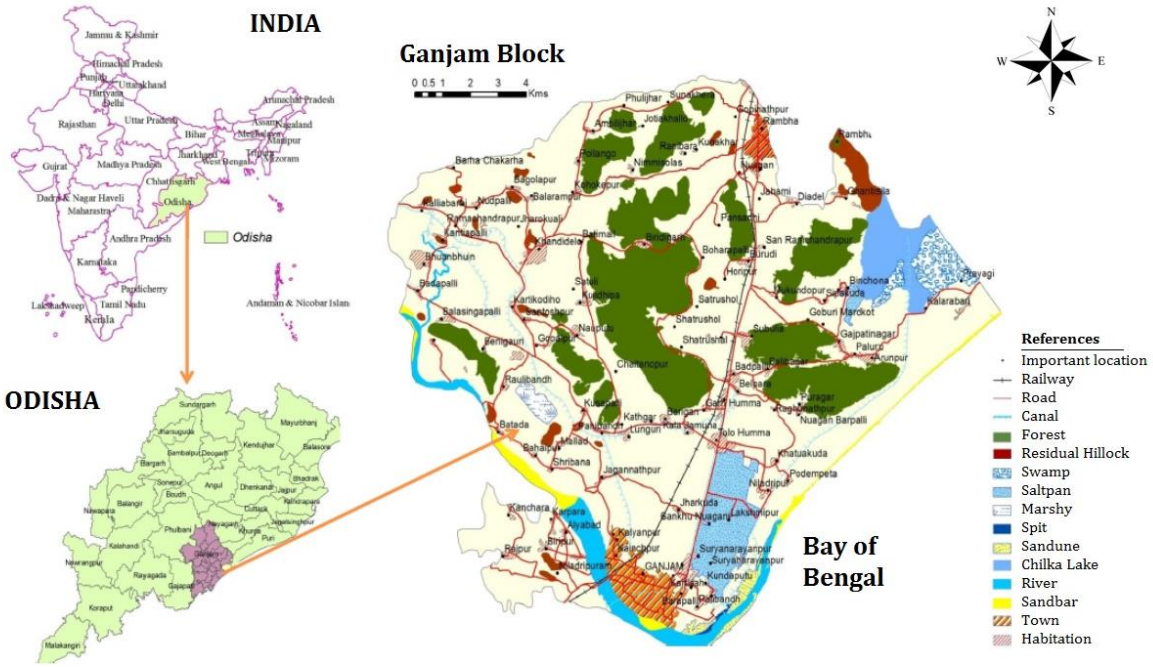

Figure 1. Location map of the study area

The block covers an area of about 246 sq km which is 2.93% of total geographical area of the district. The mean annual rainfall is 1449 mm and more than 60–70% is received during south-west monsoon (June-September). The mean maximum summer temperature is 39 °C and means minimum winter temperature is 11.5 °C. The soil temperature class is "*hyperthermic*" and moisture regime is "*ustic*" which is hot humid plain with LGP of 180–210 days. The soils are formed mainly in the deltaic alluvium of rivers. The major landforms occurred in the study area are denudation hills, lateritic uplands, pediments and inselbergs, lagoon, alluvial plains and swamps. Major soil category consists of lateritic, clayey, coastal saline sands and deltaic alluvium.

Methodology

Data sources

Rainfall erosivity (R) factor

Average rainfall data obtained from IMD last 30 years and processed in ArcGIS software and the R factor was obtained using the equation by Wischmeier and Smith (1978).

$$R = \sum_{i=1}^{12} 1.735 * 10^{(1.5 \log\left(\frac{pi^2}{p}\right) - 0.8188)} \quad (1)$$

Where R is the rainfall erosivity, Pi is the monthly amounts of precipitation and p is annual precipitation. Very less variations in R factor ranges from 679 m to 710m.

Soil erodibility factor (K)

Soil information collected from soil resource mapping (SRM) prepared by ICAR- NBSS & LUP, Govt. of India. The soil erodibility factor is the measure of the vulnerability to soil erosion as they are built-in soil properties. The K factor value ranges from 0 to 1, where the value near to 0 indicates least susceptibility to soil erosion and whereas the value closer to 1 indicated that they are very high susceptibility to soil erosion.

Topographic erosivity factor (LS)

The flow accumulation is usually derived from the digital elevation model (DEM) after processing the fill and flow direction in Arc GIS. Cell size is the extentor size of the cells being used in the DEM. The equation for computing the topographic factor (LS) in Arc GIS is computed by the formula recommended by Griffin et al. (1988).

Crop management factor (C)

By using the Landsat 8 data through supervised classification method, raster map of the land use and land cover converted to vector format file and the resultant C factor value was allocated to each of the land use classes are proposed by Hurni (1985).

Conservation supporting practice factor (P)

The conservation practice factor is calculated based on the slope of the area and equivalent P factor values derived based on each slope classes by reclassifying the slope map in ArcGIS.

Soil loss estimation

ArcGIS and ERDAS software were used to produce the desired output for the RUSLE factors such as R-Rainfall erosivity factor, K- Soil erodibility factor, LS- Slope length and steepness factor, C- cover management factor and P- Support practice factor. The USLE is the best empirical soil loss prediction equation, in spite of its limitations. That equation is A = R× K× L× S ×C ×P, where A is average annual soil loss, R is the rainfall erosivity factor, K is the soil erodibility factor, L is the slope-length factor, S is the slope steepness factor, C is the cover factor, and P is the conservation supporting-practice factor (Figure 2).

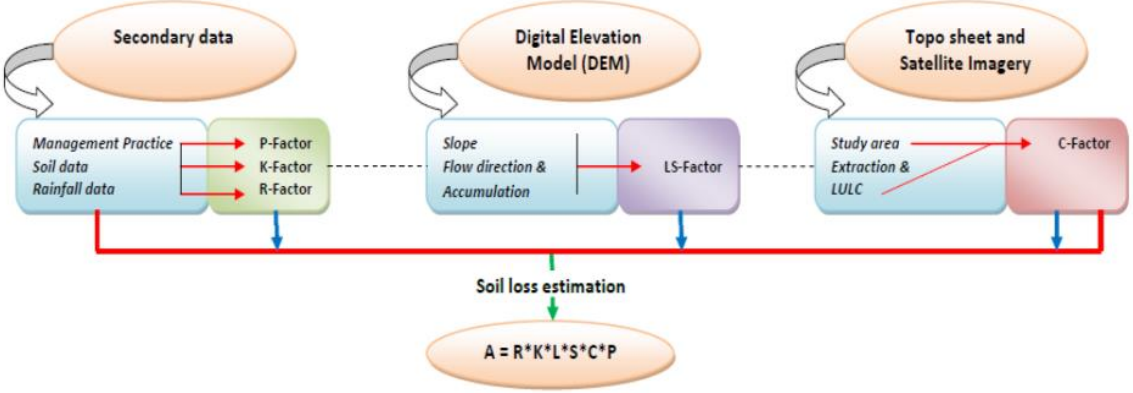

Figure 2. Flow chart of methodology

Results and Discussion

USLE analysis includes R factor, K factor, LS factor, C factor and P factor values which are determined and maps are generated using GIS.

Rainfall erosivity factor (R)

R factor is calculated based on IMD data over a period of 30 yearsof study area from equation 1 and these values are interpolated spatially through GIS technique and R factor map is generated is shown in Figure 3. The annual average rainfall erosivity factor (*R*) was found to be in the range of 697.48 to 710.16 mt $ha^{-1}cm^{-1}$. Many studies (Jain et al., 2001; Dabral et al., 2008) revealed that the soil erosion rate in the catchment is more sensitive to rainfall. The daily rainfall is a better indicator of variation in the rate of soil erosion and seasonal distribution of sediment yield. While the advantages of using annual rainfall include its ready availability, ease of computation and greater regional consistency of the exponent (Shinde et al., 2010). Therefore, in the present analysis, average annual (obtained by total rainfall divided by the total number of rainy days) rainfall was used for R factor calculation. Similar kinds of R-factor values were also calculated by Tirkey et al. (2013) and Behera (2015).

Soil erodibility factor (K)

The soil-erodibility factor (K) is represented by the susceptibility of the soil for erosion, conveyance of the detached soil and runoff resulted from rainfall. Chance of detachment of soil particles depend upon the structure, infiltration, optimum moisture content, water retentions, presence of cations, texture and composition. Soil erodability (K) of the study area was calculated using the relationship between soil texture class and organic matter content proposed by Schwab et al. (1981); Stone and Hillborn (2000). The soil erodability factor values assigned to different texture classes using GIS technique. Spatial distribution of surface soil K values of study area has shown in Figure 4. From the study (K factor map) it has been found that, in low relief areas like alluvial plains, hills and flood plains region, the K value varies from 0 to 0.36. Soil erodibility at near sea (sandbar) is comparatively high (0.88 to 1.1) because soils texture are course and generally loamy sand to sandy loam in texture and organic matter content was very low, which make more susceptible to erosion. The percentages of organic matter in soil drops erodibility, declines susceptibility of soil detachment, but enhances infiltration rates, hence the runoff by reducing erosion (Behera, 2015; Singh et al., 2002).

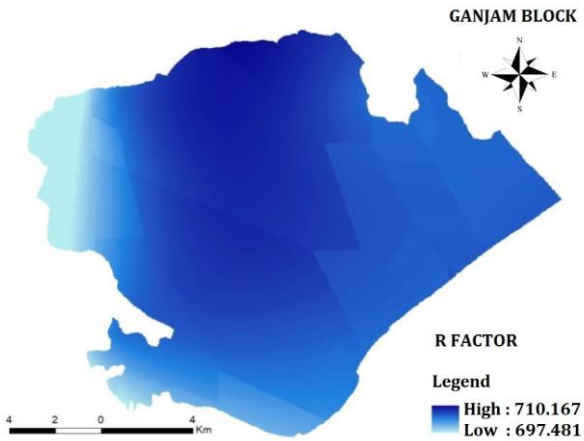

Figure 3. Spatial distribution of Rainfall (R) factor

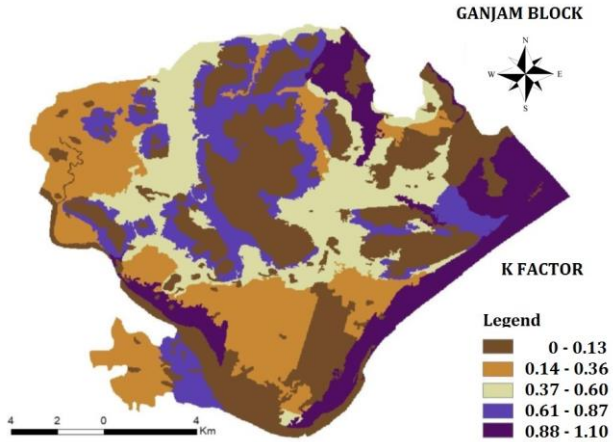

Figure 4. Soil erodibility (K) factor

Topographic factor (LS)

Topographic factor represents the influence of slope length (L) and slope steepness (S) on erosion process. LS factor was calculated by considering the flow accumulation and slope in percentage as an input. From the analysis, it is observed that the value of topographic factor increases in a range of 5 to 50 as the flow accumulation and slope increases. SRTM DEM of 30 m resolution is used to calculate LS factor, steeper the slope more will be the loss. For study area maximum slope is observed to be 0-5%. It's considered as very gently sloping area as from slope classes and LS factor map is generated and shown in Figure 5. It was found that the maximum slope varied in undulated hillock or hills side slope and foothills. According to slope map it was observed that slope at the study area is low. Analysis of the topographic factor is very important in USLE application, since this parameter characterizes surface runoff speed and quantity of sedimentation. Relationship of soil slope on topography established in different condition by Yildirim (2012) and Ozsoy et al. (2012).

Crop management factor (C)

Land use and land cover is a better understanding of the land utilization aspects of cropping pattern, fallow land, forest, wasteland and surface water bodies, which are vital for developmental planning and erosion studies. Survey of India Toposheet and Remote sensing imagery has a potential to generate a thematic layer of land use-land cover of a region. The study area has been classified into three land use classes which were assigned to different land use patterns using the values given in Table 1. Using land use-land cover map, C factor map was prepared and shown in Figure 6. C factor map shows that study area consists of high percentage vegetation cover which will reduce soil erosion (Renard et al., 2011). Soil loss is very sensible to land cover in addition to relief (Chatterjee et al., 2014). In the present study almost 50 % of the area is under forest. C factor is less significant when land use and land cover area comprises maximum percentage of natural vegetation and plantation crops. The value of which ranges from '0' in water bodies to slightly greater than '1' in barren land (Toy et al., 2002).

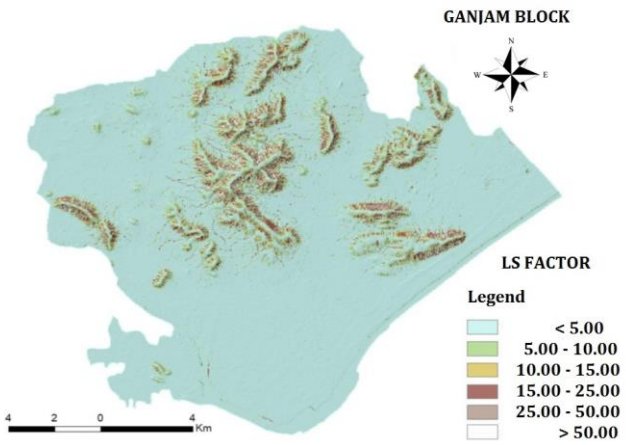

Figure 5. Slope length and steepness factor (LS)

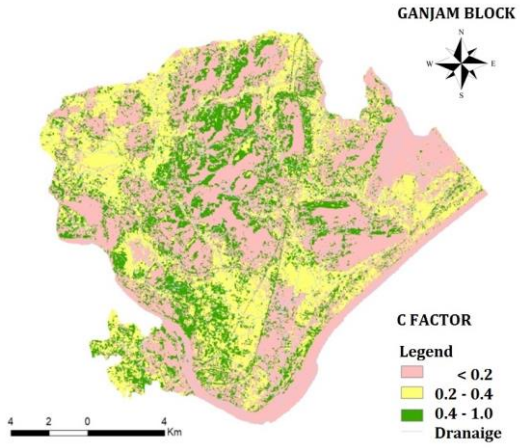

Figure 6. Cover management factor (C)

Table 1. Land use/land cover classes and respective C-factor value

C-Classes	C-factor	Area (ha)	% TGA
Forest	0-0.2	12280	49.9
Fallow land	0.2-0.4	1533	6.24
Agricultural area	0.4-1.0	10748	43.7
Total		24561	100

*TGA-Total Geographical Area

Support practice factor (P)

The support practice factor (P) is the ratio of soil loss in a normal condition to the soil loss due to ploughing in an undulating terrain. P values can be reduced by contouring, vegetative strips, strengthening the soil bunds, diversions, sediment basins and channel of an eroding area. Permanent vegetation like forest and plantation has more P values 0.7 to 1. Plain land open surface have 0.5 to 0.7. The value of P-factor is 1 for the upland and 0.50 for low land with gentle slope and cultivation of paddy and pulses (Figure 7).

Potential annual soil erosion estimation

The average annual soil erosion potential has been computed by multiplying the developed raster data from each factor of USLE analysis. The final soil erosion map displays the average annual soil loss potential of the coastal Odisha is shown in Figure 8. The GIS analysis has been carried out for RUSLE to estimate annual soil loss on a pixel-by-pixel basis and the spatial distribution of the soil erosion in the study area. The potential soil loss in the study area has been categorized into seven types viz., very slight, slight, moderate, moderate severe, severe, very severe and extremely severe erosion based on the rate of erosion (t/ha/year), i.e., More erosion corresponds to very high erosion and least rate of erosion correspond to low erosion (Table 2). It is observed that few parts of the study area have higher values of soil loss, which may be due to the steep slope and poor vegetation. It is observed that most part of the study area around 93.03% comes under low erosion category due to low slope variability. Negligible soil loss areas (5-10 t/ha/yr) have been recorded under forest and low land area. Soil erosion rate was predicted moderately high (10-15 t/ha/yr) for upland agriculture, which needs proper soil conservation measures to reduce the erosion. The high rate (20-80 t/ha/yr) of soil erosion was found in hills side slopes, foothills, barren and fallow land and sand bar of along the coastal basin (Behera, 2015; Mishra and Das, 2017).

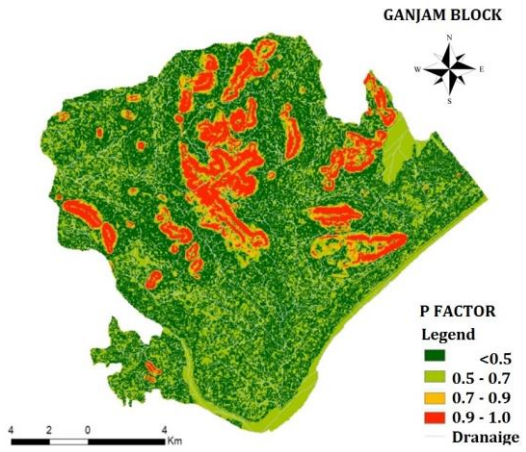

Figure 7. Conservation practices factor (P)

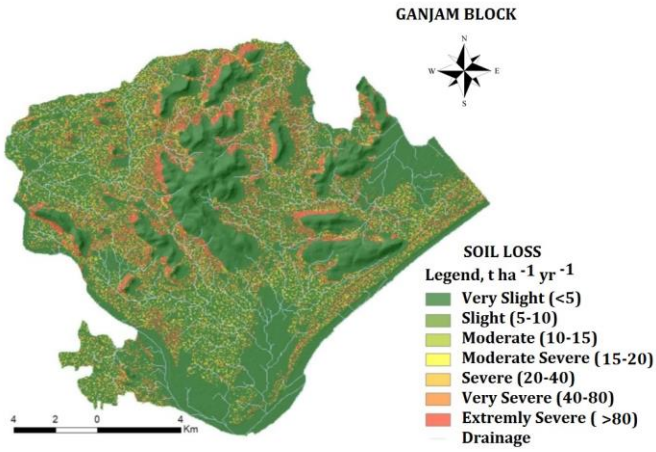

Figure 8. Soil erosion map

Table 2. Soil loss classifications according to the erosion risk classes

Erosion classes	Area (ha)	% TGA
Very low	22330	90.91
Low	721	2.93
Moderate	522	2.12
High	548	2.23
Very high	440	1.79
Total	24561	100

Conclusion

The soil erosion has been estimated and spatially distributed in the part of coastal Odisha using RUSLE and GIS technique and the soil loss map is classified into seven different erosion risk classes. According to that 23051 ha (93.03%) land has low erosion risk and 522 ha (2.12%) are moderate and 988 ha (3.72%) are high erosion risk category in Ganjam block based on variable climatic, soil and topographical condition. The average annual soil loss map is very useful to adopt soil conservation measures and protective method of agriculture practices for sustainable natural resource management.

References

Bai, Z.G., Dent, D.L., Olsson, L., Schaepman, M.E., 2008. Proxy global assessment of land degradation. *Soil Use and Management* 24(3): 223–234.

Bandyopadhyay, A.K., Bhargava, G.P., Bandyopadhyay, B.K., 1984. Coastal Saline Soils of Orissa, CSSRI, RRS, Canning Town, West Bengal, 56p.

Bandyopadhyay, B.K., Bandyopadhyay, A.K., 1983, Effect of salinity on mineralization and immobilization of nitrogen in a coastal saline soil of West Bengal. *IndianAgriculturist* 27: 41-50.

Behera, S.K., 2015. Estimation of soil erosion and sediment yield on ONG Catchment, Odisha, India. McS Thesis. National Institute of Technology, Rourkela, Department of Civil Engineering, India. Available at [Access date : 18.01.2019]: http://ethesis.nitrkl.ac.in/7561/1/2015_ESTIMATION_OF_SOIL_Behera.pdf

Bera, A., 2017. Estimation of Soil loss by USLE Model using GIS and Remote Sensing techniques: A case study of Muhuri River Basin, Tripura, India. *Eurasian Journal of Soil Science* 6(3): 206-215.

Chatterjee, S., Krishna, A.P., Sharma, A.P., 2014. Geospatial assessment of soil erosion vulnerability at watershed level in some sections of the Upper Subarnarekha river basin, Jharkhand, India. *Environmental Earth Sciences* 71(1): 357-374.

Chaudhary, D.R., Ghosh, A., Boricha, G.N., 2008. Characterization and classification of coastal saline soils of Paradip, Orissa. *Agropedology* 18(2): 129-133.

Chen, S., Chen, L., Liu, Q., Li, X., Tan, Q., 2005. Remote sensing and GIS-based integrated analysis of coastal changes and their environmental impacts in Lingding Bay, Pearl River Estuary, South China. *Ocean & Coastal Management* 48(1): 65-83.

Dabral, P.P., Baithuri, N., Pandey, A., 2008. Soil erosion assessment in a hilly catchment of North Eastern India using USLE, GIS and remote sensing. *Water Resources Management* 22(12): 1783-1798.

Devatha, C.P., Deshpande, V., Renukaprasad, M.S., 2015. Estimation of Soil loss Using USLE Model for Kulhan Watershed, Chattisgarh- A Case Study. *Aquatic Procedia* 4: 1429-1436.

Fernandez, C., Wu, J.Q., McCool, D.K., Stockle, C.O., 2003. Estimating water erosion and sediment yield with GIS, RUSLE, and SEDD. *Journal of Soil and Water Conservation* 58 (3): 128-136.

Ganasri, B.P., Ramesh, H., 2016. Assessment of soil erosion by RUSLE model using remote sensing and GIS - A case study of Nethravathi Basin. *Geoscience Frontiers* 7(6): 953-961.

Griffin, M.L., Beasley, D.B., Fletcher, J.J., Foster, G.R., 1988. Estimating soil loss on topographically non uniform field and farm units. *Journal of Soil and Water Conservation* 43(4): 326-331.

Hurni, H., 1985. Erosion-productivity conservation systems in Ethiopia. roceedings of 4th International Conference on Soil Conservation, Maracay, Venezuela, 3-9 November 1985, pp. 654-674.

Jain, S.K., Kumar, S., Varghese, J., 2001. Estimation of soil erosion for a Himalayan watershed using GIS technique. *Water Resources Management* 15(1): 41-54.

Karthick, P., Lakshumanan, C., Ramki, P., 2017. Estimation of soil erosion vulnerability in Perambalur Taluk, Tamilnadu using revised universal soil loss equation model (RUSLE) and geo information technology. *International Research Journal of Earth Sciences* 5(8): 8-14.

Kim, J.B., Saunders, P.F., Finn, J.T., 2005. Rapid assessment of soil erosion in the Rio Lempa Basin, Central America, using the universal soil loss equation and geographic information systems. *Environmental Management* 36(6): 872-885.

Lee, G.S., Lee, K.H., 2006. Scaling effect for estimating soil loss in the RUSLE model using remotely sensed geospatial data in Korea. *Hydrology and Earth System Sciences* 3: 135-157.

Lu, H., Prosser, I.P., Moran, C.J., Gallant, J.C., Priestley, G., Stevenson, J.G., 2003. Predicting sheetwash and rill erosion over the Australian continent. *Australian Journal of Soil Research* 41(6): 1037-1062.

Mishra, S.P., Das, K., 2017. Management of soil losses in South Mahanadi Delta, India. *International Journal of Earth Sciences and Engineering* 10(2): 222-232.

Monalisha, M., Panda, G.K., 2018. Coastal erosion and shoreline change in Ganjam Coast along East Coast of India. *Journal of Earth Science and Climatic Change* 9 (4): 1-6.

Narayana, D.V.V., Babu, R., 1983. Closure to estimation of soil erosion in India. *Journal of Irrigation and Drainage Engineering* 11(4): 408-410.

Ozsoy, G., Aksoy, E., Dirim, M.S., Tumsavas, Z., 2012. Determination of soil erosion risk in the Mustafakemalpasa river Basin, Turkey, using the revised universal soil loss equation, Geographic Information System, and Remote Sensing. *Environmental Management* 50(4): 679-694.

Pandey, A., Chowdary, V.M., Mal, B.C., 2007. Identification of critical erosion prone areas in the small agricultural watershed using USLE, GIS and remote sensing. *Water Resources Management* 21(4): 729-746.

Parveen, R., Kumar, U., 2012. Integrated approach of universal soil loss equation (USLE) and Geographical Information System (GIS) for soil loss risk assessment in upper South Koel Basin, Jharkhand. *Journal of Geographic Information System* 4(6): 588-596.

Parveen, R., Kumar, U., 2012. Integrated approach of universal soil loss equation (USLE) and Geographical Information System (GIS) for soil loss risk assessment in upper South Koel Basin, Jharkhand. *Journal of Geographic Information System* 4(6): 588-596.

Poyya Moli, G., Balachandran, N., 2008. Strategies for conserving ecosystem services to restore coastal habitats. UNDP-PTEI Conference on "Restoration of Coastal Habitats", 20-21 August 2008, Mahabalipuram, Tamil Nadu, India.

Renard, K.G., Yoder, D.C., Lightle, D.T., Dabney, S.M., 2011. Universal soil loss equation and revised universal soil loss equation. In: Handbook of Erosion Modeling. Morgan, R.P.C., Nearing, M.A. (Eds.). Blackwell Publishing Ltd. Oxford, England. pp. 137–167.

Renschler, C.S., Mannaerts, C., Diekkrüger, B., 1999. Evaluating spatial and temporal variability in soil erosion risk—rainfall erosivity and soil loss ratios in Andalusia, Spain. *Catena* 34(3-4): 209-225.

Schwab, G.O., Frevert, R.K., Edminster. T.W., Barnes, K.K., 1981. Soil Water Conservation Engineering, 3rd Ed, Wiley, New York, USA.

Sehgal, J., Mandal, D.K., Mandal, C., Vadivelu, S., 1992. Agro-ecological zones of India. Second Edition. Nagpur, India. Technical Bulletin, No. 24. NBSS&LUP (ICAR). 130p.

Sharda, V.N., Mandal, D., Ojasvi, P.R., 2013. Identification of soil erosion risk areas for conservation planning in different states of India. *Journal of Environmental Biology* 34(2): 219-226.

Shi, Z.H., Cai, S.F., Ding, S.W., Wang, T.W., Chow, T.L., 2004. Soil conservation planning at the small watershed level using RUSLE with GIS: a case study in the Three Gorge Area of China. *Catena* 55(1): 33-48.

Shinde, V., Tiwari, K.N., Singh, M., 2010. Prioritization of micro watersheds on the basis of soil erosion hazard using remote sensing and geographic information system. *International Journal of Water Resources and Environmental Engineering* 2(3): 130-136.

Singh, G., Babu, R., Narain, P., Bhushan L.S., Abrol, I.P., 1992. Soil erosion rates in India. *Journal of Soil and Water Conservation* 47(1): 97-99.

Singh, R., Kundu, D.K., Verma, H.N., 2002. Hydro physical characteristics of odisha soil and their water management implications, Publication 12, Water Technology center for eastern region (Indian Council of Agricultural research, Chandrasekharpur, Bhubaneswar, India. Available at [Access date: 18.01.2019]: http://www.iiwm.res.in/pdf/Bulletin_12.pdf

Srinivasan, R., Reza, S.K., Nayak, D.C., Singh, S.K., Sarkar, G.C., 2015. Characterization and classification of major vegetables growing soils of odisha coastal system- A case study. *Agropedology* 25 (2): 232-239.

Stone, R.P., Hilborn, D., 2000. Universal Soil Loss Equation (USLE), Ontario Ministry of Agriculture, Food and Rural Affairs Factsheet. Available at [Access date: 18.01.2019]: http://www.omafra.gov.on.ca/english/engineer/facts/12-051.htm#1

Tideman, E.M., 1996. Watershed management: guidelines for Indian conditions. Omega Scientific Publisher, New Delhi, India. 101p.

Tirkey, A.S., Pandey, A.C., Nathawat, M.S., 2013. Use of Satellite Data, GIS and RUSLE for estimation of average annual soil loss in Daltonganj Watershed of Jharkhand (India). *Journal of Remote Sensing Technology* 1(1): 20-30.

Toy, T.J., Foster, G.R., Renard, K.G., 2002. Soil erosion: processes, prediction, measurement, and control. John Wiley & Sons. New York, USA. p 338.

van Remortel R.D., Hamilton, M.E., Hickey, R.J., 2001. Estimating the LS Factor for RUSLE through ıterative slope length processing of digital elevation data within arclnfo grid. *Cartography* 30(1): 27-35.

Vinayaraj, P., Johnson, G., Dora, G.U., Philip, C.S., Kumar, V.S., Gowthaman, R., 2011. Quantitative estimation of coastal changes along selected locations of Karnataka, India: A GIS and remote sensing approach. *International Journal of Geosciences* 2(4): 385-393.

Wischmeier, W.H., Johnson, C.B., Cross, B.V., 1971. A soil erodibility nomograph for farmland and construction sites. *Journal of Soil Water Conservation* 26: 189–193.

Wischmeier, W.H., Smith, D.D., 1978. Predicting rainfall erosion losses - A Guide to Conservation Planning. Agriculture Handbook No. 537. US Department of Agriculture Science and Education Administration, Washington, DC, USA, 163 p.

Yildirim, U., 2012. Assessment of soil erosion at the Degirmen Creek watershed area, Afyonkarahisar, Turkey. Proceedings of ISEPP (International Symposium on Environmental Protection and Planning: Geographic Information Systems (GIS) and Remote Sensing (RS) Applications). 28-29 June 2011, İzmir, Turkey. pp. 73-80.

Eurasian J Soil Sci 2019, 8 (4) 329 - 339

Eurasian Journal of Soil Science

Journal homepage : http://ejss.fesss.org

Characterization of soil amendment potential of 18 different biochar types produced by slow pyrolysis

Hikmet Günal *, Ömer Bayram, Elif Günal, Halil Erdem

Gaziosmanpasa University, Faculty of Agriculture, Department of Soil Science and Plant Nutrition Tokat, Turkey

Abstract

Feedstock type is the most dominant factor influencing the physical characteristics and chemical composition of biochar. The main purpose of this study was to characterize and compare some of the physical and chemical properties of biochars produced by slow pyrolysis of 18 feedstocks, which are locally available agricultural residues. Moreover, elucidating the potential agronomic benefits of these biochars was the other objective of the study. Biochars were produced at 500 ^{o}C in an ingeniously developed reactor. The biochars were characterized for specific surface area (SSA), field capacity (FC), wilting point (WP), plant available water content (AW), pH, electrical conductivity (EC), cation exchange capacity (CEC), total carbon (C) and nitrogen (N), plant available phosphorus (P) and potassium (K) concentrations. Considerable variation of characteristics among biochars indicates the dominant impact of feedstock type on physical properties and chemical composition of biochars. Total C contents were highly variable with values up to 91.9% for pine sawdust. Phosphorus and K in feedstocks were concentrated in the biochars and were two to four times higher in the biochars. The CEC of biochars varied from 79.5 cmol kg^{-1} (pepper residues) to 5.77 cmol kg^{-1} (poplar sawdust). The CEC and SSA had a significant negative correlation ($P<0.01$, $r= -0.70$) that probably be attributed to the loss of functional groups during pyrolysis. The results revealed that depending on the feedstock, some biochars have potential to serve as nutrient sources as well as an additive to improve soil quality.

Keywords: Agricultural residues, feedstock type, biochar, physical and chemical properties, soil quality.

Article Info

Received : 11.01.2019
Accepted : 23.07.2019

Introduction

Biochar is a carbon-rich solid and stable material produced by pyrolysis of biomass in an oxygen-limited environment (Lehmann and Joseph, 2009). The pyrolytic conversion of the feedstocks mainly composed of agricultural residues to biochar and agricultural applications of the biochar can be considered as their environmentally and economically acceptable management (Hossain et al., 2011). The biochar can be produced from thermochemical processing of a wide variety of feedstocks with different ratios of cellulose, hemicellulose, lignin, extractives, etc. such as organic farm waste, waste treatment plant slurry, and forestry residue with high cellulose/lignin content. After pyrolysis, the solid byproduct is a porous network of carbonates and/or aromatic carbon (Herbert et al., 2012). Biochar types produced from various feedstocks have different physical and chemical characteristics as a function of variability in the composition of feedstocks (Brewer, 2012). Therefore, comparing the impacts of different biochar types on soil properties reported in the literature is difficult to extrapolate to other soils. Biochar improves fertility of soils and has no reported controversial effect on soils. The magnitude of beneficial effect is related to physical and chemical properties of biochars (Lehmann et al., 2006). Biochar improves water holding capacity of soils

* Corresponding author.
Gaziosmanpasa University, Faculty of Agriculture, Department of Soil Science and Plant Nutrition Tokat, Turkey
Tel.: +90 542 3566005 E-mail address: hikmetgunal@gmail.com
e-ISSN: 2147-4249 DOI: 10.18393/ejss.599760

(Günal et al., 2018), promotes development and bioactivity of soil micro-flora, reduces nutrient leaching (Kanthle et al., 2018), recycles soil nutrients (Oldfield et al., 2018), and increases soil organic carbon (Smith, 2016) and thus plant growth (Gaskin et al., 2010). Lim et al. (2016) stated that saturated hydraulic conductivities of the biochar amended soils were significantly influenced by the rate and type of biochar, as well as the original particle size of soil. The researchers reported that biochar addition significantly reduced the saturated hydraulic conductivity of coarse and fine sands. Cation exchange capacity (CEC) of a biochar is affected by both feedstock type and pyrolysis temperature (Brewer, 2012). CEC values decrease with higher pyrolysis temperature due to loss of functional groups. Formation of carboxylic and other oxygenated functional groups at the surface by long term oxidation of biochar increases the negative charges and CEC of a biochar (Cheng and Lehmann, 2009). Surface area is another important physical property of a biochar that has a significant impact on the extent of interactions between biochar and the soil environment (Chu et al., 2018). The nature of feedstock and pyrolysis process have significant impact on surfaces areas of biochars which might vary in the hundreds and even thousands of meters squared per gram, potentially making them suitable as the sustainable amendments of soils (Brewer, 2012).

The increasing demand for food and fiber with increasing population causes a significant amount of agricultural residues. Biochar production is a sustainable way to reduce the agricultural residues produced in food industry or farm activities (Schellekens et al., 2018) and converts them to environmentally friendly additives. Vast amounts of waste biomass are generated by agro-food industries, forestry activities and agricultural crop production in Turkey. Large portion of crops such as 2.5 t ha^{-1} of bread wheat, 13 t ha^{-1} of tomato and 10.5 t ha^{-1} of corn (Di Blasi et al., 1997) is left in the field each year following the harvest. Citak et al. (2006) reported that more than 4 million tons $year^{-1}$ of citrus and fruit pruning residues, 12.7 million tons $year^{-1}$ of tomato and eggplant residues, 350.000 tons ha^{-1} of nut slag and many other crop residues need to be reused to overcome environmental pollution problems created by these residues. Most of crop residues in Turkey are burned onsite, collected and thrown away from the field and dumped to the drainage channels or burned in the houses for energy (Günal et al., 2015). Burning or removing the crop residues for any of the stated purposes have negative impact on soil organic carbon and consequently to functioning ability of soils.

Characterization of biochars produced from several feedstocks is important to predict the stability, potential in contribution to soil quality and risks in the environment (Schellekens et al., 2018). Thus, the objective of this study was to characterize and compare some of the physicochemical properties, critical for agricultural use, of 18 biochars produced at 500 ^{o}C by slow pyrolysis of 18 feedstocks.

Material and Methods

Material

The feedstocks used to produce biochars were vegetable crop residues (tomatoes, bean, pepper, eggplant, cabbage, cauliflower, gooseberry and kidney bean), woody materials (walnut shell, pine sawdust and rosehip seed), field crop residues (rice husk, corn cob and wheat straw) and animal manure (poultry litter, sheep manure and dairy manure) collected from agricultural fields, farms and local carpenters in Tokat province of Turkey.

Methods

Biochar Production

Prior to pyrolysis processing, the biomass of the all sources were ground in a hammer mill to pass a 6 mm screen and oven dried at 60 ^{o}C to <10% moisture (Brewer et al., 2011). The biochars were produced by slow pyrolysis of feedstocks (maximum size 2 mm) at 500 ^{o}C in an ingeniously developed reactor. Slow pyrolysis process was characterized by slow heating rates (a rate of approximately 10 ^{o}C min^{-1}) and long residence times of biomass. The pyrolysis temperature was kept constant at 500 ^{o}C and biochar was held in the unit until pyrolysis gas disappeared. After heating for almost 4 to 6 hours, the biochars were allowed to cool to room temperature.

Characterization of Biochars

The biochar samples underwent the following analyzes: pH, electrical conductivity (EC), specific surface area (SSA), cation exchange capacity (CEC), total carbon (C), total nitrogen (N), plant available potassium (K) and phosphorus (P), field capacity (FC) and wilting point (WP) water contents. The biochar production rate or mass yield (MY) is defined as the ratio of carbonized product mass to the mass of feedstock (Weber and Quicker, 2018). The mass yield was calculated using the following equation:

$$MY\ (\%) = (\text{Biochar weight after pyrolysis}/\text{Feedstock weight}) \times 100.$$

The total C and N contents of the biochars were determined using a Leco CN-2000 analyzer (Leco Corp., St. Joseph, MI, USA) at 1200 °C. The pH and EC were measured in deionized water at the ratio of 1:5 wt wt^{-1} ratio. The samples were thoroughly mixed and allowed to equilibrate for 1 h; the pH and EC were then measured using an Orion 720 pH-EC meter with a combination electrode. The K and P concentrations of the biochars and raw materials were determined in duplicate following digestion at in H_2O_2 - HNO_3 acid mixture and burned in a microwave (Mars 6). The K and P concentrations in the H_2O_2 - HNO_3 solution were determined by Atomic Absorption Spectrophotometer (AAS-Agilent 240 FS). Ethylene glycol mono-ethyl ether (EGME) method was to measure specific surface area that is typically used for soils (Cerato and Lutenegger, 2002). Cation exchange capacity was determined by ammonium acetate method (Chapman, 1965). The method was modified to apply for biochars due to the low bulk density of biochars creating a problem for liquid-solid separation (Brewer et al., 2009).

Biochars were analyzed for field capacity and permanent wilting point, from which plant-available water capacity (AW) was calculated by difference between water retained at permanent wilting point and at field capacity (Laird et al., 2010). Biochars were filled in rings with a height of 10 mm and an interior diameter of 35 mm. The biochars were carefully wetted from below and drained in a pressurized chamber to either 1.1 or 15 bar on ceramic plates specific to each pressure (Chamber 1600 and 1500, Soil Moisture Equipment, Santa Barbara CA, USA), allowed to equilibrate, and weighed after reaching constant water contents. Water content was determined by drying at 105°C for overnight and field capacity and permanent wilting point were calculated.

Statistical Analyses

All data were checked for normality using by the Kolmogorov–Smirnov (Lilliefors) test. Non-normal data were transformed to meet the analysis of variances (ANOVA) assumptions. Differences between means of feedstock groups were tested with the standard least-squares mode of one-way ANOVA, followed by a Duncan comparison using SPSS 23.0 software (SPSS Inc., Chicago, IL, USA). Differences with probability larger than 95% were taken as significant. Correlation analyses were conducted among the characteristics of biochars produced.

Results and Discussion

The benefits of biochar such as a fertilizer replacement and additive to improve the nutrient availability in soil depend on characteristics of biochar types. Characterization of the biochar encompasses physical characteristics, compositional analysis and soil additive potential. Several physical and chemical characteristics of biochars produced are presented in Table 1-4. The mass yields and some physical and chemical characteristics of biochars obtained from the different sources are given in Figure 1-6. The type of feedstock had significant effect on mass yield of biochars. All feedstocks were pyrolyzed at 500 °C for almost 4 to 6 hours; however, mass yield varied from 19.68% (poplar sawdust) to 62.99% (dairy manure) with a mean of 33.48%.

Table 1. Physical and chemical properties of biochars produced from vegetable residues

	Yield, (wg),%	SSA, m^2g^{-1}	FC, %	WP, %	AW, %	pH	EC, dSm^{-1}	CEC, cmol kg^{-1}
Tomatoes	33.08	208.9	108.5	120.8	4.1	11.61	6.64	49.5
Bean	30.40	117.9	111.2	98.3	7.9c	12.18	8.75j	74.7
Pepper	34.09	133.6	128.2	128.1	5.6	11.40	4.29	79.5
Eggplant	33.02	174.2	119.9	126.8	5.7	11.60	10.30	42.9
Cabbage	34.19	78.07	86.8	76.4	10.4	11.84	18.24	43.4
Cauliflower	37.68	46.53	80.4	58.6	21.9	11.88	15.76	50.9
Gooseberry	32.09	179.7	131.6	111.7	19.9	12.42	14.79	78.2
Kidney Bean	30.62	286.6	110.1	108.8	1.3	10.52	5.72	28.9
	C, %	N, %	C:N	P in Row, g kg^{-1}	P in Bioc. , g kg^{-1}	K in Row, g kg^{-1}	K in Bioc., g kg^{-1}	
Tomatoes	65.3	0.42	156.4	1.43	3.69	10.82	34.31	
Bean	79.0	0.71	111.2	2.33	5.61	24.52	36.54	
Pepper	67.4	0.49	136.3	2.05	6.56	20.68	44.40	
Eggplant	67.7	1.17	57.8	1.65	3.88	23.58	39.51	
Cabbage	39.4	0.92	42.6	1.65	4.00	16.58	44.54	
Cauliflower	42.3	0.84	50.3	0.26	5.65	2.10	41.08	
Gooseberry	52.2	0.65	80.8	1.64	3.92	36.52	52.03	
Kidney Bean	75.8	0.75	100.6	0.96	3.08	6.27	9.29	

EC: Electrical Conductivity, CEC: Cation Exchange Capacity, SA: Specific Surface Area, FC: Field Capacity, WP: Wilting Point, AW: Available Water Content; C: Total Carbon, N: Total Nitrogen, P: Phosphorus, K: Potassium

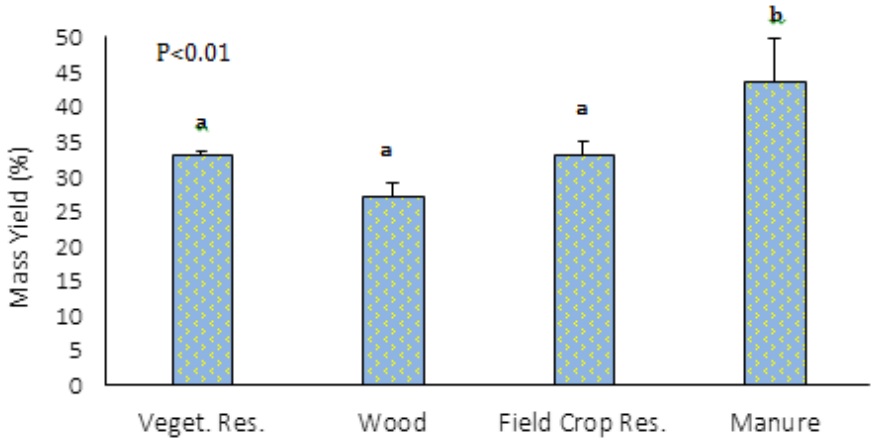

Figure 1. Mass yield (%) ± SE of means of different biochar types (n=18). Any two means sharing different letters are statistically significant (P≤0.05)

Specific surface area and cation exchange capacity of biochar types

Chemical interactions between biochar and soil environment are mostly governed by its surface chemistry. (Weber and Quicker, 2018). The type of feedstock had significant effect (P<0.01) on specific surface area (SSA) of biochars which ranged from mean value of 153.2 $m^2 g^{-1}$ (vegetable residues) to 313.9 $m^2 g^{-1}$ (wood) (Fig. 2). The lowest SSA was obtained for cauliflower (46.53 $m^2 g^{-1}$) and the highest SSA for corncob (397.5 $m^2 g^{-1}$) (Table 1 and 3). The higher the SSA of a biochar, the biochar can be more active in chemical interactions in per gram (Brewer, 2012), and hold more nutrients in addition to the direct supply of nutrients. Mean SSA of all biochar was 222.48 $m^2 g^{-1}$ which is quite high as compared to many clay minerals in soils. Lee et al. (2013) also reported surface area values for wood stem, sugarcane bagasse and palm kernel shell as over 190 $m^2 g^{-1}$ which was similar to the SSA reported in this study.

Table 2. Physical and chemical properties of biochar types produced from woody materials

	Yield, (wg),%	SSA, $m^2 g^{-1}$	FC, %	WP, %	AW, %	pH	EC, dSm^{-1}	CEC, cmol kg^{-1}
Poplar Sawdust	19.68	391.6	30.0	28.0	2.0	8.77	1.44	5.8
Walnut Shell	31.23	318.8	45.3	41.3	4.0	9.63	3.55	20.6
Pine Sawdust	25.27	267.2	58.2	18.4	39.8	7.89	5.06	13.9
Rosehip Seed	32.65	278.0	17.4	16.3	1.1	8.46	1.73	6.8
	C, %	N, %	C:N	P in Row, g kg^{-1}	P in Bioc. , g kg^{-1}	K in Row, g kg^{-1}	K in Bioc., g kg^{-1}	
Poplar Sawdust	83.6i	0.38	221.9	0.26	0.57	2.10	3.20	
Walnut Shell	85.4	0.32	267.9	1.65	0.92	4.43	5.30	
Pine Sawdust	91.9	0.26	348.9	0.31	0.31	0.61	0.63	
Rosehip Seed	87.2	1.01	86.2	1.38	3.61	1.56	1.56	

EC: Electrical Conductivity, CEC: Cation Exchange Capacity, SA: Specific Surface Area, FC: Field Capacity, WP: Wilting Point, AW: Available Water Content; C: Total Carbon, N: Total Nitrogen, P: Phosphorus, K: Potassium

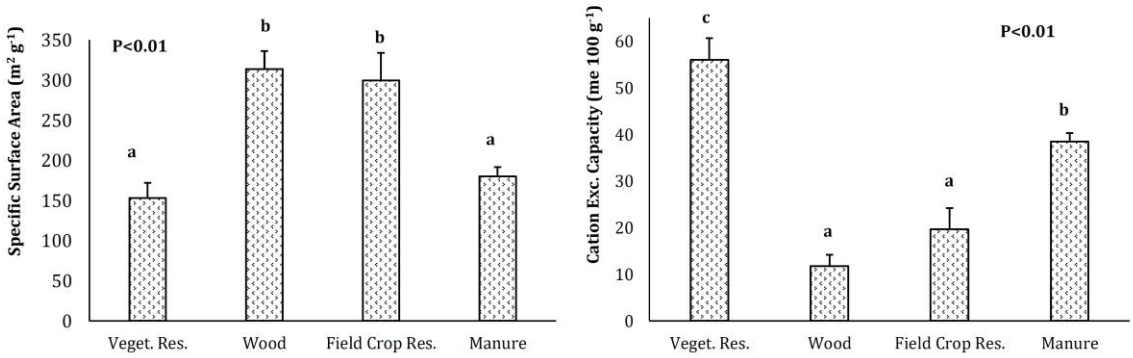

Figure 2. Specific surface area ($m^2 g^{-1}$) ± SE od means and cation exchange capacity (me 100 g^{-1}) ± SE of means of biochar types (n=18). Any two means sharing different letters are statistically significant (P≤0.05)

Cation exchange capacity (CEC) is the ability to adhere and exchange positively charged cations such as important nutrients like potassium (K), calcium (Ca), magnesium (Mg) and etc. The CEC of biochars was significantly affected by type of feedstock. Although CEC of a biochar is directly related to its surface structure and surface area (Brewer, 2012), the mean CEC of woody materials (11.8 me 100 g^{-1}) which had the highest SSA was significantly lower than the CEC of the rest of biochar groups (Figure 2). The CEC values of biochar types were considerably lower than those reported for 2:1-type clay minerals (70–250 cmol kg^{-1}) or humic substances (400–900 cmol kg^{-1}) (Sposito, 1989). The biochar produced from pepper residues had the largest CEC (79.5 cmol kg^{-1}); the CEC of biochars rated between 79.5 cmol kg^{-1} (pepper) and 5.8 cmol kg^{-1} (poplar sawdust) (Table 1 and 2). Biochars with high CEC and surface area values can be efficiently used as a soil amendment to improve soil quality. However, the CEC values obtained in this study are much lower than that reported by Yuan et al. (2011) for canola and corn straw biochars (which from 179 to 304 cmol kg^{-1}). The CEC of biochars may increase by aging. Cheng and Lehmann (2009) showed that functional groups, acidity and negative charge at the surface of oak biochar particles significantly increased in a controlled aerobic incubation experiment which resulted in increased CEC of biochar by aging.

Table 2. Physical and chemical properties of biochar types produced from woody materials

	Yield, (wg),%	SSA, m^2g^{-1}	FC, %	WP, %	AW, %	pH	EC, dSm^{-1}	CEC, cmol kg^{-1}
Rice Husk	37.83	211.8	63.3	61.9	1.4	10.20	3.29	15.2
Corncob	27.12	397.5	119.9	107.9	12.1	9.20	9.30	10.0
Wheat Straw	31.18	214.8	167.5	161.9	5.6	10.90	2.60	39.4
	C, %	N, %	C:N	P in Row, g kg^{-1}	P in Bioc. , g kg^{-1}	K in Row, g kg^{-1}	K in Bioc., g kg^{-1}	
Rice Husk	61.7	0.45	136.7	0.32	0.05	4.29	3.89	
Corncob	88.3	0.29	306.9	0.40	0.39	6.78	9.53	
Wheat Straw	71.7	0.91	78.7	0.57	1.30	14.14	27.59	

EC: Electrical Conductivity, CEC: Cation Exchange Capacity, SA: Specific Surface Area, FC: Field Capacity, WP: Wilting Point, AW: Available Water Content; C: Total Carbon, N: Total Nitrogen, P: Phosphorus, K: Potassium

Hydrological properties of biochar types

Hydrologic properties: field capacity (FC), permanent wilting point (PWP) and available water content (AW) of biochars exhibited a wide range depending on feedstock type. Similarly, Gray et al. (2014) indicated that water uptake by biochars depends on feedstock type, which controls the residual macroporosity. The FC is a measure for the water held in a material that has been saturated and allowed to freely drain. Mean biochar FC, accepted as an indication of water availability to plants ranged from 37.7% (woody materials) to 109.6% (vegetable residue) (Figure 3). The FC of biochar produced from rosehip seed was only 17.4% and wheat straw biochar had ten-fold higher water content (161.9%) at the FC (Table 2 and 3). The biochar with the most desirable hydrological property (the highest FC) was produced with the wheat straw (FC=167.5%), however, most of the water in straw biochar was also held in PWP which made only 5.6% of the water available to plant consumption. Majority of the biochars with high FC had also high WP (Table 1). The mean PWP content of biochars was between 26% (woody materials) and 103.7% (vegetable residues) (Figure 3). In contrast to FC and PWP, AW content of biochars did not significantly change (P=0.466) with the type of biochar. Biochars produced from vegetable residues, field crop residues and animal manures hold significantly higher water at FC and PWP, however, majority of water hold by these biochars is tightly held and not available for plant use.

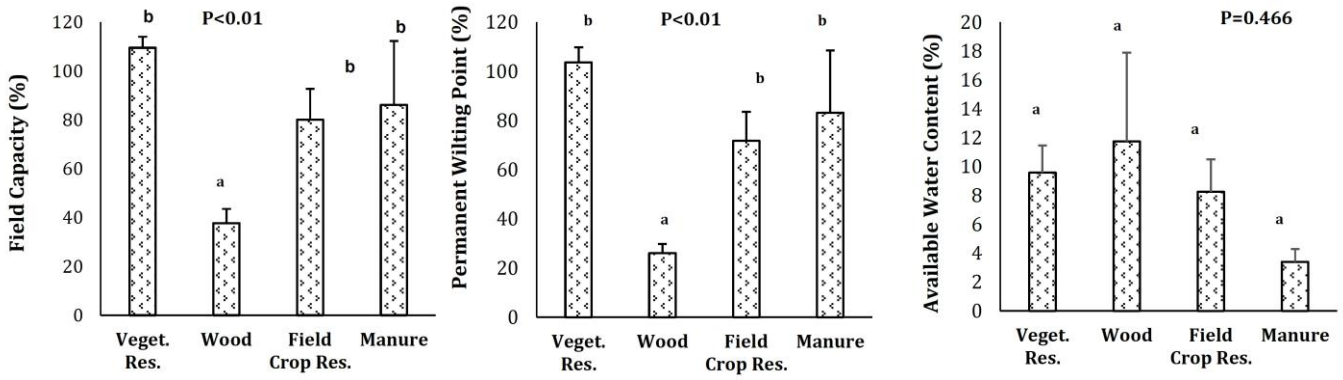

Figure 3. Field capacity (%) ± SE of means, permanent wilting point (%) ± SE of means and available water content (%) ± SE of means of biochar types (n=18). Any two means sharing different letters are statistically significant (P≤0.05)

Biochar types generated from animal manure had the lowest mean AW content (3.4%), while biochars of woody materials had the highest AW content (11.7%) (Figure 3). Pine sawdust biochars had significantly higher AW (39.8%) as compared to the rest of the biochars (mean AW was 9.25%). The AW contents of biochars produced from rosehip seed (1.1%), kidney bean (1.3%), rice husk (1.4%), ship manure (1.5%) and poplar sawdust (2.0%) were significantly lower than the other biochars (Table 1-4). In contrast to the high-water holding capacity of biochars produced in this study, Jeffery et al. (2015) reported that the biochars used in their study were highly hydrophobic and the strong hydrophobicity prevented water from infiltrating into the biochar particles, prohibiting an effect on soil water retention. Weber and Quicker (2018) indicated that hydrophobicity and water holding capacity have counteracting or overlapping effects, and the surface functional groups and the porosity of the biochar's bulk volume are responsible from the first and second factors, respectively. In another study conducted on a mesic Typic Hapludolls by Laird et al. (2010), the biochar amendment increased the water content held at gravity drained equilibrium (up to 15%), at – 1 and –5 bars soil water matric potential, (13 and 10% greater, respectively).

Table 4. Some of physical and chemical properties of biochar types produced from animal manure

	Yield, (wg),%	SSA, m^2g^{-1}	FC, %	WP, %	AW, %	pH	EC, dSm^{-1}	CEC, cmol kg^{-1}
Sheep Manure	36.80	161.3	58.1	57.7	1.5	11.82	15.37	36.0
Poultry Litter	31.83	192.9	78.7	56.1	22.6	11.60	5.00	58.0
Dairy Manure	*62.99*	163.7	32.8	29.7	3.1	10.57	4.01	40.0
	C, %	N, %	C:N	P in Row, g kg^{-1}	P in Bioc. , g kg^{-1}	K in Row, g kg^{-1}	K in Bioc., g kg^{-1}	
Sheep Manure	58.9	0.74	79.4	1.76	3.98	7.44	9.94	
Poultry Litter	58.8	0.88	66.6	*8.44*	*25.6*	25.90	44.46	
Dairy Manure	*35.9*	0.79	45.2	4.38	13.48	10.35	9.98	

EC: Electrical Conductivity, CEC: Cation Exchange Capacity, SA: Specific Surface Area, FC: Field Capacity, WP: Wilting Point, AW: Available Water Content; C: Total Carbon, N: Total Nitrogen, P: Phosphorus, K: Potassium

Carbon (C) and nitrogen (N) contents and C:N Ratio of biochar types

Total C contents of biochar types were significantly different (P<0.01) among feedstock groups. The C content of woody materials (87.03%) and field crop residues (73.90%) were significantly higher than biochars produced from vegetable residues (61.14%) and manures (51.20%) (Figure 4). Carbonization increased the total C content of pine sawdust to 91.9% and rosehip seed to 87.2%. The biochar became highly carbonaceous, with a C content ranging from 35.9% (dairy manure) to 91.9% (pine sawdust) (Table 4 and 2). The property of a biochar is a function of the feedstock origin, particle size, temperature and rate of temperature increase during pyrolysis, residence time, pressures, and conditions of the starting material (Guerro et al., 2005). Along with the C enrichment of biochars, Vaccari et al. (2011) stated that the carbon structures present in the biochar become highly resilient to the degradation by microorganisms. Therefore, the biochars with high C concentrations have capacity to store carbon for a long period of time contributing to mitigation of climate change. Lehmann et al. (2006) also indicated that biochar production from agricultural and forestry wastes or urban wastes have an estimated C sequestration capacity of 0.16 Pg C yr^{-1}.

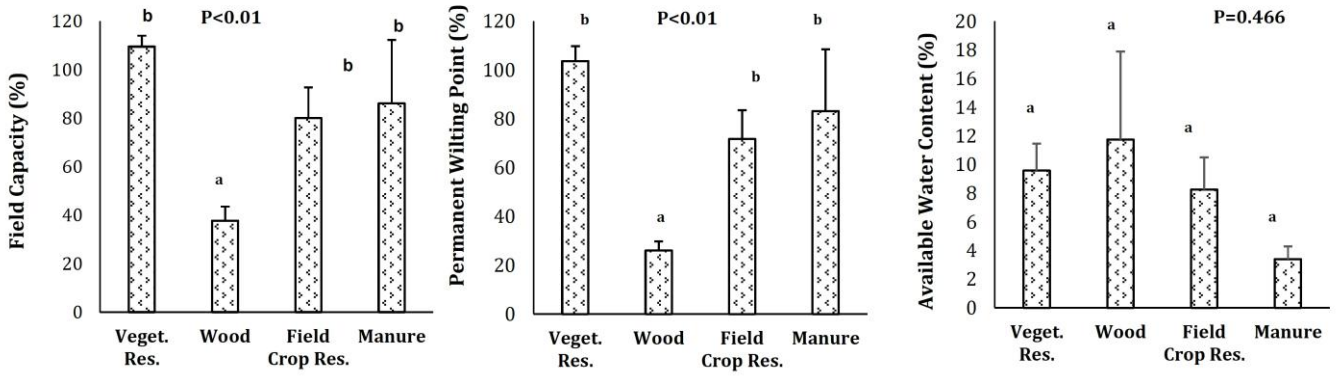

Figure 4. Total carbon (%) ± SE of means, total nitrogen (%) ± SE of means and carbon/nitrogen ratio of biochar types (n=18). Any two means sharing different letters are statistically significant (P≤0.05)

Nutrient-rich vegetable residues contained relatively more minerals than the other feedstocks, which decreased the C content. The feedstock type had no significant impact (P=0.054) on total N content of biochars. Mean total N content of biochars produced from manures (0.80%) were significantly higher than

total N content of woody materials (0.50%) (Figure 4). The amount of total N conserved in biochars ranged from 0.26% (pine sawdust) and to 1.17% (eggplant) which was inversely proportional to the total C concentrations (Table 2 and 1). Although total C contents varied widely and immobilization of N depends on relative amounts of C sources and N availability, total N contents proved equally useful to estimate N availability.

The C:N ratio is an indication of the ability for an organic substrate to release inorganic N when mixed with a soil. The effect of feedstock type on C:N ratio was statistically significant (P<0.01). The mean C:N ratio for biochars of woody materials (232.3) was almost four times higher than biochars of manures and three times higher than biochars of vegetables residues (92.2) (Figure 4). In general, the C:N ratio of biochars varied between 42.6 and (cabbage) to 348.9 (pine sawdust) (Table 1 and 2). Mukome et al. (2013) also stated that biochars produced from feedstocks high in C content (woody) had high C:N ratio. Therefore, the type of feedstock has been considered the main predictor of C:N ratio of biochar. High C:N ratios may lead to N immobilization after application of biochars to soil. Pretreating the biochar prior to soil application with a nutrient rich source such as compost or dairy effluents (Ghezzehei et al., 2014; Wang et al., 2015; Cui et al., 2016) to adsorb N and excess nutrients lowers the C:N ratio of biochars. The C:N ratio of biochars had significant negative correlations with pH, EC and CEC and positive correlation with SSA of the biochar types (Table 5).

Available phosphorus and potassium contents of biochar types

The most important characteristics of biochar types affecting the short-term crop performance were reported as the nutrient contents such as phosphorus (P) and potassium (K) (Rajkovich et al., 2012). Mean P content of biochar groups was ranked as field crop residues (0.45 g kg^{-1}), woody materials (1.35 g kg^{-1}), vegetable residue (4.55 g kg^{-1}) and animal manures (6.25 g kg^{-1}) (Figure 5). Large variations of P and K concentrations in the feedstocks and biochars indicate that feedstock type plays a significant role (P<0.01) in regulating the nutrient contents of biochars (Table 5). Biochar types contained two to four times higher P than that of the raw materials. Higher contents of K and P in the biochar types compared with their feedstocks accord with the common observation that chemical components concentrate in the solid biochar phase during the pyrolysis of feedstock (Gaskin et al., 2008; Chan and Xu, 2009; Yuan et al., 2011). Gaskin et al. (2008) reported that about 60% of P in the poultry litter and pine sawdust and 100% of the P in peanut hulls feedstock were retained in the biochars produced at 500 °C. The P and K contents of the biochar types were significantly different (P<0.05) from each other. The P content varied from 0.05 g kg^{-1} (rice husk) to 25.6 g kg^{-1} (poultry litter) (Table 2 and 4). The concentration content was between 0.63 g kg^{-1} (pine sawdust) and 52.03 g kg^{-1} (gooseberry) (Table 2 and 1). Cantrell et al. (2012) also indicated that pyrolysis of manures rich in nutrients yield nutrient rich biochars.

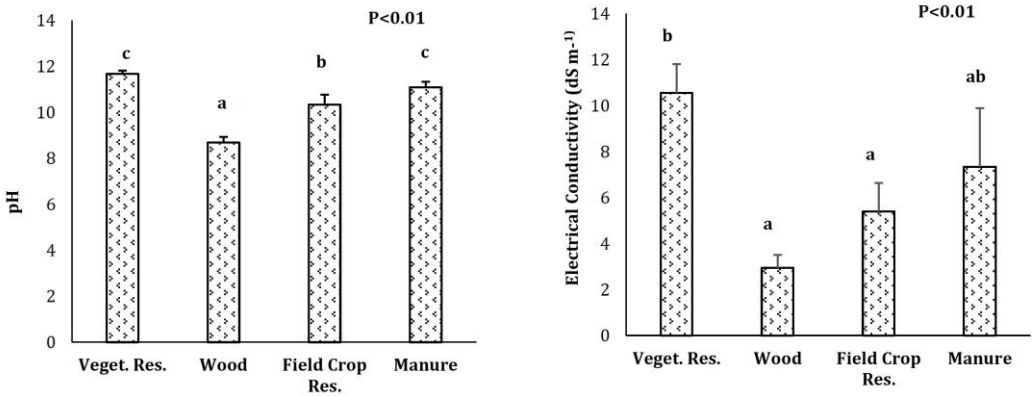

Figure 5. Available phosphorus (g kg^{-1}) ± SE of means and potassium (g kg^{-1}) ± SE of means contents of biochar types (n=18). Any two means sharing different letters are statistically significant (P≤0.05)

Desorption of plant nutrients from biochar has direct benefits for plant growth. Initial desorption rate of minerals from biochar is quite rapid and followed by a zero-order reaction that continues as long as the system is far from chemical equilibrium (Silber et al., 2010). Poultry litter was rich in P (8.44 mg kg^{-1}) and K (25.90 mg kg^{-1}), however addition to soil in fresh form may create problems due to the diseases and pathogens in fresh manure (Chan et al., 2009). Application of poultry manure in biochar form eliminates the problems, and provides higher amount of P and K as well as N. The amounts of P (25.6 mg kg^{-1}) and K (44.46 mg kg^{-1}) in poultry biochar were very high and may replace conventional P and K fertilizers for many crops (Table 4). Considering the application rates of 5 and 10 ton biochar ha^{-1}, application of poultry biochar to soil

will provide 128 kg P ha^{-1} to 256 kg P ha^{-1} and 222.3 kg K ha^{-1} to 444.6 kg K ha^{-1}. Mineral release rate of a biochar is important for the availability of nutrients in biochar. Silber et al. (2010) showed that P release of corn straw biochar produced at 500 °C significantly increased within 24 h as pH decreased from 8.9 to 4.5. The authors stated that a reasonable biochar application rate may successfully meet almost whole P need of a crop throughout the growing season. pH-dependent mineral release study of Silber et al. (2010) revealed that 1/3 of total K amount (48.7 g kg^{-1}) in the corn straw biochar was released during the first hour. The mean K content vegetable residue biochars (37.71 g kg^{-1}) is similar to that reported by Silber et al. (2010) and the significant amount of K release from the biochar may replace conventional K fertilizers for many of crops grown. However, as indicated by Silber et al. (2010), K release from the biochar will not adequately supply long-term plant K demand. In contrast to vegetable residues, biochars produced from woody biomass have lower K concentration (2.67 g kg^{-1}) and far from supplying the K demand of crops (Figure 5).

pH and electrical conductivity of biochar types

The pH and EC values of biochar types were significantly influenced by type of feedstock (P<0.01) (Figure 6). The pH value is the most important factor of a biochar in effectiveness of the agricultural applications (Weber and Quicker, 2018). The mean pH values of manures (11.1) and vegetable residues (11.7) were significantly higher than pH values of field crop residues (10.3) and woody materials (8.7) (Figure 6). All biochar types had a pH of 7.89 or greater, and the pH values ranged from slightly alkaline (pine sawdust, 7.89) to very strongly alkaline (gooseberry, 12.42) (Table 2 and 1). The addition of pine sawdust biochar to high pH biochar types may lower the pH value. Although only K concentrations of biochars have been analyzed among the alkali-earth elements, pine sawdust biochar had also the lowest concentrations of K. This could be the main reason for the lowest pH of the pine sawdust biochar. Significant positive linear correlation (r=0.86, P<0.01) between pH and K concentration of biochars supports the above discussion (Table 5). Fidel et al. (2012) also stated that the alkalinity of a biochar is influenced by organic functional groups, carbonates, and inorganic alkali composition. Low pH value of palm kernel shell (6.9) was attributed to the lowest concentrations of alkali and alkali-earth elements (Lee et al., 2013).

In many cases, biochars have been used to ameliorate acidic soils where alkalinity of biochar is favorable for improving the soil quality, and increasing the productivity of crops grown in acidic soils. Alkaline and strongly alkaline biochars may increase soil pH depending on the rate of application. However, Al-Wabel et al. (2017) indicated that biochar application in alkaline soils may not affect soil pH due to the buffering capacity of alkaline soils. Moreover, the concentration of basic sites was reported decreasing through oxidative interactions with microbes as biochar ages, thus a decrease in soil pH was obtained due to the oxidation of alkaline biochar (Liu et al., 2012). Therefore, biochars produced in this study can be used as soil additive without considering the alkalinity effect on soils.

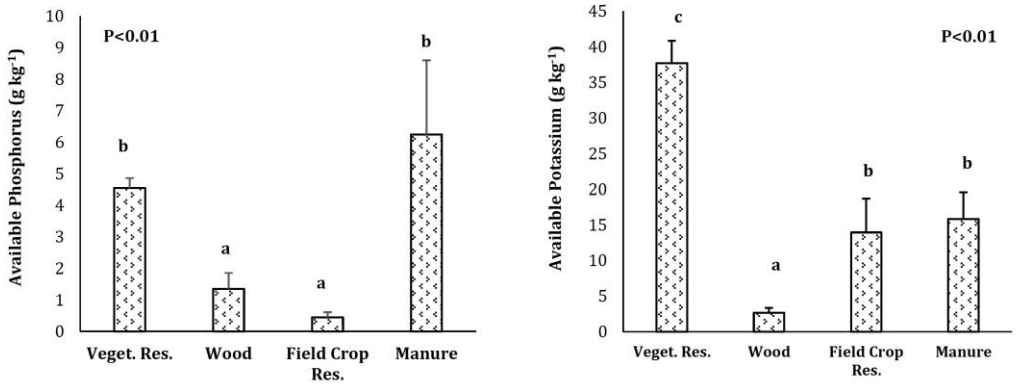

Figure 6. The pH and electrical conductivity (dS m^{-1}) ± SE of means of biochar types (n = 18). Any two means sharing different letters are statistically significant (P≤0.05)

Electrical conductivity (EC) values of biochar types should be determined to avoid salinity problems in soils, especially at high biochar application rates. The type of feedstock had significant (P<0.01) effect on EC of biochar types (Figure 6). The EC values of biochars produced from woody materials (2.95 dS m^{-1}) and field crop residues (5.39 dS m^{-1}) were significantly lower from the EC values of vegetable residue biochars (10.56 dS m^{-1}). The salinity of all biochars was high, with EC varying from 18.24 dS m^{-1} (cabbage) to 1.44 dS m^{-1} (poplar sawdust) (Table 1 and 2). The EC values of biochar types had significant positive correlations with pH, CEC, FC, WP, P and K, while it had significant negative correlations with SSA, total C and C:N ratio of biochars. The best predictor for biochar EC values was K producing r value of 0.60 (Table 5)

Relationships between physical and chemical properties of biochar types

Significantly linear relationships (P<0.01) were found between biochar pH values and all properties (except available water content) of 18 biochar types. Negative correlations indicated that surface area, total carbon content and C:N ratio of biochars were significantly decreased with increasing pH of biochars. Whereas, EC, CEC, FC and WP water contents available P and K concentrations significantly (P<0.01) increased with increased pH values of biochar types. The correlation analysis between the CEC and water contents of biochars at field capacity and wilting point showed a Pearson's correlation coefficients of 0.63 and 0.61 (P<0.01), indicating a significant positive correlation (Table 5). Surprisingly, SSA of biochars and water at FC and WP had significant negative correlations (P<0.05) which might be related to the loss of functional groups during pyrolysis process. High correlation of CEC with FC and WP also supports the negative correlations of SSA with FC and WP water contents of biochars.

Table 5. Correlations among some physical and biochemical characteristics of different biochar types

	pH	EC	CEC	SSA	FC	WP	AW	Biochar%	
pH	1.00								
EC	0.69**	1.00							
CEC	0.83**	0.49**	1.00						
SSA	-0.65**	-0.52**	-0.70**	1.00					
FC	0.50**	0.48**	0.63**	-0.33*	1.00				
WP	0.53**	0.46**	0.61**	-0.32*	0.93**	1.00			
AW	0.25	0.29	0.32*	-0.19	0.27	0.01	1.00		
Biochar%	0.36*	0.16	0.29	-0.63**	-0.09	0.03	-0.12	1.000	
	pH	**EC**	**CEC**	**SSA**	**C**	**N**	**C:N**	**P**	**K**
C	-0.62**	-0.41**	-0.59**	0.74**	1.00				
N	0.33*	0.30	0.32*	-0.37*	-0.39**	1.00			
C:N	-0.51**	-0.45**	-0.50**	0.59**	0.69**	-0.90**	1.00		
P	0.63**	0.36*	0.78**	-0.71**	-0.62**	0.52**	-0.68**	1.00	
K	0.86**	0.60**	0.87**	-0.56**	-0.56**	0.44**	-0.58**	0.67**	1.00

EC: Electrical Conductivity, CEC: Cation Exchange Capacity, SSA: Specific Surface Area, FC: Field Capacity, WP: Wilting Point, AW: Available Water Content, C: Total Carbon, N: Total Nitrogen, P: Phosphorus, K: Potassium

Positive correlation (P<0.05, r= 0.74) between SSA of biochars and total C content indicates that the higher the carbon content of the biochar the higher the surface area of the material. Biochar yields of feedstocks and SSA of biochar types had significant negative correlations (P<0.01). Lee et al. (2013) also reported very low SSA for cocopeat biochar (13.7 m^2 g^{-1}) despite its' the largest mass yield (45.9% dry ash free basis) among the biochars studied. The CEC and SSA of biochars had significant negative correlation (P<0.01, r= -0.70) (Table 5). The decrease of CEC with the increased SSA is probably related to the loss of functional groups during pyrolysis of feedstocks. Gaskin et al. (2008) found a considerable reduction of the CEC with an increase in SSA of biochars.

Conclusion

Physical and chemical properties of biochars, produced from several agricultural residues revealed that some of biochars might have many advantages in agriculture in terms of crop productivity and sustainability of soil fertility. Significant differences among biochars produced at the same pyrolysis temperature showed that the feedstock characteristics had the greatest influence on key agricultural characteristics of biochars. Application of biochar with high CEC, SSA and nutrient content can be considered an important additive to improve quality of soils with low CEC (particularly high sand content) and inadequate organic matter. Most of biochars (particularly woody materials and field crop residues) have higher SSA than sandy and comparable to or higher than clayey soils, therefore, water storage and nutrient holding capacities of sandy soils can be improved by the addition of biochars with high SSA.

Acknowledgement

This study was supported by Tokat Gaziosmanpasa University Scientific Research Project Commission (Project no: 2015/79).

References

Al-Wabel, M.I., Hussain, Q., Usman, A.R., Ahmad, M., Abduljabbar, A., Sallam, A.S. Ok, Y.S., 2018. Impact of biochar properties on soil conditions and agricultural sustainability: A review. *Land Degradation & Development* 29(7), 2124-2161.

Barton, C.F., 1948. Photometric analysis of phosphate rock. *Analytical Chemistry* 20(11): 1068-1073.

Brewer, C.E., Schmidt-Rohr, K., Satrio, J.A., Brown, R.C. 2009. Characterization of biochar from fast pyrolysis and gasification systems. *Environmental Progress & Sustainable Energy* 28(3): 386-396.

Brewer, C.E. Unger, R., Rohr, K.S., Brown, R.C., 2011. Criteria to select biochars for field studies based on biochar chemical properties. *Bioenergy Research* 4(4): 312-323.

Brewer, C.E. (2012). Biochar characterization and engineering. PhD. Dissertation, University of Iowa. USA.

Cantrell, K.B., Hunt, P.G., Uchimiya, M., Novak, J.M., Ro, K.S., 2012. Impact of pyrolysis temperature and manure source on physicochemical characteristics of biochar. *Bioresource Technology* 107: 419-428.

Chan, K.Y., Xu, Z., 2009. Biochar: Nutrient properties and their enhancement. In: Biochar for Environmental Management: Science and Technology. Lehmann, J., Joseph, S., (Eds). Earthscan, London, UK. pp.67-84.

Chapman, H.D., 1965. Cation exchange capacity. In: Methods of soil analysis Part 2 Chemical and Microbiological Properties. Black, C.A. (Ed.). Agronomy No. 9. ASA-SSSA, Madison, Wisconsin, USA. pp. 891–901.

Cheng, C., Lehmann, J., 2009. Ageing of black carbon along a temperature gradient, *Chemosphere* 75(8): 1021–1027.

Chu, G., Zhao, J., Huang, Y., Zhou, D., Liu, Y., Wu, M., Peng, H., Zhao, Q., Pan, B., Steinberg, C.E., 2018. Phosphoric acid pretreatment enhances the specific surface areas of biochars by generation of micropores. *Environmental Pollution* 240: 1-9.

Citak, S., Sonmez, S., Okturen, F., 2006. The possibility of using plant originated residues in agriculture. *Derim* 23(1): 40-53. [in Turkish]

Cerato, A.B., Lutenegger, A.J., 2002. Determination of surface area of fine-grained soils by the ethylene glycol monoethyl ether (EGME) method. *Geotechnical Testing Journal* 25(3): 315-321.

Cui, X., Hao, H., Zhang, C., He, Z., Yang, X., 2016. Capacity and mechanisms of ammonium and cadmium sorption on different wetland-plant derived biochars. *Science of the Total Environment* 539: 566-575.

Di Blasi, C., Tanzı, V., Lanzetta, M., 1997. A study on the production of agricultural residues in Italy. *Biomass and Bioenergy* 12(5): 321–331.

Di Donato, P., Fiorentino, G., Anzelmo, G., Tommonaro, G., Nicolaus, B., Poli, A., 2011. Re-use of vegetable wastes as cheap substrates for extremophile biomass production. *Waste and Biomass Valorization* 2(2): 103-111.

Downie, A., Crosky, A., Munroe, P., 2009. Physical properties of biochar. In: Biochar for Environmental Management: Science and Technology. Lehmann, J., Joseph, S., (Eds). Earthscan, London, UK. pp.13-32.

Fidel, R.B., 2012. Evaluation and ımplementation of methods for quantifying organic and ınorganic components of biochar alkalinity. MSc Thesis, Paper 12752, Iowa State University. USA.

Gaskin, J.W., Steiner, C., Harris, K., Das, K.C., Bibens, B. 2008. Effect of low-temperature pyrolysis conditions on biochar for agricultural use. *Transactions of the ASABE* 51(6): 2061-2069.

Gaskin, J.W., Speir, R.A., Harris, K., Das, K.C., Lee, R.D., Morris, L.A., Fisher, D.S., 2010. Effect of peanut hull and pine chip biochar on soil nutrients, corn nutrient status, and yield. *Agronomy Journal* 102(2): 623–633.

Ghezzehei, T.A., Sarkhot, D.V., Berhe, A.A., 2014. Biochar can be used to capture essential nutrients from dairy wastewater and improve soil physico-chemical properties. *Solid Earth* 5(2): 953-962.

Gray, M., Johnson, M.G., Dragila, M.I., Kleber, M. 2014. Water uptake in biochars: The roles of porosity and hydrophobicity. *Biomass and Bioenergy* 61: 196-205.

Guerro, M., Ruzi, M.P., Alzuet, M.U., Bilbao, R., Miller, A., 2005. Pyrolysis of eucalyptus at different heating rates: studies of char characterization and oxidative reactivity. *Journal of Analytical and Applied Pyrolysis* 74(1-2): 307-314.

Günal, H., Korucu, T., Birkas, M., Özgöz, E. Halbac-Cotoara-Zamfir, R. 2015. Threats to sustainability of soil functions in Central and Southeast Europe. *Sustainability* 7(2): 2161-2188.

Günal, E., Erdem, H. Çelik, İ., 2018. Effects of three different biochars amendment on water retention of silty loam and loamy soils. *Agricultural Water Management* 208: 232-244.

Herbert, L., Hosek, I., Kripalani, R., 2012. The characterization and comparison of biochar produced from a decentralized reactor using forced air and natural draft pyrolysis. California Polytechnic State University, San Luis Obispo Materials Engineering Department.

Hossain, M.K., Strezov, V., Chan, K.Y., Ziolkowski, A., Nelson, P.F., 2011. Influence of pyrolysis temperature on production and nutrient properties of wastewater sludge biochar. *Journal of Environmental Management* 92(1): 223-228.

Jeffery, S., Meinders, M.B., Stoof, C.R., Bezemer, T.M., van de Voorde, T.F., Mommer, L., van Groenigen, J.W., 2015. Biochar application does not improve the soil hydrological function of a sandy soil. *Geoderma* 251-252: 47-54.

Kanthle, A.K., Lenka, N.K., Tedia, K., 2018. Land use and biochar effect on nitrate leaching in a Typic Haplustert of central India. *Catena* 167: 422-428.

Laird, D.A., Fleming, P., Davis, D.D., Horton, R., Wang, B., Karlen, D.L., 2010. Impact of biochar amendments on the quality of a typical Midwestern agricultural soil. *Geoderma* 158(3-4): 443-449.

Lee, Y., Park, J., Ryu, C., Gang, K.S., Yang, W., Park, Y.K., Jung, J., Hyun, S., 2013. Comparison of biochar properties from biomass residues produced by slow pyrolysis at 500 °C. *Bioresource Technology* 148: 196-201.

Lehmann, J., Gaunt, J., Rondon, M., 2006. Bio-char sequestration in terrestrial ecosystems – a review. *Mitigation and Adaptation Strategies for Global Change* 11(2): 403–427.

Lehmann, J., Joseph, S., 2009. Biochar for Environmental Management. Science and Technology, Earthscan, London, UK.

Lim, T.J., Spokas, K.A., Feyereisen, G., Novak, J.M., 2016. Predicting the impact of biochar additions on soil hydraulic properties. *Chemosphere* 142: 136-144.

Liu, X.H., Han, F.P., Zhang, X.C., 2012. Effect of biochar on soil aggregates in the Loess Plateau: Results from incubation experiments. *International Journal of Agriculture and Biology* 14(6): 975-979.

Mukome, F.N.D., Zhang, X., Silva, L.C.R., Six, J., Parikh, S.J., 2013. Use of chemical and physical characteristics to investigate trends in biochar feedstocks. *Journal of Agricultural and Food Chemistry* 61(9): 2196-2204.

Rajkovich, S., Enders, A., Hanley, K., Hyland, C., Zimmerman, A.R., Lehmann, J., 2012. Corn growth and nitrogen nutrition after additions of biochars with varying properties to a temperate soil. *Biology and Fertility of Soils* 48(3): 271-284.

Oldfield, T.L., Sikirica, N., Mondini, C., López, G., Kuikman, P.J., Holden, N.M., 2018. Biochar, compost and biochar-compost blend as options to recover nutrients and sequester carbon. *Journal of Environmental Management* 218: 465-476.

Schellekens, J., Silva, C.A., Buurman, P., Rittl, T.F., Domingues, R.R., Justi, M., Vidal-Torrado, P., Trugilho, P.F., 2018. Molecular characterization of biochar from five Brazilian agricultural residues obtained at different charring temperatures. *Journal of Analytical and Applied Pyrolysis* 130: 106-117.

Silber, A., Levkovitch, I., Graber, E.R., 2010. pH-dependent mineral release and surface properties of corn straw biochar: agronomic implications. *Environmental Science & Technology* 44(24): 9318-9323.

Smith, P., 2016. Soil carbon sequestration and biochar as negative emission technologies. *Global Change Biology* 22(3): 1315-1324.

Sposito, G. 1989. The chemistry of soils. Oxford Univ. Press, New York, USA.

Vaccari, F.P., Baronti, S., Lugato, E., Genesio, L., Castaldi, S., Fornasier, F., Miglietta, F., 2011. Biochar as a strategy to sequester carbon and increase yield in durum wheat. *European Journal of Agronomy* 34(4): 231-238.

Wang, B., Lehmann, J., Hanley, K., Hestrin, R., Enders, A. 2015. Adsorption and desorption of ammonium by maple wood biochar as a function of oxidation and pH. *Chemosphere* 138: 120-126.

Weber, K. Quicker, P., 2018. Properties of biochar. *Fuel* 217: 240-261.

Yuan, J.H., Xu, R.K., Zhang, H., 2011. The forms of alkalis in the biochar produced from crop residues at different temperatures. *Bioresources Technology* 102(3): 3488-3497.

Eurasian J Soil Sci 2019, 8 (4) 340 - 350

Eurasian Journal of Soil Science

Journal homepage : http://ejss.fesss.org

Validation of satellite-based soil moisture retrievals from SMAP with in situ observation in the Simineh-Zarrineh (Bokan) Catchment, NW of Iran

Khaled Haji Maleki [a,*], Ali Reza Vaezi [a], Fereydoon Sarmadian [b], Wade T. Crow [c]

[a] Department of Soil Science, Faculty of Agriculture, University of Zanjan, Zanjan, Iran
[b] Department of Soil Science, Faculty of Agriculture, University of Tehran, Karaj, Iran
[c] USDA-ARS Hydrology and Remote Sensing Lab, Beltsville, MD, USA

Abstract

Soil moisture is an influential parameter in land surface hydrology and precise soil moisture data that can help researcher to realize the climate changes and land-atmosphere interactions. A initial struggle for the utilize of soil moisture data from satellite sensors is their reliability. It is important to appraise the dependability of those data before they can be regularly used at a global or local scale. In this study, the satellite soil moisture data was evaluated from the Soil Moisture Active/Passive (SMAP) over Simineh-Zarrineh Catchment in Bokan region, NW of Iran. A total of 287 soil samples as ground-based observations in the time period of 03 April to 03 December 2017 were taken for SMAP data validation. Results showed that the satellite data and in situ observation has a good correlation, with a mean correlation (r) value of 0.63 in total. This correlation level showed that, commonly, the SMAP soil moisture products over Simineh-Zarrineh Catchment (Bokan) have great quality, and it would be valuable for versatile utilization, including monitoring of land surface, weather prediction, modeling of hydrological process, soil loess monitoring, and climate studies. The results reveal that the remotely sensed data demonstrate the good correlation with in situ observation across the dry land with mean correlation (r) values of 0.67 throughout the time period. Particularly, SMAP soil moisture reveal a constant structure for obtain the spatial distribution of surface soil moisture. Additional researches are necessary for well realizing the SMAP data.

Keywords: Dry land, NDVI, RMSE, Soil water.

Article Info

Received : 03.10.2018
Accepted : 01.08.2019

Introduction

Soil moisture is a main control on many hydrological phenomena, particularly runoff formation, evaporation of soil and transpiration of plant. Soil moisture is one of the most difficult variables to prospect, because of its interaction with parameters as an example soil types, topography and vegetation (Wilson et al., 2004). The utilize satellite data has become a potent tool to increase our knowledge of the impress of soil moisture in the hydrological phenomena in some regions, e.g., land-atmosphere phenomena (Miralles et al., 2012; Taylor et al., 2012); weather and runoff prediction (Brocca et al., 2010; Bisselink et al., 2011); landslides (Brocca et al., 2012); agricultural drought monitoring (Sánchez et al., 2018) and precipitation products (Chen et al., 2012).

In the last two decades, several researches have illustrated that soil moisture can be recaptured by satellite missions, the most important ones are the Soil Moisture Ocean Salinity (SMOS) (Kerr et al., 2010) and Soil Moisture Active/Passive (SMAP) (Entekhabi et al., 2014). Lately, NASA's Soil Moisture Active/Passive (SMAP) satellite mission was inaugurated on January 31, 2015. The goal of the operation is monitoring of

* Corresponding author.
Department of Soil Science, Faculty of Agriculture, University of Zanjan, Zanjan, Iran
Tel.: +98 9194017683
E-mail address: khaled.hajimaleki@yahoo.com
e-ISSN: 2147-4249
DOI: 10.18393/ejss.608005

soil moisture and landscape freeze/thaw state at global scale. The SMAP measurements will, therefore, donate to enhanced predictions of water, energy and carbon movement between the land and atmosphere (Entekhabi et al., 2010). Nevertheless, as an outcome of the several procedures used for various satellite data, the quality and continuity of passive microwave soil moisture data changes in spatially and temporally (Owe et al., 2001; Parinussa et al., 2011; Dorigo et al., 2016). The appraisal of remotely sensed data is essential to guide their accurate apply and to enhance our comprehension of their advantages and disadvantages under various situation over the world and at various times.

In the circumstance of the SMAP mission, the requirement is an accuracy of 0.04 $cm^3.cm^{-3}$ for volumetric soil moisture (Entekhabi et al., 2014). Moreover mission demands standard, validation prepares the users with quality confidence, which in theory should comprise higher assurance and acceptation, resulting in further to extensive utilize of the mission products. This in turn prepares encourage for the mission and its substitutes. Eventually, from the scientific viewpoint remote sensing in special, there will be approximately uncertainty in the data because of lack of clarity in defining contributing area and depth for the different satellite operation sensors and frequencies. Validations help us to find a solution for these subjects and enhance algorithms through a careful appraisal of algorithm efficiency and anomalies.

Some researchers have appraised soil moisture data based on passive microwave sensors versus in situ observation across various areas (Brocca et al., 2011; Albergel et al., 2012; Parinussa et al., 2015; Wu et al., 2016). Former studies have also concentrated on the comparison of some soil moisture data (Kerr et al., 2012; Albergel et al., 2012; Dorigoet al., 2015). Leroux et al. (2014) performed comparisons between the SMOS, ASCAT, and ECMWF (European Centre for Medium-Range Weather Forecasts) soil moisture data and the outcomes show that SMOS retrievals are adjacent to the ground measurements with a low average root mean square error of 0.061$cm^3.cm^{-3}$. Al-Yaari et al. (2014) conducted a comparison among the SMOS and AMSR-E data used by extended period of time and shown that in terms of correlation values, the SMOS data was discovered to better capture the soil moisture temporal dynamics in generously vegetated biomes while good outcomes for AMSR-E were obtained over arid and semi-arid biomes. Zeng et al. (2015) analyzed comparison the AMSRE, AMSR2 and ASCAT data applying annual and seasonal succession, and the outcomes show that the AMSR-E and AMSR2 data were underestimated generally. Zeng et al. (2016) performed a introductory assessment of the SMAP radiometer data versus in situ observations gathered from various networks that contain disparate climatic and land surface situations, and the outcomes demonstrate that the SMAP data is in excellent concurrence with the in situ observations, despite the fact that it show dry or wet bias at various areas.

Because of the lack of long time period SMAP soil moisture; there is an absence of sufficient investigation compared to other soil moisture data. The SMAP data has been appraised in comparison with the uncertainty of downscaled brightness temperature obtained from airborne and ground remarks concurrently (Leroux et al., 2014; Das et al., 2016).

Due to the lack of systematic ground based monitoring of soil moisture and irregular topographies in the region such as studies would be essential and should be done. SMAP data can be used to understanding hydrological processes in the region because of good temporal resolution. In this research, it would be efforts to comparison SMAP data at daily time scales over the Simineh-Zarrineh catchment in Bokan city, NW of IRAN used by in situ observation from soil samples for 03 April to 03 December 2017. It would be the evaluation of SMAP data by ground based soil moisture in various land uses of semi-arid region to achieve the overall outlook of the SMAP soil moisture data accuracy and prepare a more practical outline for the applicability and accuracy of SMAP for various implementation.

Material and Methods

Study area

The Simineh-Zarrineh catchment with an area of 17563 km^2 is placed in the mountainous area of northwest of Iran and covered West Azarbaijan, East Azarbaijan and Kurdistan provinces with 56, 16 and 28 percentage of the catchment area respectively. (Urmia Lake Restoration National Committee, 2015). The Simineh-Zarrineh catchment is located (latitude $35^0 42' 14''$ to $37^0 44' 31''$ N, longitude $45^0 31' 32''$ to $47^0 22' 21''$ E) in the southern and southeastern parts of Urmia Lake and regarding the size it is the largest sub-basin of Urmia Lake basin (Figure 1). The lowest and highest elevation above sea level in the area is 1254 and 3389 meter respectively. Dominant crop in dry lands are barely, wheat and in irrigated agricultural land are sugar beet, alfalfa and apple.

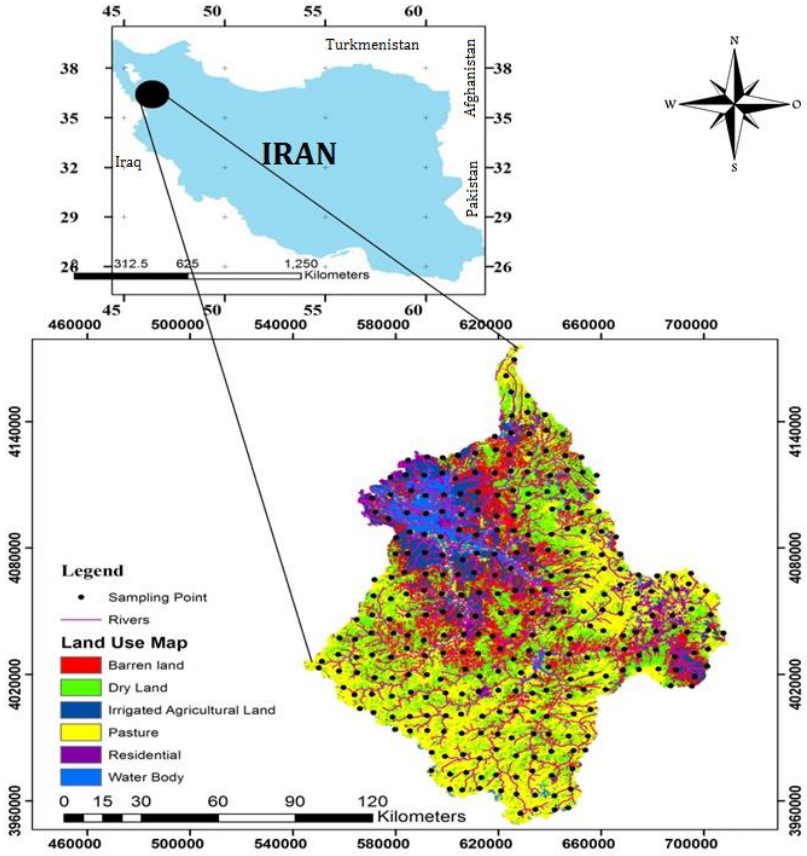

Figure 1. The 2018 Land Use Map of Simineh_Zarrineh Catchment (Bokan), in-situ soil moisture observations sites and rivers.

The rivers of Zarrinehrud and Siminehrud are perennial streams in this catchment with a highest discharge of about 3 billion cubic meters annually in the period 1995–2014 are regarded as water full rivers in the country. Zarrinehrud and Siminehrud river basins supply about 52% of environmental flow of Urmia Lake in each year. The length of Zarrinehrud and Siminehrud river is about 240 and 200 km and the area of the basin is 11642 and 5921 km^2 respectively. (Ahmadaali et al., 2018). The local climate is characterized by a dry steppe, hot summers, cold winters, low precipitation, high evaporation and low humidity. The annual average temperature and annual average precipitation are 12.1 C^0 and 423 mm respectively.

Datasets

SMAP satellite was launched on January 2015 by the National Aeronautics and Space Administration (NASA) (Entekhabi et al., 2010). SMAP supplies soil moisture data that envelopment the upside 5 cm of the soil column with an preciseness of 0.04 cm^3.cm^{-3} and a spatial resolution of 3, 9, 36 km, and envelopments the earth every three days (Entekhabi et al., 2010; Leroux et al., 2016; Das et al., 2011; Reichle et al., 2016). The SMAP criterion science data are demonstrated in the Table 1. on the whole, the SMAP task will create 15 distributable data representing four levels of data processing.

Table 1. Product Information of SMAP Mission

No.	Product	Description	Resolution
1	L1A_Radiometer	Radiometer Data in Time-Order	-
2	L1A_radar	Radar Data in Time-Order	-
3	L1_TB	Radiometer T_B in Time-Order	(36×47 km)
4	L1B_S0_LoRes	Low-Resolution Radar σ_B in Time-Order	(5×30 km)
5	L1C_S0_HiRes	High-Resolution Radar σ_B in Half_Orbit	1 km (1-3 km)
6	L1C_TB	Radiometer T_B in Half-Orbit	36 km
7	L2_SM_A	Soil Moisture(Radar)	3km
8	L2_SM_P	Soil Moisture(Radiometer)	36km
9	L2_SM_AP	Soil Moisture(Radar+Radiometer)	9km
10	L3_FT_A	Freeze/Thaw State(Radar)	3km
11	L3_SM_A	Soil Moisture (Radar)	3km
12	L3_SM_P	Soil Moisture (Radiometer)	36km
13	L3_SM_AP	Soil Moisture (Radar+Radiometer)	9km
14	L4_SM	Soil Moisture (Surface and Root Zone)	9km
15	L4_C	Carbon Net Ecosystem Exchange (NEE)	9km

Level 1 product contains instrument-related data and appears in granules that are based on half orbits of the SMAP satellite. Level 2 products are geophysical retrievals of soil moisture on a fixed Earth grid based on Level 1 products and ancillary information; the Level 2 products are output on a half-orbit basis. Level 3 products are daily composites of Level 2 surface soil moisture and freeze/thaw state data. These level products are daily global composites of the Level 2 geophysical retrievals for an entire UTC (Coordinated Universal Time) day. Level 4 products are model-derived value-added data products of surface and root zone soil moisture and carbon net ecosystem exchange that support key SMAP applications and more directly address the driving science questions. These level products contain output from geophysical models utilizing SMAP data (https://smap.jpl.nasa.gov/data/). In addition, the SMAP soil moisture data supplies measurements and analysis update data including pertinent geophysical fields reported as 3-hourly time averages, allocated over a 9-km grid (Reichle et al., 2015). In this research Level 4 products was used for validation and verification. All of SMAP data is downloadable from https://nsidc.org

In Situ Soil Moisture and Land Use Data

Sampling strategy based on regular sampling grid and in accordance with the pixel size of the satellite. In situ soil moisture samples in depth of 0 to 5 cm were collected from 287 soil sample points at six time periods in this paper (Figure 1). It has been attempt to select number of point based on the percentage of area covered by each land uses (Table 2). At each monitoring point, soil samples of topsoil (0–5 cm) were collected using a core sampler with 5-cm diameter and 12 cm height on six occasions from 03 April to 03 December 2017. Soil samples were taken in accordance with satellite data acquisition time. But when the surface was covered with snow, sampling was not done. The minimum and maximum intervals of soil samples point were 10.7 and 7.2 km respectively. After collecting, samples were put in plastic bag with tight fitting lids. Soil moisture was measured using mass method by the oven in the lab. After weighing, samples for 24 to 48 hours were dried in an oven at 105 ° C and then volumetric soil moisture percentage had been determined.

Data acquired in time period of 03 April to 03 December 2017. The soil moisture observation points acquired data for six days according to time table of SMAP mission. During the sampling process it has also been tried to the spatial distribution of the samples are located in all land uses.

The land use map is classified in accord with the 2018 Landsat 8 satellite data with a spatial resolution of 30 m in July (Figure 1). It was utilized to analyze the efficiency of SMAP data for various land use types over the Simineh-Zarrineh catchment (Bokan). The Land use map 2018 covering soil samples and rivers location is displayed in Figure 1. The number of soil samples distributed in various spatial areas and land use types is displayed in Table 2. Total of 287 soil samples were chosen for daily analysis.

Table 2. The number of soil sample sites situated in various land use over the Simineh_Zarrineh Catchment (Bokan).

Land Use	Percentage of Area(%)	Number of Soil Samples
Water body	4.65	0
Pasture	35.65	106
Irrigated agricultural land	8.43	41
Barren land	19.56	57
Dry land	28.22	83
Residential land	3.51	0

Methods

Previous researches have follow various approaches to compare remotely sensed soil moisture with in situ measurements (Entekhabi et al., 2010; Wu et al., 2016; Crow et al., 2012; Wang et al., 2016). In this study, the qualities of SMAP data were appraised by comparing them to the in situ soil moisture measurement from ground points. Four statistical indicators were used, containing the mean difference (MD), the root mean square difference (RMSD), the unbiased root mean square error (ubRMSE) and the correlation coefficient (R).

The accuracy of SMAP data are assessed regarding the MD, the RMSD, and the R. The MD represents the bias, namely the systematic difference between satellite soil moisture retrievals and in situ soil moisture observation. The MD was determined by the following equation (1):

$$MD = \frac{\sum_{i=1}^{n} \left(Q_s(i) - Q_m(i)\right)}{N} \quad (1)$$

The RMSD is a frequently used measure of the differences between SMAP data and in situ observation. RMSD is the square root of the average of squared errors. The RMSD was expressed by following equation (2):

$$RMSD = \sqrt{\frac{\sum_{i=1}^{N} (Q_s(i) - Q_m(i))^2}{N}} \quad (2)$$

Where; Q_s represents as a remotely sensed soil moisture ($cm^3.cm^{-3}$), Q_m is the in situ soil moisture observation ($cm^3.cm^{-3}$) and N expressed by total number of samples, and i represents a specific sample.

So that get an enhanced authentic prediction of RMSD, the bias can be absolutely eliminate by determining the ubRMSE that illustrates random error. The ubRMSE is computed by the following equation (3) (Entekhabi et al., 2014).

$$ubRMSE = \sqrt{(RMSD)^2 - (MD)^2} \quad (3)$$

The r reveal the proportionate of preciseness among SMAP data and in situ soil moisture observation. The correlation coefficient(r) expressed by following equation (4):

$$r = \frac{\sum_{i=1}^{n}(\theta_s(i) - \mu_s)(\theta_m(i) - \mu_m)}{(N-1)\sigma_s\sigma_m} \quad (4)$$

Where; σ_s and σ_m are the standard deviation of satellite and in situ data ($cm^3.cm^{-3}$), respectively and μ_s is the mean of SMAP soil moisture throughout the whole appraisal time period ($cm^3.cm^{-3}$), and μ_m is the mean of in situ soil moisture observation ($cm^3.cm^{-3}$). Normalized Difference Vegetation Index (NDVI) is the extensive used vegetation index to recognize healthy vegetation from others or from non-vegetated areas. NDVI was calculated following equation (5):

$$\text{NDVI} = \left(\frac{NIR - R}{NIR + R}\right) \quad (5)$$

Where; NIR is Near Infra-Red band(band 5 for both Landsat 8 and ETM+ sensor) and R is Red band (band 4 in case of Landsat 8 and ETM+ sensor).

Results

SMAP data was appraised by comparing with in situ observation with four statistical criteria during 03 April to 03 December 2017 were used to analyze and validation in various land use types. The outcomes of MD, RMSD, ubRMSE and R were computed for SMAP product with in situ observation. As seen in Figure 2, the MD for SMAP soil moisture had positive values of 0.011, 0.009, 0.023, 0.012 $cm^3.cm^{-3}$ in 08 May, 03 July, 13 September and 03 November respectively, despite in another times, MD had negative values of 0.007 $cm^3.cm^{-3}$ and 0.021 $cm^3.cm^{-3}$ in 03 April and 03 December, respectively. The SMAP soil moisture demonstrates good performance with RMSD values ranging from 0.18 $cm^3.cm^{-3}$ to 0.33 $cm^3.cm^{-3}$ and ubRMSE value from 0.17 $cm^3.cm^{-3}$ to 0.33 $cm^3.cm^{-3}$. Figure 2 demonstrates that, SMAP data compared to the in situ measurement is well correlated, with r equal 0.77 and 0.72in 03 July and 03 November respectively and great correlated with r equal 0.62 in 03 April respectively also good correlated with r equal 0.56, 0.57 and 0.52 in 08 May, 13 September and 03 December respectively. The SMAP soil moisture demonstrated the good correlation with in situ measurement in 03 July.

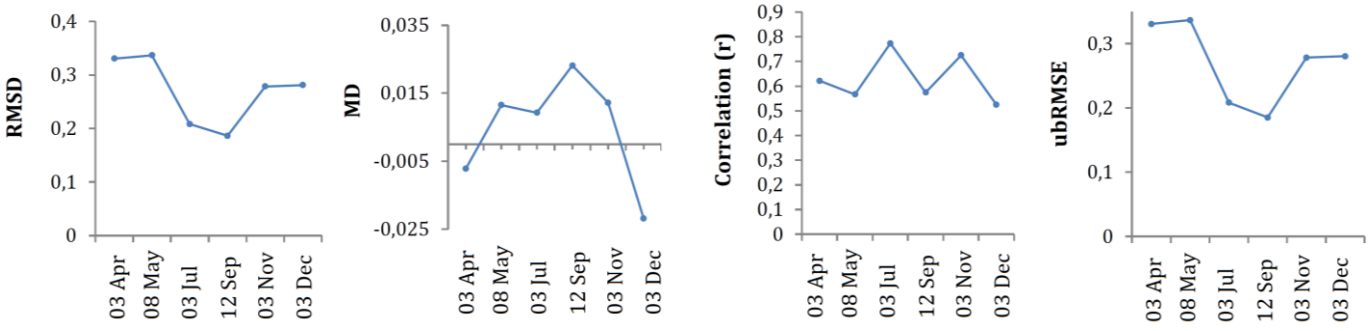

Figure 2. Evolution of four statistics results for SMAP daily data of Simineh-Zarrineh Catchment (Bokan).

As shown in Figure 3, the correlation coefficients for the daily data, as appraised by the different time period, the SMAP data is mostly have great performance. SMAP soil moisture displays distinguish variation. The correlation between SMAP and in situ data were shown in Figure 3. Correlation values between the data sets

are great along most of the time period in variation of biomes and climate circumstances in 03 July and 03 November with averaged values of r=0.77 and r=0.72 respectively. In 03 April, 03 September, 08 May and 03 December the correlation between SMAP and in situ data was good with r values of 0.61, 0.57, 0.56 and 0.52, respectively. So that SMAP soil moisture data had been great performed, as indicated by higher r values (Figure 2), in the 03 July and November also SMAP soil moisture had the lowest correlation with in situ data in the 03 December relative to the other times.

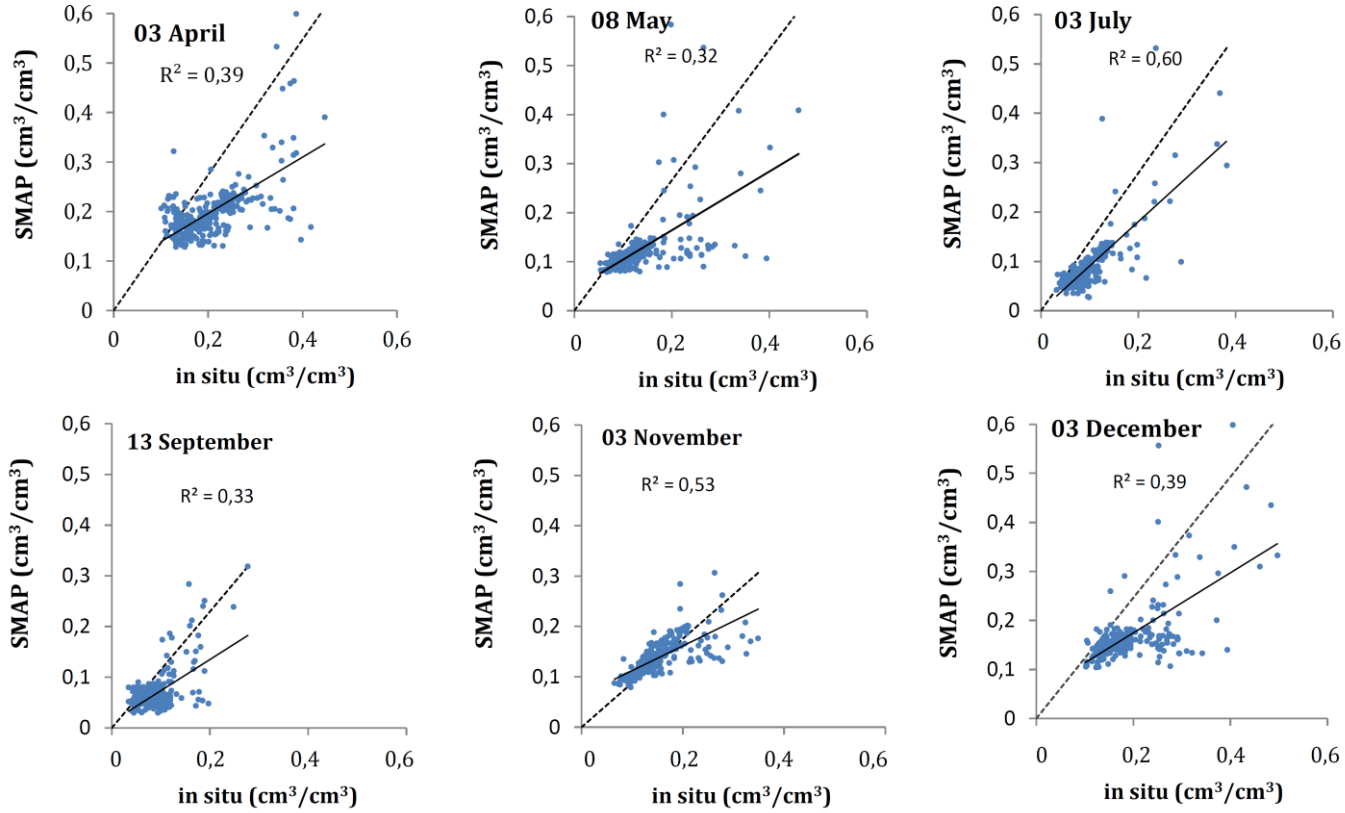

Figure 3. Correlation between SMAP daily data and in situ data in different land use of Simineh-Zarrineh Catchment (Bokan). 1:1 dot line and fitted solid line.

The accuracy of SMAP data is influenced by the kind of land use. The MD, RMSD, ubRMSE and R were computed for the SMAP data with various land use (Figure 4).

For the SMAP soil moisture data, the good efficiency was achieved in 03 July for the dry lands, where the MD, RMSD and ubRMSE values were 0.08, 0.18 and 0.17 respectively. Low range of soil moisture variation in pasture partially donates to the low RMSD and ubRMSE, as showed in the correlation coefficients (Figure 4). The average value of correlation coefficients for the dry land and irrigated agricultural land were 0.67 and 0.54 ($p > 0.05$), respectively. Compared with other land uses, the dry land showed the best r values for SMAP soil moisture data (0.67 $cm^3.cm^{-3}$).

SMAP soil moisture data obtained in barren land showed negative MD in 03 April and 03 December, a partly high RMSD (0.31 $cm^3.cm^{-3}$) and a good r value (0.75) in comparison with in situ data. The minimum MD and the good average value of r outcomes were achieved in dry land for SMAP soil moisture data in 03 July (Figure 4). Daily SMAP data demonstrated the lowest r value for irrigated agricultural land, with an average r value of 0.54 in 03 April to 03 December. The efficiency of the SMAP data retrieved from different land use of Simine-Zarrineh catchment was analyzed. Daily averaged SMAP data were in comparison with in situ data by correlation coefficient (Table 3).

Negative MD values in the 03 April for barren land and irrigated agricultural land and in the 03 December for all land use types had been seen in daily average SMAP soil moisture, which means that the data are underestimates (Figure 4a,f). Low positive MD values in SMAP soil moisture data for whole land use types had been seen in 03 July (Figure 4d). The highest MD values connect to SMAP soil moisture were achieved in the 08 May and for Pasture (Figure 4b). The good results for SMAP soil moisture in the 13 September for dry land obtained in RMSD and ubRMSE (Figure 4c). The SMAP soil moisture showed the lowest RMSD (0.33

$cm^3.cm^{-3}$) and ubRMSE (0.32 $cm^3.cm^{-3}$) in the 03 April and 03 November for irrigated agricultural land (Figure 4a,e). Small MD values occurred in 03 July and 03 November for all land uses, showing that more precise soil moisture predict were achieved for SMAP soil moisture (Figure 4d,e).

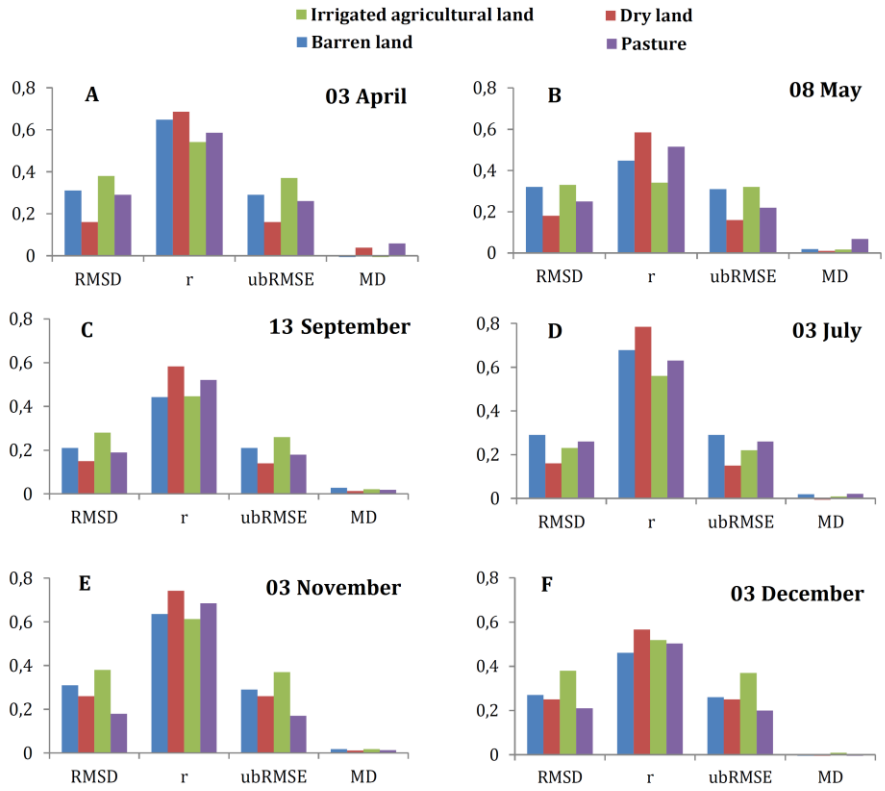

Figure 4. Results of cross validation for SMAP soil moisture daily data with different Land use types of Simineh-Zarrineh Catchment (Bokan).

Table 3. Mean correlation and standard deviation for SMAP daily data versus in situ data in different land use of Simineh-Zarrineh Catchment (Bokan).

	Land use type	03 April	08 May	03 July	13 September	03 November	03 December
Average correlation (r)	Barren land	0.64	0.57	0.75	0.55	0.71	0.67
	Dry land	0.69	0.63	0.81	0.61	0.76	0.61
	Irrigated agricultural land	0.54	0.52	0.58	0.51	0.59	0.51
	Pasture	0.59	0.47	0.66	0.57	0.63	0.59
Standard deviation	Barren land	0.25	0.19	0.21	0.23	0.18	0.29
	Dry land	0.22	0.17	0.12	0.2	0.15	0.26
	Irrigated agricultural land	0.26	0.23	0.27	0.29	0.25	0.33
	Pasture	0.29	0.21	0.23	0.24	0.22	0.31

With regard to land uses, dry land, barren land, pasture and irrigated agricultural land the average r value were 0.76, 0.61, 0.57 and 0.54 respectively (Figure 5). The best average R value for dry land, Pasture, Barren land and irrigated agricultural land in this time period were in 03 July, 03 November, 03 July and 03 November respectively (Figure 5). SMAP soil moisture had the good results regarding r values (r>0.70) in the 03 July for dry land (Figure 5).

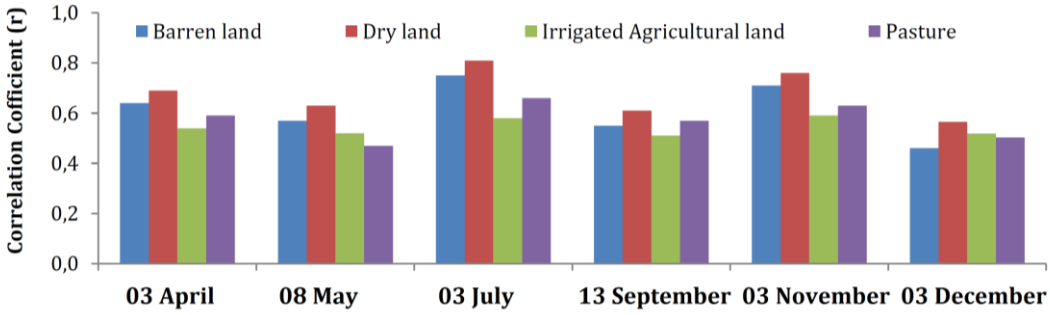

Figure 5: Results of correlation among SMAP data and in situ data for various land use types and different times of Simineh-Zarrineh Catchment (Bokan).

Discussion

The vegetation diversity, soil and climate features are the critical parameters that affect the outcomes. Moreover, there is significant spatial variety in various land use types and temporal and dynamical modification in their features, which lead to various grades of efficiency in spatial-temporal assessment. The weak outcomes of this appraisal would be described by some causes. First, uncertainties result from several complicated parameters that influence the radiative transfer model (Wu et al., 2016). Second, there exist dissimilarity in the vertical depth checked out by the satellite SMAP soil moisture and the in situ data. The soil water content of the surface layer (5 cm) detected by SMAP soil moisture will be different from the deeper layer which observed by the soil sampling (5 cm). The soil water content in the surface layer that detected by satellite tends to react further quickly to atmospheric process than the deeper soil layer.

The SMAP protocol utilize an Ensemble Kalman Filter (EnKF) to be revealed SMAP data with soil moisture prediction from the NASA Catchment land surface model (Reichle et al.,2016). Various recovery procedure and brightness temperature measurement was utilized by SMAP (Das et al., 2016; Das et al., 2011), which contributes to the differences evaluation results. The immense nonuniformity in each pixel comparative to the in situ observation negatively affected the accuracy of the appraisal (Jackson et al., 2010). The parameters discussed above may also use to the SMAP soil moisture. The SMAP soil moisture ordinary demonstrated well concurrence with the reference data and successfully captured the spatial and temporal changes showed in Figures 2–5 and Tables 3. As an example, SMAP soil moisture performed good in the areas covered by dry land, because of low fluctuation of vegetation in this time period (Dorigo et al., 2010). The apposite, SMAP soil moisture showed poor correlations among the reference data in irrigated agricultural land (Figures 4 and 5), since that fluctuation of vegetation in its area is very high. These impacts would be originated to the high range of changes in soil moisture in these areas, which approximately fit to the anticipated retrieval accuracy of the satellite data (Al-Yaari et al., 2014). Meanwhile SMAP soil moisture also showed low correlations with the in situ data in Pasture areas in 08 May. As shown in Figure 1, about 35.65 percentage of this study area covered with its.

The outcomes approved that vegetation performs a great role in the appraisal efficiency of the SMAP product. It could be seen from Figure 6 the NDVI were large through the year for Irrigated agricultural land. The correlation among the SMAP soil moisture calculated r with in situ and NDVI is relative numerous with a high value of 0.53 (Figure 7), which revealed the effect of vegetation to soil moisture data. The quality of remotely sensed data reduces with increasing vegetation severity in dry land, Pasture and Irrigated agricultural land (Figure 7). These results were accordant with former researches (Brocca et al., 2013a,b,c). While Barren land areas did not exhibit same correlation structure with other land use types, this can be partially described by the very low vegetation in Barren land (Figure 7).

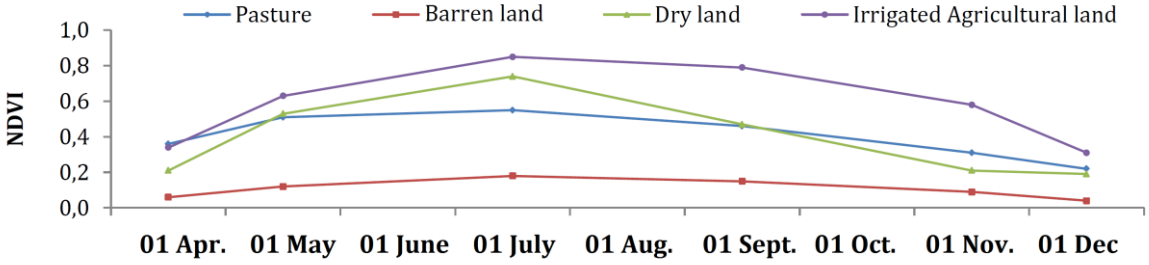

Figure 6. The temporal variation of mean NDVI for various land uses.

Investigating the temporal trends further nearly, SMAP soil moisture oriented to underestimate soil moisture in 03 April and 03 December and presents properly throughout the dry season (e.g., from 08 May to 03 September) than throughout the rest of the year. The causes can be linked to some aspects. First of all, low frequency of precipitation in summer than other time periods, that partially showed the good performance of SMAP data in summer. Meantime, the April to September in addition has plentiful vegetation, which more intensifies the incompatibility with in situ soil moisture. In this research, with NDVI of various land use types from April to December 2017 (Figures 6) and the correlation among SAMP soil moisture appraised r versus in situ and NDVI (Figure 7), impact of vegetation for soil moisture data can be measurable described.

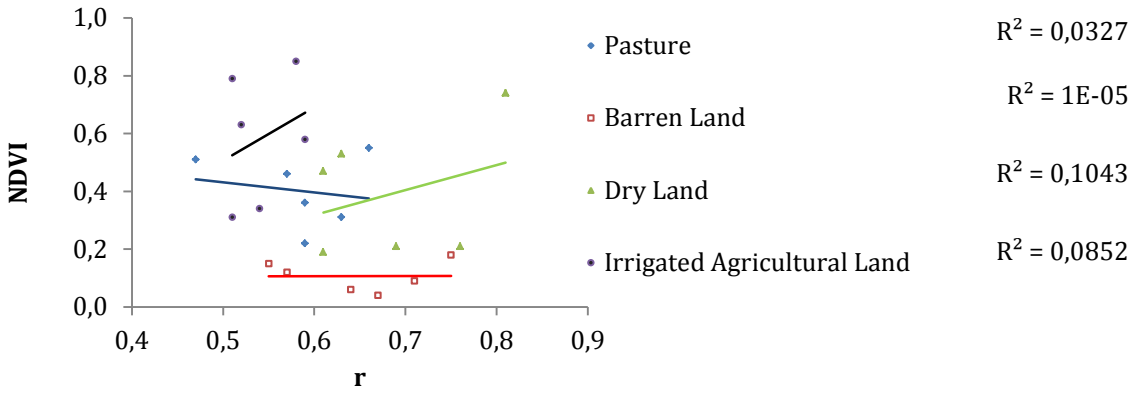

Figure 7. Correlation coefficient (r) between NDVI and SMAP soil moisture evaluation results with in situ (r).

Moreover, several aspects of the spatiotemporal data would be underlined. From Figure 4, it would be understand that the dry land outperforms the other land use throughout almost the whole time period. As exhibit from Figure 7, bigger NDVI in irrigated agricultural land donated to the poor performance. In spite the fact that in dry land the NDVI exhibit great effect on the appraisal of SMAP soil moisture data, in other words several parameters as an example large spatial intricacy of topography and surface characteristic may principally affect the appraisal outcomes. Nevertheless, the SMAP soil moisture show reverse outcomes for correlation from 03 April and 03 December in barren land as shown in Figure 4. This outcome would be because of a number of parameters, comprising greater vegetation coverage or variation in precipitation. Regarding the complete divergence among satellite and in situ soil moisture data, SMAP soil moisture exhibited relatively low mean RMSD and ubRMSE (Figure 2). In Figure 4, the dry land and pasture shows lower RMSD for the SMAP data. Meanwhile, the dry land exhibits relatively smaller RMSD and ubRMSE over the time period. It is mostly shown from Figure 4 that the dry land is principally situated in area with low NDVI variation over the year (Figure 6). The small range and change of soil moisture in these land uses partially donated to the small RMSD and ubRMSE. For validation of remotely sensed data, the greatest interesting subject is the representativeness of the in situ observations; both in situ sensor errors and the taken sampling of the true field mean soil moisture on the basis of a finite number of point samples can reason bias and magnitude errors in the predictions (Entekhabi et al., 2014). Despite the fact that SMAP data exhibit well concurrence with in situ data in r, for instance, dry land executed good with daily mean measurements for SMAP data, moderate executes were found for irrigated agricultural land for SMAP data, however the ubRMSE value of SMAP data in different land use and time periods can't meet the design criteria. Anyway, systematic deviations among remotely sensed and in situ data are frequently discovered although the temporal dynamics are highly similar (Loew and Schlenz, 2011). In this research, in situ data near water body were eliminated. Therefore, differences may seem somewhat. It has been conclude that SMAP soil moisture products over Simineh- Zarrineh catchment (Bokan) are practical for different utilization such as predicting rainfall, monitoring of climate change and hydrological modeling, that based on good remarked universal soil moisture datasets from remotely sensed.

Conclusion

This research prepared an inclusive assessment of the SMAP data across the Simineh- Zarrineh catchment (Bokan) using in situ data of 287 sampling point distributed through this catchment as ground control. The results indicate the SMAP soil moisture data appear relatively good agreement with in situ data placed in various land uses and arranged in a time periods. This conclusion can be supported well by the four statistical criteria (MD, RMSD, ubRMSE and R). Our analysis evaluation mentions that the efficiency of the SMAP soil moisture changes rely on their spatial distribution, time periods distribution and land use types. Regarding that spatial series analysis, SMAP data in the land use covered by dry land exhibit well concurrence with in situ data. Poor correlation coefficient in 03 December and a good correlation coefficient in 03 July have been shown. Generally results demonstrate best performances of the product to retrieve surface soil moisture as well as short term variability. Correlation values among the data sets are very satisfactory across most of the inspected sites situated in contrasted various land use types with mean values of 0.68, 0.64, 0.58 and 0.54 for dry land, barren land, pasture and irrigated agricultural land respectively. It is important to express that although the appraised SMAP soil moisture products utilized in this research were discovered to be very dependable in accord with the spatial and temporal analysis. Concentrated on the effect of spatial-temporal characteristics, the land use types with pasture, irrigated

agricultural land, barren land and dry land were significantly influenced by seasonal variation. Generally, the conducted validation assessment permitted definition of the dependability of SMAP data through a strong and standardized compared by ground measurements for assessment of spatiotemporal series on daily time scales across the Simineh- Zarrineh catchment (Bokan). In summary, the accuracy and reliability of the SMAP data predicts changes rely on land uses. These outcomes are in concurrence with our anticipation that SMAP data are mostly of best quality over low vegetation covered regions. This subject would be addressed in future researches to enhance the accuracy of SMAP data predicts.

Acknowledgements

The authors appreciate to Por Bare Baghestan Company for conducted to analyze the soil samples. We are very much thankful to Dr. Luca Brocca from IRPI for their valuable guidance.

References

Ahmadaali, J., Barani, GH.A., Qaderi, K., Hessari, B., 2018. Analysis of the effects of water management strategies and climate change on the environmental and agricultural sustainability of Urmia Lake Basin, Iran. *Water* 10(2): 160.

Albergel, C., de Rosnay, P., Gruhier, C., Munoz-Sabater, J., Hasenauer, S., Isaksen, L., Kerr, Y., Wagner, W., 2012. Evaluation of remotely sensed and modeled soil moisture products using global ground-based in situ observations. *Remote Sensing of Environment* 118: 215–226.

Al-Yaari, A., Wigneron, J.P., Ducharne, A., Kerr, Y., de Rosnay, P., de Jeu, R., Govind, A., Al Bitar, A., Albergel, C., Muñoz-Sabater, J., 2014. Global-scale evaluation of two satellite-based passive microwave soil moisture datasets (SMOS and AMSR-E) with respect to land data assimilation system estimates. *Remote Sensing of Environment* 149: 181–195.

Al-Yaari, A., Wigneron, J.P., Kerr, Y., de Jeu, R., Rodriguez-Fernandez, N., van der Schalie, R., Al Bitar, A., Mialon, A., Richaume, P., Dolman, A., 2016. Testing regression equations to derive long-term global soil moisture datasets from passive microwave observations. *Remote Sensing of Environment* 180: 453–464.

Barichivich, J., Briffa, K.R., Myneni, R., van der Schrier, G., Dorigo, W., Tucker, C.J.,Osborn, T.J., Melvin, T.M., 2014. Temperature and snow-mediated moisture controls of summer photosynthetic activity in northern terrestrial ecosystems between 1982 and 2011. *Remote Sensing* 6(2): 1390–1431.

Brocca, L., Melone, F., Moramarco, T., Wagner, W., Naeimi, V., Bartalis, Z., Hasenauer, S., 2010. Improving runoff prediction through the assimilation ofthe ASCAT soil moisture product. *Hydrology and Earth System Sciences* 14(10): 1881–1893.

Brocca, L., Hasenauer, S., Lacava, T., Melone, F., Moramarco, T., Wagner, W., Dorigo, W., Matgen, P., Martinez-Fernandez, J., Llorens, P., Latron, J., Martin, C., Bittelli, M., 2011. Soil moisture estimation through ASCAT and AMSR-E sensors: An intercomparison and validation study across Europe. *Remote Sensing of Environment* 115(12): 3390–3408.

Brocca, L., Ponziani, F., Moramarco, T., Melone, F., Berni, N., Wagner, W., 2012. Improving landslide forecasting using ASCAT-derived soil moisture data: A case study of the Torgiovannetto Landslide in Central Italy. *Remote Sensing* 4(5): 1232–1244.

Brocca, L., Melone, F., Moramarco, T., Wagner, W., Albergel, C., 2013a. Scaling and filtering approaches for the use of satellite soil moisture observations. In: Remote Sensing of Energy Fluxes and Soil Moisture Content. Petropoulos, G.P. (Ed.). CRC Press, Taylor and Francis Group, Boca Raton, New York, USA. pp. 411–426.

Brocca, L., Moramarco, T., Melone, F., Wagner, W., 2013b. A new method for rainfall estimation through soil moisture observations. *Geophysical Research Letters* 40(5): 853–858.

Brocca, L., Tarpanelli, A., Moramarco, T., Melone, F., Ratto, S.M., Cauduro, M., Ferraris, S., Berni, N., Ponziani, F., Wagner, W., Melzer, T., 2013c. Soil moisture estimation in alpine catchments through modeling and satellite observations. *Vadose Zone Journal* 12(3): vzj2012.0102

Chen, F., Crow, W.T., Holmes, T.R.H., 2012. Improving long-term, retrospective precipitation datasets using satellite-based surface soil moisture retrievals and the soil moisture analysis rainfall tool. *Journal of Applied Remote Sensing* 6(1): 063604

Crow, W.T., Berg, A.A., Cosh, M.H., Loew, A., Mohanty, B.P., Panciera, R., de Rosnay, P., Ryu, D., Walker, J.P., 2012. Upscaling sparse ground-based soil moisture observations for the validation of coarse-resolution satellite soil moisture products. *Reviews of Geophysics* 50(2): RG2002.

Das, N.N., Entekhabi, D., Dunbar, R.S., Njoku, E.G., Yueh, S.H., 2016. Uncertainty estimates in the SMAP combined active-passive downscaled brightness temperature. *IEEE Transactions on Geoscience and Remote Sensing* 54(2): 640–650.

Das, N.N., Entekhabi, D., Njoku, E.G., 2011. An algorithm for merging SMAP radiometer and radar data for high-resolution soil-moisture retrieval. *IEEE Transactions on Geoscience and Remote Sensing* 49(5): 1504–1512.

Dorigo, W.A., Scipal, K., Parinussa, R.M., Liu, Y.Y., Wagner, W., de Jeu, R.A.M., Naeimi, V., 2010. Error characterisation of global active and passive microwave soil moisture datasets. *Hydrology and Earth System Sciences* 14(12): 2605–2616.

Dorigo,W.A., Gruber, A., de Jeu, R.A.M., Wagner, W., Stacke, T., Loew, A., Albergel, C., Brocca, L., Chung, D., Parinussa, R.M., Kidd, R., 2015. Evaluation of the ESA CCI soil moisture product using ground-based observations. *Remote Sensing of Environment* 162: 380–395.

Entekhabi, D., Njoku, E.G., O'Neill, P.E., Kellogg, K.H., Crow, W.T., Edelstein, W.N., Entin, J.K., Goodman, S.D., Jackson, T.J., Johnson, J., 2010. The Soil Moisture Active Passive (SMAP) mission. *Proceedings of the IEEE* 98(5): 704–716.

Entekhabi, D., Yueh, S., O'Neill, P.E., Kellogg, K.H., Allen, A., Bindlish, R., Brown, M., Chan, S., Colliander, A., Crow, W.T., Das, N., De Lannoy, G., Dunbar, R.S., Edelstein, W.N., Entin, J.K., Escobar, V., Goodman, S.D., Jackson, T.J., Jai, B., Johnson, J., Kim, E., Kim, S., Kimball, J., Koster, R.D., Leon, A., McDonald, K.C., Moghaddam, M., Mohammed, P., Moran, S., Njoku, E.G., Piepmeier, J.R., Reichle, R., Rogez, F., Shi, J.C., Spencer, M.W., Thurman, S.W., Tsang, L., Van Zyl, J., Weiss, B., West, R., 2014. SMAP Handbook–Soil Moisture Active Passive: Mapping Soil Moisture and Freeze/Thaw from Space. Jet Propulsion Laboratory (JPL) Publication. Pasadena, CA.

Jackson, T.J., Cosh, M.H., Bindlish, R., Starks, P.J., Bosch, D.D., Seyfried, M., Goodrich, D.C., Moran, M.S., Du, J.Y., 2010, Validation of advanced microwave scanning radiometer soil moisture products. *IEEE Transactions on Geoscience and Remote Sensing* 48(12): 4256–4272.

Kerr, Y., Waldteufel, P., Wigneron, J.P., Delwart, S., Cabot, F., Boutin, J., Escorihuela, M.J., Font, J., Reul, N., Gruhier, C., Juglea, S.E., Drinkwater, M.R., Hahne, A.,Martin-Neira, M., Mecklenburg, S., 2010. The SMOS mission: new tool formonitoring key elements of the global water cycle. *Proceedings of the IEEE* 98(5): 666–687.

Kerr, Y.H., Waldteufel, P., Richaume, P., Wigneron, J.P., Ferrazzoli, P., Mahmoodi, A., Al Bitar, A., Cabot, F., Gruhier, C., Juglea, S.E., Leroux, D., Mialon, A., Delwart, S., 2012. The SMOS soil moisture retrieval algorithm. *IEEE Transactions on Geoscience and Remote Sensing* 50(5): 1384–1403.

Leroux, D.J., Kerr, Y.H., Al Bitar, A., Bindlish, R., Jackson, T.J., Berthelot, B., Portet, G., 2014. Comparison between SMOS, VUA, ASCAT, and ECMWF soil moisture products over four watersheds in US. *IEEE Transactions on Geoscience and Remote Sensing* 52(3): 1562–1571.

Loew, A., Schlenz, F., 2011. A dynamic approach for evaluating coarse scale satellite soil moisture products. *Hydrology and Earth System Sciences* 15(1): 75–90.

Miralles, D.G., van den Berg, M.J., Teuling, A.J., de Jeu, R.A.M., 2012. Soil moisture-temperature coupling: A multiscale observational analysis. *Geophysical Research Letters* 39(21): L21707.

Owe, M., de Jeu, R., Van de Griend, A., 2001. Estimating long term surface soil moisture from satellite microwave observations in Illinois, USA. Remote Sensing and Hydrology 2000 (Proceedings of a symposium held at Santa Fe, New Mexico, USA, April 2000). IAHS Publication No. 267, 2001.

Parinussa, R., Meesters, A.G.C.A., Liu, Y.Y., Dorigo, W.; Wagner, W.; de Jeu, R.A.M., 2011 An analytical solution to estimate the error structure of a global soil moisture data set. *IEEE Geoscience and Remote Sensing Letters* 8(4): 779–783.

Parinussa, R.M., Holmes, T.R.H., Wanders, N., Dorigo,W.A., de Jeu, R.A.M., 2015. A preliminary study toward consistent soil moisture from AMSR2. *Journal of Hydrometeorology* 16: 932–947.

Reichle, R., Koster, R., De Lannoy, G., Crow, W., Kimball, J., 2016. Level 4 Surface and Root Zone Soil Moisture (L4_SM) Data Product. Available at [Access date: 03.10.2018]: https://nsidc.org/sites/nsidc.org/files/technical-references/272_L4_SM_RevA_web.pdf

Sanchez, N., González-Zamora, Á., Martínez-Fernández, J., Piles, M., Pablos, M., 2018. Integrated remote sensing approach to global agricultural drought Monitoring. *Agricultural and Forest Meteorology* 259: 141–153.

Seneviratne, S.I., Corti, T., Davin, E.L., Hirschi, M., Jaeger, E.B., Lehner, I., Orlowsky,B., Teuling, A.J., 2010. Investigating soil moisture-climate interactions in a changing climate: a review. *Earth-Science Reviews* 99(3-4): 125–161.

Taylor, C.M., de Jeu, R.A.M., Guichard, F., Harris, P.P., Dorigo, W.A., 2012. Afternoon rain more likely over drier soils. *Nature* 489: 423–426.

Urmia Lake Restoration National Committee. 2015. Necessity of Lake Urmia Resuscitation, Causes of Drought and Threats; Report No: ULRP-6-4-3-Rep 1; Urmia Lake Restoration National Committee: Tehran, Iran.

Wang, S., Mo, X., Liu, S., Lin, Z., Hu, S., 2016. Validation and trend analysis of ECV soil moisture data on cropland in North China plain during 1981–2010. *International Journal of Applied Earth Observation and Geoinformation* 48: 110–121.

Wilson, D. J., Western, A. W., Grayson, R.B., 2004. Identifying and quantifying sources of variability in temporal and spatial soil moisture observations. *Water Resources Research* 40(2): W02507.

Wu, Q.S., Liu, H.X., Wang, L., Deng, C.B., 2016. Evaluation of AMSR2 soil moisture products over the contiguous united states using in situ data from the international soil moisture network. *International Journal of Applied Earth Observation and Geoinformation* 45: 187–199.

Zeng, J.Y., Chen, K.S., Bi, H.Y., Chen, Q., 2016. A preliminary evaluation of the SMAP radiometer soil moisture product over United States and Europe using ground-based measurements. *IEEE Transactions on Geoscience and Remote Sensing* 54(8): 4929–4940.

Eurasian J Soil Sci 2019, 8 (4) 351 - 363

Eurasian Journal of Soil Science

Journal homepage : http://ejss.fesss.org

Evaluation of soil fertility in citrus planted areas by geostatistics analysis method

Fulsen Özen*

Ege University, Faculty of Agriculture, Department of Soil Science & Plant Nutrition, İzmir, Turkey

Abstract

The aim of this study is to map citrus planted areas, which have been detected by traditional methods to date, with a high accuracy method and to reveal the land characteristics and fertility conditions. A database was created for citrus planted areas with the help of high-resolution Worldview 2 satellite images in this study. By creating the digital elevation model, orthorectification of satellite images was made and slope, aspect and elevation characteristics were determined. Using soil maps, maps showing terrain characteristics were produced. 43 soil samples were taken to represent citrus planted areas; geostatistical maps showing their pH, salinity, lime, texture, organic matter, total N, available P; exchangeable K, Ca, Mg, Na, available Fe, Cu, Zn, Mn levels were created and their statistical analyses were performed 2,132.08 ha citrus planted area was found in the study area. The parameters obtained from the digital elevation model (slope, aspect, elevation), the data of the land from the soil maps and the physical properties-macro/micro nutritional contents of the soil produced by the geostatistics method were evaluated together. It was determined that the features in all areas mapped as citrus planted area are quite suitable for citrus production. However, it is thought that Fe and Zn uptake from the soil will decrease due to the fact that the pH level is slightly alkaline and high lime contents. Identifying and sustainable monitoring of citrus production areas, which are very important in terms of economy, accurately, up-to-date, without causing loss of time and labor, will be possible with integrated use of GIS and RS techniques.

Keywords: Citrus, soil fertility, geostatistics, Worldview 2 satellite imagery.

Article Info

Received : 03.11.2018
Accepted : 20.08.2019

Introduction

Citrus, which can be grown in tropical and subtropical climate regions, is a plant association containing the citrus fruit tree species of Rutaceae family including not only the ones that are common and have economical value such as orange, mandarin, grapefruit, bitter orange and lemon species but also shaddock, citron and bergamot (Uysal and Polatöz, 2017). Especially rich in vitamin C, it can be consumed as fresh fruit, fruit juice, and jam; extracts can be taken from its flowers, fresh sprouts, and peels; whereas its peels can also be used in making animal feed. (Gamze and Kısmalı, 2003). Total phenolic matter, mineral matter and vitamin content of the peels were found to be higher than fruit and fruit juice (Belitz and Grosch, 1999; Güzel and Akpınar, 2017). Our country is extremely suitable for the production of citrus fruits in terms of ecological conditions. Turkey is located on the northern edge of the world citrus fruit production (Akgün, 2006). The production of citrus fruits, which is an economic vegetable product, has seen to increase considerably in recent years. The most important factors in the choice of citrus production are the presence of multiple uses in the national economy, its importance in the health-nutrition chain, its high employment potential and its ability to adapt to regional conditions. For this reason, it has become a necessity of our age to use more modern and reliable methods in order to increase the productivity of citrus production areas, to maintain its sustainability and to meet the nutritional needs of people accurately and healthily.

* Corresponding author.
Ege University, Faculty of Agriculture, Department of Soil Science & Plant Nutrition, Bornova, İzmir, Turkey
Tel.: +90 232 3112684 E-mail address: fulsen.ozen@ege.edu.tr
e-ISSN: 2147-4249 DOI: 10.18393/ejss.616689

The Geographical Information System (GIS) and remote sensing technique have emerged as reliable and effective data providers and methods for sustainable management of agricultural areas. Remote sensing including satellite images, aerial photographs, LIDAR images, different image processing techniques and algorithms (NDVI, EVI, SAVI, NDWI) pixel/object-based classification are used in many applications such as determination of the plant pattern in agricultural activities, yield estimation and determination of field use and disease/ harm/damage detection. On the other hand, GIS is an application that has the ability to visualize information obtained from different sources (vector, raster, text data) as well as to produce, store, process and analyze. Das et al. (2009) by using the remote sensing technique and GIS in their study, made an assessment of the yield that can be obtained from citrus planted areas. Areas that may affect crops such as different plant conditions, water stress, and soil erosion are mapped. Lopez et al. (2010) conducted a multistage classification study to identify citrus orchards in the Comunidad Valenciana region of Spain using GIS. By automatic classification, an accuracy of 85% was achieved. Supported by field studies, the method reached 94.38% accuracy with the proposed methodology in recent conditions. In a study conducted in Iran, temperature, co-elevation maps and topographic maps produced for 30 years since 1980 were transferred into GIS and statistical analyses were performed. In this study, it was determined that minimum temperature value and elevation from the sea had a significant negative effect on citrus production. As a result, it was emphasized that citrus fruits are affected more from low temperatures and the maximum elevation is suitable up to 700 m for a profitable production (Zabihi et al., 2016). In Pakistan, Naseem et al. (2016), has aimed to reveal the relationship between citrus and environmental conditions in order to identify the citrus tristeza virus. The geographic information system was used to determine the spatial distribution of citrus areas, the formation of citrus tristeza virus and effects of environmental factors; temperature and precipitation. The effect of yearly incidence of temperature, precipitation, and associated citrus tristeza virus has shown that the annual average temperature has a negative correlation with the frequency of citrus tristeza virus. However, a positive correlation was observed between the incidence of citrus tristeza virus and precipitation factor. Digital maps created by the data involving topography, land use, soil, and climate were used to determine the characteristics of citrus planted areas in Chongqing, China. A total of 50 randomly selected orchards (2032 ha) were examined and the topographic features of the orchards were determined using the digital elevation model DEM. The data obtained and produced were analyzed and it was determined that approximately 33% of the total area of Chongqing city was suitable for citrus development (Wu et al., 2011). In the study carried out in citrus fields in Ramsar region of Iran, it was aimed to form a citrus land conformity assessment model based on five (slope, elevation, lowest temperature, highest temperature, precipitation) biophysical factors. A number of decision strategies and scenarios have been successfully developed by changing the critical factors by using the Ordered Weighted Averaging (OWA) and the analytical hierarchy process (AHP) method together. As a result, it was determined that citrus cultivation was suitable in 6.7% of the study area (Zabihi et al., 2019).

In recent years, multivariate geostatistics and spatial analyzes have been used to determine the relationship between soil properties and soil fertility in spatial analysis (Goovaerts 1997, 1998). In addition to GIS, geostatistical methods are a different technique for evaluating the spatial variability of land and soil (Foroughifar et al., 2013). These techniques can fully characterize soil properties according to their distribution (Chen et al., 2009). The variogram is generally used in geostatistics. The interpolation technique, known as kriging, provides an unbiased, linear estimation of a regional variable in an unsampled area, where it is best defined in terms of least squares (Oliver and Webster, 2014). Başayigit and Şenol (2009) made an application for the preparation of efficiency maps of the areas where fruit growing potential of Isparta province is high with GIS. For this purpose, soil samples at two different depths (0-20 cm, 20-40 cm) were collected from 120 different points and available P, exchangeable cations and extractable Fe, Cu, Mn, Zn analyses were performed. By using inverse distance weighting technique (IDW), point data were converted to spatial data and thematic maps were produced for each soil characteristic. Shen et al. (2019) have compared inverse distance weighted (IDW) interpolation methods, radial basis functions (RBF), ordinary kriging (OK), co-kriging (COK), multiple linear regression (MLR), geographic weighted regression (GWR), regression kriging (RK) and geographically weighted regression (GWRK) methods. In four Mollisol regions in Northeast China, the areas where landscape pattern, land use type, topographic characteristics, soil tillage method, sample density, sample accuracy, and total phosphorus content are different were selected as research areas. As a result, GWRK and RK were determined as the most suitable interpolation methods and when the cost, time and process were considered, it was explained that the OK method was also relatively acceptable. Santos France et al. (2017a,b) used the kriging interpolation method to produce the spatial distribution of heavy metal content of soils in northern Spain and northern Peru. In a study conducted in

Bara, Nepal, 109 surface soil samples (0-15 cm depth) were taken and pH, organic matter (OM), nitrogen (N), phosphorus (P,), potassium (K), zinc (Zn) and boron (B) contents were determined. Digital map layers were produced by kriging method for each soil chemical properties. It was emphasized that these maps will enable farmers to evaluate their land, allowing them to make easier and more efficient management decisions and to maintain the sustainability of productivity.

The aim of this study was to determine citrus planted areas in Aydın province by remote sensing technique and geographical information system. Soil samples (0-30 cm) were randomly taken from 43 different points in order to determine the soil fertility level of citrus production areas and their physical and chemical properties were analyzed in the laboratory. Each soil feature spatial distributions were determined and a digital database was created in which every existing and produced data could be evaluated.

Material and Methods

Research area and geographical location

Aydın Province; is located between the 37th and 38th northern latitudes and 27th and 29th eastern longitudes in the southwest of Turkey. The area of the city is 811,600 ha and according to data provided from TUIK in 2017, 366,608 thousand ha (approximately 45%) of the region is used for agricultural activities. Aydın is surrounded by the Aegean Sea from the west, Denizli from the east, İzmir and Manisa from the north and Muğla from the south (Figure 1). It is the Menderes basin that affects the agricultural structure of the city at a high rate. The city of Aydın is known as the Lower Greater Menderes section of the Greater Menderes basin, formed by the Greater Menderes River and its tributaries. There are 17 districts in Aydın, including the central district. Development levels of agriculture, industry and tourism sectors vary according to districts (Anonymous, 2018). Citrus planted areas distributed in Kuyucak, Nazilli, Sultanhisar and Yenipazar districts constitute the research area.

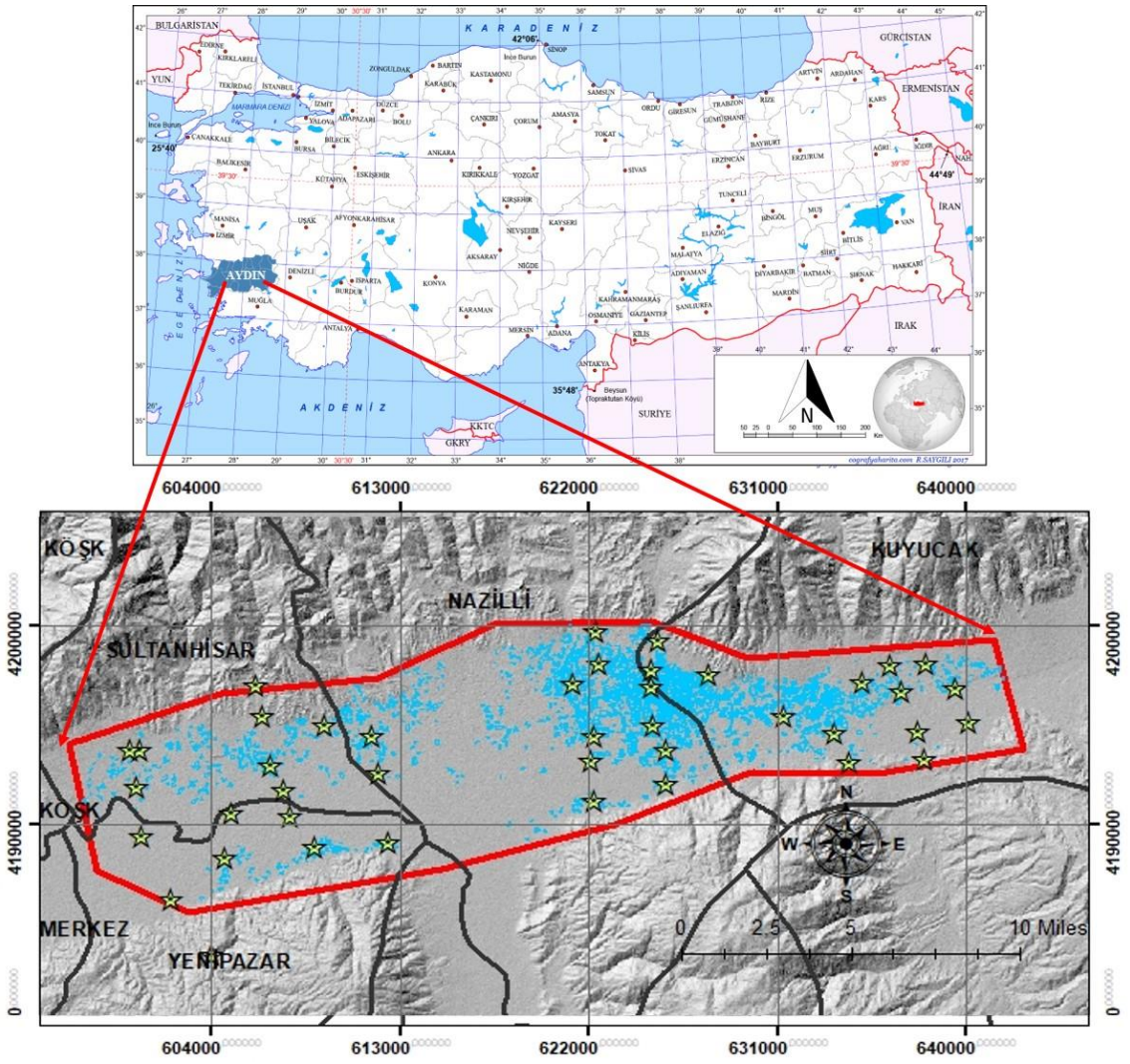

Figure 1. The geographical location of the research area, distribution of citrus planted areas and soil sampling points

The city of Aydın has a Mediterranean climate and the average annual rainfall is 645.1 mm. Most of the annual rainfall occurs in winter, spring, and autumn. 8.9% of precipitation occurs in summer, 44.5% in winter, 22.7% in autumn and 23.9% in spring. When long-term meteorological data are analyzed, the average temperature was found to be 8.2 ^{0}C in January and 28.4 ^{0}C in July (Anonymous, 2017). The average relative humidity is 61.2% (Anonymous, 2018).

Material

Sultanhisar, Yenipazar, Nazilli and Kuyucak Köşk districts where the citrus planted areas in Aydın province are found as orchard facilities were chosen as the research areas. The purchase of 10 1/25.000 scaled contour maps that are necessary for the creation of the digital elevation model and which covers the research area was made by the General Directorate of Mapping. Three Worldview-2 satellite images of 45 cm resolution belonging to June 2013 were used for the determination of citrus areas. During the research, Trimble Geoexplorer 2005 series GPS was used in field studies. ArcGIS 10.5 was used to create a digital elevation model (DEM) by using contour curves, ENVI software was used to transform images into pansharpened, and PCI software was used for orthorectification of images. Forthythree soil samples, which were representative of the characteristics of the research area were taken by random sampling method. Depth of taking soil samples is approximately 30 cm depending on soil properties. SPSS 15.0 software was used to interpret the results of the analysis. Soil characteristics required to determine the fertility status of citrus planted areas were evaluated in ArcGIS 10.5 software in the digital database and mapped geostatistically.

Method

Topographical maps, soil maps, satellite imagery and similar data of the research area were collected and entered into the database by using GeoMedia and ArcGIS, which are GIS software, and an updateable database was created. Universal Transverse Mercator (UTM) projection and WGS-84 (World Geodetic System 1984) datum were used for all data. Field surveys were carried out for orthorectification of Worldview-2 satellite images and points were collected from 71 points with sensitive GPS. Orthorectification of the satellite images was performed using DEM generated from contour lines. Digital terrain models with elevation information are used to rearrange the numerical reflection values according to the topography (topographic normalization) by eliminating the shadow effect which is a problem in the classification of satellite images (McCormick, 1999). The main purpose of orthorectification is to eliminate the differences that occur due to topographic changes seen on the surface of the earth, and shifts in satellite and aerial photographs (Düzgün, 2010). Image sharpening process was carried out in satellite images by "Gram-Schmidt Spectral Sharpening" method in ENVI software. (Yuhendra et al., 2011; Matsuoka, 2012, Özdemir, 2017). This method allows benefiting from the spectral characteristics of the sensors with a high spatial resolution of the image (Marangoz et al., 2005). In order to enrich the properties of the soil layer in the digital database, each feature in 1/25.000 scaled soil maps was transferred as attribute information.

Soil samples were taken from 0-30 cm depth according to general rules (Ballinger et al., 1966). Soil samples brought to the laboratory were dried in the laboratory and passed through 2 mm sieves and prepared for analysis (Soil Survey Staff, 1951). Contents of the soils including pH (Jackson, 1967), electrical conductivity (Jones, 2001), structure (Bouyoucos, 1962, Black, 1965), $CaCO_3$ (Schlichting and Blume, 1966), organic matter (Rauterberg and Kremkus, 1951), total nitrogen (Bremner, 1965), available phosphorus (Olsen and Sommers, 1982), exchangeable potassium, calcium, magnesium and sodium (Knudsen et al., 1982), available iron, zinc, copper and manganese (Lindsay and Norvell, 1978) were determined. Statistical Package Program named SPSS 15.0 (Statistical Package for Social Science) was used to compare the soil analysis values, to perform statistical analyses and to interpret the results. 95% confidence level (5% level of significance) was taken into consideration in performing these analyses.

Soil characteristics show spatial variability due to the effects of the basic and external factors that form them (Heuvelink and Webster, 2001) and this change may occur depending on soil type, topography, climate, vegetation and anthropogenic activities (Shi et al., 2009). Geostatistics, which is defined as the tools used to examine and estimate the spatial distribution of related variables, is used to show the spatial distribution of soil properties (Burrough 1993; Cambardella et al., 1994) and spatial variability in various natural phenomena (Mousavifard et al., 2013). The results of 17 soil properties analyzed for the determination of soil fertility were evaluated by using geostatistics analysis methods. In general, the concept of geostatistics refers to stochastic methods used to determine and estimate the distinctive characteristics of spatially referenced data (Mulla and McBratney, 2002). As being one of the stochastic interpolation methods, Ordinary Kriging (OK) was used to determine the spatial distribution of soil properties. Kriging is a linear

geostatistics interpolation technique that provides the Best Linear Neutral Estimator (BLUE) for space-dependent variables. Kriging estimates are calculated as weighted sums of sampled adjacent densities (Robinson and Metternicht, 2006). In most cases, ordinary kriging proves that forest resistance values are sufficiently robust in unsampled areas. Ordinary kriging is the most common method of kriging (Krasilnikov and Sidorova, 2008; Mousavifard et al., 2013) and general equality is expressed as follows:

$$\gamma=1/2\ N(h) \sum_{i=1}^{N(h)} [Z(\chi_i)- Z(\chi_j+h)]^2 \quad (1)$$

According to Yeşilkanat et al. (2014)," γ (x) semi-variance value, the distance between h, i and j points, N (h): the number of pairs of points on the h length (or the number of h vectors in the region), Z (xi): The measured value of the variable at point i, Z (xj + h): is the measured value at the point of the variable".

Results

Orthorectification and image sharpening processes were completed and Worldview 2 satellite images were manually vectorized by Geomedia 6.0 screen digitizing method. The satellite image was studied with NIR 1/Rededge/Red band combination to better determine the citrus trees and tree species that can be mixed with citrus in the study area (Figure 2). A significant part of the data collection studies carried out at this stage was executed as a result of field studies. Mapped citrus planted areas were accepted as boundaries, instead of the tree parcel boundaries. For this reason, artificial (home, other reinforced concrete structures, etc.) and natural (other tree species, etc.) elements outside the citrus tree, which is within the boundaries of the agricultural parcel are not included in the mapping. It was determined that citrus planted areas distributed in the research area occupy an area of 2132.08 ha.

Figure 2. Digitized citrus planted areas in Worldview 2 satellite images (Aydın-Nazilli)

The elevation varies between 53-830 m in the research area. Citrus planted areas at an elevation of 0-200 m, 201-305 m, 351-500 m, 501-650 m and 651-830 m cover respectively 94.66%, 3.27%, 1.59%, 0.41% and %0.07 of the areas. As the elevation up to 700 m is not seen as a limiting factor in citrus production (Zabihi et al., 2019), the entire area of the research area is suitable for citrus production. When the citrus production areas were examined for the aspect parameter, it was found that they showed an approximate distribution in all directions. While flat areas cover 10.28% of the total area; the northern, the northeastern, the eastern, the southeastern, the southern, the southwestern, the western and the northwestern directions have a distribution of 11.34%, 10.99%, 9.20%, 11.44%, 11.03%, 12.48%, 10.73% and 12.50% in the total area respectively. The slope characteristics of the areas where citrus production is made are as follows: Lands with a slope of 2-6%, 0-2%, 6-12%, +30%, 12-20% and 20-30% have a distribution of 54.71%, 18.78%, 18.77%, 3.04%, 2.74% and 1.95% in the total area respectively.

1/25.000 scaled soil maps containing the great soil group, slope, depth, land use capability class (LUCC), stoniness, rockiness, erosion, drainage, texture, land use and other characteristics (salinity-alkalinity) of the research area were vectorized. The thematic map of each soil feature was produced and their spatial size and % distributions were determined. Due to various land types and geological structures, colluvial soils occupy the most area with 51.06%, followed by alluvial soils with 46.21% and non-agricultural areas, regosols, rendzinas and limeless brown soils with a total of 2.73%. When the distribution of land use capability classes in the area was examined, it was determined that citrus planted areas were mostly on Class I lands (41.54%). In terms of the area they occupy, Class III lands (33.37%), Class II lands (20.46%), Class IV lands (1.93%) and others (Class VI, VII, VII, 2.71%) follow Class I. In terms of soil depth, most of the citrus planted areas are located in areas with a depth of 90 cm and above (97.05%). It is known that in citrus the effective root depth is between 30-90 centimeters in aerated and well-drained soil conditions (e.g. sandy-loamy) (YAYÇEP, 2010). Therefore, the research area meets the soil requirements of citrus in terms of its characteristics. When the erosion characteristics of the area are examined, the areas defined as having little or no erosion show a distribution of 85.42%, while the areas exposed to moderate erosion cover an area of 11.97%. The remaining areas have a very small area, even though they are considered non-agricultural and severe in terms of erosion severity. When the research area is classified according to other soil properties, the areas that do not have any problems have a value of 47.84%. Additionally, 26.96% of the areas are found to have slightly saline or insufficient drainage, 15.31% of the areas to have insufficient drainage, 5.67% of the areas to be stony, 1.56% of areas to have salty-insufficient drainage, 0.06% of the areas to have poor drainage and non-agricultural areas to cover 2.60% of the area.

The coefficient of variation, which is considered as an important index for explaining changes in soil properties, is classified as low (<15%), medium (15-35%) and high (> 35%) according to the values it takes (Wilding, 1985; Mulla and Mc Bratney, 2000; Özyazıcı et al., 2016). In this study, except the properties including pH (4.75%), sand (27.19%) and P (33.64%), the soil properties were determined to have high variability, while the most variable soil property was found to be Mn (117.08%) (Table 1). In many studies, it was explained that the coefficient of variation of pH contents found in soil was low (Tsegaye and Hill, 1998; Aimrun et al., 2007; Dengiz et al., 2015).

Table 1. Some descriptive statistics of soil properties

Soil properties	Min	Max	Avarege	Variance	Standart Deviation	Standart Error	Variance Coefficients
pH	6,08	7,82	7,46	0,1263	0,3554	0,0542	4,7534
EC, µs/cm	97,20	1542	531,08	0,0003	0,0186	0,0028	54,7362
$CaCO_3$, %	0,62	22,51	7,87	52,8930	7,2728	1,1091	92,3757
Sand, %	19,52	84,96	58,85	260,9826	16,1550	2,4636	27,1922
Silt, %	7,28	42,56	27,49	99,4464	9,9723	1,5208	36,9026
Clay, %	6,32	41,76	13,66	82,5271	9,0844	1,3854	67,1926
OM, %	0,41	6,62	2,27	1,6795	1,2960	0,1976	57,0497
N, %	0,02	0,33	0,11	0,0042	0,0648	0,0099	57,0008
P, mg kg^{-1}	3,30	141	38,90	16,9080	4,1119	0,6271	33,6403
K, mg kg^{-1}	116,40	970	281,98	0,2174	0,4663	0,0711	64,6586
Ca, mg kg^{-1}	588	4900	3132,58	37,7459	6,1438	0,9369	39,2229
Mg, mg kg^{-1}	16,86	242,15	139,81	0,2234	0,4727	0,0721	40,5594
Na, mg kg^{-1}	9,60	422,40	110,51	0,0857	0,2927	0,0446	64,5504
Fe, mg kg^{-1}	2,86	19,97	8,83	25,8747	5,0867	0,7757	57,5754
Zn, mg kg^{-1}	0,16	6,30	1,11	1,4136	1,1890	0,1813	106,7328
Cu, mg kg^{-1}	0,32	8,78	2,14	2,9585	1,7200	0,2623	80,5680
Mn, mg kg^{-1}	1,24	58,30	11,18	171,2380	13,0858	1,9956	117,0806

Correlation analysis results of soil chemical properties are given in Table 2. According to the analysis results, 58 of 153 correlation pairs between soil properties were found to be statistically significant at 1% and 5%. The most positive significant correlation was found between N and OM ($p < 0.01$) and lowest between Mn and $CaCO_3$ (0.291*). On the other hand, the highest negative correlation was found between sand and clay values (-0.857**), while the lowest correlation was found between sand content and Ca (-0.293*).

Distribution maps showing soil physical and chemical properties were classified using limit data belonging to different groups of each parameter. The distribution maps of the research area soils according to pH, salinity, lime, sand, alluvion, clay, and organic matter contents are given in Figure 3.

Table 2.Correlation analyzes results of soil chemical properties

	pH	EC	$CaCO_3$	Sand	Silt	Clay	OM	N	P	K	Ca	Mg	Na	Fe	Zn	Cu	Mn
pH	1.000																
EC	0.420**	1.000															
$CaCO_3$	0.519**	0.448**	1.000														
Sand	-0.517**	-0.385**	-0.654**	1.000													
Silt	0.449**	0.270ns	0.468**	-0.857**	1.000												
Clay	0.422**	0.387**	0.644**	-0.829**	0.423**	1.000											
OM	0.189ns	0.256ns	0.183ns	-0.211ns	0.144ns	0.223ns	1.000										
N	0.189ns	0.255ns	0.183ns	-0.210ns	0.144ns	0.222ns	1.000**	1.000									
P	-0.530**	-0.413**	-0.600**	0.476**	-0.394**	-0.415**	-0.102ns	-0.103ns	1.000								
K	0.328*	0.425**	0.290*	-0.449**	0.296*	0.473**	0.340*	0.341*	-0.321*	1.000							
Ca	0.672**	0.340*	0.583**	-0.293*	0.265ns	0.228ns	0.101ns	0.102ns	-0.463**	0.281ns	1.000						
Mg	0.662**	0.580**	0.761**	-0.737**	0.611**	0.635**	0.239ns	0.237ns	-0.503**	0.418**	0.423**	1.000					
Na	0.516**	0.658**	0.325*	-0.439**	0.343*	0.396**	0.172ns	0.173ns	-0.532**	0.331*	0.316*	0.405**	1.000				
Fe	-0.147ns	0.100ns	0.086ns	-0.116ns	0.040ns	0.160ns	0.280ns	0.280ns	0.140ns	-0.078ns	-0.246ns	0.048ns	0.091ns	1.000			
Zn	-0.133ns	0.152ns	-0.045ns	0.164ns	-0.120ns	-0.156ns	0.154ns	0.154ns	-0.202ns	0.076ns	-0.006ns	-0.048ns	0.096ns	-0.176ns	1.000		
Cu	-0.214ns	-0.087ns	-0.173ns	-0.202ns	0.315*	0.011ns	-0.034ns	-0.035ns	0.342*	0.145ns	-0.143ns	-0.002ns	-0.147ns	0,122ns	0,114ns	1.000	
Mn	0.156ns	0.177ns	0.291*	-0.268ns	0.025ns	0.431**	-0.024ns	-0.025ns	-0.155ns	-0.011ns	0.192ns	0.209ns	0.081ns	0,086ns	-0.138ns	-0.024ns	1.000

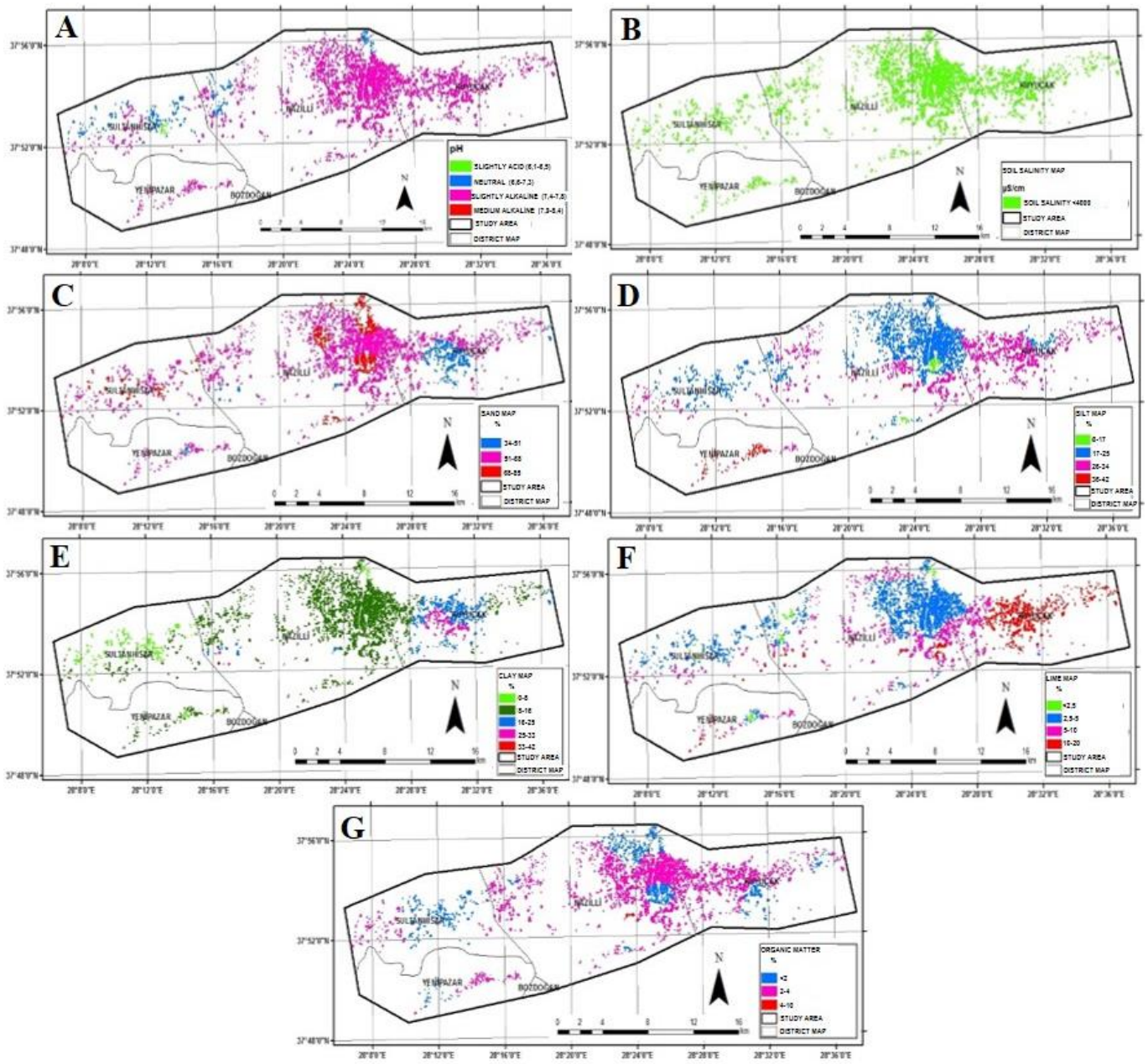

Figure 3. pH (A), salinity (B), sand (C), silt (D), clay (E), calcium carbonate (F) and organic matter (G) distribution maps of the study area.

The pH of soil samples varies between 6.08- 7.82 and when classified according to limit values (Richards, 1954; Ülgen and Yurtseven, 1995), the largest area is covered by the light alkaline soils (90.88%). This is followed by neutral soils (8.58%), light acid soils (0.51%), and moderate alkaline soils (0.03%). Citrus trees are highly susceptible to excess salts and their tolerance to soil salinity is associated with the ability to restrict the entry of toxic ions [sodium (Na), chlorine (Cl) and boron (B)] into roots and their transportation to shoots (Srivastava and Singh, 2009). Total salt values of soil samples range between 0.006-0.099. Due to the total salt content of soil samples being less than 0.150% (US Soil Survey Staff, 1951), there is no salt problem that will cause the above-mentioned effects to occur. Lime contents of soil samples vary between 0.61% and 22.5%. When the lime contents of soils are classified, 57.21% of the areas are found to be limy (2.5-5%), 22.80% to be rich in lime (5-10%), 17.46% to have texture+marn (10-20%) and 2.53% to be lime-poor (0-2.5%). The structure of the soil samples taken in the study is generally light and moderate. It was found that 65.1% of the soil was sandy loam and 18.6% had a loamy texture (Black, 1965). The soil content of ideal citrus cultivation is required to be between 8-10% (not exceeding 20%), sand content to be 50% and loam content to be 20% (Yayçep, 2010). The class of the soil in the research area, where the sand amount is distributed the most (51-68%), covers 69.08% of the whole area. According to the clay quantity, the areas containing 8-16% of clay have a distribution of 69.94%. According to the findings obtained in terms of the properties of the structure, it was determined that the desired properties for citrus production were present

in the research area. The level of organic matter in the soil is important to help maintain an active population of microorganisms. Organic matter is therefore considered as an indicator of the sustainability of the soil management system (Srivastava and Singh, 2009). Organic matter contents of the research area range from 0.41% to 6.62%. When the soils are examined in terms of the amount of organic matter, 74.53% are found to be in the class of humic (2-4%), whereas 24.94% to be poor and 0.53% to be in the class of strong humic (4-10%) (Akalan, 1965).

The distribution maps according to the contents of the soils in the research area, which includes: total nitrogen (N), available phosphorus (P), exchangeable potassium (K), exchangeable calcium (Ca), exchangeable magnesium (Mg), exchangeable sodium Na, available iron (Fe), available copper (Cu), available zinc (Zn), and available manganese (Mn) are given in Figure 4.

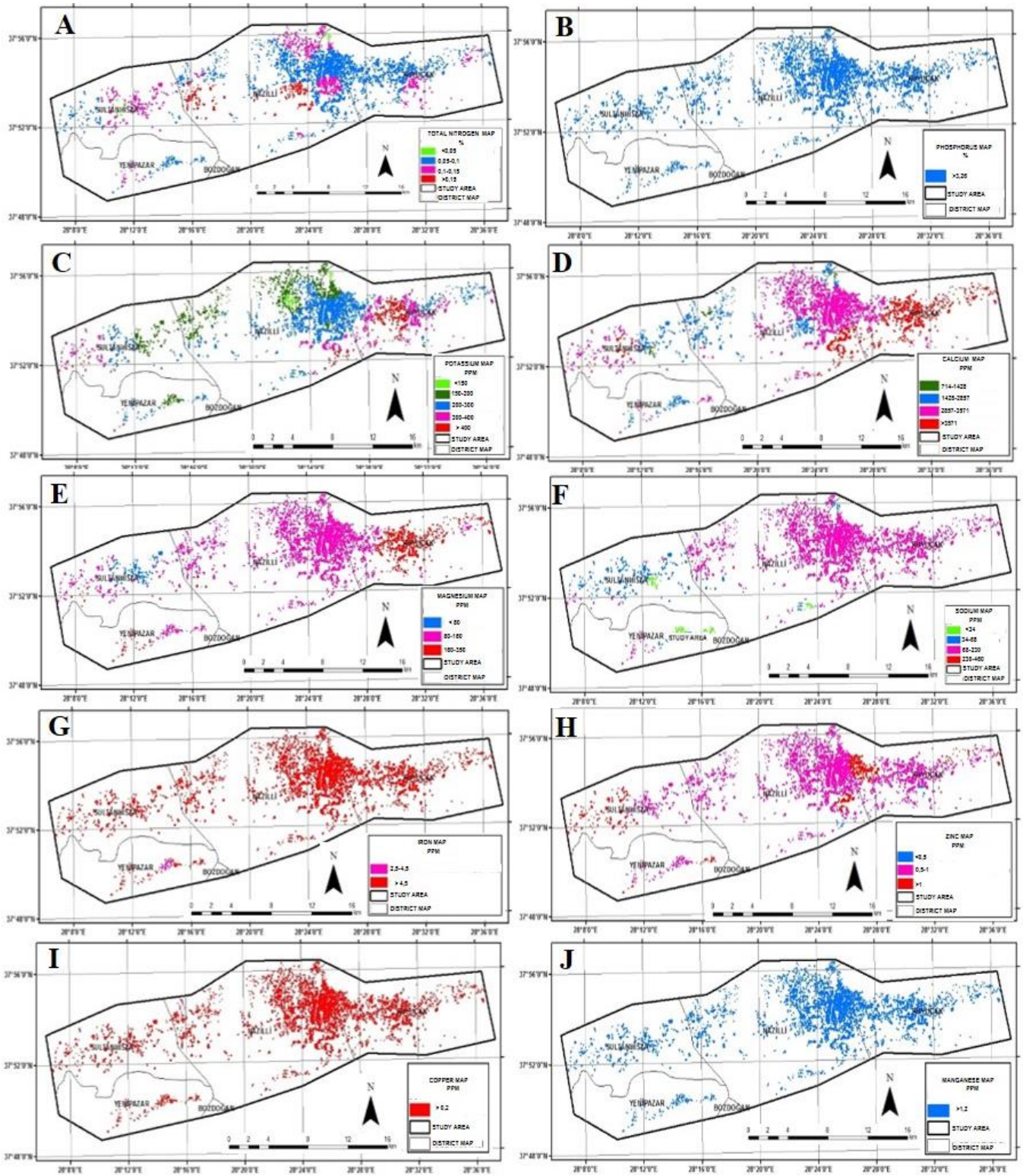

Figure 4. N (A), P (B), K (C), Ca (D), Mg (E), Na (F), Fe (G), Zn (H), Cu (I) and Mn (J) distribution maps of the study area.

Total nitrogen content of the soils varies between 0.021% and 0.331%. According to the total nitrogen distribution map, the areas in the good category with N content of 0.1-0.15% have 72%, the areas with the N content in the moderate category (0.05-0.1%) have 25.15%, the areas with N content in the rich category (> 0.15%) have 1.62% and the areas with N content in the poor category (0-0.05%) have 1.23% of the distribution (Çokuysal and Erbaş, 2004). Nitrogen content is in parallel with the organic matter content of soils. Soils are characterized as humus, which confirms the high amount of beneficial nitrogen. The absorbable phosphorus content of the soils varies between 4.2 and 19.9 mg kg^{-1}. According to Çokuysal and Erbaş (2004), soils with beneficial phosphorus content being >3.26 mg kg^{-1} are classified as a good level. Accordingly, the useful phosphorus content in the entire area is defined as good. The exchangeable potassium content of the soils was determined between 116.40 and 970 mg kg^{-1}. The class defined as sufficient according to the exchangeable potassium content (200-300 mg kg^{-1}) was distributed in the research area by 50.01% ratio. This was followed by the class with 23.37% ratio, which is defined as low according to the potassium content (200-300 mg kg^{-1}), the class defined as high (300-400 mg kg^{-1}) with 16.16% ratio, the class defined as very high (>400 mg kg^{-1}) with 8.85% ratio and the class defined as deficient (<150 mg kg^{-1}) with 1.61% ratio (Çokuysal and Erbaş, 2004).

The variable calcium content of the soils was determined between 588 and 4900 mg kg^{-1}. The class, defined as excess relative to the exchangeable calcium content (2857-3571 mg kg^{-1}), is the most common with 58.02%. This is followed by the class with 20.87% ratio, which is defined as good according to the calcium content (1428-2857 mg kg^{-1}), the class defined as to excess (> 3571 mg kg-1) with 19.77% ratio and the class defined as poor (715-1428 mg kg^{-1}) with 1.34% ratio (Çokuysal and Erbaş, 2004). The exchangeable magnesium content of the study area soils was determined between 16.86 and 242.15 mg kg^{-1}. The class defined as moderate according to the exchangeable magnesium content (80-160 mg kg^{-1}) has 80,70%, the class defined as high (160-350 mg kg^{-1}) has 14.49% and the class defined as poor (<80 mg kg^{1}) has 4.81% of the distribution (Çokuysal and Erbaş, 2004). The varying sodium content of the research area soils was determined between 9.60 and 422.40 mg kg^{-1}. The class defined as moderate (68-230 mg kg^{-1}), according to the exchangeable sodium content, has an 86.95% ratio, the class defined as low (34-68 mg kg^{-1}) has a 10.41% ratio, the class defined as very low (<34 mg kg^{1}) has a 2.58% ratio and the class defined as very high (230-460 mg kg^{1}) has a 0.06% ratio (Loue, 1968).

The available iron contents of the study area were determined between 2.86 and 19.97 mg kg^{-1}. The class, defined as sufficient according to the exchangeable iron content (>4.5 mg kg^{-1}) covers a very large proportion of the area with 99.998% (Lindsay and Norvel, 1978). However, due to the fact that the majority of citrus production areas are at the level of mild alkaline and medium level alkaline pH, have high lime content and sufficient levels of P and Cu in the soil, it is likely that Fe will be transformed into ineligible form by plants (Kacar and Katkat, 2007). According to the exchangeable zinc content (0.5-0.1 mg kg^{-1}), the class is defined as deficient and is in the first place with 88.04% rate. This is followed by of the class defined as sufficient (> 0.1 mg kg^{-1}) with 10.87% and the class defined as deficient (<0.5 mg kg^{-1}) with the ratio of 1.09% (Lindsay and Norvel, 1978). Since high soil pH lime content is determined in citrus production areas, it is predicted that this situation may have negative effects on Zn availability (Kacar and Katkat 2007; Karaman et al., 2007; Karaçal 2008). In addition, because of the antagonistic interaction between P and Zn (Kacar and Katkat, 2007), Zn uptake of plants decreases and Zn deficiency can be seen as the P content of soils increases. Considering the good P content of the research area, it may be a problem in terms of Zn nutrition. The copper contents of the study area were determined between 0.32 and 8.78 mg kg^{-1}. It covers the entire class area defined as sufficient according to the exchangeable copper content (>.2 mg kg^{-1}) (Lindsay and Norvel, 1978). The available manganese contents in the study area were determined between 1.24 and 58.30 mg kg^{-1}. The class, which is defined as sufficient according to the exchangeable manganese content (> 1.2 mg kg^{-1}) covers the entire area (Lindsay and Norvel, 1978).

Conclusion

As a result, it was determined that citrus planted areas distributed in the research area occupy an area of 2132.08 ha. In a topographic look, these areas are on an elevation of <200 m, are mostly flat and slightly slopped and distributed to 69.78% of the land facing to the north and south. Their production areas are mainly concentrated on alluvial and colluvial soil groups, they have land use talent classes I II and III, +90 cm soil depth, and are on areas that erosion and other problems are mostly not observed. Soil pH levels have a slightly alkaline reaction, the salt content is very low and lime content is high. The structure classes in most of the areas are determined as sandy loam and loam for citrus production. The organic matter coverage of the soils is mostly sufficient. In terms of macronutrients; total nitrogen, available phosphorus contents of

soils are good and exchangeable potassium contents are sufficient. Exchangeable calcium, magnesium, and sodium scopes are again generally determined to be sufficient. When the levels of micronutrients were examined, it was found that exchangeable iron, copper and manganese element contents were sufficient and zinc contents were deficient.

The citrus products, which are important in many ways for both the agricultural sector and a country's economy, provide employment opportunities to many people in sectors including production, market development, industry-processing, transportation, imports and exports in the world and in Turkey. For this reason, citrus planted areas have an important potential to be followed within environmentally friendly production strategies and sustainable production/consumption concepts. With the research carried out, an updateable database was created for mapping the production areas, revealing the productivity conditions, determining the disease and pest control, determining the infrastructure opportunities for the sub-industries, preparing fertilizer production and consumption plans and most importantly for examining the yield/quality values in the coming years. In addition, it is thought that it will be an important source of information for future studies on the subject.

References

Aimrun, W., Amin, M.S.M., Ahmad, D., Hanafi, M.M., Chan, C.S., 2007. Spatial variability of bulk soil electrical conductivity in a Malaysian paddy field: Key to soil management. *Paddy Water Environment* 5(2): 113-121.

Akalan, İ.,1965. Toprak Oluşu, Yapısı ve Özellikleri. Ankara Üniversitesi Ziraat Fakültesi Yayınları No: 231. 332s. [in Turkish].

Akgün, C., 2006. Turunçgiller Sektör Profili. Dış Ticaret Şubesi Uygulama Servisi. Ankara. [in Turkish].

Anonymous, 2017. Turkish State Meteorological Service. Available at [Access date: 14.02.2017]: https://mgm.gov.tr/?il=Aydin

Anonymous, 2018. Aydın Tarım Master Planı. Aydın Tarım ve Orman İl Müd. Available at [Access date: 14.02.2017]: https://aydin.tarimorman.gov.tr/Belgeler/Ayd%C4%B1n%20Tar%C4%B1m%20Master%20Plan%C4%B1/MASTER%20PLAN%20%20%2816.01.2019%29-converted.pdf

Ballinger, W.E., Bell, H.K., Childers, N.F., 1966. Peach nutrition. In: Fruit Nutrition. Childers, N.F. (Ed.). Somerset Press, New Jersey, pp. 276-390.

Başayiğit L., Şenol H., 2009. The production of fertility maps of potential land for orchards using geographical ınformation systems. *Journal of Plant & Environmental Sciences* 1: 36-45 [in Turkish].

Belitz, H.D., Grosch, W., 1999. Fruits and fruit products. In: Food chemistry. Belitz, H. D., Grosch, W. (Eds.). Springer, Berlin, Heidelberg. pp. 748-800.

Black, C.A., 1965. Method of soil analysis. Part 1 Chemical and Microbiological Properties. Agronomy No. 9. American Society of Agronomy, Madison, Wisconsin, USA.

Bouyoucos, G.J., 1962. Hydrometer method improved for making particle size analyses of soils. *Agronomy Journal* 54(5): 464-465.

Bremner, J.M., 1965. Total Nitrogen. In: Method of Soil Analysis, Part 2. Chemical and Microbiological Properties. Black, C.A. et al. (Eds.) American Society of Agronomy, Madison, Wisconsin, USA. pp. 1149-1178.

Burrough, P.A., 1993. Soil variability: a late 20th century view. *Soils and Fertilizers* 56: 529-562.

Cambardella, C.A., Moorman, T.B., Parkin, T.B., Karlen, D.L., Novak, J.M., Turco, R.F., Konopka, A.E., 1994. Field-scale variability of soil properties in central Iowa soils. *Soil Science Society of America Journal* 58(5): 1501-1511.

Chen, H., Shen, Z., Liu G., Tong, Z., 2009. Spatial heterogeneity of available zinc, copper, and manganese in Xiangcheng tobacco planting fields, Henan Province, China. *Frontiers of Biology in China* 4(4): 469–476.

Çokuysal, B., Erbaş, E., 2004. Bitkilerde besin maddeleri noksanlıkları ve toprak tahlillerinin değerlendirilmesi. Ege Üniversitesi Tarımsal Uygulama ve Araştırma Merkezi, Çiftçi Broşürü: 55, İzmir. [in Turkish].

Das, P.T., Tajo, L., Goswami, J., 2009. Assessment of citrus crop condition in Umling block of Ri-Bhoi district using RS and GIS technique. *Journal of the Indian Society of Remote Sensing* 37: 317–324.

Dengiz, O., Özyazıcı, M.A., Sağlam, M.. 2015. Multi-criteria assessment and geostatistical approach for determination of rice growing suitability sites in Gokirmak catchment. *Paddy and Water Environment* 13(1): 1-10.

Düzgün, Ş., 2010. Uzaktan Algılamaya Giriş Ünite 6: Görüntü Ortorektifikasyonu. TÜBA-Türkiye Bilimler Akademisi, Ulusal Açık Ders Malzemeleri. Available at [Access date: 14.02.2017]: http://www.acikders.org.tr/pluginfile.php/637/mod_resource/content/0/Ders_Notlari/Unite6_Goruntu_Ortorektifikasyonu.pdf

Foroughifar, H., Jafarzadeh, A.A., Torabi, H., Pakpour, A., Miransari, M. 2013. Using geostatistics and geographic information system techniques to characterize spatial variability of soil properties, including micronutrients. *Communications in Soil Science and Plant Analysis* 44(8), 1273-1281.

Gamze, Ö., Kısmalı, Ş., 2003. An investigations on the population, distribution and damage of the Wooly whitefly, Aleurothrixus floccosus (Maskell) (Homoptera: Aleyrodidae) on citrus areas in Izmir province of Turkey. *Turkish Journal of Entomology* 27(1): 61-72. [in Turkish]

Goovaerts, P., 1997. Geostatistics for natural resources evaluation. Oxford Univ. Press, NewYork, USA. 483 p.

Goovaerts, P., 1998. Accounting for estimation optimality criteria in simulated annealing. Mathematical Geology, 30(5); 511–534.

Güzel, M., Akpınar, Ö., 2017. Turunçgil kabuklarının biyoaktif bileşenleri ve antioksidan aktivitelerinin belirlenmesi. *Gümüşhane Üniversitesi Fen Bilimleri Enstitüsü Dergisi* 7(2): 153-167. [in Turkish]

Heuvelink, G B.M., Webster, R., 2001. Modelling soil variation: past, present, and future. *Geoderma* 100(3-4): 269-301.

Jackson, M.L., 1967. Soil Chemical Analysis. Prentice Hall of India Pvt. Ltd., New Delhi. 498p.

Jones, Jr.J.B., 2001. Laboratory guide for conducting soil tests and plant analysis. CRC Press, New York, USA. 363p.

Kacar, B, Katkat, V., 2007. Bitki Besleme. Nobel Yayın Dağıtım, Ankara, Turkey. 678s.[in Turkish].

Karaçal, I., 2008. Toprak Verimliliği. Nobel Yayın Dağıtım, Ankara. Turkey. 222s.[in Turkish].

Karaman, R., Brohi, A.R., Müftüoğlu, N.M., Öztaş, T., Zengin, M., 2007. Sürdürülebilir Toprak Verimliliği. Detay Yayın Dağıtım, Ankara, Turkey. 224s. [in Turkish].

Krasilnikov, P., Sidorova, V., 2008. Geostatistical analysis of the spatial structure of acidity and organic carbon in zonal soils of the Russian plain. In: Soil geography and geostatistics: Concepts and Applications. Krasilnikov, P., Carré, F., Montanarella, L. (Eds.). Institute for Environment and Sustainability, European Communities, Luxembourg, pp. 55-67.

Lindsay, W.L., Norvell, W.A., 1978. Development of a DTPA Test for zinc, iron, manganese and copper. *Soil Science Society America Journal* 42(3): 421-428.

Loue A.T., 1968. Diagnostic petiolaire des prospectian etudes sur la nutrition at la fertilization potassiques de la vigne. Societe Commerciale des Potasses d'Alsace. Services Agronomiques, pp.31-41

López-García, F., Andreu-García, G., Blasco, J., Aleixos, N., Valiente, J.M., 2010. Automatic detection of skin defects in citrus fruits using a multivariate image analysis approach. *Computers and Electronics in Agriculture* 71(2): 189-197.

Marangoz, A.M., Karakış, S., Oruç, M., Büyüksalih, G., 2005. Nesne-tabanlı görüntü analizi ve ıkonos pan-sharpened görüntüsünü kullanarak yol ve binaların çıkarımı. TMMOB Harita ve Kadastro Mühendisleri Odası 10. Türkiye Harita Bilimsel ve Teknik Kurultayı 28 Mart - 1 Nisan 2005, Ankara, Turkey. [in Turkish]

Matsuoka, M., 2012. Comparison of the spectral properties of pansharpened images generated from AVNIR-2 and prism onboard Alos. XXII ISPRS Congress, 25 August – 01 September 2012, Melbourne, Australia.

Mc Cormick, N., 1999. Satellite-based forest mapping using the silvics software, user manual. Space Applications Institute, EGEO, Commission of the European Communities, Joint Research Centre, I-21020 Ispra (VA), Italy, 13-28 p.

Mousavifard, S.M., Momtaz, H., Sepehr, E., Davatgar, N., Sadaghiani, M.H.R., 2013. Determining and mapping some soil physico-chemical properties using geostatistical and GIS techniques in the Naqade region, Iran. *Archives of Agronomy and Soil Science* 59(11): 1573-1589.

Mulla, D.J., Mc Bratney, A.B., 2000. Soil Spatial Variability. In: Handbook of Soil Science. Sumner, M.E. (Ed.). CRC Press, New York, USA. pp. A321-A352

Mulla, D.J., McBratney, A.B., 2002. Soil spatial variability. In: Soil physics companion, Warrick, A.W. (Ed.). CRC Press, New York, USA. pp.343-373.

Naseem, S., Mahmood, S., Ali, Z., 2016. Occurrence of Citrus tristeza virus in Pakistan: a GIS based approach combining host distribution and disease reports. *Pakistan Journal of Agricultural Sciences* 53(3): 513-521.

Oliver, M.A., Webster, R., 2014. A tutorial guide to geostatistics: Computing and modelling variograms and kriging. *Catena* 113: 56–69.

Olsen, S.R., Sommers, L.E., 1982. Phosphorus. In: Methods of Soil Analysis Part 2 Chemical and Microbiological Properties. Page, A.L. (Ed.). American Society of Agronomy, Soil Science Society of America, Madison, USA. pp. 403-430.

Özdemir, M., 2017. Evaluation of image pan-sharpening methods in terms of object-oriented classification. *Harita Dergisi* 158: 26-34. [in Turkish].

Özyazıcı, M.A., Dengiz, O., Aydoğan, M., Bayraklı, B., Kesim, E., Urla, Ö., Yıldız, H., Ünal, E., 2016. Levels of basic fertility and the spatial distribution of agricultural soils in Central and Eastern Black Sea Region. *Anadolu Journal of Agricultural Sciences* 31(1): 136-148.

Panday, D., Maharjan, B., Chalise, D., Shrestha, R.K., Twanabasu, B., 2018. Digital soil mapping in the Bara district of Nepal using kriging tool in ArcGIS. *PloS one* 13(10): 1-20.

Knudsen, D., Peterson, G.A., Pratt, P.F., 1982. Lithium, Sodium, and Potassium. In: Methods of Soil Analysis Part 2 Chemical and Microbiological Properties. Page, A.L. (Ed.). American Society of Agronomy, Soil Science Society of America, Madison, USA. pp. 225-246.

Rauterberg, E., Kremkus, F., 1951. Bestimmung von Gesamthumus und Alkalilöslichen Humusstoffen im Boden. Z.F. Planzenernaehrung, Düngung und Bodenkunde, Verlag, Chemice Gmbh, Weinheim.

Richards, L.A., 1954. Diagnosis and improvement of saline and alkali soil. U.S. Salinity Lab. Staff, U.S. Department of Agriculture, Agricultural Research Service, Handbook 60. Washington D.C. USA. 160p.

Robinson, T.P., Metternicht, G., 2006. Testing the performance of spatial interpolation techniques for mapping soil properties. *Computers and Electronics in Agriculture* 50(2): 97-108.

Santos-Francés, F., Martínez-Graña, A., Zarza C.A., García Sánchez, A., Rojo, P.A., 2017a. Spatial distribution of heavy metals and the environmental quality of soil in the Northern Plateau of Spain by Geostatistical Methods. *International Journal of Environmental Research and Public Health* 14(6):568.

Santos-Francés, F., Martínez-Graña, A., Rojo, P.A., García Sánchez, A., 2017b. Geochemical background and baseline values determination and spatial distribution of heavy metal pollution in soils of the andes mountain range (Cajamarca-Huancavelica, Peru). *International Journal of Environmental Research and Public Health* 14(8): 859.

Schlichting, E., Blume, H.P., 1966. Bodenkundliches Praktikum, Verlag Paul Parey, Hamburg-Berlin.

Shen, Q., Wang, Y., Wang, X., Liu, X., Zhang, X., Zhang, S., 2019. Comparing interpolation methods to predict soil total phosphorus in the Mollisol area of Northeast China. *Catena* 174: 59-72.

Shi, W., Liu, J., Du, Z., Song, Y., Chen, C., Yue, T., 2009. Surface modelling of soil pH. *Geoderma* 150(1-2): 113-119.

Srivastava, A.K., Singh, S., 2009. Citrus decline: Soil fertility and plant nutrition. *Journal of Plant Nutrition* 32(2): 197-245.

Soil Survey Staff, 1951. Soil survey manual. Agricultural Research Administration, United States Department of Agriculture, Agricultural Handbook No.18, Washington, USA. 503p.

Tsegaye, T., Hill, R.L., 1998. Intensive tillage effects on spatial variability of soil test, plant growth and nutrient uptake measurement. *Soil Science* 163(2): 155-165.

Uysal, O., Polatöz, S., 2017. Dünyada ve Türkiye'de turunçgil üretimi ve dış ticareti. TÜRKTOB Dergisi 22: 6-11 [in Turkish].

Ülgen, N., Yurtsever, N., 1995. Türkiye gübre ve gübreleme rehberi. Toprak ve Gübre Araştırma Enstitüsü Yayınları, Genel Yayın No: 209, Teknik Yayınlar No: T.66, Ankara. [in Turkish].

Wilding L.P., 1985. Spatial Variability: It's documentation, accommodation and implication to soil surveys. In: Soil Spatial Variability. Nielsen, D.R., Bouma J. (Eds.). Pudoc, Wageningen, The Netherlands, pp: 166-194.

Wu, W., Liu, H.B., Dai, H.L., Li, W., Sun, P.S., 2011. The management and planning of citrus orchards at a regional scale with GIS. *Precision Agriculture* 12(1): 44-54.

Yayçep, 2010. Turunçgil Yetiştiriciliği. Televizyon Yoluyla Yaygın Çiftçi Eğitimi Projesi (YAYÇEP). Tarım ve Köyişleri Bakanlığı Yayın Dairesi Başkanlığı. Yayın No:54. Ankara. Available at [Access date: 17.03.2017] : http://www.katipogluziraat.com/kitap/turuncgil_cesitleri.pdf

Yeşilkanat, C., Kobya, Y., Taşkın, H., Çevik, U., 2014. Jeoistatistik tahmin ve simülasyon yöntemleri ile Artvin ilindeki doğal kaynak suları için toplam alfa ve toplam betanın ara değer modellemesi ve haritalanması. *Cumhuriyet Üniversitesi Fen-Edebiyat Fakültesi Fen Bilimleri Dergisi* 35(4): 11-35 [in Turkish].

Yuhendra, Sumantyo, J.T.,, Kuze, H., 2011. Performance analyzing of high resolution pan-sharpening techniques: Increasing image Quality for Classification using supervised kernel support vector machine. *Research Journal of Information Technology* 8(1): 12-28.

Zabihi, H., Vogeler, I., Amin, Z.M., Gourabi, B.R., 2016. Mapping the sensitivity of citrus crops to freeze stress using a geographical information system in Ramsar, Iran. *Weather and Climate Extremes* 14: 17-23.

Zabihi, H., Alizadeh, M., Kibet Langat, P., Karami, M., Shahabi, H., Ahmad, A., Nor Said, M., Lee, S., 2019. GIS multi-criteria analysis by ordered weighted averaging (OWA): toward an integrated citrus management strategy. *Sustainability* 11(4): 1009.

Eurasian J Soil Sci 2019, 8 (4) 364 - 377

Eurasian Journal of Soil Science

Journal homepage : http://ejss.fesss.org

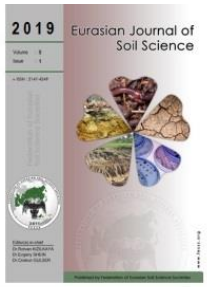

Organic-inorganic interactions in an aridisoil of Oman along vertical and lateral trends of the soluble major, trace and rare-earth elements

Khadija Semhi [a], Norbert Clauer [b,*], Malik Al Wardy [a]

[a] Sultan Qaboos University, P.O. Box 36, Al-Khod 123, Muscat, Sultanate of Oman

[b] Institut de Physique du Globe de Strasbourg (UdS-CNRS), 1 rue Blessig, 67084 Strasbourg, France

Abstract

Major, trace and rare-earth elements "(REEs)" dissolved by successive water and acetic-acid leaching of soil samples were quantified along a vertical and a lateral trend relative to a reference aridisoil covered by palm trees. The total content of the organic carbon ranges from 0.07 to 2.7% with the highest values in the topsoil closely below vegetation, confirming a higher organic activity. The water-removed elements decrease irregularly with depth and with increasing distance to the vegetated area, the highest concentrations being observed at 20 cm depth and 18 m away from vegetation. The nutrients removed by acetic-acid decrease with depth and until 22 m from vegetation. Maximum leaching was observed in the surface sample and 32 m away from vegetation. In fact, no straight trends were obtained in both the vertical and horizontal samplings; it looks that the elemental contents of each soil layer are only representative for themselves. The metallic trace elements are more abundant in the topsoil than in the subsoil, suggesting some anthropogenic supply. Mainly controlled by solid organic exudates, the REEs are the only ones with general vertical and horizontal trends: they decrease at depth, together with an increase laterally away from vegetation. The Ce and Eu positive anomalies increase deeper below the vegetation and away: an oxidation-reduction change is visible for the former anomaly, probably due to decreasing organic activity. The latter anomaly away from vegetation could reflect a larger contribution of soluble minerals to the leachates.

Keywords: Lateral and vertical distribution records; vegetated aridisoil; major, trace and rare-earth elements; water and acetic-acid leachings; organic matter activity; anthropogenic supply.

Article Info

Received : 02.04.2019
Accepted : 26.07.2019

Introduction

Plant roots and their soil interface constitute an intense interactive zone where many biochemical reactions take place. In the light of such reactions, the nutrient dynamics control the activity of the microorganisms, the growth of the plants, as well as a variable dissolution and alteration of minerals from hosting soils (Jobbágy and Jackson, 2001; Shen et al., 2011; Camenzind et al., 2018). Understanding of such vital reactions is fundamental and may be investigated by characterizing the role and distribution of the nutrients, especially in the rhizosphere. Varied studies focused on the distribution of specific elements, such as phosphorus in the host soils (Hedley et al., 1982a; Helal and Dressler, 1989; Gahoonia and Nielsen 1992; Zoyza et al., 1997). Others outlined the vertical distribution of nitrogen and carbon (Nielsen et al., 1988; Knops and Bradley, 2009), or the pH variations in the rhizosphere (Hedley et al., 1982b). Manea et al. (2011) investigated the vertical distribution of Cu, showing that it decreases with depth, the highest content in the topsoil being due to anthropic human activity. Fekiacova et al. (2013) described the vertical distribution of Fe in soils, while other studies (Mathan, 1991; Jayaganesh et al., 2011) investigated the vertical distribution

* Corresponding author.
Institut de Physique du Globe de Strasbourg (UdS-CNRS), 1 rue Blessig, 67084 Strasbourg, France
Tel.: +33 88 67 03 01
E-mail address: nclauer@unistra.fr
e-ISSN: 2147-4249
DOI: 10.18393/ejss.616903

of Mg, still in soils, Wood and de Turk (1940) and Hirekurabar et al. (2000) examining that of K. However, only a few investigations established a clear relationship between the vertical distribution in the rhizosphere and the lateral trend of elements, such as of the lanthanides for instance, that can be useful for soil management and plant preservation. In turn, understanding the elemental dynamics in soils by using their spatial distribution is necessary to decrypt the elemental evolution and their impact on their immediate environment.

The objectives of this study carried in a region under arid climate were then in an identification of the vertical partitioning of essential and non-essential elements in a soil with a vegetal cover, and the lateral distribution of the same elements in the same soil at an increasing distance from vegetation to identify best the local interactions of the vegetal and mineral worlds. This experiment was also undertaken to estimate the availability of nutrients to plants and their immediate mobility. Micronutrients of soils may be associated with different phases, such as exchangeable cations, carbonates, Fe and Mn oxides, organic matter, sulphides and silicates, as well as salts in arid countries, because these chemical forms can influence their mobility, toxicity and bioavailability. Furthermore, soil characteristics, such as the pH and Eh, the clay content and cation-exchange capacity, and the occurrence of Mn, Fe oxides and organic matter are also contributing to the distribution of heavy metals and their availability to plants in soils (Martínez and Motto, 2000; Sterckeman et al., 2000; Aydinalp and Marinova, 2003). Water-exchangeable and acid-extractable soluble fractions contain mobile compounds that are easily bioavailable. Since nutrients of the accessible fractions are mostly involved in the growth of plants and in the activity of microorganisms in soils, reflecting potentially both the soil bedrock supply and anthropogenic inputs, the present study was based on the examination of major, trace and rare-earth elements removed by successive water and acetic-acid leaching experiments. As examination of rare earth-elements (REEs) in soils has repetitively shown specific applications (e.g., Tyler, 2004; Semhi et al., 2009; Chang et al., 2016) in the assessment of soil genesis, the increase of soil fertility, the evaluation of anthropogenic impacts, and also the identification of pedogenic processes, we have dedicated a special interest to these elements.

REEs also identified as lanthanides consist of elements that are characterized by a ground state electronic configuration with at least one electron in the 4f electronic orbitals, mostly non-interactive but with a strong ionic bonding character making them as strong acids (Piper and Bau, 2013). REEs occur generally with three electrons removed from their d, s and f orbitals; only Eu has a half-filled f-orbital that allows stability for the Eu^{2+} species, and Ce exhibits an oxidation-reduction state that allows Ce to occur as either Ce^{3+} or Ce^{4+}, especially in soils (Taylor and McLennan, 1985). Wyttenbach et al. (1998) studied REEs of leaves from plants and the associated soils and found that Ce yields a negative anomaly in all plants with respect to the corresponding soil. Miao et al. (2008) reported that the geochemical characteristics of REEs from plants depend on the types of soils, that their concentrations are higher in B and C soil horizons than in the above A horizon, and that they outline an Eu negative anomaly and a Ce positive anomaly. They also described REE fractionations from soil to plant roots, stems and leaves, with heavy REEs (HREEs) relatively less available relative to the light REEs (LREEs). Alternatively, Loell et al. (2011) reported a Ce negative anomaly in German soils, as did Wyttenbach et al. (1998) in plants, together with correlations between REEs and clay, Fe, and Mn oxide contents.

Material and Methods

The selected site is the palm-tree nursery of the Agricultural Experiment Station from the Sultan Qaboos University in Oman. The station covers an area of 70 hectares and among the variety of fruit crops grown at the station, are date palm trees (*Phoenix dactylifera L*) that account for about 500 trees distributed in open fields and along road paths. The area is characterized by an average relative humidity of 46% and an average annual temperature of 29°C, the minimum night and maximum day temperatures ranging from 13 to 48°C, respectively. The evapotranspiration rate was measured at 3-12 mm/day. The samples belong to the groves and vicinity of a date palm cultivar called “Khalas”. This cultivar has an average production of 120 kg/season dates at the station. The date palms are irrigated with a bubbler system with two bubblers in each grove supplying 280 to 320 L/day of low salinity groundwater (< 2 dS/m) to each date palm tree. The soils were collected at different depths and distances from palm trees with determination of the pH values during sampling. For the vertical investigation, the samples were collected 10 cm below the surface, as well as at 20, 50 and 100 cm depths in the subsoil. For the lateral investigation, a second set of samples was collected at a constant depth of 50 cm at 10, 12, 18, 22 to 32 m from the vegetation.

All soil samples were dried for 2 days at room temperature and then were placed in an oven at 60 °C for about 10 h before being hand-crushed in a mortar. One gram of dry soil sieved at <63 µm was first leached with double-distilled water during 15 min at a room temperature of 20 °C. The extracts were separated from

residues by centrifugation at 4,000 rpm (SIGMA model 3-15). The residues were washed again afterwards with double-distilled water by shaking and centrifugation. Then, the residue was treated with 40 ml of acetic acid (CH_3COOH at 0.1 mol/L). The extracts were also separated from solid residues by centrifugation for their chemical analysis.

The elemental contents were determined on an inductively coupled plasma atomic emission spectrometer (ICP-AES of the Laboratoire d'Hydrologie et de Géochimie de Strasbourg, France) for the major (Si, Al, Mg, Ca, Na, K and P) and some trace elements (Sr, Fe, Mn and Zn), and on an inductively coupled plasma mass spectrometer (ICP-MS also of the Laboratoire d'Hydrologie et de Géochimie de la Surface de Strasbourg, France) for the other trace elements (V, Cu, Ba, Cr, Co, Ni, Rb, As, Zr, Cd, U and Th) and the rare-earth elements (REEs). Repeated analysis of international standards such as B-EN and GL-O on a weekly basis provided an analytical precision of $\pm$2.5% for the major elements, $\pm$5% for the trace elements and $\pm$10% for the REEs, on the basis of the analytical procedure by Samuel et al. (1985). The total organic carbon (TOC) was measured with a TOC analyzer (Simadzu Model TOC-V) on a precision better than $\pm$5% and a detection limit of 0.05 mg/kg).

Results

The results include pH, TOC (in %) and concentrations (in mg/g, µg/g and ng/g) of the elements analyzed in the collected leachates by either water or dilute acetic-acid action. In the study site, the soils are alkaline with a pH ranging from 7.34 to 8.71 (Table 1), the vertical and lateral variability being very limited.

The TOC ranges from 0.07 to 2.7% with the highest value in the surface horizon close to vegetation, decreasing vertically and horizontally away from vegetation, which confirms the expected organic activity decrease away from vegetation (Table 1). The vertical TOC are higher than the lateral ones, confirming that the organic activity in the vegetation area is higher than in the corresponding de-vegetated one. As organic matter plays a determining role in binding heavy metals in soils and sediments (Akan et al., 2003), it is also considered to immobilize them and reduce their uptake by the plants, which is not what was found here. Alternatively, organic complexation of heavy metals in soils (Weng et al., 2002; Silveira et al., 2003; Tukura et al., 2007; Ashworth and Alloway, 2008) reduces heavy-metal pollution of plants including consumable vegetables.

The elements removed by water leaching

The contents of the major elements

The water extracts contain mainly elements that are easily removable, mainly adsorbed on the mineral particles and organic compounds sensitive to water contact. The most extracted elements here are Na, Ca and Mg with a vertical distribution indicating an important extraction of Ca, Mg, Na, K, Mn and P at 20-cm depth, while the highest extraction of Fe and Al occurred further down in the horizon at a 50-cm depth (Fig. 1), Si being most leached in the uppermost 10-cm deep horizon. To be noticed also is the parallel changes of the Ca and Na contents in both the vertical and the horizontal trend. On the other hand, the P contents are drastically decreasing when sampling is away from vegetation, vertically and horizontally. The K contents appear more complex as they decrease when buried, which could relate to increasing distance to vegetation. However, in the horizontal display, they increase with increasing distance to vegetation (Figure 1).

The lateral distribution indicates that Al and Fe are enriched 10-m away from vegetation with ups and downs beyond: decrease at 12 m, increase again at 18 and 22 m, before another decrease at 32 m. Ca, Si and K yield also waving contents when collected away from vegetation. None outlines a constant change, either increasing or decreasing, which suggests that the interference between organic and inorganic influences is not straight (Figure 1). In summary, the total amounts of major elements leached by water decrease with depth by about half between the uppermost and lowermost samples. On the other hand, it fluctuates by a similar ratio when the distance to vegetation increases, the lower contents being recorded at 10 and 22 m away from vegetation (Figure 2).

The Na/K ratio varies between 1.6 and 29.1, the highest value being observed in the vertical trend at the 100-cm depth, which suggests crystallization of Na salts at depth rather than in the topsoil due to the arid climate. The lateral distribution of this ratio indicates also a decrease of Na soluble phases when the distance from vegetation increases, even at similar depth (Table 1; Figure 3). The highest value for the K/Rb ratio is at a 50-cm depth in the vertical profile. Along the horizontal display, the same ratio decreases first when distance to vegetation increases, then it increases until 22 m away from vegetation. The Ca/Sr ratio increases with depth, while zigzagging horizontally when distance increases (Figure 3). The Mg/Ca ratio ranging from 0.2 to 1.35 tends to decrease with depth and with distance from vegetation due to an increase of the Ca content. Its highest value is observed in the topsoil due to a higher Mg concentration relative to Ca.

Table 1. Major, trace and rare-earth elemental compositions of the water and acetic acid leachates along the vertical and horizontal trends. The contents of the analyzed elements are plotted in the data columns of each. bdl stands for below detection limit and nd for not determined.

Water leachates	Depth (m)	Si (µg/g)	Al (µg/g)	Mg (µg/g)	Ca (µg/g)	Fe (µg/g)	Mn (µg/g)	Na (µg/g)	K (µg/g)	P (µg/g)	Sr (µg/g)	Zn (µg/g)	Na/K	Ca/Sr	K/Rb	TOC (%)	pH values
1 W	0.10	45.5	0.32	193	170	0.59	0.04	650	90.3	44.0	2.69	2.25	7.20	63.0	1859	2.09	8.29
2 W	0.20	30.8	1.85	400	297	1.52	0.25	948	108	43.9	4.60	2.11	8.75	64.6	2062	2.66	8.45
3 W	0.50	23.8	4.84	83.1	127	3.44	0.06	538	103	26.5	1.21	1.17	5.22	105	5886	0.70	8.97
4 W	1.00	40.5	1.73	111	177	1.25	0.20	640	22,0	24.5	1.74	0.79	29.1	102	2200	0.45	8.68
	Distance (m)																
5 W	10.0	82.3	23.0	77.7	312	14.8	0.43	184	62.8	4.45	2.72	0.40	2.93	111	1569	0.08	8.89
6 W	12.0	26.3	0.11	65.2	200	0.08	0.14	313	56.3	5.80	13.4	0.43	5.56	14.9	4500	0.09	8.90
7 W	18.0	31.5	4.94	141	719	2.76	1.02	468	132	4.68	10.1	1.93	3.53	71.1	5878	0.07	9.03
8 W	22.0	40.0	4.37	46.4	154	2.78	0.21	192	117	7.95	9.26	1.08	1.63	16.6	6700	0.07	8.75
9 W	32.0	33.5	0.32	93.2	467	0.20	0.05	370	114	5.68	4.81	0.30	3.24	96.9	4570	0.07	8.95
Acid leachates	Depth (m)	Si (mg/g)	Al (mg/g)	Mg (mg/g)	Ca (mg/g)	Fe (mg/g)	Mn (mg/g)	Na (mg/g)	K (mg/g)	P (mg/g)	Sr (mg/g)	Zn (µg/g)	Na/K	Ca/Sr	K/Rb		
1 AC	0.10	0.22	0.23	2.97	326	0.16	0.15	0.83	0.33	0.14	0.45	14.5	2,49	724	1335		
2 AC	0.20	0.25	0.20	7.60	175	0.06	0.28	1.41	0.24	1.07	0.36	24.5	5,86	491	2008		
3 AC	0.50	0.36	0.36	6.32	172	0.14	0.39	1.12	0.39	1.26	0.26	27.8	2,86	670	4255		
4 AC	1.00	0.29	0.10	9.98	130	0.07	0.51	1.52	0.36	4.70	0.42	66.8	4,21	311	2395		
	Distance (m)																
5 AC	10,0	0.61	0.19	9.87	127	0.12	0.59	1.34	0.36	4.52	0.49	0.116	3.69	259	2851		
6 AC	12,0	0.25	0.35	4.69	174	0.08	0.10	0.86	0.39	0.17	0.36	0.008	2.18	484	3154		
7 AC	18,0	0.22	0.22	2.97	307	0.12	0.13	0.58	0.36	0.073	0.54	0.007	1.62	572	7189		
8 AC	22,0	0.18	0.23	3.37	155	0.08	0.12	0.97	0.33	0.14	0.38	0.007	2.94	410	8835		
9 AC	32,0	0.22	0.17	3.67	390	0.11	0.16	0.83	0.36	0.093	0.69	0.006	2.29	565	6908		

Table 1. (continued)

Water leachates	Depth (m)	V (ng/g)	Ba (ng/g)	Cr (ng/g)	Co (ng/g)	Ni (ng/g)	Cu (ng/g)	As (ng/g)	Rb (ng/g)	Zr (ng/g)	Cd (ng/g)	Zn (ng/g)	Pb (ng/g)	Th (ng/g)	U (ng/g)	Zn/Cu
1 W	0.10	182	123	89.8	4.61	192	379	24.3	48.5	16.8	2.79	2.25	8.25	6.07	2.91	5.94
2 W	0.20	163	168	92.5	7.25	210	373	42 .5	52.5	12.8	2.33	2.11	9.25	1.25	2.25	5.66
3 W	0.50	225	85.0	123	5.75	485	498	27.5	17.5	10.0	2.43	1.17	7.00	1.50	3.00	2.35
4 W	1.00	255	103	85.0	7.00	383	265	37.5	10.0	9.50	1.58	0.79	6.25	0.75	1.00	2.96
	Distance (m)															
5 W	10.0	129	273	188	22.8	655	420	37.5	40.0	18.8	0.60	0.40	20.0	2.00	2.00	0.94
6 W	12.0	131	398	45.0	6.50	60.0	52.5	37.5	12.5	bdl	0.30	0.43	2.75	bdl	0.50	8.14
7 W	18.0	45.5	235	42.5	27.5	218	113	15.0	22.5	bdl	1.63	1.93	14.3	bdl	0.50	17.1
8 W	22.0	96.5	230	62.5	12.8	95.0	0.09	32.5	17.5	2.50	1.48	1.08	5.75	bdl	1.25	12.7
9 W	32.0	30.5	143	57.5	2.75	67.5	0.04	10.0	25.0	bdl	0.03	0.30	nd	bdl	0.75	7.44
Acetic acid leachates	Depth (m)	V (µg/g)	Ba (µg/g)	Cr (µg/g)	Co (µg/g)	Ni (µg/g)	Cu (µg/g)	As (µg/g)	Rb (µg/g)	Zr (µg/g)	Cd (µg/g)	Zn (µg/g)	Pb (µg/g)	Th (µg/g)	U (µg/g)	Zn/Cu
1 AC	0.10	1.10	17.6	9.75	1.65	11.6	7.35	0.62	0.25	0.19	0.20	14.5	0.90	0.49	0.48	8.82
2 AC	0.20	0.54	17.4	7.54	2.58	10.0	1.72	0.32	0.12	0.17	0.12	24.5	0.47	0.11	0.25	9.50
3 AC	0.50	0.70	11.6	11.0	3.38	11.5	1.07	0.46	0.09	0.27	0.15	27.8	0.27	0.08	0.45	8.22
4 AC	1.00	0.32	21.1	6.60	2.46	4.17	1.06	0.28	0.15	0.18	0.19	66.8	0.24	0.04	0.26	27.1
	Distance (m)															
5 AC	10.0	0.93	20.2	14.3	3.99	10.4	0.72	0.72	0.13	0.19	0.23	1.00	0.24	37.2	0.62	29.1
6 AC	12.0	0.14	10.1	6.79	2.32	9.87	1.16	0.27	0.12	0.06	0.06	8.00	0.37	118	0.25	3.45
7 AC	18.0	0.92	17.4	7.04	1.51	8.75	0.84	0.49	0.05	0.04	0.10	6.75	0.48	236	0.41	4.47
8 AC	22.0	0.19	6.84	5.55	2.33	8.21	0.68	0.28	0.04	0.03	0.05	7.25	0.30	130	0.17	3.11
9 AC	32.0	1.47	28.3	7.95	1.91	10.9	0.98	0.40	0.05	0.03	0.13	6.00	0.53	260	0.52	3.15

Table 1. (continued)

Water leachates	Depth (m)	La (ng/g)	Ce (ng/g)	Pr (ng/g)	Nd (ng/g)	Sm (ng/g)	Eu (ng/g)	Gd (ng/g)	Tb (ng/g)	Dy (ng/g)	Ho (ng/g)	Er (ng/g)	Tm (ng/g)	Yb (ng/g)	Lu (ng/g)	Total (ng/g)
1 W	0.10	4.37	9.22	1.07	3.40	0.83	0.46	0.97	0.34	0.66	0.29	0.46	0.22	0.49	0.17	22.9
2 W	0.20	3.00	7.25	0.73	2.25	0.58	0.30	0.72	0.23	0.45	0.18	0.33	0.15	0.25	0.13	16.5
3 W	0.50	4.50	9.25	1.23	4.25	0.95	0.33	1.08	0.25	0.95	0.23	0.45	0.10	0.53	0.10	24.2
4 W	1.00	2.25	6.50	0.55	2.50	0.55	0.18	0.50	bdl	0.53	bdl	0.20	0.05	0.23	0.05	14.1
	Distance (m)															
5 W	10.0	10.3	21.5	2.30	9.75	1.95	0.80	2.10	0.28	1.40	0.40	0.75	0.13	0.65	0.10	52.4
6 W	12.0	bdl	1.00	bdl	bdl	bdl	bdl	bdl	bdl	bdl	bdl	bdl	bdl	bdl	bdl	nd
7 W	18.0	1.50	10.8	0.43	1.75	0.38	bdl	0.50	bdl	0.28	bdl	0.15	bdl	0.13	bdl	nd
8 W	22.0	1.00	4.25	bdl	1.00	bdl	bdl	0.18	bdl	bdl	bdl	bdl	bdl	bdl	bdl	nd
9 W	32.0	0.25	0.75	bdl	0.25	bdl	bdl	bdl	bdl	bdl	bdl	bdl	bdl	bdl	bdl	nd
Acetic acid leachates	Depth (m)	La (µg/g)	Ce (µg/g)	Pr (µg/g)	Nd (µg/g)	Sm (µg/g)	Eu (µg/g)	Gd (µg/g)	Tb (µg/g)	Dy (µg/g)	Ho (µg/g)	Er (µg/g)	Tm (µg/g)	Yb (µg/g)	Lu (µg/g)	Total (µg/g)
1 AC	0.10	3.34	4.76	0.95	4.01	1.00	0.24	0.96	0.15	0.85	0.17	0.42	0.057	0.31	0.005	17.3
2 AC	0.20	1.29	1.88	0.32	1.49	0.38	0.11	0.42	0.06	0.37	0.08	0.20	0.027	0.15	0.002	6.81
3 AC	0.50	1.29	1.93	0.31	1.51	0.39	0.12	0.46	0.07	0.44	0.09	0.25	0.034	0.20	0.003	7.12
4 AC	1.00	0.38	0.52	0.08	0.37	0.09	0.03	0.11	0.15	0.09	0.02	0.05	0.001	0.04	0.007	1.80
	Distance (m)															
5 AC	10.0	0.45	0.66	0.10	0.49	0.13	0.04	0.16	0.02	0.13	0.03	0.08	0.01	0.07	0.01	2.38
6 AC	12.0	1.47	1.65	0.40	1.71	0.43	0.10	0.40	0.06	0.35	0.07	0.17	0.02	0.13	0.02	6.98
7 AC	18.0	2.28	3.00	0.63	2.69	0.66	0.16	0.63	0.01	0.58	0.11	0.29	0.04	0.22	0.03	11.4
8 AC	22.0	1.09	1.40	0.29	1.22	0.29	0.07	0.29	0.04	0.25	0.05	0.12	0.02	0.09	0.01	5.22
9 AC	32.0	2.83	3.79	0.79	3.41	0.85	0.21	0.82	0.12	0.76	0.14	0.38	0.05	0.28	0.04	14.5

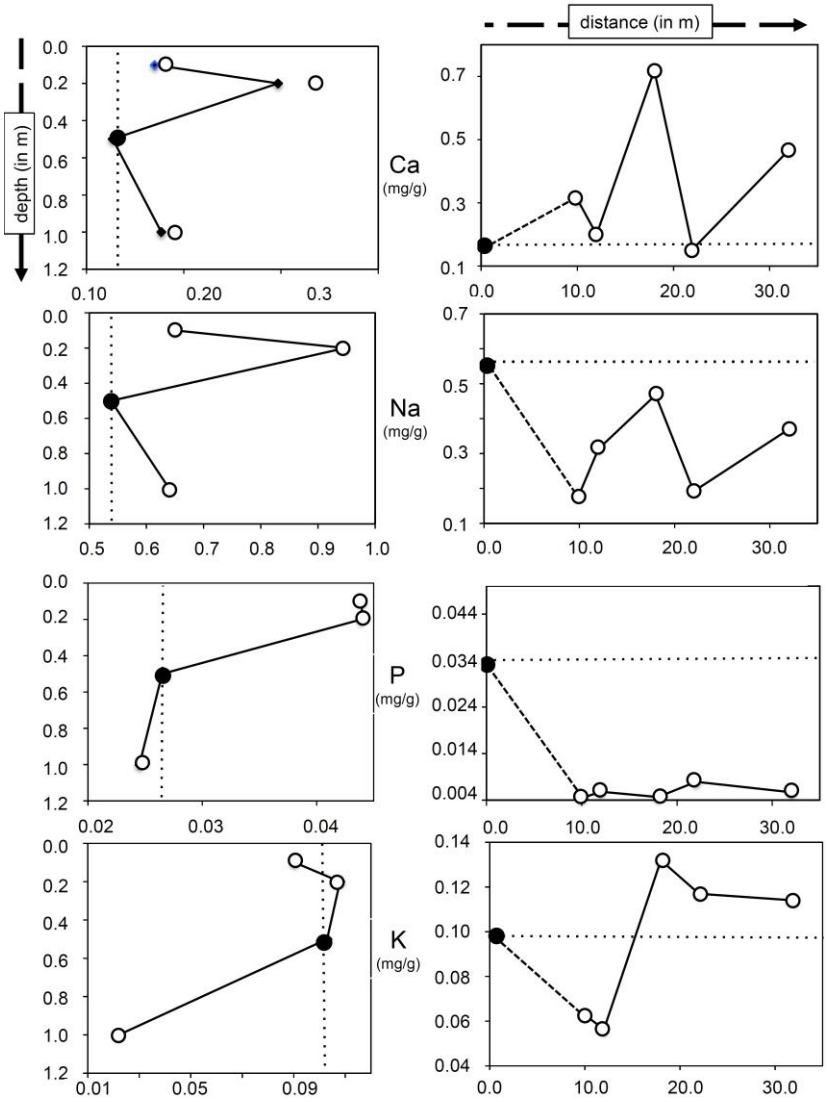

Figure 1. Vertical and lateral variations of some major element in the water leachates relative to depth in the left column and to distance to vegetation in the right column. The black dot in the graphs corresponds to the reference sample in both trends. The finely dotted lines represent the reference contents in the vertical and horizontal samplings.

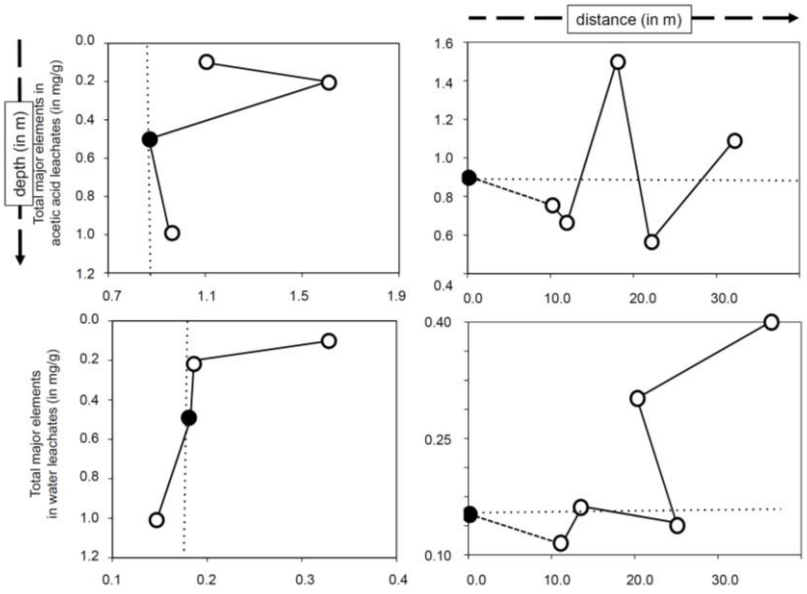

Figure 2. Total major elemental contents of the water leachates in the top row and of the acetic leachates in the bottom row, relative to depth to the left and to distance to the vegetation to the right. The black dot in the graphs corresponds to the reference sample in both trends. The finely dotted lines represent the reference contents in the vertical and horizontal samplings.

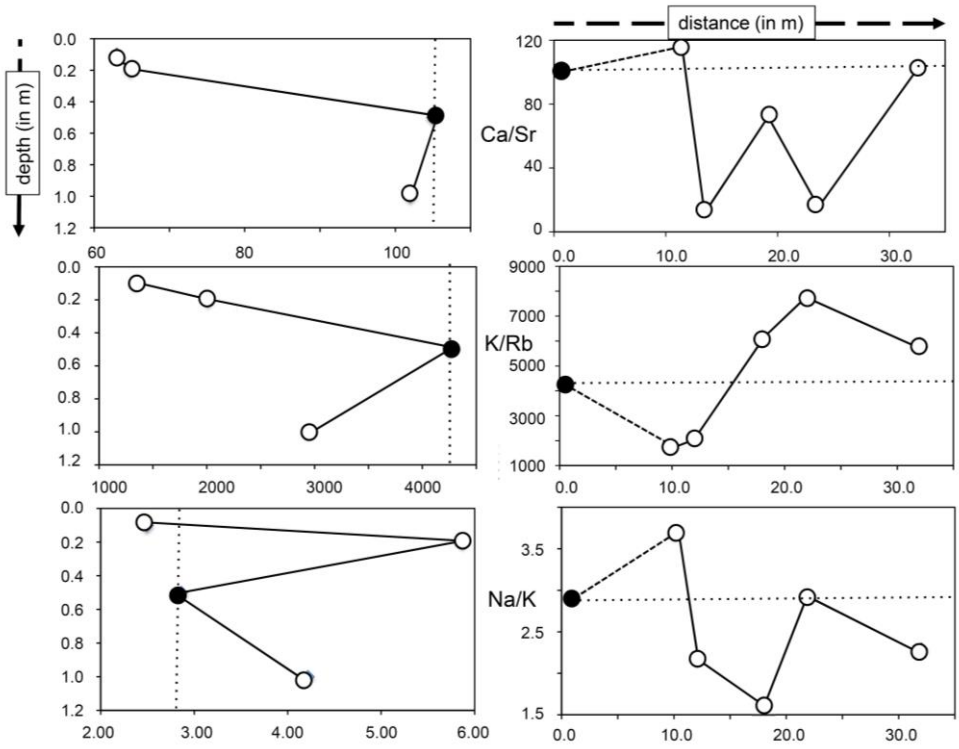

Figure 3. The Ca/Sr, K/Rb and Na/K ratios of the water leachates relative to depth in the left column and to distance to vegetation in the right column. The black dot in the graphs corresponds to the reference sample in both trends. The finely dotted lines represent the reference contents in the vertical and horizontal samplings.

The contents of the trace elements

Vertical distribution of the trace elements shows a progressive decrease with depth for the Rb, Th, Zr, Pb, Cu, Cd and U contents. While Ni increases with depth, the contents of Cr do not show any significant change except at 50 cm depth where it increases. Ba decreases with depth with an increase at 20 cm depth. Co and As increase at 20 cm and at 1 m depth, whereas the V contents decrease at 20 cm depth and increase at the 50 cm and 100 cm. Zn increases progressively, while Sr increases at 20 cm and decreases deeper. The lateral distribution of the trace elements in the water extracts highlights increasing Co, Rb, Cr and Ni contents at 10 m from vegetation that decrease at 12 m away. The concentrations of Cu and V decrease with increasing distance from vegetation. The concentration of As is characterized by a significant reduction 32-m away from vegetation, Cd and U are decreasing with increasing distance from vegetation, Cd having a significant decrease at 12 m and 32 m from vegetation. The concentration of Pb waves away from vegetation with an increase at 10 m, a decrease at 12 m, an increase at 18 m and a decrease again at 22 m. The Sr content of the leachates increases significantly at 12 m, while Zn decreases until 12 m, increasing at 18 m and decreasing at 32 m.

In sum, the trace elements removed by water and expressed as the total dissolved elements decrease generally irregularly with depth and with increasing distance from vegetation. The highest availability is observed in the 20-cm deep horizon and at 18 m away from vegetation (Figure 1).

The contents of the REEs

The total REE contents of the water extracts from vertical trend are about 23 ng/g at 10 cm below the surface, 17 ng/g at 20 cm and 25 ng/g at 50 cm, decreasing to about 14 ng/g at 1-m depth (Table 1). Relative to the surface, transfer of REEs to the deeper horizons occurred without any major fractionation, as their distribution patterns remain flat relative to that of the most surficial sample (Figure 4A). The small ups and downs among the element contents are most probably due, at least partly, to the analytical uncertainty of very small amounts. Only a slight decrease towards the heavy REEs (HREEs) can be observed, which is probably not significant analytically either. However, the slope has the tendency to increase with depth even if only slightly. Also to be noticed are the positive Eu anomaly for the deepest leachate and the negative Eu anomaly in the two deeper leachates. Changing oxidation-reduction conditions for the former and an increasing inorganic impact for the latter could explain these modifications that will be discussed in a further section.

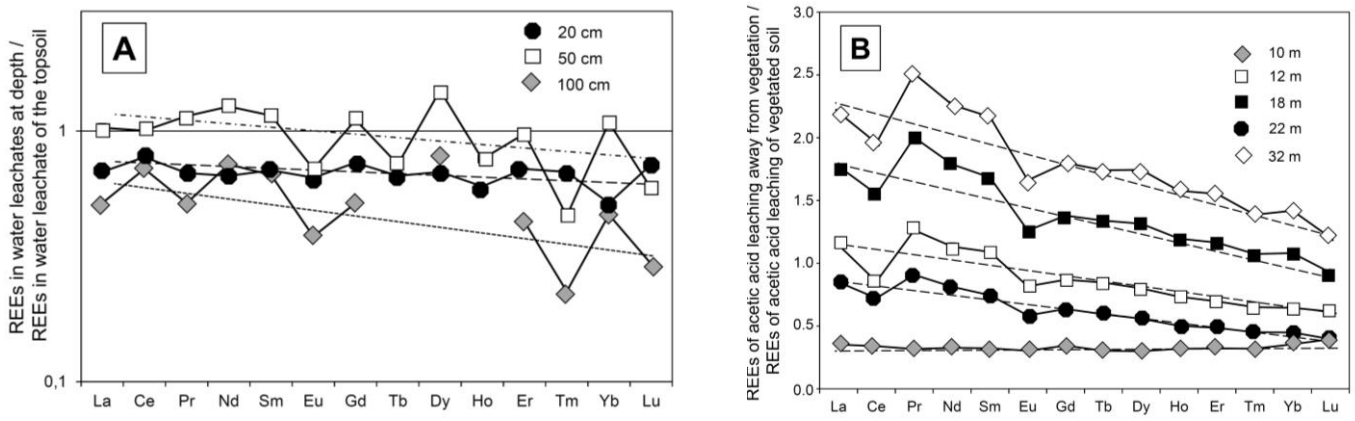

Figure 4. (A) The REE distribution patterns from water leachates of the vertical trend, relative to the topsoil leachate. (B) The REE distribution patterns of the acetic acid leachates along the horizontal trend.

The lateral distribution could only be examined at 10 m away from vegetation as most REE contents of the water leachates were below detection limit of the used equipment. When compared to the water leached of the soil sample at 50 cm below vegetation, that located 10 m away from vegetation shows a pattern with a significant decrease in the heavy REEs' contents (HREEs; Figure 5A). Furthermore, together with a significant negative Tb anomaly that is yet difficult to explain, a small positive Nd anomaly and a more significant positive Eu anomaly are visible.

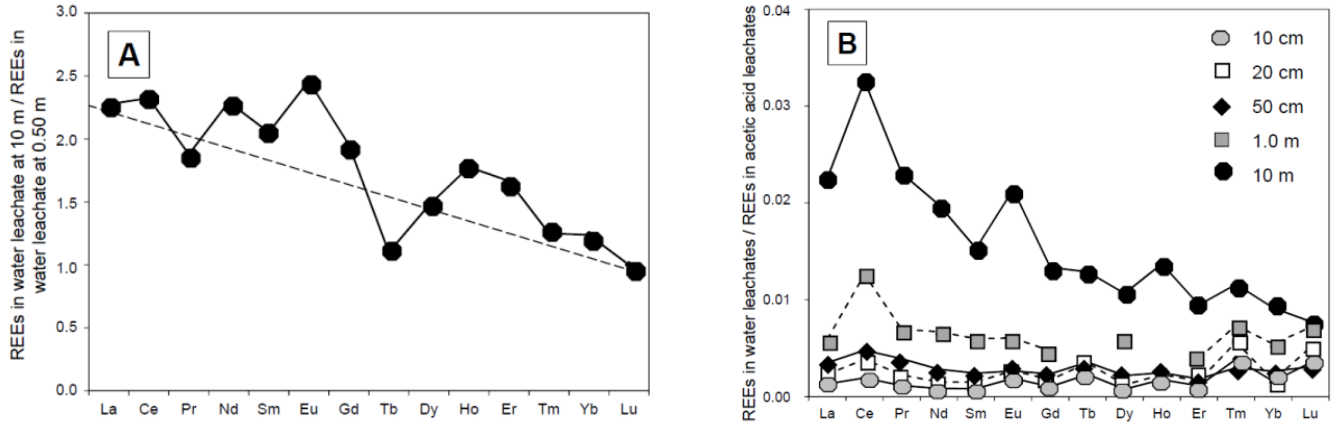

Figure 5. (A) The REE distribution pattern of the water leachate at 10-m distance from vegetation relative to the same pattern of the reference water leachate at 0.50 m depth. (B) The REE distribution patterns of the water leachates relative to the equivalent acetic acid leachates along the vertical trend and in the horizontal sample from 10-m distance.

The elements removed by acetic acid leaching

The contents of the major elements

Acetic acid is often used to leach metallic elements present in exchangeable mineral fractions that are sensitive to changing pH in sediments (Sahuquillo et al., 2003). The acetic-acid extracts from soil samples collected here contain elements that were released subsequently at the initial water-leaching step, meaning that basically the samples did no longer contain such adsorbed elements. In fact, Ca and Fe are the most removed elements near the surface, to the opposite of Mn, Na, P and Mg that accumulate at depth (Figure 6), and of Si, Al and K that accumulate at 50 cm. The vertical elemental trends indicate that Mg, P, Mn and Na increase with depth, Al increases at 50 cm depth and decreases above at 20 cm and below at 100 cm, while Si increases in the upper horizons and decreases at 100 cm depth.

The lateral distribution relative to vegetation indicates a reduction of Mg, P, Si, Fe and Al, an irregular increase of Ca and no change for K with increasing distance (Figure 6). The content of Na increases slightly at 10-m distance and decreases beyond, while Fe decreases significantly at 12 m and 22 m, Mn increases at 10 m before decreasing to the opposite to Al that decreases strongly at 10 m. The availability of nutrients illustrated by the total removed major elements by acetic-acid leaching decreases 22 m away from vegetated area, as it did with increasing depth. Compared to the soil with the vegetal cover at 50 cm depth, the maximum availability of the major elements is obtained 32 m away from vegetation, as it was in the topsoil under vegetation. In summary, the total amounts of major elements leached by water and acetic acid are very different, but unexpectedly they mimic also each other. The patterns relative to the distance to

vegetation are especially quite identical, those obtained for the vertical profile being very similar (Figure 2). Even if not leaching the same fractions, water and acetic acid have a similar impact on similar soil compositions.

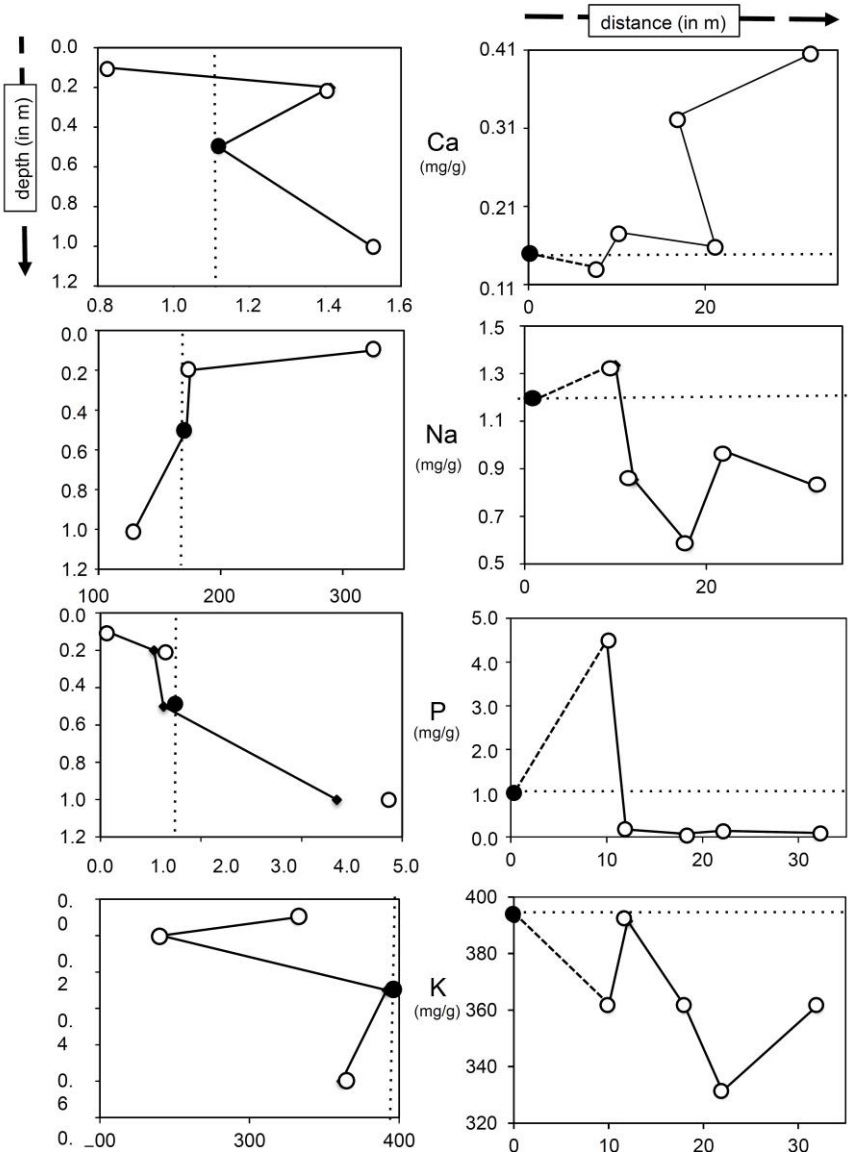

Figure 6. Vertical and lateral variations of major elements in the acetic-acid leachates relative to depth in the left column and to distance to vegetation in the right column. The black dot corresponds to the reference sample in both trends.

The Na/K ratio ranges from 2.5 to 5.9, this latter value being observed in the topsoil at 20 cm depth. The ratio decreases at 50 cm depth and increases in the subsoil along the vertical trend. Relative to the soil around the vegetation, the same Na/K ratio does not outline any lateral variation away from vegetation. After a significant decrease in the 10 initial meters, the Ca/Sr ratio remains quite identical when distance to vegetation increases (Figure 7). Ranging from 0.01 to 0.08, the Mg/Ca ratio tends to increase with depth and to decrease with distance from vegetation as for the leachates by water do, in fact, to an increase of Ca (Table 1).

The contents of the trace elements

The vertical distribution of the trace elements outlines progressive decreases of the As, Rb, Th, Pb, U, Ni, Cu and V contents with depth, those of Cr decreasing at 20 cm, increasing at 50 cm, and those of Co increasing until 50 cm and decreasing at 100 cm. Ba decreases at 50-cm depth, decreasing further at 100 cm, while Zr increases at 50 cm depth and again at 100 cm. The lateral distribution relative to vegetation of the elements leached by acetic acid outlines increases in the Pb and Th contents with increasing distance, while those of Zr decrease. The Ni contents decrease progressively until an increase at 32-m distance. The contents of Cr and Co increase at 10 m and then decrease, while those of V and Cu decrease at 12 m and 22 m. The As contents increase at 10 m and 18 m, while Rb increases at 10 m and 12 m, decreasing further away. Ba is more concentrated at 32 m than near the vegetation. The U and Cd contents increase at 10 m, decrease at 12 m and 22 m, increasing again at 32 m.

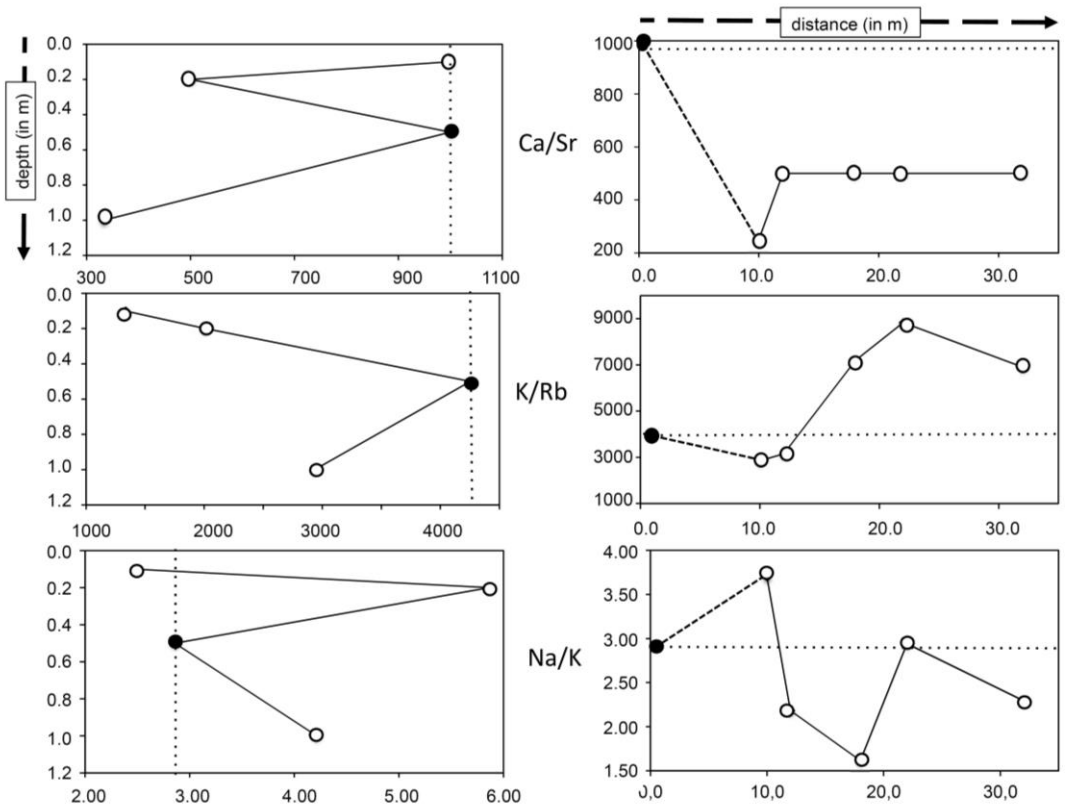

Figure 7. The Ca/Sr, K/Rb and Na/K ratios of the acetic-acid leachates relative to depth in the left column and to distance to vegetation in the right column. The black dot corresponds to the reference sample in both trends.

No correlation was observed between the contents of the elements leached by water and those of the elements leached by the acetic acid except for Na and Si, especially in the lateral distribution. There seems to be a competition between the water and acetic-acid leachates for these two elements, suggesting the leaching of phases that are soluble in either water or acetic acid are of varied sources, unless they were incorporated into mineral phases variably sensitive to the leaching solutions. This outline may also indicate that soil washing with water may have decreased the solubility of Na and Si in the acetic acid. Among the trace elements, only the water-leached Cr is proportional to the acetic-acid leached Cr, suggesting the same source for both phases, while Rb behaves as do Na and Si.

The contents of the REEs

The total contents of REEs in the acetic-acid leachates from vertical trend is much higher than in the water leachates: at about 17.3 μg/g near the surface close to the plants, it decreases to 1.8 μg/g at 100 cm depth. The overall distribution shows a somehow higher accumulation in the topsoil. The lateral REE distribution indicates that the lowest amount occurs at 10 m from vegetation with a progressive increase at 32 m away from vegetation (Table 1). The REE patterns of the acetic-acid leachates from vertical sampling plotted relative to their contents in the reference soil at 50 cm depth outline increasing heavy REEs (HREEs) at 20 and 50 cm depth, while the distribution pattern is flat for the leachate from 1-m deep sample (Figure 8). Also to be noticed are the two positive Ce and Eu anomalies. In sum, this very different pattern relative to those of the water leachates confirms that the REEs extracted by water and acetic acid were located in different components of different origins.

Relative to the REEs contents of the 50-cm deep reference level below vegetation, the distribution patterns at increasing distance from vegetation yield a significant enrichment in light REEs (LREEs) as well as increasing negative anomalies in Ce and Eu (Figure 4B). Earlier studies showed that higher concentrations of LREEs are observed in soils developed on phosphate and carbonate rocks (Chen and Yang, 2010), which is not the case here. The already mentioned negative Ce anomaly also visible in most leachates is often considered to characterize oxidizing environments (McLennan, 1989). The distribution patterns of the REEs trends are very similar, except varied extends of the Ce and Eu anomalies, with only an increasing slope from La on the light side of the REE distribution to Lu at the heavy side correlated with the distance to the vegetation. At the 32-m distance, the pattern has the steepest slope, while completely flat at the 10-m distance.

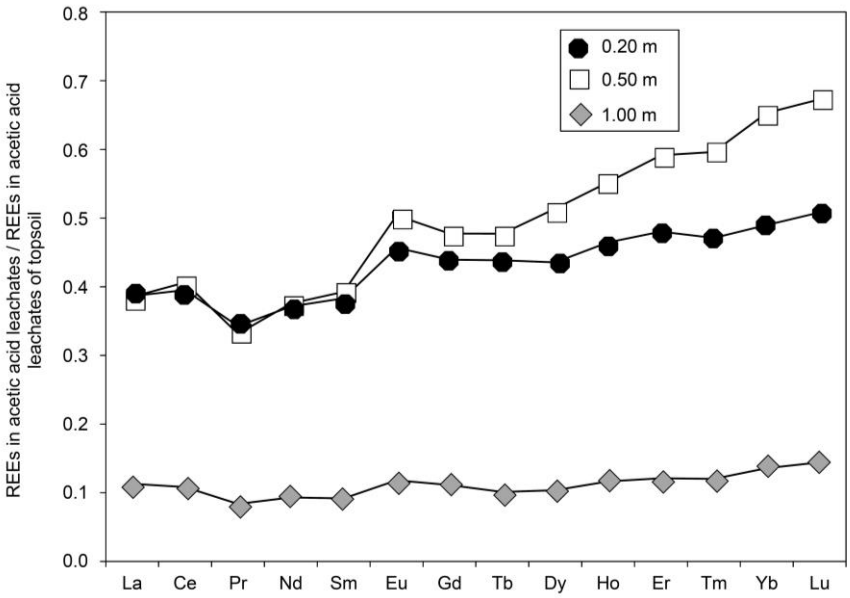

Figure 8. REE distribution patterns of the acetic-acid leachates relative to the acetic-acid leachate of the topsoil sample along the vertical trend at 0.20-m, 0.50-m and 1-m depth.

Of interest is the progressive increase of the Ce negative anomaly from 10 to 32 m distance to vegetation, which suggests a progressive change in the oxidation-reduction conditions in the soil when the distance to vegetation increases. From a somewhat reduced environment imposed by the vegetation, the conditions become more oxidizing away. The negative Eu anomaly that basically is representative for increasing contents of silicate minerals (Weill and Drake, 1973) is also increasing progressively with the distance to the vegetation. This progressive change could record a progressive input of an inorganic REE supply to the leachates relative to the organic supply.

When possible, comparison of the REE patterns of the water and acetic acid leachates from the same samples outlined instructive displays. In fact, the water and acid-acetic solutes of the soil samples close to vegetation at 10, 20 and 50 cm are very similar with flat patterns (Figure 5B). Only two leachates yield different patterns: that from 1-m depth outlines a significant positive Ce anomaly, the rest of the pattern being still flat, and that from 10 m away yields a downwards slope for the HREEs, and very visible positive Ce and Eu anomalies that have been already mentioned.

Discussion

Differences in the vertical and lateral distributions of elements can be assigned to changes in the physicochemical properties of the studied soil including pH, amount and activity of the occurring organic matter, as well as amount and type of minerals, especially clays such as smectite characterized by high cation-exchange capabilities. As a preliminary hypothesis, the vertical downwards increase of elements could indicate either some dissolution of secondary phases or leaching of elements adsorbed on crystal surfaces in the topsoil, while a vertical decrease may indicate either the supply of elements into a plant activity volume in the rhyzosphere near the surface, or an input from anthropogenic sources via the atmosphere at the upper soil level and a decrease downwards. The lateral increase of elements can be due to either dissolution of secondary phases, a decrease of the micro-organic soil components, or even fixation of anthropogenic supplies by the micro-organisms near the vegetation and a lateral decrease focusing on their role in plant growth.

The message of the elements leached by water

Increasing of the Al, Ca, Mg, Fe, Mn, K and Na contents from water leachates at 20 cm depth relative to those of the topsoil above suggests an evapo-transpiration that usually induces such increase of nutrient concentrations (Cramer et al., 2008; Onwuka and Mang, 2018). On the other hand, while elements primarily taken up by plants, such as K and P, decrease with depth, the important increase of Al and Fe at 50 cm depth may indicate a downwards leaching with possible incorporation into secondary phases. Ifansyah (2013) reported that humic acid is able to increase the P availability and to reduce the Al and Fe solubility in soils. High solubility of Al and Fe, together with a P decrease at 50 cm depth, does not correlate here with a change of the pH, which increased only slightly from 8.29 to 8.97 at 50 cm, compared to the topsoil. Ifansyah (2013) reported also that the high Al and Fe solubility is accompanied by hydrolysis that induces a release of

hydrogen ions into the soil fluids and consequently an acidification of the soil. The interpretation of the data obtained here is different. As humic substances are strongly complexing Al and $Fe_{(III)}$, the total Al concentration and its speciation in the soil depend mainly on the pH and the chemical environment of the pore waters (Gerke, 1997; Kisnierienė and Lapeikaitė, 2015). On the other hand, Al has no specific biological function (Poschenrieder et al., 2008). Adsorption affinity of phosphate by ferro-hydrite complexes (Wang et al., 2015) could also explain the P decrease at 50 cm depth.

The lateral distribution of the leached elements most probably highlights a progressive decrease of the plant activity; the lower K leaching obtained close to vegetation may then be due to the soil contribution to the plant cycling. This hypothesis is confirmed by the K increase in the samples away from vegetation. It is also supported by the P contents decreasing progressively in the leachates away from vegetation. Elements such as Si, Al and Ca, which contents increase with the distance from vegetation, may also be indicative of a progressively increased contribution of altering minerals from soil. Na decreasing away from vegetation, while Mg and Fe rather fluctuate with the distance to the vegetation, could then relate to either decreasing minerals containing the former or varied amounts of minerals with the latters. Elements such as Cu, Cr and Pb are enriched in the upper horizons and depleted at depth, which suggests some anthropogenic supply. Conversely, As, V and Ni are enriched at depth, which could result from a more active leaching near the surface and a transfer downwards. In general, elements, which contents decrease with distance to vegetation as is the case for V, Cu, Cd and U, suggest also a complexation process with organics of the soil that are also expectedly decreasing when the distance to vegetation increases.

The message of the elements dissolved by acetic acid

Elements such as Mg, Na, P, Si and Mn are increasing at depth that results from a combined leaching and precipitation of secondary phases in the deeper soil. Relative to the topsoil close to vegetation, the Al, Si, Mg, Mn, Na and P contents increase at 10 m, and then decrease with distance, while Fe shows a lateral decrease. The Ca contents decrease at 10 m, while increasing at the other sampling stations. The content of K remains unchanged with distance, which suggests that when involved in plant activities it contributes more to the water leachates as a potential nutrient than to the acetic-acid leachable phases.

The message of the trace elements

The increasing contents of the trace elements relative to depth characterize a leaching from topsoil downwards as the contents may originate from soluble minerals, while any decrease at depth reflects rather a precipitation with increasing pH. Alternatively, leached trace elements characterized by decreasing contents with depth may also indicate surficial supplies of anthropogenic sources. The elements most leached from soil surface are V, Ni, Cu, Th, As and Rb (with an important decrease at 50 cm). Co increases downwards with an important step at 50 cm. The REEs are more accumulated in the topsoil, whereas the decrease of the trace elements relative to depth parallels the increase of pH.

The REE contents of the leachates decrease at depth relative to those from topsoil with, laterally, an increase at 18 m, a decrease at 22 m, and a renewed increase at 32 m. The distribution confirms that there is a higher plant activity and/or amount of organic matter in the topsoil that complexes and fixes REEs. Alternatively, the irregular increases of the REE contents with distance could illustrate local inputs from dissolved minerals. A comparison of the water and acetic acid leachates in the vertical trend shows that the Ce and Eu positive anomalies are significantly larger when sampling is deeper in the vertical trend and further away from vegetation in the unique available pattern. These anomalies point to the fact that the earlier reported negative anomalies in soils (Wyttenbach et al., 1998; Loell et al., 2011) seem not to be general rules. Here, the Ce anomaly indicates apparently that there is a progressive oxidation-reduction change when sampling is more distant from plant activity, surprisingly towards a more reduced environment, which could relate to some lower activity of the microorganisms, or even to a more or less decrease of their occurrence. The increasing Eu anomaly obtained away from vegetation might reflect a larger contribution of mineral compounds in the leachates, confirming in turn a decreasing organic contribution. The higher contents in the HREEs relative to the LREEs in the leachates away from vegetation, vertically and horizontally, seem to be quite systematic (Figure 4A and B; Figure 5A and B).

The K/Rb, Ca/Sr and Na/K ratios

The K/Rb ratio of the water-soluble fractions ranges from about 1,569 to 6,700 in the different soil samples. As reported by Chaudhuri et al. (2007), these high values are more common for organic than mineral materials. The vertical distribution indicates a higher ratio in the subsoil relative to the topsoil, as is the case

in the lateral distribution. This trend is somewhat to the opposite to that of the associated total organic carbon.

The Ca/Sr ratio ranges from about 14.9 to 111 with the highest value 10 m away from vegetation and the lowest 12 m away. It is lower in the topsoil than in the subsoil because of Sr decrease with depth. In its lateral fluctuation, the changes of the Ca/Sr ratio parallel the changes in the Ca of the acetic acid leachates (r^2=-0.65), while they parallel the Sr changes (r^2=0.80) in the water extracts. No alternative correlations between Ca/Sr ratio and Ca contents are observed in the water extracts and between Ca/Sr ratio and Sr contents in the acetic acid extracts.

The K/Rb ratio ranges from about 1,335 to 8,835 in the acetic-acid leachates of the analyzed samples. Its fluctuations are better correlated with Rb than with K. The general tendency is an increase with depth and with distance from vegetation, because of a preferential Rb decrease. The Ca/Sr ranges from 259 to 670 with no clear trend in the subsoil, the fluctuations being correlated with the Ca rather than with the Sr changes (Figure 3).

The Na/K ratio ranges from about 1.63 to 29.1 in the water leachates. The vertical fluctuations show a higher ratio in the subsoil because of an increased content in Na. Alternatively, the lateral distribution of the ratio outlines a decrease with the distance from vegetated area except at 12 m where no change relative to samples collected close to vegetation is visible. In the acetic acid leachates, the Na/K ratio ranges less widely from 1.62 to 5.86. For both the water and acetic-acid leachates, a positive correlation is observed between Na/K ratio and the concentration of Na, which suggests a uniform supply of Na along both the vertical and the lateral trend.

Conclusion

The elemental distribution in water and acetic-acid leachates shows that plant cycling is not systematically the dominant control of the nutrient distribution in soils. However, elements such as Mg, Na, P, Si and Mn enriched here at depth in the acetic acid leachates appear to be controlled essentially by the organic cycle. Usually involved in plant cycling, K remains unchanged in the acetic-acid solutes with depth and distance to the plants. For the water leachates, its vertical distribution outlines a decrease with depth because essentially involved in the plant activity. Opposite results characterize the P contents that decrease in the water and acetic acid leachates away from vegetation. A human impact is suspected for the metallic trace elements that are enriched in the acetic-acid leachates at the surface relative to the subsoil. The vertical distribution of the K/Rb ratio ranging from about 1,569 to 6,700 in the water-soluble fractions indicates a higher ratio in the subsoil than the topsoil. It ranges from about 1,335 to 8,835 in the acetic acid leachates, increasing with depth and distance to vegetation. In turn, this experiment raises the basic heterogeneity of soils below and away from vegetation: no constant trend being observed in both directions. It looks like the soluble elements of each soil sample are only representative for themselves.

Not controlled directly by the plants but more probably by solid organic exudates, REEs are more accumulated in the acetic-acid leachates of the topsoil. Their contents in the leachates decrease at depth relative to those in the leachates of the topsoil with an irregular increase laterally away from vegetation. The REEs distribution confirms a higher amount of organic matter in the topsoil that complexes and fixes REEs. Alternatively, the irregular increases of the REE with distance illustrate local irregular inputs from solid phases dissolved by acetic acid. Ce and Eu positive anomalies are significantly larger when sampling is deeper in the soil and away from vegetation. The Ce anomaly apparently indicates that there is a progressive oxidation-reduction change when sampling is distant from plant activity, probably induced by a significantly lower activity of the microorganisms. On the other hand, the increasing Eu anomaly away from vegetation might reflect a larger contribution of the mineral compounds to the leachates. Higher contents in the HREEs relative to the LREEs in the leachates away from vegetation, vertically and horizontally, seem to be quite systematic outlines.

References

Akan, J.C., Audu, S.I., Mohammed, Z., Ogugbuaja, V.O., 2013. Assessment of heavy metals, pH, organic matter and organic carbon in roadside soils in Makurdi metropolis, Benue State, Nigeria. *Journal of Environmental Protection* 4(6): 618-628.

Ashworth, D.J., Alloway, B.J.. 2008. Influence of dissolved organic matter on the solubility of heavy metals in sewage-sludge-amended soils. *Communications in Soil Science and Plant Analysis* 39(3-4): 538-550.

Aydinalp, C., Marinova, S.. 2003. Distribution and forms of heavy metals in some agricultural soils. *Polish Journal of Environmental Studies* 12(5): 629-633.

Camenzind, T., Hattenschwiler, S., Treseder, K.K., Lehmann, A., Rillig, M.C.. 2018. Nutrient limitation of soil microbial processes in tropical forests. *Ecological Monographies* 88(1): 4-21.

Chang, C., Li, F., Liu, C., Gao, J., Tong, H., Chen, M., 2016. Fractionation characteristics of rare earth elements (REEs) linked with secondary Fe, Mn and Al minerals in soils. *Acta Geochimica* 35(4): 329-339.

Chaudhuri, S., Clauer, N., Semhi, K., 2007. Plant decay as a major control of river dissolved potassium: A first estimate. *Chemical Geology* 243(1-2): 178-190.

Chen, J., Yang, R., 2010. Analysis on REE geochemical characteristics of three types of REE-rich soil in Guizhou Province, China. *Journal of Rare Earths* 28(S1): 517-522.

Fekiacova, Z., Pichat, S., Cornu, S., Balesdent, J., 2013. Inferences from the vertical distribution of Fe isotopic compositions on pedogenetic processes in soils. *Geoderma* 209-210: 110-118.

Gahoonia, T.S., Nielsen, N.E., 1992. The effects of root-induced pH changes on the depletion of inorganic and organic phosphorus in the rhizosphere. *Plant and Soil* 143(2): 185-191.

Gerke, J., 1997. Aluminum and iron(III) species in the soil solution including organic complexes with citrate and humic substances. *Journal of Plant Nutrition and Soil Science* 160(3): 427-432.

Cramer, M.D, Hoffmann, V., Verboom, G.A., 2008. Nutrient availability moderates transpiration in Ehrharta calycina. *New Phytologist* 179(4): 1048-1057.

Hedley, M.J., Nye, P.H., White, R.E., 1982a. Plant induced changes in the rhizosphere of rape (Brassica napus var. Emerald) seedlings. II. Origin of the pH change. *New Phytologist* 91(1): 31-44.

Hedley, M.J., Stewart, J.W.B., Chauhan, B.S., 1982b. Changes in inorganic and organic soil phosphorus fractions induced by cultivation practices and by laboratory incubations. *Soil Science Society of America Journal* 46(5): 970-976.

Helal, H.M, Dressler, A., 1989. Mobilization and turnover of soil phosphorus in the rhizosphere. *Zeitschrift of Pflanzenernaehrung und Bodenkunde* 152(2): 175-180.

Hirekurabar, B.M., Satyanarayana, T., Sarangmath, P.A., Manjunathaiah, H.M., 2000. Forms of potassium and their distribution in soils under cotton based cropping system in Karnataka. *Journal of the Indian Society of Soil Science* 48, 604-608.

Ifansyah, H., 2013. Soil pH and solubility of aluminum, iron, and phosphorus in ultisols: the roles of humic acid. *Journal of Tropical Soils* 18(3): 203-208.

Jayaganesh, S., Venkatesan, S., Senthurpandian, V.K., Poobathiraj, K., 2011. Vertical distribution of magnesium in the laterite soils of South India. *International Journal of Soil Science* 6(1) 69-76.

Jobbágy, E.G., Jackson, R.B., 2001. The distribution of soil nutrients with depth: Global patterns and the imprint of plants. *Biogeochemistry* 53(1): 51-77.

Kisnieriené, V., Lapeikaité, I., 2015. When chemistry meets biology: the case of aluminium- a review. *Chemija* 26(3): 148-158.

Knops, J.M.H., Bradley, K.L., 2009. Soil carbon and nitrogen accumulation and vertical distribution across a 74-year chronosequence. *Soil Science Society of America Journal* 73(6): 2096-2104.

Loel, M., Reiher, W., Felix-Henningsen, P., 2011. Contents and bioavailability of rare earth elements in agricultural soils in Hesse (Germany). *Journal of Plant Nutrition and Soil Science* 174(4): 644-654.

McLennan, S.M., 1989. Rare earth elements in sedimentary rocks; influence of provenance and sedimentary processes. *Reviews in Mineralogy and Geochemistry* 21(1): 169-200.

Manea, A., Dumitru, M., Vranceanu, N., Dumitru, S., Isnoveanu, I., 2011. Vertical distribution of copper content in soil from Zlatna area. *Research Journal of Agricultural Science* 43(3): 118-124.

Martínez, C.E., Motto, H.L., 2000. Solubility of lead, zinc and copper added to mineral soils. *Environmental Pollution* 107(1): 153-158.

Mathan, K.K., 1991. Magnesium distribution pattern in a soil toposequence in Doddabetta series of Nilgiris. *Journal of Indian Society of Soil Science* 39, 368-370.

Miao, L., Xu, R., Ma, Y., Zhu, Y., Wang, J., Cai, R., Chen, Y., 2008. Geochemistry and biogeochemistry of rare earth elements in a surface environment (soil and plant) in South China. *Environmental Geology* 56(2): 225-235.

Nielsen, N.E., Schjørring, J.K., Jensen, H.E., 1988. Efficiency of fertilizer nitrogen uptake by spring barley. In: Nitrogen Efficiency in Agricultural Soils. Jenkinson, D.S., Smith, K.A., (Eds.). Elsevier Applied Science, London and New York, USA. pp.62-72.

Onwuka, B., Mang, B., 2018. Effects of soil temperature on some soil properties and plant growth. *Advanced Plants & Agricultural Research* 8(1): 34-37.

Piper, D.Z., Bau, M., 2013. Normalized rare earth elements in water, sediments, and wine: Identifying sources and environmental redox conditions. *American Journal of Analytical Chemistry* 4(10A): 69-83.

Poschenrieder, C., Gunsé, B., Corrales, I., Barceló, J., 2008. A glance into aluminum toxicity and resistance in plants. *Science of The Total Environment* 400(1-3): 356-368.

Sahuquillo, A., Rigol, A., Rauret, G., 2003. Overview of the use of leaching/extraction tests for risk assessment of trace metals in contaminated soils and sediments. *Trends in Analytical Chemistry* 22(3): 152-159.

Samuel, J., Rouault, R., Besnus, Y., 1985. Analyse multi-élémentaire standardisée des matériaux géologiques en spectrométrie d'émission par plasma à couplage inductif. *Analusis* 13(7): 312-317.

Semhi, K., Chaudhuri, S., Clauer, N., 2009. Fractionation of rare-earth elements in plants during experimental growth in varied clay substrates. *Applied Geochemistry* 24(3): 447-453.

Shen, J., Yuan, L., Zhang, J., Li, H., Bai, Z., Chen, X., Zhang, W., Zhang, F., 2011. Phosphorus dynamics: From soil to plant. *Plant Physiology* 156(3): 997-1005.

Silveira, M.L.A., Alleoni, L.R.F., Guilherme, L.R.G., 2003. Biosolids and heavy metals in soils. *Scientia Agricola* 60(4): 793-806.

Sterckeman, T., Proix, N., Douay, F., Fourrier, H., 2000. Vertical distribution of Cd, Pb and Zn in soils near smelters in the North of France. *Environmental Pollution* 107(3): 377-389.

Taylor, S.R., McLennan, S.M., 1985. The Continental Crust: its Composition and Evolution. Blackwell, Oxford, 312 p.

Tukura, B.W., Kagbu, J.A., Gimba, C.E., 2007. Effects of pH and total organic carbon (TOC) on the distribution of trace metals in Kubanni Dam sediments, Zaria, Nigeria. *Science World Journal* 2(3): 1-6.

Tyler, G., 2004. Rare earth elements in soil and plant systems – A review. *Plant and Soil* 267(1-2): 191-206.

Wang, H., Zhu, J., Fu, Q.L, Xiong, J.W, Hong, C., Hu, H.Q., Violante A., 2015. Adsorption of phosphate onto ferrihydrite and ferrihydrite-humic acid complexes. *Pedosphere* 25(3): 405-414.

Weill, D.F., Drake, M.J., 1973. Europium anomaly in plagioclase feldspar: experimental results and semiquantitative model. *Science* 180(4090): 1059-1060.

Weng, L., Temminghoff, E.J.M., Lofts, S., Tipping, E., Van Riemsdijk, W.H., 2002. Complexation with dissolved organic matter and solubility control of heavy metals in a sandy soil. *Environmental Science Technology* 36(22): 4804-4810.

Wood, L.K., de Turk, F.E., 1940. The absorption of potassium in soil in non-replaceable forms. *Science Society of America Journal* 5: 152-161.

Wyttenbach, A., Furrer, V., Schleppi, P., Tobler, L., 1998. Rare earth elements in soil and in soil-grown plants. *Plant and Soil* 199(2): 267-273.

Zoysa, A.K.N, Loganathan, P., Hedley, M.J., 1997. A technique for studying rhizosphere processes in tree crops: soil phosphorus depletion around camellia (Camellia japonica L.) roots. *Plant and Soil* 190(2): 253-265.